

**Characterisation of the interactions between the KSHV ORF57  
protein and the human TREX complex**

**Sophie Schumann**

Submitted in accordance with the requirements for the degree of  
Doctor of Philosophy

The University of Leeds  
Faculty of Biological Sciences  
School of Molecular and Cellular Biology

September 2014

The candidate confirms that the work submitted is her own and that appropriate credit has been given where reference has been made to the work of others.

This copy has been supplied on the understanding that it is copyright material and that no quotation from the thesis may be published without proper acknowledgement.

© 2014 The University of Leeds and Sophie Schumann

## Acknowledgements

I would like to express my gratitude to my supervisor Professor Adrian Whitehouse, for his continuing trust, guidance and support throughout my thesis. He always had an open door for me. Many thanks also to my co-supervisor Dr Richard Foster, who played an invaluable part in the rational-based drug design of my project.

My deepest appreciation to my colleagues and friends from the Whitehouse and Hewitt groups, past and present, for creating such a great work environment. You have often provided me with scientific advice and support, as well as a good laugh.

Many thanks go to Dr Ian Yule, for his help with compound selection and *in silico* modelling. Acknowledgments also to Dr Brian Jackson for performing the thermophoresis experiment presented within this thesis and to Dr Belinda Baquero-Perez for proof reading sections of my work.

I am grateful to the Wellcome Trust for funding my studies and for putting me in a position where I could design and shape my own project.

A huge thank you to my family, for believing in me and making me believe in myself.

Last, but definitely not least, I would like to thank John, who gave me his unlimited support at every step of my PhD and to whom I can say; without you, this would have been so much harder.

## Abstract

Kaposi's sarcoma-associated herpesvirus (KSHV) is a human oncovirus associated with multiple malignancies, including Kaposi's sarcoma (KS). Like all herpesviruses, KSHV can establish either a latent or a lytic infection in host cells. During latency the virus remains in a dormant state, with limited gene expression. After reactivation, KSHV enters the lytic life cycle, characterised by production of infectious virions and subsequent dissemination of the virus from its latent reservoir. Importantly, lytic replication is critical for KS tumourigenesis.

KSHV replicates in the nucleus of the host cell and requires cellular mRNA export factors to efficiently export viral mRNAs from the nucleus, allowing their translation in the cytoplasm. But while mammalian mRNA export is linked to splicing, the majority of the KSHV genome encodes intronless mRNAs, prompting the virus to circumvent this step. KSHV therefore expresses ORF57, a multifunctional protein essential for lytic replication. ORF57 recruits members of the cellular human transcription/export (hTREX) complex to form an export competent viral ribonucleoprotein particle (vRNP), facilitating efficient nuclear export of intronless KSHV mRNAs.

This study presents a novel mechanism for the specific disruption of the vRNP and subsequent inhibition of virus lytic replication. Results suggest an ATP-cycle dependent remodelling of hTREX, which affects the ability of ORF57 to interact and form an export competent vRNP. Specifically, inhibiting ATP hydrolysis by the hTREX component and ATPase UAP56 prevents ORF57 from recruiting the hTREX complex, while key components of the endogenous complex remain able to interact.

Following this finding, UAP56 was targeted by small molecule inhibitors, using a structure-based drug design approach, to prevent ATP hydrolysis and thereby inhibiting vRNP formation. Strikingly, a hit compound identified was shown to disrupt formation of the vRNP, lytic protein expression and infectious virion production, while allowing endogenous hTREX formation within a therapeutic window, where no cytotoxicity was observed.

Bearing in mind the conserved mechanism for herpesvirus intronless mRNA export, this study finally presents a series of compounds that are able to prevent both KSHV and HSV-1 lytic replication.

# Contents

<b>Acknowledgements</b> .....	<b>ii</b>
<b>Abstract</b> .....	<b>iii</b>
<b>Contents</b> .....	<b>iv</b>
<b>List of figures</b> .....	<b>ix</b>
<b>List of tables</b> .....	<b>xiii</b>
<b>Abbreviations</b> .....	<b>xiv</b>
<b>1 Introduction</b> .....	<b>2</b>
1.1 <i>Herpesviridae</i> .....	2
1.1.1 Classification of Herpesviruses .....	2
1.1.1.1 <i>Alphaherpesvirinae</i> .....	2
1.1.1.2 <i>Betaherpesvirinae</i> .....	3
1.1.1.3 <i>Gammaherpesvirinae</i> .....	4
1.1.2 Virion architecture .....	4
1.1.3 Genomic structure .....	5
1.1.4 Life cycle.....	6
1.1.4.1 Latency .....	8
1.1.4.2 Lytic replication.....	8
1.2 The <i>Gammaherpesvirinae</i> .....	9
1.2.1 Epstein Barr virus (EBV) .....	10
1.2.1.1 EBV life cycle .....	12
1.2.2 Kaposi's sarcoma-associated herpesvirus (KSHV).....	13
1.2.2.1 KSHV associated diseases .....	15
1.2.2.1.1 Kaposi's sarcoma (KS) .....	15
1.2.2.1.2 Primary effusion lymphoma (PEL) .....	19
1.2.2.1.3 Multicentric Castleman disease (MCD).....	19
1.2.2.2 KSHV life cycles .....	19
1.2.2.2.1 Latency .....	20
1.2.2.2.2 Lytic replication.....	22
1.3 Cellular mRNA export.....	25
1.3.1 Cellular mRNA processing.....	25
1.3.2 The human transcription/export (hTREX) complex .....	26
1.3.2.1 Assembly and function of the hTREX complex .....	27

1.3.2.2	The hTREX complex and the export receptor Nxf1.....	31
1.3.2.3	The hTREX complex and the exon junction complex (EJC) .....	33
1.3.3	Alternative mRNA export pathways .....	33
1.3.3.1	CRM1-dependent mRNA export .....	33
1.3.3.2	Nuclear budding of mRNPs .....	34
1.3.3.3	Export of intronless mRNA.....	35
1.4	Viral mRNA export.....	36
1.4.1	Herpesvirus mRNA export.....	36
1.4.2	mRNA export by other viruses .....	36
1.5	KSHV ORF57 protein.....	39
1.5.1	ORF57-mediated mRNA export .....	41
1.5.2	Other roles of ORF57 .....	44
1.5.2.1	Transcriptional enhancement by ORF57.....	45
1.5.2.2	Stabilisation of mRNA by ORF57 .....	45
1.5.2.3	Translational enhancement by ORF57 .....	46
1.5.2.4	Regulation of splicing of viral transcripts by ORF57 .....	47
1.6	KSHV drug discovery.....	48
1.6.1	KSHV inhibitors.....	48
1.6.1.1	Current treatment options.....	48
1.6.1.2	Novel approaches of herpesvirus therapy.....	51
1.6.2	Drug development .....	51
1.6.2.1	Rational-based drug design.....	53
1.7	Thesis aim.....	57
<b>2</b>	<b>Material and Methods.....</b>	<b>59</b>
2.1	Materials.....	59
2.1.1	Chemicals .....	59
2.1.2	Cell culture reagents .....	59
2.1.3	Antibodies .....	59
2.1.4	Enzymes .....	60
2.1.5	Oligonucleotides .....	61
2.1.6	Plasmid expression constructs.....	61
2.1.7	Screening compounds.....	62
2.2	Methods .....	63
2.2.1	Molecular cloning.....	63

2.2.1.1	Transformation of <i>E. coli</i> BL21 and DH5 $\alpha$ .....	63
2.2.1.2	Plasmid purification .....	63
2.2.2	Cell culture .....	64
2.2.2.1	Cell lines .....	64
2.2.2.2	Cell maintenance .....	64
2.2.2.3	Transient transfection.....	65
2.2.2.4	siRNA knock-down .....	66
2.2.2.5	Treatment with small molecule inhibitors.....	66
2.2.2.6	Cytotoxicity assays .....	66
2.2.3	Virus based assays.....	67
2.2.3.1	Induction of KSHV lytic replication.....	67
2.2.3.2	KSHV late protein expression.....	67
2.2.3.3	KSHV replication assay .....	68
2.2.3.4	HSV-1 primary infection.....	68
2.2.3.5	Viral re-infection assays .....	69
2.2.3.6	HSV-1 plaque assay .....	70
2.2.4	Large scale expression and purification of proteins .....	70
2.2.4.1	Recombinant protein expression in <i>E. coli</i> BL21.....	70
2.2.4.2	Solubilisation of bacterially expressed protein.....	71
2.2.4.3	Purification of GST-tagged proteins.....	71
2.2.5	Analysis of proteins.....	72
2.2.5.1	Determination of protein concentration .....	72
2.2.5.2	SDS-polyacrylamide gel electrophoresis.....	72
2.2.5.3	Coomassie blue staining .....	73
2.2.5.4	Western blotting .....	73
2.2.6	Analysis of protein-protein interactions .....	74
2.2.6.1	GST-pulldown assay .....	74
2.2.6.2	Co-immunoprecipitation assay .....	74
2.2.6.3	Immunofluorescence microscopy.....	75
2.2.7	Biochemical assays.....	76
2.2.7.1	ATPase assay .....	76
2.2.8	Analysis of mRNA .....	76
2.2.8.1	Fluorescence <i>in situ</i> hybridisation (FISH).....	76
2.2.8.2	Nucleocytoplasmic fractionation for viral mRNA export assay .....	77

2.2.8.3	Total RNA isolation.....	77
2.2.8.4	DNase treatment .....	78
2.2.8.5	Reverse transcription.....	78
2.2.8.6	Quantitative real-time PCR (qPCR) .....	79
<b>3</b>	<b>A novel interaction of ORF57 with CIP29, a hTREX component .....</b>	<b>81</b>
3.1	Introduction.....	81
3.2	GST pulldowns show an interaction between CIP29 and ORF57 .....	82
3.3	Co-Immunoprecipitation assays confirm an interaction between CIP29 and ORF57 .....	84
3.4	Immunofluorescence microscopy shows ORF57 dependent relocalisation of CIP29 .....	85
3.5	Role of CIP29 in UAP56-mediated ATP hydrolysis .....	87
3.6	An ATP-dependent interaction of hTREX components affects the ability of ORF57 to interact with CIP29.....	90
3.7	Role of CIP29 in ORF57-mediated export of viral intronless mRNAs.....	91
3.8	Loss of CIP29 does not affect KSHV late protein expression .....	94
3.9	Discussion.....	95
<b>4</b>	<b>ATP-cycle dependent remodelling of hTREX complex affects ORF57-induced viral RNP formation and can be exploited as a therapeutic target .....</b>	<b>99</b>
4.1	Introduction.....	99
4.2	ATP-dependent formation of the ORF57-mediated vRNP .....	100
4.3	ATP-cycle dependent remodelling of the ORF57-mediated vRNP .....	102
4.4	High-throughput screening for UAP56 ATPase inhibitors.....	105
4.5	Confirmation of UAP56 inhibition by small molecule inhibitor C2 .....	109
4.6	Disruption of vRNP formation <i>in vitro</i> by ATPase inhibitor C2 .....	111
4.7	ATPase inhibitor C2 prevents recruitment of hTREX by ORF57 but does not inhibit cellular bulk mRNA export .....	115
4.8	C2 prevents ORF57-mediated export of viral mRNAs.....	117
4.9	Cytotoxicity of C2 in TREx BCBL-1 Rta cells .....	118
4.10	Disruption of vRNP formation by C2 in KSHV infected cells .....	119
4.11	Treatment of TREx BCBL1-Rta cells with C2 prevents export of viral intronless mRNA.....	120
4.12	Small molecule inhibitor C2 prevents expression of viral late proteins in KSHV infected cells.....	121

4.13	Inhibition of viral replication and production of infectious virus particles in the presence of C2.....	124
4.14	Discussion.....	126
<b>5</b>	<b>Structural analogues of UAP56 ATPase inhibitor C2 and the inhibitory effect on HSV-1 .....</b>	<b>130</b>
5.1	Introduction.....	130
5.2	Effect of close structural analogue An1 on KSHV late protein expression and viral load in KSHV lytic replication .....	131
5.3	Effect of close structural analogue An3 on KSHV late protein expression and viral load in KSHV lytic replication .....	135
5.4	Effect of close structural analogue SKW032 on KSHV late protein expression and viral load in KSHV lytic replication.....	138
5.5	Effect of close structural analogue SKW036 on KSHV late protein expression and viral load in KSHV lytic replication.....	142
5.6	Effect of C2 on HSP90 and HSP90 client proteins .....	145
5.7	Effect of inhibitor C2 on HSV-1 replication .....	151
5.8	Effect of inhibitor C2 on HSP90 and HSP90-client proteins in HFF cells .....	157
5.9	Discussion.....	158
<b>6</b>	<b>Discussion .....</b>	<b>161</b>
6.1	ORF57 and CIP29.....	162
6.2	ORF57 and hTREX: ATP-dependency and complex remodelling .....	163
6.3	Identification of a novel KSHV-inhibitor.....	168
6.4	Implication of the inhibitor as anti-KSHV drug.....	170
6.5	Inhibition of HSP90 and off-target effects .....	171
6.6	Hit to lead development and future work .....	173
	<b>References .....</b>	<b>I</b>

## List of figures

Figure 1.1: Phylogenetic tree for <i>Herpesviridae</i> .....	3
Figure 1.2: Herpesvirus structure. ....	5
Figure 1.3: Herpesvirus genome structures. ....	6
Figure 1.4: Herpesvirus entry mechanisms. ....	7
Figure 1.5: Herpesvirus lytic replication. ....	9
Figure 1.6: KSHV genome map. ....	14
Figure 1.7: KSHV prevalence worldwide.....	15
Figure 1.8: Kaposi's sarcoma incidence rate worldwide. ....	16
Figure 1.9: Proposed mechanism of KSHV-induced sarcoma. ....	18
Figure 1.10: Schematic of KSHV genome segregation during mitosis.....	21
Figure 1.11: RTA-mediated transactivation mechanisms.....	24
Figure 1.12: Structure of the mRNA 5'-cap. ....	25
Figure 1.13: The hTREX complex associates to the 5'-end of mRNA via an interaction with the cap binding complex.....	28
Figure 1.14: UAP56 assembles the hTREX complex sequentially, in an ATP-dependent manner.....	31
Figure 1.15: The hTREX complex interacts with the export receptor Nxf1.....	32
Figure 1.16: RNP export by nuclear envelope budding.....	35
Figure 1.17: Strategies in viral mRNA export. ....	37
Figure 1.18: ORF57 aa sequence, secondary structure and putative motifs. ....	40
Figure 1.19: ORF57 recruits the complete hTREX complex onto the viral mRNA.....	43
Figure 1.20: ORF57 recruits the translational enhancer PYM onto viral mRNA. ....	47
Figure 1.21: Mechanism of action of ganciclovir and cidofovir. ....	49
Figure 1.22: Stages of research and development during a drug discovery cascade. ....	52
Figure 1.23: Target-based vs. system-based approaches in drug discovery.....	53
Figure 1.24: Knowledge plot highlighting the approach of rational-based drug design.....	54
Figure 1.25: Methods in fragment-based drug design: Fragment linking and fragment evolution. ....	55
Figure 1.26: Range of potency and molecular mass of fragments, HTS hits and drugs/drug candidates.....	56
Figure 3.1: Induction of bacterially expressed GST and GST-CIP29. ....	82
Figure 3.2: Binding of GST and GST-CIP29 to glutathione-conjugated agarose beads. ....	83

Figure 3.3: GST-pulldown assay shows CIP29 interacting with ORF57 and UIF. ....	84
Figure 3.4: Co-Immunoprecipitations confirm an interaction of CIP29 with ORF57 and UIF. .....	85
Figure 3.5: Overexpression of ORF57 causes re-localisation of endogenous CIP29. ....	86
Figure 3.6: Overexpression of ORF57 leads to a redistribution of recombinant CIP29. ....	87
Figure 3.7: Purification of GST-tagged hTREX components. ....	88
Figure 3.8: CIP29 stimulates UAP56 ATPase activity <i>in vitro</i> . ....	89
Figure 3.9: ATP needs to be present for ORF57 to interact with CIP29. ....	91
Figure 3.10: Knock-down of CIP29 using siRNA in 293T cells. ....	92
Figure 3.11: CIP29 knock-down does not affect ORF57-mediated mRNA export. ....	93
Figure 3.12: Knock-down of CIP29 using siRNA in latent 293 rKSHV.219 cells. ....	94
Figure 3.13: CIP29 knock-down does not affect viral late protein expression. ....	95
Figure 4.1: ATP-dependent formation of the ORF57-mediated vRNP. ....	101
Figure 4.2: Dose-dependent effect of ATP and ATP $\gamma$ S on ORF57-mediated vRNP formation. .....	102
Figure 4.3: ATP-cycle dependent remodelling of the ORF57-mediated vRNP. ....	103
Figure 4.4: Dose-dependency of ATP-cycle dependent remodelling of the ORF57-mediated vRNP. ....	104
Figure 4.5: Schematics of ATP-cycle dependent remodelling of central hTREX components and the ORF57-mediated vRNP. ....	105
Figure 4.6: Determination of assay conditions for UAP56-ATPase assay. ....	106
Figure 4.7: Inhibition of UAP56 ATPase activity by ATP $\gamma$ S. ....	107
Figure 4.8: Screening of small molecules and fragments against UAP56 ATPase activity identified four potential inhibitors. ....	108
Figure 4.9: Compound C2 is predicted to bind to the ATP binding pocket of UAP56. ....	109
Figure 4.10: IC <sub>50</sub> measurements of C2 for UAP56. ....	110
Figure 4.11: Thermophoresis binding curve for UAP56 and C2. ....	111
Figure 4.12: Disruption of vRNP formation by UAP56 ATPase inhibitor C2. ....	112
Figure 4.13: Cell viability of 293T cells in the presence of C2. ....	113
Figure 4.14: Disruption of UAP56 co-localisation with ORF57 in the presence of C2. ....	114
Figure 4.15: Disruption of CIP29 co-localisation with ORF57 in the presence of C2. ....	115
Figure 4.16: Fluorescence <i>in situ</i> hybridisation (FISH) demonstrates C2 prevents hTREX sequestration by ORF57, but does not inhibit cellular bulk mRNA export. ....	116
Figure 4.17: Inhibitor C2 reduces ORF57-mediated mRNA export. ....	117



Figure 5.22: Expression of HSP90 client protein CDC2 by HFF cells in the presence of C2.	157
Figure 6.1: Schematics of ATP-cycle dependent remodelling of central hTREX components and the ORF57-mediated vRNP. ....	164
Figure 6.2: Crystal structure of UAP56 N-terminal and C-terminal domains. ....	165
Figure 6.3: Initial strategy for advancing hit compound C2. ....	175

## List of tables

Table 1.1: EBV associated diseases. ....	11
Table 1.2: Overview of EBV latency programmes, their associated malignancies and gene expression profiles. ....	13
Table 1.3: Known components of hTREX. ....	27
Table 2.1: List of cell culture reagents and their suppliers. ....	59
Table 2.2: Primary antibodies, their working dilution and suppliers. ....	60
Table 2.3: List of enzymes and their suppliers. ....	61
Table 2.4: List of oligonucleotides and their sequences ....	61
Table 2.5: Plasmid expression constructs, their source and reference literature. ....	62
Table 2.6: List of small molecule inhibitors and their suppliers. ....	62

## Abbreviations

%	percentage
<	less than
°C	degrees Celsius
α	Alpha
β	beta
γ	gamma
κ	kappa
μg	microgram
μl	microlitre
μm	micrometre
μM	micromolar
aa	amino acid
AAA-ATPase	ATPase associated with diverse cellular activities
ADP	adenosine diphosphate
AIDS	acquired immune deficiency syndrome
AREX	alternative mRNA export
ART	antiretroviral therapy
ATP	adenosine triphosphate
ATPγS	adenosine 5'-O-(3-thio)triphosphate
BARTS	BamHI A rightward transcripts
BCBL	body cavity based lymphoma
BLA	biological license application
BoHV	bovine herpesvirus
bp	base pair
BSA	bovine serum albumin
bZIP	basic leucine zipper domain
CAR	cytoplasmic accumulation region
CAR-E	cytoplasmic accumulation region consensus element
CBC	cap binding complex
CBP80	cap binding protein 80

CC <sub>50</sub>	half maximal cytotoxic concentration
cDNA	complementary DNA
CIP29	cytokine induced protein 29 kDa
CRM1	chromosomal region maintenance 1
CTE	constitutive transport element
C-terminus	carboxy-terminus
DAPI	4', 6-diamidino-2-phenylindole
DE	delayed early
dH <sub>2</sub> O	distilled water
DMEM	Dulbecco's modified Eagles medium
DMSO	dimethyl sulphoxide
DNA	deoxyribonucleic acid
DNase	deoxyribonuclease
dNTP	deoxyribonucleoside (5'-) triphosphate
dox	doxycycline hyclate
DP	diphosphate
ds	double stranded
dT	deoxythymidine
DTT	dithiothreitol
E	early
EBER	Epstein-Barr virus-encoded small RNA
EBNA	Epstein-Barr nuclear antigen
EBV	Epstein-Barr virus
EC <sub>50</sub>	half maximal effective concentration
ECL	enhanced chemiluminescence
EDTA	ethylenediaminetetraacetic acid disodium salt
EGFP	enhanced green fluorescent protein
EJC	exon junction complex
EphA2	ephrin receptor tyrosine kinase A2
FBS	foetal bovine serum
FDA	food and drug administration
FLIP	FLICE-inhibitory protein
Fnorm	normalised fluorescence

g	gram
<i>g</i>	gravitational force
GaHV	gallid herpesvirus
GAPDH	glyceraldehyde 3-phosphate dehydrogenase
gB	glycoprotein B
GCV	ganciclovir
GDP	guanosine diphosphate
GFP	green fluorescent protein
gH	glycoprotein H
GI <sub>50</sub>	half maximal growth-inhibitory concentration
gL	glycoprotein L
gp	glycoprotein
GST	glutathione S-transferase
GTP	guanosine triphosphate
h	hours
HAART	highly active antiretroviral therapy
HBV	hepatitis B virus
HCl	hydrochloric acid
HCMV	human cytomegalovirus
HCV	hepatitis C virus
HEK	human embryonic kidney
HHV	human herpesvirus
HIF	hypoxia-inducible factor
HIV	human immunodeficiency virus
HLA	human leukocyte antigen
hpi	hours post induction
HPMPC	cidofovir
HRE	hypoxia response element
HRP	horseradish peroxidase
HSP90	heat shock protein 90
HSV-1	herpes simplex virus 1
HTLV	human T-cell leukemia virus
hTREX	human transcription/export

HTS	high-throughput screening
HVS	herpesvirus saimiri
IC <sub>50</sub>	half maximal inhibitory concentration
ICP27	infected cell polypeptide 27
ICTV	International Committee on Taxonomy of Viruses
IE	immediate early
IF	immunofluorescence
IFN	interferon
IgG	immunoglobulin G
IL-6	interleukin-6
IP	immunoprecipitation
IPTG	isopropyl- $\beta$ -D-thio-galactoside
IR	internal repeat
IRF	interferon regulatory factor
ISRE	interferon-stimulated response element
JNK	c-Jun aminoterminal kinase
Kb	kilobase
Kbp	kilobase pair
KCl	potassium chloride
K <sub>D</sub>	dissociation constant
kDa	kiloDalton
K-RBP	KSHV RTA binding protein
KS	Kaposi's Sarcoma
KSHV	Kaposi's Sarcoma associated herpesvirus
L	late
LAMP	latency-associated membrane protein
LANA	latency-associated nuclear antigen
LAT	latency-associated transcripts
LB	lysogeny broth
LCL	lymphoblastoid cell lines
LMP	latency-associated membrane protein
lncRNA	long non-coding RNA
M	molar

m <sup>7</sup> G	7-methyl-guanine
MCD	multicentric Castleman's disease
MCMV	murine cytomegalovirus
mCP	minor capsid protein
MDa	megaDalton
MgCl <sub>2</sub>	magnesium chloride
MHC	major histocompatibility complex
MHV-68	murine gammaherpesvirus 68
miRNA	microRNA
ml	millilitre
mM	millimolar
mm	millimetre
MP	monophosphate
MPMV	Mason Pfizer Monkey Virus
mRNA	messenger RNA
mRNP	messenger ribonucleoprotein particle
MTA	mRNA transcript accumulation
MTS	3-(4,5-dimethylthiazol-2-yl)-5-(3-carboxymethoxyphenyl)-2-(4-sulfophenyl)-2H-tetrazolium
n	sample size
NaCl	sodium chloride
NaOH	sodium hydroxide
ncRNA	non-coding RNA
NDA	new drug application
NES	nuclear export signal
NF-κB	nuclear factor kappaB
ng	nanogram
NLS	nuclear localisation signal
nm	nanometre
nM	nanomolar
NMD	nonsense-mediated decay
NP	nucleoprotein
NP40	tergitol-type NP-40

NPC	nuclear pore complex
N-terminus	amino-terminus
Nups	nucleoporins
Nxf1	nuclear RNA export factor 1
Nxt1	nuclear transport factor 2-like export factor 1
Oct	octamer transcription factor
OD	optical density
ORE	ORF57 response element
ORF	open reading frame
<i>ori-Lyt</i>	lytic origin of DNA replication
<i>ori-P</i>	latent origin of DNA replication
p	p-value
PABP	polyadenylate binding protein
PABPC1	polyadenylate-binding protein cytoplasmic 1
PAGE	polyacrylamide gel electrophoresis
PAN	polyadenylated nuclear
PBS	phosphate buffered saline
PCR	polymerase chain reaction
PDGF	platelet-derived growth factor
PEL	primary effusion lymphoma
pfu	plaque forming units
PHAX	phosphorylated adaptor for RNA export
PML	promyelocytic leukemia protein
pmol	picomole
poly(A)	polyadenylated
PRE	post-transcriptional regulatory element
pre-mRNA	precursor-messenger RNA
PrV	pseudorabies virus
PTL	post-transplant lymphoma
PTM	post-translational modification
qPCR	quantitative PCR
qRT-PCR	quantitative reverse transcriptase PCR
QSAR	quantitative structure-activity relationship

R&D	research and development
RanGAP	Ran GTPase-activating protein
Rb	retinoblastoma
RBM14	RNA binding protein 14
RBP-jk	recombination signal-binding protein 1 for J-kappa
RFP	red fluorescent protein
RGG	arginine- and glycine-rich
RIPA	radioimmunoprecipitation assay
RNA	ribonucleic acid
RNAP II	RNA polymerase II
RNase	ribonuclease
RNP	ribonucleoprotein particle
ROS	reactive oxygen species
RPMI	Roswell Park Memorial Institute medium
RRE	RTA response element
rRNA	ribosomal RNA
RT	reverse transcriptase
RTA	replication and transcription activator
sec	seconds
SAR	structure-activity relationship
SD	standard deviation
SDS	sodium dodecyl sulphate
siRNA	small interfering RNA
siScr	scrambled siRNA
snRNA	small nuclear RNA
sORF	small open reading frame
Sqrt	square root
SR	serine/arginine rich
SSC	saline-sodium citrate
SuHV	suid herpesvirus
SV40	Simian vacuolating virus 40
TBS	tris buffered-saline
TEMED	N-N-N'-N'-tetramethylethylenediamine

THV	tupaïid herpesvirus
TLR	toll-like receptors
TP	triphosphate
TPA	12- <i>O</i> -tetradecanoylphorbol-13-acetate
TR	terminal repeat
TREX	transcription/export
Tris	tris(hydroxymethyl)aminoethane
tRNA	transfer RNA
U	unit
UIF	UAP56-interacting factor
U <sub>L</sub>	unique long region
uORF	upstream open reading frame
U <sub>s</sub>	unique short region
UTR	untranslated region
UV	ultraviolet
V	volts
v/v	volume per volume
VEGF	vascular endothelial growth factor
vFLIP	viral FLICE inhibitory protein
vGPCR	viral G protein-coupled receptors
VHS	virus host shut-off
vHTS	virtual high-throughput screening
vIL-6	viral interleukin 6
vRNP	viral ribonucleoprotein particle
vTK	viral thymidine kinase
VZV	varicella-zoster virus
w/v	weight per volume
Xbp	X-box binding protein

## **Bases**

A	adenine
C	cytosine
G	guanine
T	thymine

## **Amino acids**

Alanine	Ala	A
Arginine	Arg	R
Asparagine	Asn	N
Aspartate	Asp	D
Cysteine	Cys	C
Glutamate	Glu	E
Glutamine	Gln	Q
Glycine	Gly	G
Histidine	His	H
Isoleucine	Ile	I
Leucine	Leu	L
Lysine	Lys	K
Methionine	Met	M
Phenylalanine	Phe	F
Proline	Pro	P
Serine	Ser	S
Threonine	Thr	T
Tryptophan	Trp	W
Tyrosine	Tyr	Y
Valine	Val	V

# Chapter 1

~

## Introduction

# 1 Introduction

## 1.1 *Herpesviridae*

### 1.1.1 Classification of Herpesviruses

Herpesviruses are a class of viruses with distinct architecture and morphology. The order of *Herpesvirales*, all members of which are related to each other by a very distant common ancestor, comprises of three families: *Herpesviridae*, including all mammalian, avian and reptilian herpesviruses, *Alloherpesviridae*, infecting fish and amphibians, and *Malacoherpesviridae*, which cause disease in invertebrates (Davison et al., 2009). Estimates put the point of evolutionary divergence of the *Herpesvirales* families between 180–200 million and up to 400 million years ago (Davison, 2007). Only three conserved genes have been identified across the *Herpesvirales*, whereas more than 40 genes are conserved across all *Herpesviridae* (McGeoch et al., 2008).

In 1979, the largest of all Herpesvirus families, the *Herpesviridae* was further divided into three subfamilies: *Alpha-*, *Beta-* and *Gammaherpesvirinae* (Figure 1.1) (Matthews, 1979). While the original classification occurred based on biological properties, such as host range, site of infection, cytotoxicity and length in reproductive cycle (Roizmann et al., 1992), more recent developments in genome sequencing now allows classification based on genome comparison (Davison, 2010).

#### 1.1.1.1 *Alphaherpesvirinae*

Herpesviruses belonging to the *Alphaherpesvirinae* subfamily establish latent infection in neuronal cells, primarily sensory ganglia, with lytic replication often occurring in epidermal cells. They distinguish themselves from other subfamilies through a short reproductive cycle and the ability to progress rapidly in cell culture. *Alphaherpesvirinae* also have a variable and broad host range.

Prominent members of the *Alphaherpesvirinae* subfamily include the human pathogens herpes simplex virus type I and II (HSV-1/2) and varicella zoster virus (VZV), also known as human herpesvirus (HHV) type 1, 2 and 3, respectively. Important herpesviruses in animal

virology also belonging to the *Alphaherpesvirinae* include; porcine herpesvirus 1 (*Suid herpesvirus 1*, SuHV-1), which causes pseudorabies in pigs, gallid herpesvirus 2 (GaHV-2), responsible for Marek’s disease in chicken, as well as bovine herpesvirus 1 (BoHV-1), which is known to cause several worldwide diseases in cattle.

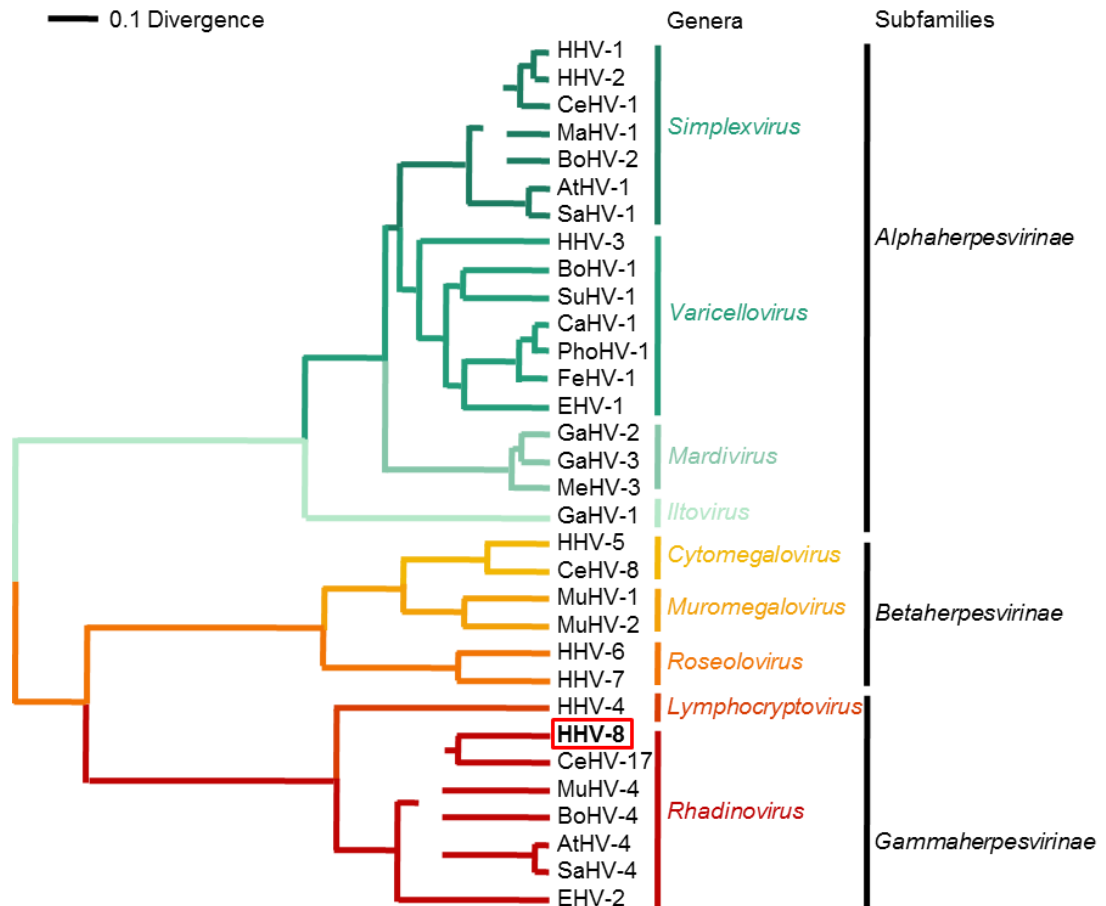


**Figure 1.1: Phylogenetic tree for *Herpesviridae*.** The phylogenetic tree shows the evolutionary relationship of *Herpesviridae* based on amino acid sequence alignments. Adapted from (Strauss and Strauss, 2007).

### 1.1.1.2 *Betaherpesvirinae*

Betaherpesviruses latently infect lymphoreticular cells, secretory glands and kidneys (Strauss and Strauss, 2007). They have a long reproductive cycle, are restricted in their host range and spread very slowly in tissue culture, compared with other members of the *Herpesviridae* family. Cells infected with betaherpesviruses are often found enlarged, forming cytomegaly.

*Betaherpesvirinae* include the human pathogens human cytomegalovirus (HCMV, HHV-5), as well as HHV-6 and HHV-7, both belonging to the *Roseolovirus* genera.

#### 1.1.1.3 *Gammaherpesvirinae*

Latent infection of *Gammaherpesvirinae* occurs in lymphoblastoid cells, with most viruses specific for either T- or B-lymphocytes. Some members of this subfamily are also able to lytically replicate in epithelial cells and fibroblasts. *Gammaherpesvirinae* have a narrow host range and can only infect members of the family or order to which their natural host belongs.

To date, two human gammaherpesviruses are known: Epstein-Barr virus (EBV, HHV-4) and Kaposi's sarcoma-associated herpesvirus (KSHV, HHV-8), belonging to the *Lymphocryptovirus* and *Rhadinovirus* genera, respectively.

#### 1.1.2 Virion architecture

Herpesviruses have a unique architecture and morphology (Figure 1.2), which was previously used to be the distinguishing criteria in their taxonomy. The large, linear, double stranded (ds) DNA genome is packaged into an icosahedral capsid in the form of a torus (Furlong et al., 1972). The capsid is assembled out of 162 capsomers, to form an icosahedron with T = 16 symmetry, with a final size of around 100 nm in diameter. One pentameric capsomere in the capsid is replaced by the so-called portal complex, which allows packaging and release of the genetic material (Cardone et al., 2007; White et al., 2003). The viral capsid is surrounded by the tegument, an amorphous protein coat, consisting of about 20 different viral and cellular proteins, that can vary in thickness. The roles of the tegument are diverse, from host cell shut-off, evasion of host immune response, to capsid transport and envelopment (Kelly et al., 2009; Mettenleiter, 2004). The tegument layer is enclosed by a viral envelope. This envelope consists of a lipid bilayer and contains several viral glycoproteins necessary for host cell binding and membrane fusion

(Mettenleiter et al., 2009). The final size of a virus particle varies from 100–300 nm, due to the difference in tegument thickness.

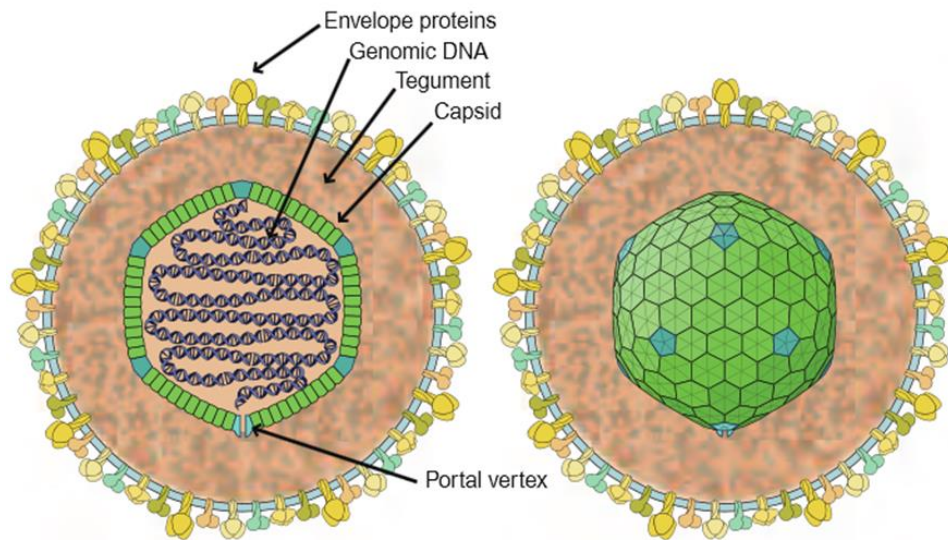


**Figure 1.2: Herpesvirus structure.** Schematic representation of structural components of a herpesvirus particle. Figure taken from *Viral structures and antibodies*, abcam®.

### 1.1.3 Genomic structure

The genome of herpesviruses consist of a single, linear double-stranded DNA, ranging from 125 to 291 kbp in length. The genomic ends contain unpaired nucleotides, which are neither covalently closed nor covalently linked to a protein. The majority of the herpesvirus genome consists of unique sequences, but most viruses also have some repeated sequence elements. These repeated sequences can be  $10^3$ – $10^4$  bp in size and their unique distribution pattern can be used to classify *Herpesviridae* genomes into six distinct types (Figure 1.3). Interestingly, classification of genome type does not correlate with evolutionary relatedness, and all genome types occur throughout the *Alpha-*, *Beta-* and *Gammaherpesvirinae*. Genomes of type A have two identical, large terminal repeat (TR) sequences at either end of the genome. Amongst others, HHV-6 belongs to group A. Herpesviruses of type B, such as KSHV, have genomes with multiple direct repeats at both termini. Type C genomes, as is found in EBV, have similar multiple repeat regions at the end of the genome, but in addition contain several internal repeat (IR) sequences scattered throughout the unique genome region. Genome type D is distinguished by two inverted repeat sequences, one internally and one occurring at a terminus. This creates

the characteristic unique short ( $U_S$ ) and the unique long ( $U_L$ ) sequence in between these repeats. An example of genome type D is VZV. Members of genome group E, such as HSV-1 and 2, also contain  $U_S$  and  $U_L$  sequences; however, here both are flanked by separate inverted repeat domains. In contrast, genomes of type F, exemplified by MCMV-1, do not contain any extended DNA repeat sequences (Roizman et al., 1981).

During evolution, many herpesviruses have acquired pirated genes from their host cells. These cellular homologues help regulate host defence mechanisms and apoptosis, as well as function in immune evasion.

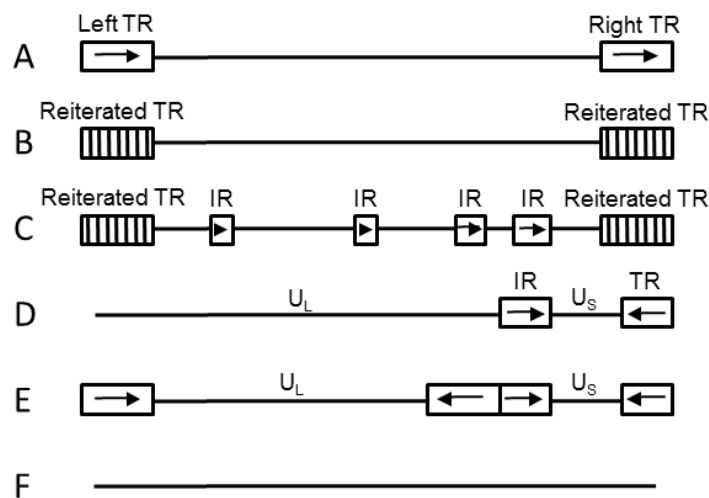


**Figure 1.3: Herpesvirus genome structures.** Schematic representation of the six *Herpesviridae* genome types. Unique regions are shown by lines and repeat domains are represented as boxes. Arrows indicate the orientation of the repeat elements. TR, terminal repeat; IR, internal repeat;  $U_L$ , unique long region;  $U_S$ , unique short region. Adapted from (McGeoch et al., 2008).

#### 1.1.4 Life cycle

The herpesvirus life cycle begins when an infectious virus particle binds to the cell surface. This contact is established through glycoproteins embedded in the virus envelope. The genes for three glycoproteins are conserved across all herpesviruses and accordingly, these three glycoproteins are essential for entry of all *Herpesvirales*: gB, gH and gL. The viral envelope proteins bind to cellular receptors during entry. Some of these receptors function as binding receptors, which increase the concentration of viruses on the cell surface, others are entry receptors, which activate fusion of the viral envelope with the cell membrane (Spear and Longnecker, 2003) (Figure 1.4a). Common cellular receptors are

proteoglycans, such as the glycosaminoglycan heparan sulphate that is responsible for KSHV and HSV-1 binding. However, some herpesviruses require endocytosis to enter cells, with membrane fusion occurring after acidification of the endosomal compartment (Figure 1.4b). The type of entry mechanism is dependent on herpesvirus and cell type. After fusion, the capsid and tegument proteins are released into the cytoplasm of the cell. From here, the uncoated capsid traffics via the microtubule network to the nucleus, where the viral DNA enters through the nuclear pore complex (Shukla and Spear, 2001; Mabit et al., 2002; Naranatt et al., 2005). Once inside the nucleus the viral DNA circularises immediately (Mabit et al., 2002). The virus can then enter one of two distinct life cycles: latency or lytic replication.

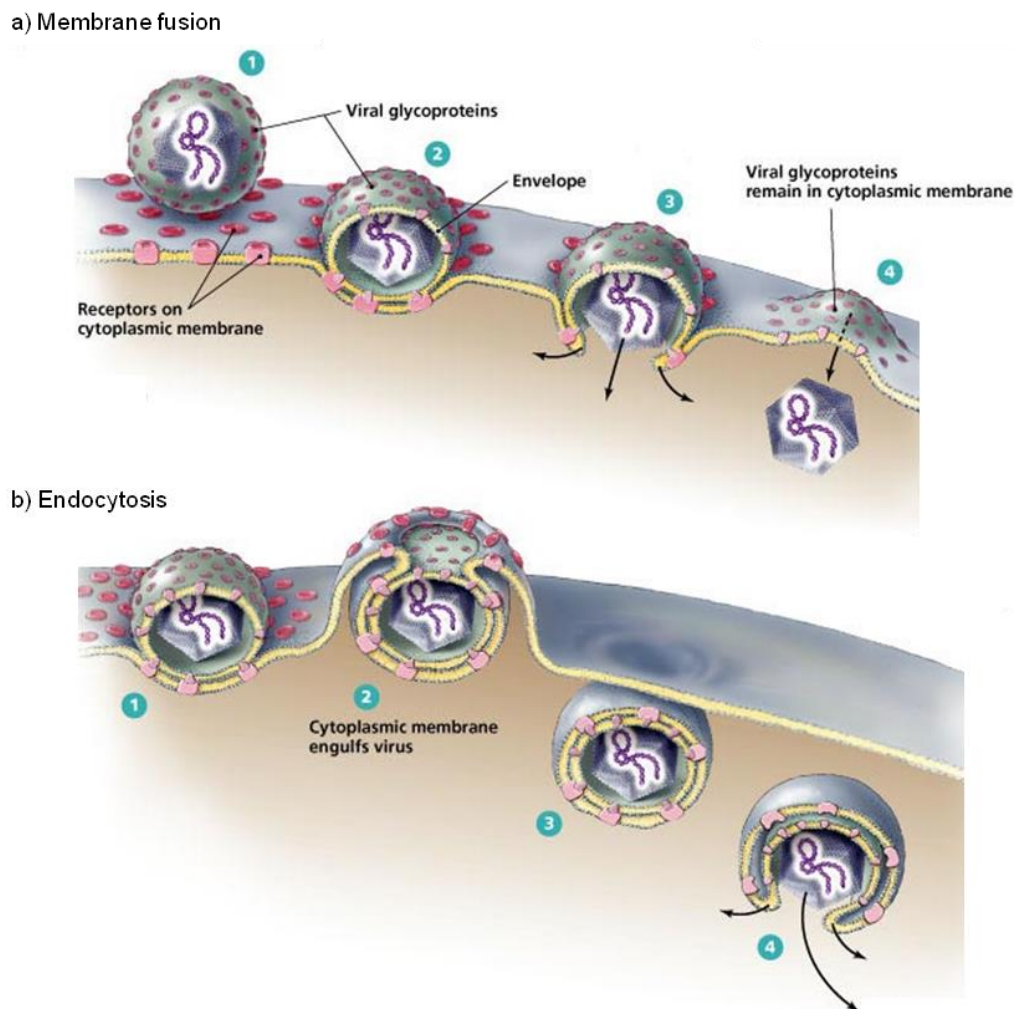


**Figure 1.4: Herpesvirus entry mechanisms.** a) Membrane fusion: (1) Virus particles approach the cell surface. (2) The virus attaches via cell surface receptors, which induces (3) fusion of the viral and cell membrane. (4) The virus capsid and tegument layer are released into the cytoplasm. b) Endocytosis: (1) The virus attaches via cell surface receptors, which induces (2) invagination of the virus into endosomes. (3) Acidification of the endosome leads to (4) membrane fusion and release of the capsid and tegument into the cytoplasm. Taken from (Tortora et al., 2012).

#### 1.1.4.1 Latency

During latency the virus remains in a dormant state with no infectious progeny virions being produced (Werner et al., 1978; Kaschka-Dierich et al., 1982). The viral genome is maintained as a non-integrated episome in the nucleus of the infected cell (Collins and Medveczky, 2002; Griffiths and Whitehouse, 2007). Usually latency is established in a specific cell type dependent on the virus. Only a small number of genes are expressed during latency, producing the so called latency-associated transcripts (LATs). Most of these LATs code for proteins involved in persistence of the viral genome, prevention of apoptosis and immune evasion (Croen, 1991; Friborg et al., 1999).

#### 1.1.4.2 Lytic replication

Reactivation of latent virus leads to lytic replication, the second distinct life cycle all herpesviruses can enter. During lytic replication, an expression cascade regulates the strong increase in viral gene expression: three main temporal phases control the *de novo* protein synthesis (Figure 1.5). All viral genes are transcribed in the nucleus by the host cell RNA polymerase II, whereas translation occurs in the cytoplasm of the host cell after the viral mRNA has been exported. The first viral proteins to be expressed are called immediate early (IE). These are required for the efficient expression of delayed early (DE) genes. DE genes encode proteins that are essential for viral DNA synthesis by the viral DNA polymerase or function in immunomodulation of the host cell. The circular DNA is replicated in a rolling circle manner, producing concatamers which are subsequently cleaved into monomers within the terminal repeat region. In turn, expression of DE genes and DNA synthesis regulates the expression of late (L) genes. Late genes include those coding for structural proteins involved in capsid formation and virion production. The capsid is assembled in the nucleus of the host cell and packages the newly replicated DNA. The capsid matures by budding from the nuclear double membrane, resulting in primary envelopment and de-envelopment of the capsid (Skepper et al., 2001). The tegument layer is then added in the cytoplasm through a series of intricate protein-protein interactions (Mettenleiter, 2002). Finally, re-envelopment and thereby production of mature progeny virions takes place in the cytoplasm. For a long time it was believed that this occurred

through budding into trans-Golgi vesicles, however, a more recent report has also implicated a role for endocytic tubules (Hollinshead et al., 2012). Following secondary envelopment, the infectious virions are released by exocytosis, resulting in lysis of the host cell.

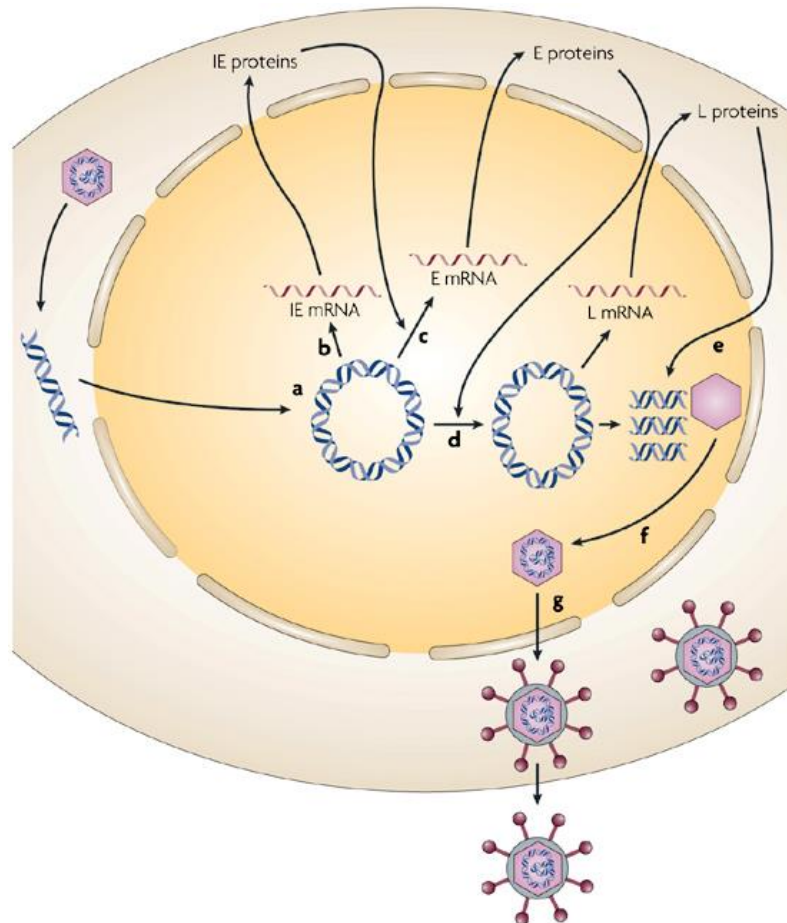


**Figure 1.5: Herpesvirus lytic replication.** a) After infection of the host cell the capsid is transported to nuclear pores, where viral DNA enters the nucleus and circularises immediately. b) Reactivation of the virus causes expression of immediate-early (IE) genes. c) IE gene products promote an expression cascade where delayed-early (E) genes are expressed d) Delayed-early genes are required for viral DNA replication, which in term stimulates late (L) genes expression. e) Structural proteins, encoded by late genes, assemble viral capsids, f) which encapsulate the newly synthesised viral DNA. g) The nucleocapsids travel through the nuclear membrane and acquire their envelope when budding from the golgi, before exiting the cell. Taken from (Knipe and Cliffe, 2008).

## 1.2 The *Gammapesvirinae*

The *Gammapesvirinae* subfamily contains four genera: *Lymphocryptovirus* (gamma-1), *Rhadinovirus* (gamma-2), *Macavirus* and *Percavirus* (Davison et al., 2009). Gamma-

herpesviruses latently infect either B- or T-lymphocytes, however, they undergo lytic replication in epithelial cells or fibroblasts. The genomes of *Gammaherpesvirinae* show a high degree of conservation. They contain a conserved central region, arranged in four gene blocks and interspersed with unique open reading frames (ORFs), which is flanked by a variable number of terminal repeat (TR) sequences. Due to high similarity in orientation and arrangement of core genes in their central sequence, genomes of gamma-herpesviruses are described as co-linear (Albrecht and Fleckenstein, 1990; Nicholas et al., 1992; Russo et al., 1996).

While *Alphaherpesvirinae* establish latency in non-dividing cells, Gamma-herpesviruses undergo latent infection in replicating cells. To ensure propagation of the viral genome during cell division, several copies of the genome are tethered to host mitotic chromosomes (Cotter and Robertson, 1999). Furthermore, *Gammaherpesvirinae* express a number of proteins that function to enhance survival of the host cell, by suppression of apoptosis, subversion of the host immune system and enhancement of cell cycle progression (Friborg et al., 1999; Li et al., 1997; Sarid et al., 1999). Subsequently, through manipulation of host cell mechanisms, many gamma-herpesviruses have the ability to induce neoplasia in their hosts and transform cells in culture (Damania, 2004). Both EBV and KSHV are human gamma-herpesviruses capable of causing cancers and other proliferative disorders.

### **1.2.1 Epstein Barr virus (EBV)**

Over 50 years ago, EBV was identified as the first human oncogenic virus, after the virus was isolated from lymphoblasts cultured from a Burkitt's lymphoma (Epstein et al., 1964). In the following years, EBV has been implicated in a series of malignancies summarised in Table 1.1.

**Table 1.1: EBV associated diseases.**

Associated Malignancy	Name
B-cell lymphoma	Burkitt's lymphoma
	Hodgkin's lymphoma
	Post-transplant lymphoma (PTL)
T-cell lymphoma	Extranodal natural killer/T-cell lymphoma
Carcinoma	Nasopharyngeal carcinoma
	Gastric carcinoma

EBV infection occurs usually asymptotically in early childhood and leads to lifelong persistence of the virus. In contrast, primary infection taking place during adolescence often results in infectious mononucleosis, characterised by flu-like symptoms and severe fatigue. Here, proliferation of B-cells infected with lytic replicating EBV causes a hyperproliferation of T-cells, including EBV-specific CD8<sup>+</sup> cytotoxic T-cells (Callan et al., 1996). While this system-wide response leads to the pathology of infectious mononucleosis, it is a self-limiting process ending with most EBV infected cells cleared after a few weeks. However, some B-cells with latent EBV can avoid immune surveillance and thus, the virus is able to establish a lifelong reservoir. In addition to B-lymphocytes, EBV can also establish an initial infection and replicate in oral epithelial cells, allowing transmission of the virus via contaminated saliva (Kurth et al., 2000; Webster-Cyriaque et al., 2006; Tugizov et al., 2003). As a result, over 90% of the global adult population is seropositive for EBV. Development of malignant diseases following EBV infection is extremely rare and invariably associated with immune suppression; such as through co-infection with human immunodeficiency virus (HIV) or malaria, or after tissue and organ transplants (iatrogenic immune suppression) (Pagano, 2008; Taylor and Blackbourn, 2011).

In contrast to many other herpesviruses, EBV does not attach to the host cell via the proteoglycan heparan sulphate, but utilises the cellular receptor CR2 (also known as CD21), expressed on mature B-lymphocytes by binding of the viral gp350 (Fingerroth et al., 1984). Furthermore, a second glycoprotein, gp42, binds to human leukocyte antigen (HLA) class II molecules, functioning as a co-receptor (Borza and Hutt-Fletcher, 2002). Infection of endothelial cells occurs in a much less efficient manner; however, this distinct pathway is to date poorly understood.

### 1.2.1.1 EBV life cycle

After initial EBV infection, a brief phase of lytic replication occurs, leading to a pool of infectious virions. These can establish a reservoir of latently infected cells, which does not require re-infection through rounds of lytic replication to be maintained. Four distinct EBV latency expression programmes have been described, which are essential for host colonisation and persistence, termed latency 0, I, II and III. After initial infection of naive B-cells, latency III, the broadest of all latency expression programmes, drives proliferation and differentiation in these cells. While many of these infected B-lymphocytes are removed by the primary T-cell response, some are transformed into a proliferating lymphoblastoid cell line (a process called B-cell activation). To avoid host immune responses in healthy individuals, a down regulation of gene expression is induced, giving way to an expression programme known as latency II. A further reduction of expressed proteins and RNAs, leads to latency I. Though this process is highly complicated and not well understood, it is believed that this reduction in EBV transcription takes place during transit through a germinal centre reaction, resulting in EBV-positive memory B-cells (Young and Rickinson, 2004). These resting memory B-cells enter circulation and form the latent reservoir in immunocompetent individuals (Babcock et al., 1998). This state, also known as latency 0, is characterised by almost complete suppression of viral antigen expression (Young and Rickinson, 2004).

While all EBV-induced malignancies are driven by viral latency, the contrasting expression programmes are linked to different diseases (summarised in Table 1.2). Latency I, the most restrictive expression programme associated with a malignancy, is observed in all cases of endemic Burkitt's lymphoma. These tumours are often found in children co-infected with malaria and therefore have a high incidence rate in regions of Africa and New Guinea, in which malaria is holoendemic. Transcription of the EBV genome in latency I is limited to EBNA1 (an EBV-encoded nuclear antigen essential for episomal maintenance) and the Epstein-Barr virus-encoded small RNAs (EBERs), a group of non-coding RNAs (ncRNAs). Latency II, which is found in Hodgkin's lymphoma and EBV-associated carcinomas, such as nasopharyngeal carcinoma and gastric carcinoma, is characterised by expression of EBNA1, the latent membrane proteins (LMP) 1, 2A and 2B, as well as the EBERs and certain virally encoded microRNAs (miRNAs), often referred to as BARTs. LMP1 has anti-apoptotic function, whereas LMP2A and 2B promote cell survival and motility (Huen et al., 1995;

Caldwell et al., 1998). Latency III is characterised by the expression of all EBV-encoded nuclear antigens (EBNA1, 2, 3A, 3B, 3C and leader protein), the LMPs, as well as the EBERs and BARTs (Pagano, 2008; Klein et al., 2007; Speck and Ganem, 2010). As only EBNA1 is able to evade the CD8<sup>+</sup> immune response, whereas some other EBNAs are immunodominant, a healthy immune system is able to suppress development of lymphoproliferative diseases through latency III. Hence this expression programme is only associated with malignancies in severely immunocompromised patients and found in B-cells of post-transplant lymphomas (PTLs) that develop in the absence of effective T-cell surveillance.

**Table 1.2: Overview of EBV latency programmes, their associated malignancies and gene expression profiles.** ncRNAs = non-coding RNAs, miRNAs = microRNAs.

	Latency 0	Latency I	Latency II	Latency III
<b>Associated malignancy</b>	-	Burkitt's lymphoma	Hodgkin's lymphoma & Carcinomas	Post-transplant lymphomas
<b>EBNA-1</b>	-	+	+	+
<b>EBNA-2, 3A, 3B, 3C, LP</b>	-	-	-	+
<b>LMP-1, 2A, 2B</b>	-	-	+	+
<b>EBERs (ncRNAs)</b>	+	+	+	+
<b>BARTs (miRNAs)</b>	-	-	+	+

### 1.2.2 Kaposi's sarcoma-associated herpesvirus (KSHV)

In 1994, herpesvirus-like DNA fragments were first isolated from KS tumours and subsequently identified as a novel human herpesvirus. Thus, KSHV is the eighth and most recently identified human herpesvirus, and one of the currently known seven human oncoviruses.

The viral genome is 138 Kb in length and encodes 87 open reading frames (ORFs), 12 pre-miRNAs expressing 25 mature miRNAs, (Grundhoff et al., 2006; Cai et al., 2005; Pfeffer et

al., 2005), as well as long non-coding RNAs (lncRNAs) (Sun et al., 1996). Furthermore, the existence of another 50 upstream and small ORFs (uORFs and sORFs, respectively) has recently been proposed (Arias et al., 2014). Figure 1.6 displays a genome map of KSHV ORFs.

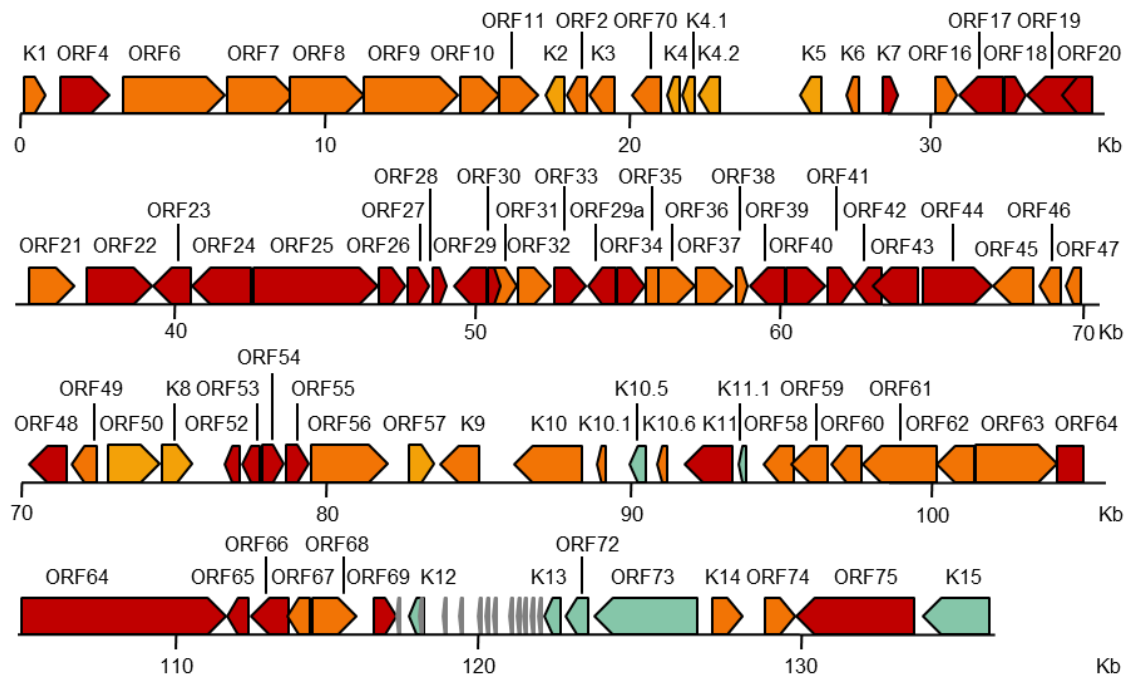


**Figure 1.6: KSHV genome map.** Viral latent genes are shown in teal, early, delayed-early and late lytic genes are shown in shades from orange to red. KSHV encoded miRNA are shown as gray arrowheads. Adapted from (Coscoy, 2007) after data in (Paulose-Murphy et al., 2001) and (Arias et al., 2014).

Unlike EBV, KSHV infection is not ubiquitous across the world's population (Figure 1.7). The prevalence is highest in sub-Saharan Africa, with seropositivity rates of over 50%, but is less common in Mediterranean countries (20–30%) and most of Europe, Asia and the US (less than 10%) (Uldrick and Whitby, 2011). Infectious KSHV virions are shed from oral epithelial cells and hence make transmission via saliva the most common route of infection (Ambroziak et al., 1995; Webster-Cyriaque et al., 2006; Blackburn et al., 1998; Pauk et al., 2000). This is especially important, as this route is thought to be responsible for the high prevalence of childhood infections in certain regions of Africa (Bagni and Whitby, 2009). It has furthermore been reported that transmission can also occur via blood (Whitby et al., 1995; Hladik et al., 2006) and sexual contact (Martin et al., 1998).

However these findings are still subject of discussion (Engels et al., 2007; Martin and Osmond, 2000).

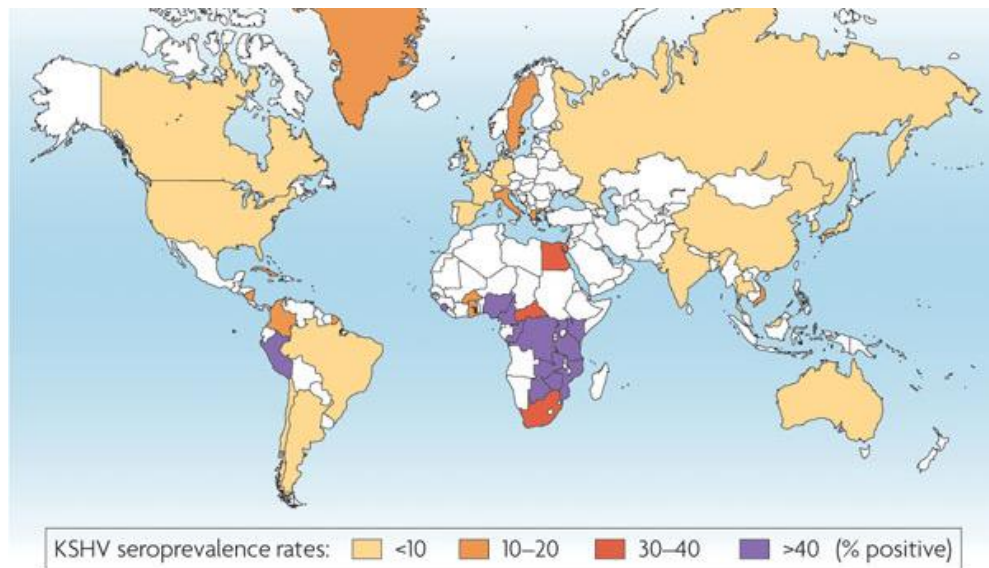


**Figure 1.7: KSHV prevalence worldwide.** A high seroprevalence is visible in sub-Saharan Africa. In contrast, Asia, the US and most part of Europe have low infection rates. No data is available for countries shown in white. Taken from (Mesri et al., 2010).

#### 1.2.2.1 KSHV associated diseases

KSHV was first identified as the aetiological agent of HIV-associated Kaposi's sarcoma (KS) (Chang et al., 1994) and has since been shown to cause all forms of KS. In recent years, KSHV involvement has also been shown in primary effusion lymphoma (PEL) (Cesarman et al., 1995) and multicentric Castleman disease (MCD) (Soulier et al., 1995).

##### 1.2.2.1.1 Kaposi's sarcoma (KS)

KS was first described by the Hungarian dermatologist Moritz Kaposi in 1872 (Kaposi, 1872). Due to the geographically constrained distribution of KS incidents (Oettle, 1962) and the association with immune suppression (Penn, 1978), it was suggested well before the first KS epidemic occurred that the tumours might be caused by an infectious agent. With the onset of the AIDS epidemic in 1989, KS morbidity increased drastically: Studies showed more than 15% of people in the US infected with AIDS also reported with KS (Beral

et al., 1990). This epidemic-like morbidity and the high mortality of KS led to intense research into the etiology of KS, which ultimately resulted in the identification of herpesvirus DNA fragments in KS biopsies and subsequently the discovery of KSHV (Chang et al., 1994).

Even though the introduction of effective anti-retroviral therapies led to a decrease in the occurrence of KS, tumours have been reported in individuals with well controlled HIV (Grulich et al., 2001; Maurer et al., 2007). Furthermore, as KS has become one of the most common cancers in sub-Saharan Africa (termed endemic KS) (Parkin et al., 2008), many people in resource poor countries are still greatly affected by KSHV (Figure 1.8).

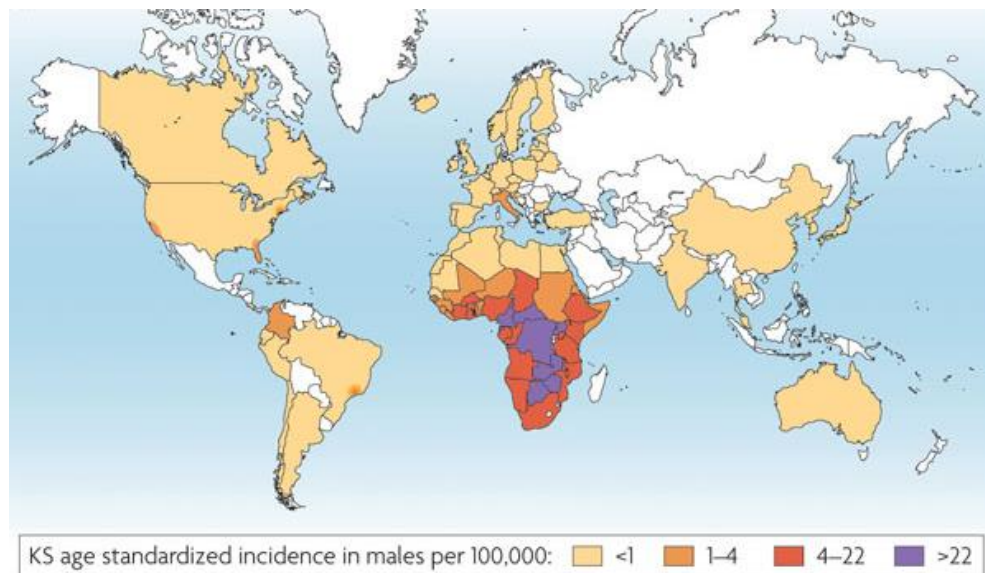


**Figure 1.8: Kaposi's sarcoma incidence rate worldwide.** Concurrent with the high seroprevalence and HIV-epidemic a high KS incidence rate is visible in parts of Africa. No data is available for countries shown in white. Taken from (Mesri et al., 2010).

In addition to AIDS-associated KS, patients receiving organ transplants or chemotherapy are also at a higher risk of developing so called iatrogenic KS, due to immune suppression. While healthy individuals are less likely to be affected by the onset of KS, the so called classic KS commonly affects elderly men from the Mediterranean. However, opposed to the aggressive forms of cancer found in AIDS-associated or iatrogenic KS, which spreads rapidly to internal organs and lymph nodes (Ganem, 2010), classic KS tumours are usually benign.

KS presents itself as a spindle cell tumour of endothelial origin, which is highly vascularised. These microvascular channels fill with blood and give KS skin lesions their characteristic dark appearance. Through its association with the infectious agent KSHV, KS tumours progress and regress based on the host immune system and as such withdrawal of immunosuppressive medication (in iatrogenic KS) or treatment with HAART (in AIDS-associated KS) can lead to a remission of the skin lesions.

Several KSHV genes expressed in tumour cells exhibit direct pro-oncogenic activities by inhibiting the tumour suppressor genes p53 and Rb, and inducing NF- $\kappa$ B (Cai et al., 2010; Mesri et al., 2010). Viral proteins, especially the products of “pirated” host cell genes, subvert cell signalling pathways and lead to the expression and secretion of pro-inflammatory, angiogenic and proliferative cytokines (Ballon et al., 2011; Bottero et al., 2011). This effect is aggravated by KS tumour cells expressing receptors for these cytokines on the cell surface and thereby creating an autocrine signalling system (Hengge et al., 2002).

In contrast to EBV, where all malignancies are associated with viral latency, both latent and lytic replication cycles are indispensable for KS occurrence (Ye et al., 2011). For example, only lytic replication allows dissemination of infectious virions from the B-cell reservoir into the blood stream allowing infection of other cells types, including endothelial cells. Furthermore, while the majority of tumour cells are latently infected, sporadic rounds of lytic replication are essential for maintenance of the viral episome in endothelial cells (Staskus et al., 1997). Finally, in addition to the pro-oncogenic activities of latent gene products, lytic proteins also contain tumourigenic properties (Figure 1.9).

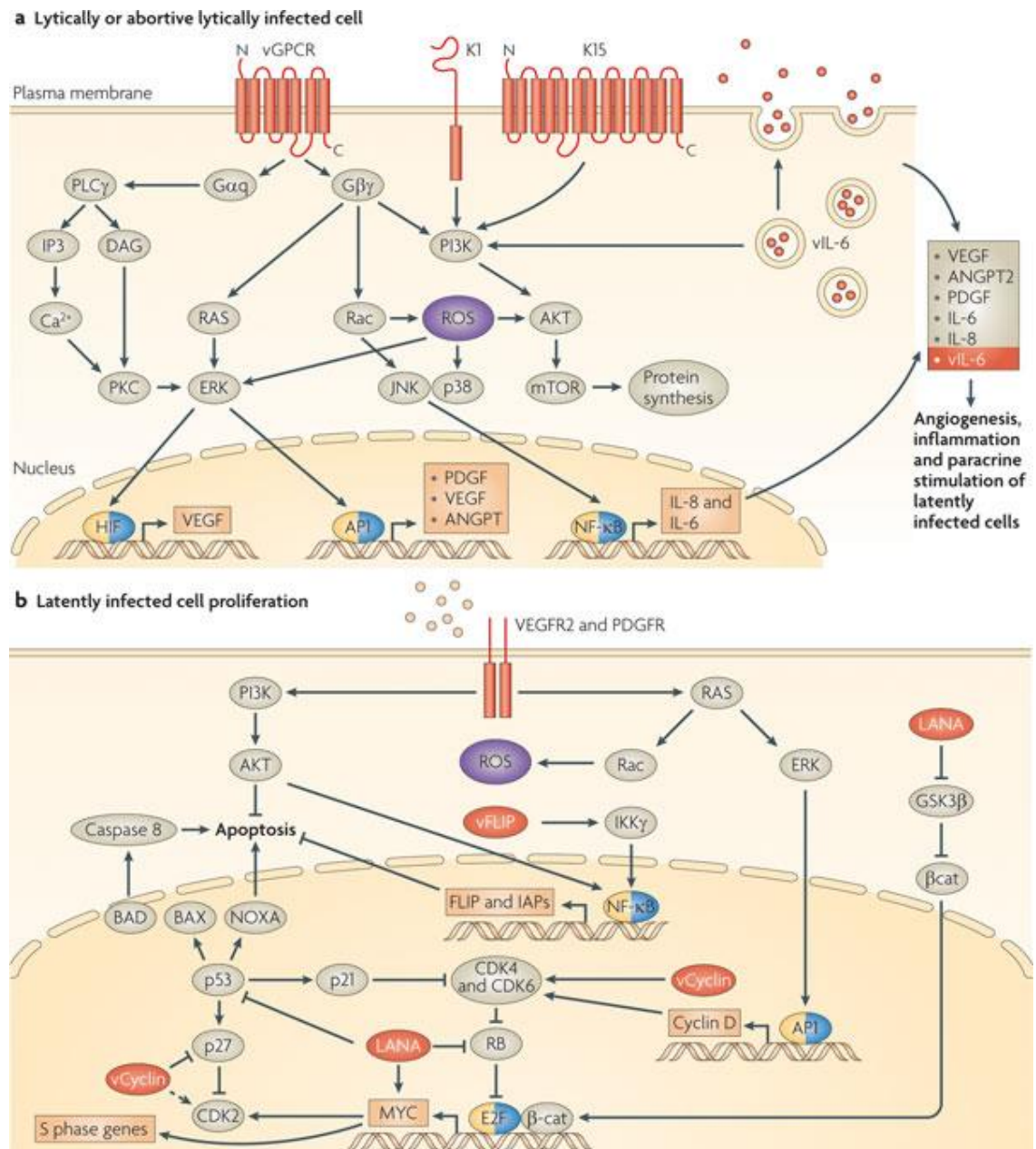


**Figure 1.9: Proposed mechanism of KSHV-induced sarcoma.** a) The early lytic genes vGPCR, K1, vIL-6 and K15 (shown in red) manipulate host cell signalling pathways, leading to the expression and secretion of inflammatory, angiogenic, proliferative cytokines (including, vascular endothelial growth factor (VEGF), platelet-derived growth factor- $\beta$  (PDGF $\beta$ ), angiopoietin 2 (ANGPT2), IL-6 and IL-8). b) Secreted factors from lytic cells in turn act on receptors in latently infected cells through a paracrine mechanism. Together with direct pro-oncogenic activities of KSHV latent genes, such as vFLIP, vCyclin and latency-associated nuclear antigen (LANA), as well as the KSHV-encoded microRNAs, this enhances the tumourigenic potential of KSHV infection. Taken from (Mesri et al., 2010).

#### 1.2.2.1.2 *Primary effusion lymphoma (PEL)*

PEL, originally called body cavity based lymphoma, is a rare non-Hodgkin's lymphoma mostly affecting patients with end stage AIDS. During PEL, transformed, proliferating B-cells enter serosal cavities of the body, such as the pleura, pericardium, and peritoneum, where they establish lymphomatic growth. To date, no effective treatment against PEL is known and as such, survival rates are very poor, with a median of 6 months after diagnosis (Chen et al., 2007; Boulanger et al., 2005). All tumour cells contain several copies of the KSHV genome, are fully immortalised and grow readily in culture (Ganem, 2007). PEL-derived cell lines are commonly used in the laboratory, as they present a useful tool to study KSHV *in vitro* (Pagano, 2008).

#### 1.2.2.1.3 *Multicentric Castleman disease (MCD)*

MCD is a rare disease, characterised by extreme hyperproliferation of lymphoid tissue which frequently spread to multiple organs as the disease progresses. Most cases of MCD are associated with AIDS, however, MCD is also known to occur in HIV-negative individuals. In AIDS patients, co-infection of HIV and KSHV is found in 100% of cases, whereas in non-HIV infected individuals only 40% of MCD cases are associated with KSHV infection (Soulier et al., 1995). While the involvement of KSHV in the development of MCD is still poorly understood, a link might involve the "pirated" KSHV-gene coding for the IL-6 homologue, vIL-6. It is proposed that lymphoproliferation in MCD occurs via an IL-6 mediated pathway and high levels of IL-6 are often found in tumour cells (Oksenhendler et al., 2000). It is therefore speculated that vIL-6 contributes to the development of MCD.

#### 1.2.2.2 KSHV life cycles

Initial infection with KSHV occurs via attachment of the virus to the host cell plasma membrane. Adhesion is facilitated by the viral glycoproteins K8.1, gB, gH and gL, that bind to cell surface receptors. Specifically, K8.1 and gB interact with the proteoglycan heparan sulphate (Birkmann et al., 2001), while gB also interacts with the integrin  $\alpha 3\beta 1$  (Akula et

al., 2002). Furthermore, the glycoproteins gB, gH and gL are also important for mediating membrane fusion. Additional interactions with co-receptors and integrins on the cell surface are believed to take place prior to fusion of the viral envelope with the plasma membrane, allowing infection of different cell types (Garrigues et al., 2008; Kaleeba and Berger, 2006; Rappocciolo et al., 2006; Pagano, 2008).

After KSHV has entered a host cell and inserted its genome into the host cell nucleus, primary infection is cleared through a cytotoxic T-cell response. However, virus which has established the latent state in B-cells is able to escape this host response, allowing persistence in infected individuals (Wang et al., 2001).

#### 1.2.2.2.1 Latency

The KSHV genome circularises rapidly after entering a cell and is maintained as a non-integrated episome in the nucleus of the infected host cell (Collins and Medveczky, 2002; Griffiths and Whitehouse, 2007). Only seven KSHV genes are expressed during latency, which are referred to as latency-associated transcripts (LATs). Three of these genes are transcribed from the same locus as a polycistronic mRNA undergoing alternative splicing, as well as translation initiation to produce LANA (*ORF73*), v-cyclinD (*ORF72*) and vFLIP (*K13*) (Jeong et al., 2004; Dittmer et al., 1998).

The viral latency-associated nuclear antigen (LANA) is responsible for attaching the circular viral episomes to the host chromosome during mitosis, allowing even distribution and maintenance of the KSHV episome upon B-cell division (Figure 1.10) (Ballestas et al., 1999). Furthermore, LANA facilitates KSHV genome replication during latency, by binding to the *ori-P* and recruiting it to the nuclear matrix, where the cellular DNA replication machinery assembles in a cell cycle-dependent manner (Ohsaki et al., 2009). LANA has also been reported to influence expression of cellular and viral genes through transcriptional regulation mechanisms (Ballestas et al., 1999; Renne et al., 2001). Furthermore, an interaction with p53 and subsequent inhibition of the tumour suppressor protein has also been described (Friborg et al., 1999), suggesting LANA-mediated modulation of cell cycle control and cell growth mechanisms. KSHV v-cyclinD is the viral homologue of cyclinD and as such able to perform similar cellular functions. While it is able to deregulate the cell

cycle through interaction with cdk6 and phosphorylation of the retinoblastoma protein (Rb) (Godden-Kent et al., 1997), it is less responsive to cdk inhibitors p21, p27 and p16. Recently, v-cyclinD has also been shown to functionally cooperate with vFLIP: this viral homologue of the FLICE-inhibitory protein (FLIP) is known to inhibit apoptosis through activation of NF- $\kappa$ B (Liu et al., 2002; Matta et al., 2003). Specifically, although vFLIP-dependent activation leads to p21 and p27 overexpression and subsequent G1 cell cycle arrest, v-cyclinD prevents this senescence through degradation of p27 (Zhi et al., 2014). Therefore, through its ability to resist p21/p27 inhibition and degrade p27, v-cyclinD can contribute to permanent vFLIP-dependent NF- $\kappa$ B activation.

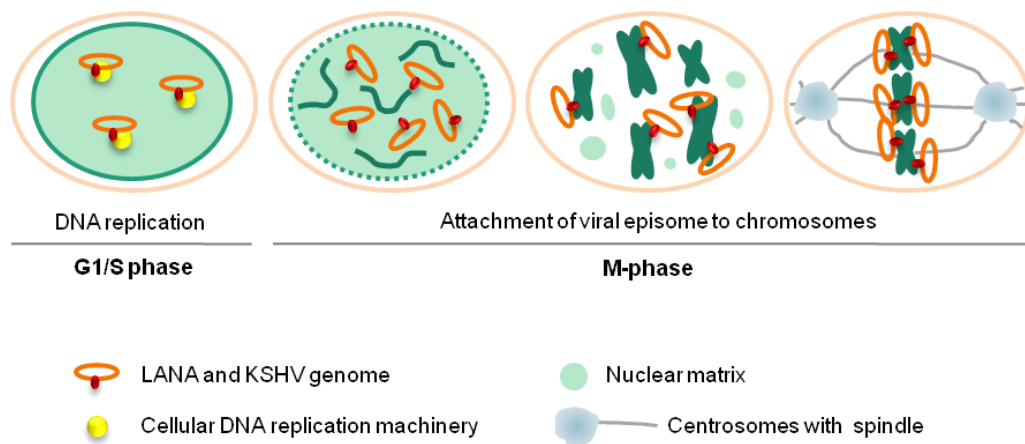


**Figure 1.10: Schematic of KSHV genome segregation during mitosis.** The viral protein LANA facilitates viral latent DNA replication by recruiting the *ori-P* to the nuclear matrix, where the cellular DNA replication machinery is assembled. LANA then functions to attach the viral episome to host chromosomes during mitosis to ensure even distribution of viral genome during cell division. Adapted from (Ohsaki and Ueda, 2012).

The four other proteins expressed during latency include the Kaposin transcripts (A, B and C from the *K12* locus), which are also expressed during lytic replication. Kaposin A has been shown to stabilise cellular cytokine transcripts and has transforming potential (Muralidhar et al., 1998), whereas Kaposin B has been implicated in activation of the proto-oncogene *STAT3*, causing chronic inflammation characteristically found in KS (McCormick and Ganem, 2005; King, 2013). Similarly, the latent and lytic protein LAMP is also associated with generating an inflammatory environment (Pietrek et al., 2010). Another latent protein, vIRF2, is able to act like its cellular homologues and thereby deregulate mechanisms controlled by interferon regulatory factors (IRFs) (Burysek et al., 1999). Finally, the last latently expressed protein is B-cell specific: LANA2 (or vIRF3) is

known to interact with p53 and thereby regulates antiviral mechanisms as well as apoptosis (Rivas et al., 2001).

KSHV latently infected cells also express viral miRNAs. While they are believed essential for maintenance of latency (Cai et al., 2005), their function is still not fully elucidated.

#### *1.2.2.2.2 Lytic replication*

External stimuli, such as a suppressed immune system, inflammation or stress stimuli can cause reactivation of the virus from the latent state, allowing entry into the lytic life cycle. The precise mechanisms of this process are yet to be completely understood. However, the role of the regulator of transcription activation (RTA, expressed from *ORF50*), which functions as the viral latent/lytic switch protein, has been established. Expression of RTA alone is sufficient to induce KSHV lytic replication (Lukac et al., 1998; Lukac et al., 1999). Following reactivation and expression of RTA, the temporal cascade of gene expression is activated, culminating in assembly, egress and finally budding of infectious KSHV virions from B-cells (as described before under 1.1.4.2).

Hypoxia is known to cause KSHV reactivation via a RTA response. During this process, transcription factors, called hypoxia-inducible factors (HIFs), bind to the RTA promoter and induce RTA expression, subsequently inducing KSHV lytic replication (Davis et al., 2001; Haque et al., 2003). Hypoxia also activates the X-box binding protein 1 (XBP-1), which can in turn transactivate the RTA promoter (Dalton-Griffin et al., 2009). Moreover, XBP-1 is induced upon B-cell differentiation, which is also believed to initiate reactivation of the virus (Wilson et al., 2007). A further cell stimuli involved in the induction of KSHV lytic replication is signalling of the inflammatory cytokine interferon-gamma (IFN- $\gamma$ ) (Blackbourn et al., 2000). KSHV reactivation can also be initiated by co-infection with other herpesviruses, such as HSV-1 and CMV (Qin et al., 2008; Vieira et al., 2001). The HIV-1 transactivator Tat is also able to induce expression of RTA and thereby KSHV lytic replication (Zeng et al., 2007). Furthermore, activation of toll-like receptor signalling, which occurs during innate immune response to some viral infections, has been implicated in KSHV reactivation (Gregory et al., 2009).

The expression of the *ORF50* gene leads to the presence of RTA, the first protein following KSHV reactivation (Sun et al., 1998; Sun et al., 1999). RTA functions as a viral transactivator that can initiate gene expression through three distinct mechanisms: direct, indirect and via its E3 ubiquitin ligase activity (Figure 1.11).

RTA is a transcription factor that is able to directly bind multiple promoters using a consensus RTA response element (RRE) (Goodwin and Whitehouse, 2001). The C-terminal domain of the protein contains the transcriptional activation domain, similar to that of many cellular transcription factors (Lukac et al., 1999), whereas the N-terminus facilitates binding to DNA (Song et al., 2001). RTA is also able to induce itself in a positive feedback loop (Deng et al., 2000).

While RTA activates many genes containing the RRE, such as the polyadenylated nuclear (PAN) RNA promoter, it is also known to induce expression of genes lacking this sequence, such as *ORF57*, via an indirect mechanism. While these interactions are generally weaker, RTA recruits cellular transcription factors, namely Rbp-jk (Liang et al., 2002), C/EBP $\alpha$  (Wang et al., 2003) and AP-1 (Wang et al., 2004a) to enhance the effect. Once RTA promoter binding has occurred, efficient recruitment of the transcription machinery occurs, enabling RNA polymerase II (RNAP II) to transcribe the immediate early (IE) genes and promoting the gene expression cascade. Hence, RTA expression is sufficient to initiate a cascade of events leading to the production of infectious virions.

In addition to its role as transcription factor, RTA has intrinsic E3 ubiquitin ligase activity (Yang et al., 2008). This enables RTA to target cellular and viral proteins for proteasomal degradation. Specifically, RTA is known to degrade the transcriptional repressor Hey1 through a ubiquitination-mediated process (Gould et al., 2009). This leads to upregulation of RTA expression and lytic replication, as Hey1 occupies the *ORF50* promoter to inhibit RTA protein production during latency.

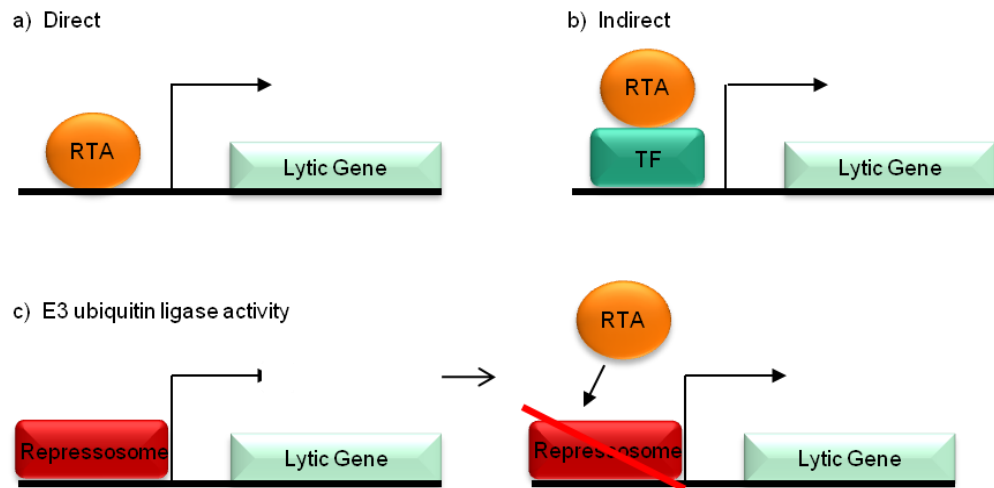


**Figure 1.11: RTA-mediated transactivation mechanisms.** a) RTA can act directly as a transcription factor, binding to the RRE. b) RTA can act indirectly, by recruiting cellular transcription factors (TF) onto viral promoters lacking the RRE. c) Through its E3 ubiquitin ligase activity, RTA can degrade transcriptional repressor, upregulating the target gene expression.

RTA is also involved in lytic DNA replication, through binding of the lytic origin of replication (*ori-Lyt*) via a conserved RRE (Wang et al., 2004b; AuCoin et al., 2002). Together with the viral protein K-bZIP, RTA facilitates formation of a replication initiation complex. These large, multi-protein complexes form distinct, globular replication compartments within the nucleus that are associated with sites of DNA synthesis during lytic replication (Wu et al., 2001). The viral DNA is replicated via a rolling-circle mechanism and subsequently cleaved into monomers within the TR region, which leads to an approximately 100-fold increase of viral DNA copy numbers within the cell during the lytic cycle.

Alongside RTA, the second immediate-early protein essential for lytic replication is encoded by the *ORF57* gene. ORF57 is a multifunctional protein involved in all stages of viral RNA processing, particularly mRNA export. To highlight the role of ORF57, the basic concept of mammalian mRNA export will first be explored, before describing ORF57 and its function in KSHV lytic replication and KSHV-mediated diseases (section 1.5).

### 1.3 Cellular mRNA export

Eukaryotic cells are characterised by compartmentalisation, with physical boundaries separating organelles, which perform different biological functions. This has several advantages, such as the ability to maintain a specific micro-environment and to keep macromolecules within a region or exclude them when they are not required. However, this spatial separation necessitates specific transport mechanisms to be present, which in turn allows for regulatory and quality control pathways to be incorporated. Such is the case with mRNAs, which are produced in the nucleus, but must be exported into the cytoplasm for translation to take place. The export pathway is tightly coupled to specific maturation processes that turn a precursor mRNA (pre-mRNA) into an export competent mRNA. Unsuccessful pre-mRNA processing results in nuclear retention and degradation, preventing faulty mRNAs from being used as templates for translation (Fasken and Corbett, 2009; Hilleren et al., 2001; Brodsky and Silver, 2000; Lei and Silver, 2002; Libri et al., 2002; Zenklusen et al., 2002). In contrast, successful maturation through splicing and 5'- and 3'-end processing leads to a stepwise assembly of all RNA binding protein complexes required for efficient mRNA export.

#### 1.3.1 Cellular mRNA processing

The first mRNA processing step occurs concurrent to transcription, after just 25–30 nucleotides have been added to the growing pre-mRNA. The 5'-end of the nucleic acid is protected from 5'-3' degradation, by a so called cap structure (Figure 1.12). The cap consists of a guanine nucleotide which is added to the 5'-end via an unusual 5'-5' linkage. After addition, the guanine is then methylated to create a 7-methyl-guanine ( $m^7G$ ) cap.

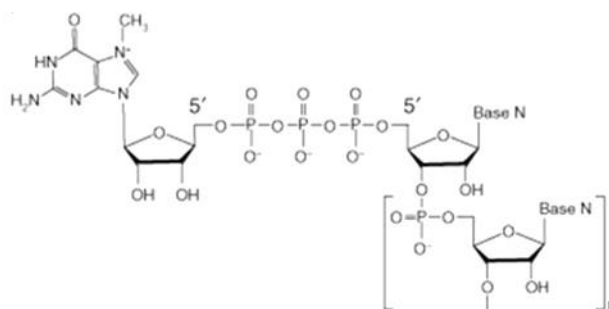


**Figure 1.12: Structure of the mRNA 5'-cap.** Taken from (Gu and Lima, 2005).

Next, the pre-mRNA undergoes splicing. During this process introns of the nascent transcript are removed and the exons are ligated together. The spliceosome, which facilitates this procedure, contains approximately 125 different proteins and several small nuclear RNAs (snRNAs) (Hocine et al., 2010). Each of the snRNAs is part of a ribonucleoprotein particle (RNP), which catalyses the splicing process. In addition to performing excision and ligation of the pre-mRNA, the spliceosome also has to negotiate the site of splicing, as transcripts often present multiple splicing sites in order to generate several proteins from one gene. Additional SR (serine/arginine-rich) proteins are often involved into this process (Long and Caceres, 2009).

Finally, 5'-capped and spliced pre-mRNA is polyadenylated at the 3'-end to generate mature mRNA. A poly(A) tail protects the mRNA from degradation and is required for recognition as mature mRNA by cell surveillance mechanisms, allowing export and translation initiation (Doma and Parker, 2007). The polyadenylation process is again subject of a multiprotein complex, comprising about 85 proteins (Shi et al., 2009). This complex recognises polyadenylation signals transcribed in the 3'-end and cleaves the mRNA 10–30 nucleotides downstream of this signal, before the poly(A) tail is added. Both, aberrant polyadenylation as well as hyperadenylation are associated with retention of the mRNA in the nucleus and subsequent degradation.

### **1.3.2 The human transcription/export (hTREX) complex**

Cellular bulk mRNA export is facilitated by the human transcription/export (hTREX) complex, which allows recruitment of the export receptor Nxf1 (TAP) and Nxt1 (p15) onto mature mRNA and subsequent shuttling through the nuclear pore (Reed and Hurt, 2002; Aguilera, 2005; Kohler and Hurt, 2007). Several studies employing model organisms have shown the TREX complex to be highly conserved across plants, yeast and higher eukaryotes (Reed and Hurt, 2002; Reed and Cheng, 2005; Cullen, 2003; Stutz and Izaurralde, 2003). All known components of hTREX are listed in Table 1.3.

**Table 1.3: Known components of hTREX.** Taken from (Schumann et al., 2013).

<b>hTREX Component</b>	<b>Alternative Name</b>	<b><i>S. cerevisiae</i> Ortholog</b>	<b>Known Interactions in hTREX</b>
<b>UAP56</b>	BAT1, DDX39B	Sub2	Aly, CIP29 (Dufu et al., 2010), Chtop (Chang et al., 2013), UIF (Hautbergue et al., 2009), THO (Masuda et al., 2005)
<b>DDX39</b>	URH49, DDX39A	Sub2	Aly (Golovanov et al., 2006), UIF (Hautbergue et al., 2009), CIP29 (Yamazaki et al., 2010)
<b>Aly</b>	Ref, Alyref, Thoc4, Bef	Yra1	UAP56 (Taniguchi and Ohno, 2008), Chtop (Chang et al., 2013), Thoc5, Thoc2 (Chi et al., 2013)
<b>CIP29</b>	HCC1, Tho1, Sarnp	Tho1	UAP56 (Dufu et al., 2010)
<b>UIF</b>	-	-	UAP56 (Hautbergue et al., 2009)
<b>Chtop</b>	SRAG, CAO77 FOP	-	UAP56, Aly (Chang et al., 2013)
<b>SKAR</b>	pDIP3, PoDIP3	-	(Folco et al., 2012)
<b>ZC11A</b>	ZC3H11A	-	(Folco et al., 2012)
<b>Thoc1</b>	Hpr1, p84	Hpr1	Part of THO (Chi et al., 2013)
<b>Thoc2</b>	Tho2	Tho2	Aly, Part of THO (Chi et al., 2013)
<b>Thoc5</b>	fSAP79, Fmip	-	Aly, Part of THO (Chi et al., 2013)
<b>Thoc6</b>	fSAP35, WDR58	-	Part of THO (Chi et al., 2013)
<b>Thoc7</b>	fSAP24	-	Part of THO (Chi et al., 2013)
<b>Tex1</b>	Thoc3	Tex1	Part of THO (Chi et al., 2013)
<b>ELG</b>	-	-	(Dufu et al., 2010)
<b>ERH</b>	DROER	-	(Dufu et al., 2010)

#### 1.3.2.1 Assembly and function of the hTREX complex

As mRNAs differ greatly in length, structure and sequence, assembly of the hTREX complex has to be independent of these features and is instead coupled to the above mentioned steps of mRNA biogenesis. In 1999, research first showed that splicing events are linked to

mRNA export from the nucleus (Luo and Reed, 1999). Subsequently, two core proteins of the hTREX complex, the export adaptor Aly and the conserved RNA helicase UAP56, have been implicated in both processes (Zhou et al., 2000; Luo et al., 2001). UAP56, which is involved in spliceosome assembly, interacts with Aly directly during spliceosome formation and recruits the export adaptor onto the spliced mRNP. UAP56 is then believed to play a major role in assembly of the remaining hTREX complex, whereas Aly functions later to mediate binding of the export receptor Nxf1.

In yeast, a synergy of 3'-end processing and mRNA export has also been demonstrated. Here, the Aly homologue Yra1 is bound by the polyadenylation factor Pcf11 at the same binding site used by Sub2, the UAP56 homologue, suggesting mutually exclusive interactions (Johnson et al., 2009b). Furthermore, a RNA- and ATP-bound Sub2 is able to displace Pcf11 from its interaction with Yra1, allowing Pcf11 to bind Clp1, a subunit of the cleavage-polyadenylation factor CF1A (Johnson et al., 2011). This interaction of Pcf11 and Clp1 is essential for a functioning polyadenylation complex, whereas Sub2 binding of Yra1 is necessary for TREX formation, successfully coupling both processes. As the interaction of Aly and Pcf11 is conserved in metazoans (Johnson et al., 2009b), a similar combination of both processes can easily be imagined occurring in humans.

Finally, hTREX is associated with the 5'-end of the mRNA (Figure 1.13). Localisation is determined by a direct interaction of Aly and the cap binding protein 80 (CBP80), a component of the cap binding complex (CBC) (Cheng et al., 2006; Chi et al., 2013; Lejeune et al., 2002). As such, uncapped transcripts are poorly exported (Cheng et al., 2006), highlighting again the cooperation between mRNA processing and export.

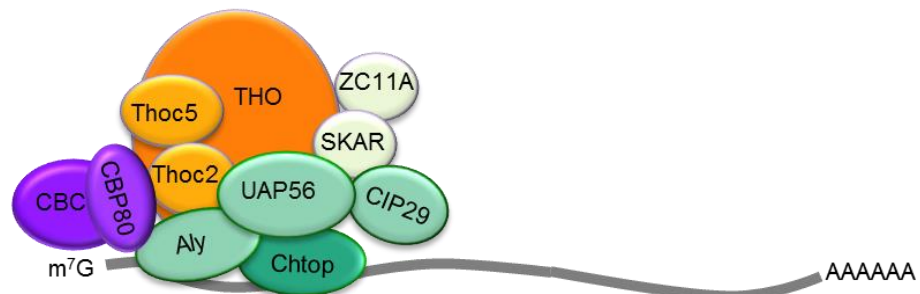


**Figure 1.13: The hTREX complex associates to the 5'-end of mRNA via an interaction with the cap binding complex.** All components of hTREX are shown with their known interaction partner. Modified from (Schumann et al., 2013).

The THO complex, a sub-complex of hTREX formed by a number of closely-associated proteins, also binds CBP80 and is believed to bridge the interaction to UAP56 (Dufu et al., 2010). However, recent contrary reports indicated THO might only associate with Aly and not UAP56 (Chi et al., 2013). In this study, direct interactions were detected between the THO components, Thoc2 and Thoc5, with Aly. These contradicting results of two independent studies highlight the complexity of working with a dynamically remodelled multi-protein complex. While a clear role has been given to THO in yeast, coupling transcription to mRNA export, metazoan THO subunits remain comparably poorly understood. In yeast, THO binding of the nascent mRNA during transcription has been shown, which enables the recruitment of the remaining TREX complex after mRNA binding (Strässer et al., 2002). No such link between transcription and export is found in metazoans and knockdown of THO subunits only results in a minor export block, with the vast majority of mRNAs still exported (Rehwinkel et al., 2004).

In contrast, UAP56 is thought to be responsible for the recruitment and assembly of hTREX in metazoans. The DExD-box RNA helicase shows ATPase activity *in vitro*, a process now believed essential for complete assembly of the hTREX complex. ATP-dependency of hTREX was first shown for the interaction of Aly and hTREX component CIP29 (Dufu et al., 2010). CIP29 was first identified after analysis of hepatocellular carcinoma cell proteome and has been implicated in several other studies in connection with cancer (Choong et al., 2001; Fukuda et al., 2002; Hashii et al., 2004). However, bioinformatic predictions showed an N-terminal SAP domain and sequence homology to a variety of heterogeneous nuclear ribonucleoproteins (Choong et al., 2001). Following this, recent proteomic-based research has identified CIP29 as a new putative member of the hTREX complex, where it forms a trimeric complex with Aly and UAP56 (Dufu et al., 2010).

An interaction of CIP29 and the UAP56 paralogue DDX39 has also been previously described (Sugiura et al., 2007). It was proposed that together, CIP29 and DDX39 form part of an export complex targeting a functionally distinct subset of mRNAs compared to the hTREX complex (Yamazaki et al., 2010). DDX39 shares 90% sequence identity and 96% sequence similarity with UAP56 and has also been shown to interact with Aly (Golovanov et al., 2006). While redundant and overlapping functions of DDX39 and UAP56 have been reported, the export complex formed around DDX39 was termed AREX (alternative mRNA export) (Yamazaki et al., 2010). Knock-down of both UAP56 and DDX39 together were

found to eliminate cellular bulk mRNA export, whereas loss of DDX39 or UAP56 individually were found to cause distinct mitotic defects, consistent with each helicase targeting specific groups of mRNAs (Yamazaki et al., 2010). However, the function of DDX39 still remains poorly studied in the context of hTREX and cellular mRNA export and further work is required to clarify the individual roles of UAP56 and DDX39.

UAP56 is not the only hTREX component for which redundancy has been shown. The serine/arginine rich proteins (SR proteins) 9G8, SRp20 and SF2/ASF can also bind the export receptor Nxf1, recruiting it onto spliced mRNA (Huang et al., 2003). Furthermore, UIF (UAP56 interacting factor) bridges the interaction of UAP56 with Nxf1, making Aly redundant (Hautbergue et al., 2009). Depletion of Aly or UIF individually only causes a minor inhibition of mRNA export, however, double knock-down causes a severe block in mRNA export, showing a phenotype similar to UAP56/DDX39 knock-down.

More recently, another novel hTREX component has been identified by proteomics studies of the immunopurified complex: Like CIP29, Chtop was also found to bind to UAP56 in an ATP-dependent manner (Chang et al., 2013). However, while CIP29 binds UAP56 concurrently with Aly, Chtop binding can be outcompeted by the presence of Aly. Both Aly and Chtop bind the mRNA, which is essential for mRNA export. Interestingly, this process is facilitated by UAP56 and can be prevented *in vitro*, if UAP56 is incubated with a non-hydrolysable ATP analogue. Furthermore, Chtop, Aly and CIP29 have been shown to stimulate UAP56 ATPase activity *in vitro*. It seems therefore likely, that UAP56 loads Chtop and Aly sequentially onto mRNA and facilitates hTREX assembly in an ATP-cycle dependent manner (Figure 1.14).

Finally, the proteins SKAR and ZC11A have also been identified as hTREX components. Both have been shown to interact with UAP56 in an ATP-dependent manner and function in mRNA export, however, their individual roles remain to be fully elucidated.

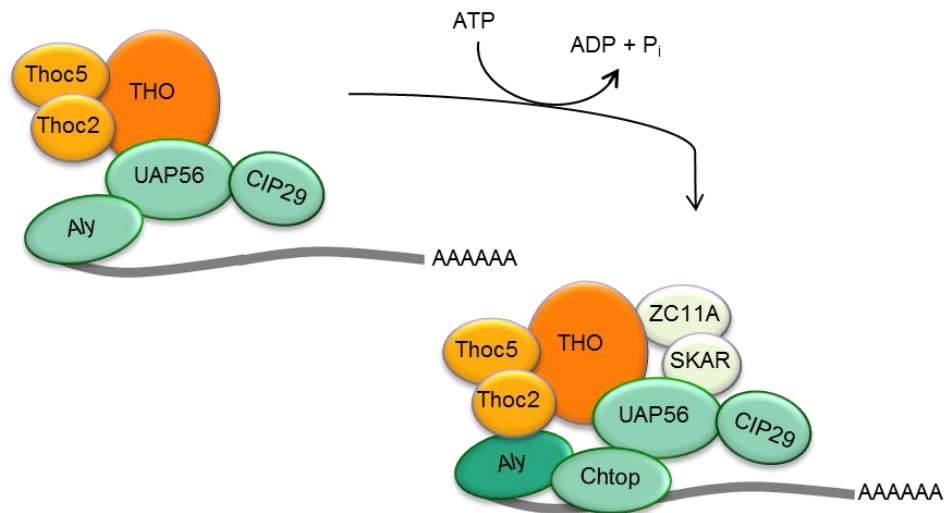


**Figure 1.14: UAP56 assembles the hTREX complex sequentially, in an ATP-dependent manner.** All proteins affected in the ATP-dependent assembly are shown in shades of green. Proteins not affected by the ATP-dependency are shown in orange. Modified from (Schumann et al., 2013).

### 1.3.2.2 The hTREX complex and the export receptor Nxf1

As previously mentioned, bulk mRNA exported from the nucleus into the cytoplasm of the cell needs to travel through selective and well controlled channels in the nuclear envelope, termed the nuclear pore complexes (NPCs). These NPCs are composed of around 30–50 different nucleoporins (Nups), functioning as structural proteins, membrane anchors and flexible gates (phenylalanine/glycine (FG)-rich nucleoporins), which interact directly with nuclear export receptors. It is therefore essential that all export-competent ribonucleoproteins particles (RNPs) contain specific export receptors that are targeted to the NPC. For this, the hTREX complex recruits Nxf1 and its co-factor Nxt1, by providing a docking platform for the non-karyopherin heterodimer. Both Aly and Thoc5 bind Nxf1 directly, upon assembly of the complete hTREX complex (Katahira et al., 2009). This induces a conformational change in Nxf1, which enables the export receptor to bind mRNA (Viphakone et al., 2012). Furthermore, as RNA- and Nxf1-binding domains in Aly overlap, binding of the export receptor induces a handover of mRNA from Aly to Nxf1 (Hautbergue et al., 2008). This process is controlled through post-translational methylation of the binding site in Aly. Moreover, binding of Nxf1 to Aly causes displacement of UAP56 from the hTREX complex (Figure 1.15).

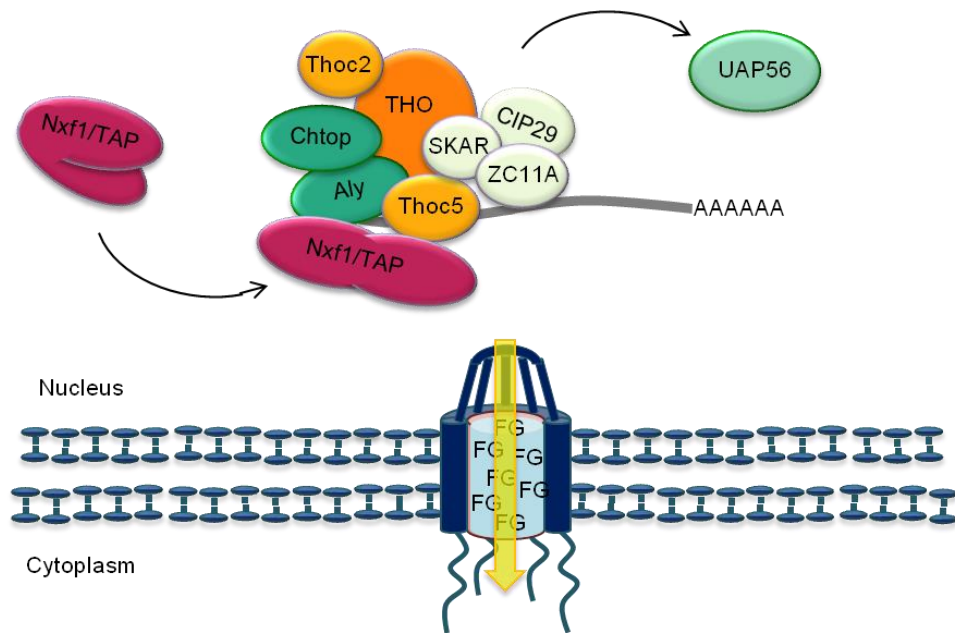


**Figure 1.15: The hTRES complex interacts with the export receptor Nxf1.** The interaction with hTRES induces a conformational change in the export receptor. This in turn allows mRNA handover from Aly and leads to the dissociation of UAP56 from the complex. After Chtop binding to Nxf1 and potentially further remodelling (not shown here), the export competent RNP can pass through the NPC. Modified from (Schumann et al., 2013).

Chtop, which during the earlier stages of hTRES assembly is directly associated with Aly, is also able to bind Nxf1 (Teng and Wilson, 2013). In addition to the above mentioned process, this interaction is also necessary for complete handover of mRNA from Aly to Nxf1 (Chang et al., 2013). The change in interacting protein partners by Chtop is regulated by methylation, as unmethylated Chtop was found *in vivo* to bind Aly, whereas methylated Chtop subsequently interacts with Nxf1 (Teng and Wilson, 2013). While both Chtop and Thoc5 are reported to bind Nxf1 directly, their interaction with the export receptor is mutually exclusive and yet, both proteins exist in the same complex (Chang et al., 2013). This suggests further remodelling of the hTRES complex upon binding of Nxf1 and prior to mRNA export occurring. Once transfer of mRNA to Nxf1 has taken place, the mRNP can traverse the NPC via a transient interaction of Nxf1 and Nxt1 with the FG-nucleoporins (Stewart, 2007).

### 1.3.2.3 The hTREX complex and the exon junction complex (EJC)

The exon-junction complex (EJC) is a multiprotein complex deposited on the mRNA during splicing. While initially believed to be also involved in mRNA export, the EJC has more recently been shown to function in distinct processes, such as translational enhancement, mRNA localisation and nonsense-mediated decay (NMD) (Giorgi and Moore, 2007; Nott et al., 2004; Chang et al., 2007). Also in contrast to the hTREX complex, the EJC binds mRNA in more than one distinct location: proteins are deposited 20–24 nucleotides upstream of each exon-exon junction (Le Hir et al., 2000). This marks the spliced mRNA as mature, a process essential for translational enhancement of spliced transcripts (Nott et al., 2004).

The EJC consists of four core proteins; MLN51, Magoh, Y14 and the DEAD-box protein eIF4AIII (DDX48) (Le Hir and Andersen, 2008). Both Y14 and Magoh are able to recruit the translational enhancer, PYM. PYM then functions to increase the pioneer round of translation, through recruitment of the 40S ribosomal subunit and assembly of the pre-initiation complex (Diem et al., 2007). Furthermore, SKAR, a protein also found in the hTREX complex has been implicated in EJC functioning, where SKAR increases translation efficiency of spliced mRNA in response to mTOR signalling (Ma et al., 2008). This indicates that both complexes might be linked through individual proteins functioning in both processes and dynamic remodelling of both complexes.

## 1.3.3 Alternative mRNA export pathways

### 1.3.3.1 CRM1-dependent mRNA export

In contrast to cellular bulk mRNA export, most other cargos that are moved between the nucleus and cytoplasm are transported via the Ran-dependent pathway. Here, proteins and non-coding RNAs are exported by the conserved family of karyopherin export receptors (exportins), namely CRM1, exportin-5 and exportin-t. While exportin-5 and exportin-t are utilised for miRNAs, some proteins and tRNAs, respectively, CRM1 is commonly used to export ribosomal RNAs (rRNAs), small nuclear RNAs (snRNAs) (Cullen, 2003), and proteins (Kudo et al., 1997), as well as a minor subset of mRNAs. Prominent

examples of these mRNAs are *Cd83*, *Fos* and *cyclin D1* (Prechtel et al., 2006; Brennan et al., 2000; Alt et al., 2000).

CRM1 is structurally different from Nxf1 and lacks an RNA binding domain (Fornerod et al., 1997). It therefore requires the presence of an adaptor protein that bridges the CRM1-RNA interaction. PHAX (phosphorylated adaptor for RNA export) has been named as CRM1-RNA adaptor protein, however, it binds exclusively to snRNAs (Ohno et al., 2000) and an adaptor protein for mRNA therefore remains to be identified. Recognition of known adaptor proteins by CRM1 occurs via a leucine-rich-type nuclear export signals (NES). The subsequent shuttling process is regulated by the small GTPase Ran (Moore and Blobel, 1993; Moore, 1998). Binding of GTP-loaded Ran (RanGTP) by CRM1 allows binding of the cargo, whereas the interaction with RanGDP, after GTP hydrolysis, leads to a release of the cargo. Directionality of transport from the nucleus into the cytoplasm is ensured via a gradient of RanGTP across the nuclear membrane. This gradient is generated by RanGAP (Ran GTPase-activating protein), which is only present in the cytoplasm (Görlich and Kutay, 1999) and hence drives export into the cytoplasm and release of the cargo from CRM1.

### 1.3.3.2 Nuclear budding of mRNPs

For a long time it was believed that all mRNA was exported via the NPC, however, recently it was reported that, surprisingly, some mRNAs can leave the nucleus by budding through the nuclear membrane (Speese et al., 2012) (Figure 1.16). This process was described in *Drosophila* muscle cells during synapse development. Here, the mRNAs are packaged into large mRNP granules, which then bud into the perinuclear space between the inner and outer membrane. Interestingly, this process is mediated by Lamin C, a protein that has been previously implicated in muscular dystrophies when mutated (Speese et al., 2012; Burke and Stewart, 2002; Méjat et al., 2009). Budding from the perinuclear space into the cytoplasm was later found to be facilitated by the AAA-ATPase torsin (Jokhi et al., 2013). A similar budding mechanism has previously been described for egress of herpesvirus capsids after assembly in the nucleus. These multimegadalton complexes bud from the nucleus through inner-nuclear-membrane envelopment and outer-nuclear-membrane de-envelopment (Lee and Chen, 2010).

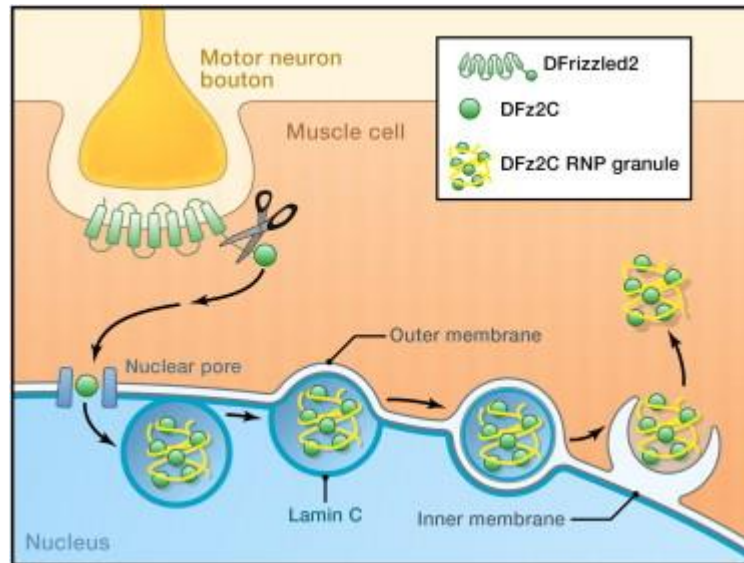


**Figure 1.16: RNP export by nuclear envelope budding.** Fragments (DFz2C) of the wnt receptor (DFrizzled2) are internalised and transported to the nucleus. In the nucleus DFz2C forms large granules with RNP complexes and lamin C, which bud from the nucleus by envelopment and de-envelopment. Exported mRNAs function locally in synapse assembly. Taken from (Hatch and Hetzer, 2012).

### 1.3.3.3 Export of intronless mRNA

Export of spliced mRNA is relatively well studied, in contrast, it is fairly poorly understood how naturally intronless mRNAs are exported from the nucleus. Only recently, it was shown that some intronless transcripts can be exported via the hTREX/Nxf1 pathway (Lei et al., 2011). A large cytoplasmic accumulation region (CAR) is essential for export of the mRNA, circumventing the splicing requirement. Subsequently, a 10-nt consensus element (CAR-E) was found in the naturally intronless genes *HSPB3*, *c-Jun*, *IFN $\alpha$ 1* and *IFN $\beta$ 1* (Lei et al., 2013). Components of the hTREX complex, the Prp19 complex and splicing factor U2AF2 associate to the CAR-E and thereby facilitate mRNA export.

An alternative mechanism has also been previously described for the transcripts of replication-dependent histone genes, which are intronless and lack polyadenylation. These mRNAs also contain consensus elements, however, they serve to recruit cellular SR proteins and export factors (such as 9G8 and SRp20), which in turn are able to bind the export receptor Nxf1 (Huang and Carmichael, 1997; Huang et al., 2003; Hargous et al., 2006).

## **1.4 Viral mRNA export**

Viruses that replicate in the nucleus of the host cell require export of their mRNAs into the cytoplasm. While utilising the host machinery, viruses face the challenge of circumventing crucial control mechanisms to allow export of their own mRNA. The following section highlights how different viruses have evolved ways to exploit cellular export pathways and utilise them for their own need (an overview is given in Figure 1.17).

### **1.4.1 Herpesvirus mRNA export**

Many human herpesviruses, including KSHV, EBV, HSV-1 and HCMV, recruit the complete or part of the hTREX complex onto their mRNA, in order to facilitate export of viral transcripts. However, as herpesviruses contain numerous intronless lytic genes, they face the conundrum of efficiently exporting these mRNAs to allow lytic replication. Therefore, all herpesviruses have evolved to express a highly conserved viral SR protein, which is able to recruit the necessary cellular proteins and facilitate export. As this forms the focus of this research study, herpesvirus mRNA export will be discussed in detail, as exemplified by KSHV and its SR protein ORF57 (section 1.5.1).

### **1.4.2 mRNA export by other viruses**

The hTREX complex and Nxf1 export pathway is not only utilised by herpesviruses, but also by other viruses, such as influenza A and hepatitis B virus (HBV). While influenza A expresses a spectrum of different mRNAs, including intronless, intron-containing (unspliced) and spliced, all require the export receptor Nxf1 to be exported from the nucleus (Read and Digard, 2010). Viral intronless mRNAs coding for early proteins were shown to weakly depend on Nxf1 for export, whereas intronless transcripts coding for late proteins were strongly dependent on the presence of Nxf1. Unspliced, intron-containing mRNAs were also reliant on Nxf1, but in addition also needed to recruit UAP56. Export of spliced viral mRNAs, which were proposed to be exported analogous to cellular spliced mRNAs, showed strong dependency on UAP56, Nxf1 and weak dependency on Aly. In contrast, a more recent study also detected an interaction of Aly and UAP56 with the

intronless transcripts of the early nucleoprotein (NP), as well as for the unspliced mRNAs of M1 and NS1 (Yin et al., 2013). Furthermore, the same study also reported binding of spliced mRNA by the SR protein, 9G8. Together, this data suggests that influenza A relies heavily on the hTREX complex and Nxf1 export pathway. However, while spliced transcripts may be processed in a manner similar to cellular mRNA, it appears that intronless mRNA and unspliced mRNAs must employ a viral adaptor protein to bridge the interaction to UAP56 or Nxf1. While this protein remains yet to be identified, an interaction of the highly pathogenic avian influenza NP protein with Aly has recently been identified (Balasubramaniam et al., 2013). However, while knock-down of Aly did not decrease the levels of viral mRNA export; a further interaction of NP with UAP56 was suggested based on molecular docking evidence, and knock-down of UAP56 significantly reduced the viral titre. It would therefore be interesting to see if redundancy of Aly by UIF might be involved in this system.

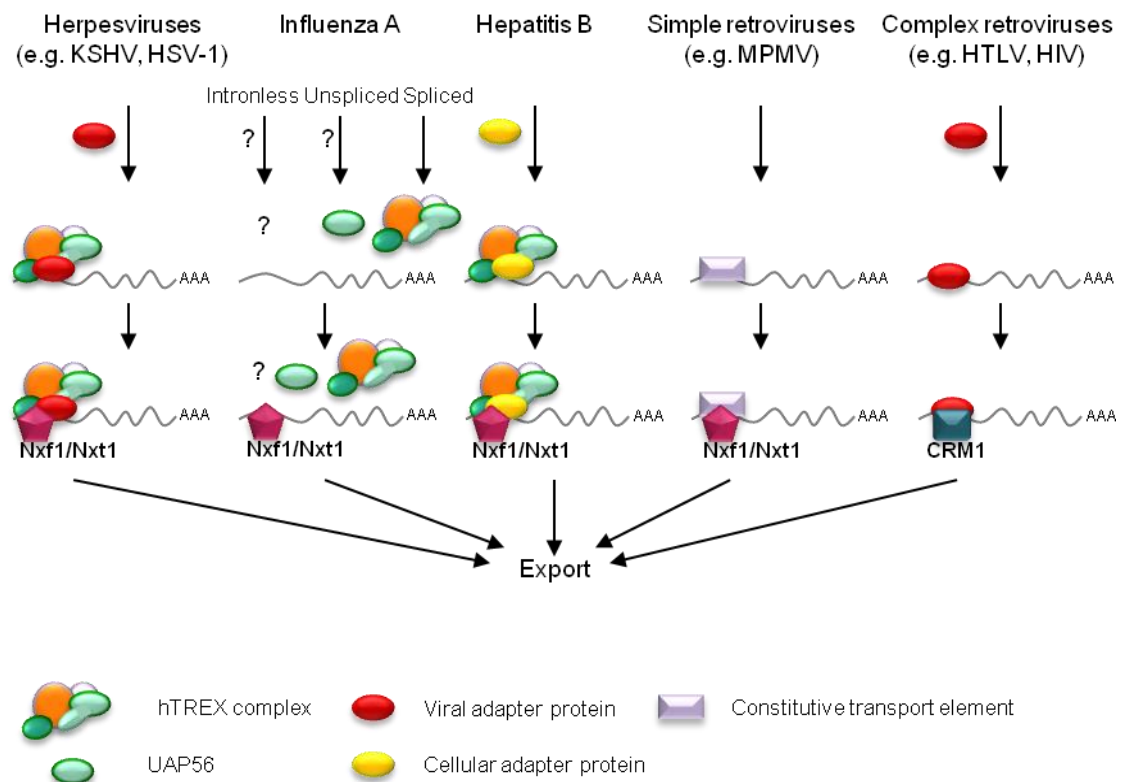


**Figure 1.17: Strategies in viral mRNA export.** Herpesviruses and hepatitis B recruit the hTREX complex onto their viral mRNAs to allow export via the Nxf1/Nxt1-dependent pathway. Influenza A virus is believed to also utilise this pathway, even though the mechanism appears to differ for subsets of mRNAs, whereas simple retroviruses recruit Nxf1/Nxt1 via a constitutive export element (CTE). In contrast, complex retroviruses utilise the CRM1-dependent export pathway.

Hepatitis B virus (HBV) also encodes several intronless genes. These genes contain a post-transcriptional regulatory element (PRE), which has previously been described as essential for export of intronless HBV transcripts (Huang and Liang, 1993). Only very recently, the PRE has now been shown to specifically recruit the hTREX complex, via a cellular adaptor protein called ZC3H18 (Chi et al., 2014). This zinc finger protein binds to a sub-element within the PRE and bridges the interaction to Thoc5. Binding of Thoc5 is sufficient to recruit other hTREX components, as well as Nxf1 and Nxt1, for nuclear export.

In addition to influenza viruses and HBV, simple retroviruses are also known to utilise Nxf1 and Nxt1, to allow nuclear export of viral mRNAs. Interestingly, Nxf1 was first identified as a nuclear export receptor in metazoans, after it was linked with the nuclear export of incompletely spliced mRNAs from Mason Pfizer Monkey Virus (MPMV) (Bray et al., 1994; Grüter et al., 1998). These mRNAs were found to contain a constitutive transport element (CTE); a highly structured, *cis*-acting sequence sufficient for nuclear export (Bray et al., 1994). Nxf1 was subsequently shown to bind directly to the CTE of type D retrovirus RNAs and thereby facilitate nuclear export (Grüter et al., 1998). Interestingly, a CTE can be found in both spliced and unspliced viral mRNAs, though it is only required for efficient export of the unspliced transcripts (Strasser et al., 2000).

Finally, complex retroviruses, such as HIV or human T-cell leukemia virus (HTLV), are known to utilise the CRM1-dependent export pathway. To export viral unspliced or partially spliced mRNAs, HIV expresses a viral adaptor protein, termed Rev, that interacts with a highly structured, *cis*-acting motif called the Rev response element (RRE) (Malim and Cullen, 1991). Furthermore, Rev, which is found expressed by all members of the lentivirus subfamily, contains a leucine-rich sequence, serving as an NES, which recruits CRM1 (Fischer et al., 1995). Interestingly, Rev has been shown to suppress the Nxf1 export pathway via a direct interaction with CBP80, a component of the cap-binding complex (Taniguchi et al., 2014). Through binding of the CBC, Rev can outcompete the essential interaction with Aly and hence disrupt hTREX assembly and Nxf1 recruitment. Similar to HIV, HTLV, a member of the orthoretrovirus subfamily, encodes a Rev-like protein called Rex, which acts as viral interaction partner for CRM1 and functions via a similar mechanism (Shida, 2012).

## 1.5 KSHV ORF57 protein

ORF57, also called MTA (mRNA transcript accumulation), is 455 aa in length, encoding a 51 kDa protein translated from a monocistronic mRNA, containing one small intron. ORF57 is essential for production of infectious virions during lytic replication (Han and Swaminathan, 2006). Expression of ORF57 is initiated indirectly by RTA, which recruits other transcription factors to bind to the *ORF57* promoter region. ORF57 is highly conserved across all *Herpesviridae*. Homologues in other human herpesviruses include: SM (also called EB2 or Mta) in EBV (Semmes et al., 1998; Ruvolo et al., 2004), ICP27 in HSV-1 (Sandri-Goldin, 2008; Sandri-Goldin, 1998), UL69 in HCMV (Toth and Stamminger, 2008) and ORF4 in VZV (Ote et al., 2009). While these proteins are conserved in their function, they each have a distinct size and share little sequence homology, with similarities only described amongst the *Gammaherpesvirinae*. For example, the ORF57 homologues of KSHV, EBV and the classical gammaherpesvirus prototype herpesvirus saimiri (HVS), only share about 30% identity of aa residues.

The crystal structure of ORF57 is to date not known, however, computer simulations of the ORF57 secondary structure suggest a largely unstructured N-terminus, while the C-terminal domain forms primarily alpha-helices (Taylor et al., 2011). Furthermore, several putative functional and structural motifs have been described after analysis of the aa sequence (Figure 1.18) (Majerciak and Zheng, 2009). Detailed studies have revealed three NLS to be located within the arginine-rich region of KSHV ORF57, each of which alone is adequate to work as an independent NLS (Boyne and Whitehouse, 2006). However, mutation of any two of the three NLSs is sufficient to abolish ORF57 function (Majerciak et al., 2006). Concurringly, the first two of these NLSs have been shown to function together as a nucleolar localisation signal and it has been suggested that this nucleolar localisation is necessary for efficient viral mRNA export (Boyne and Whitehouse, 2006; Boyne and Whitehouse, 2009).

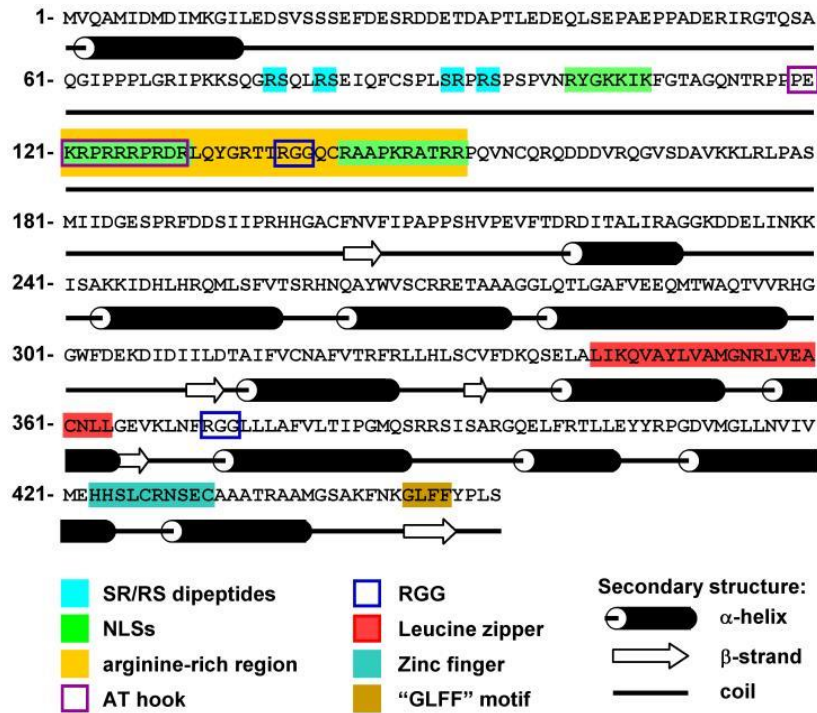


**Figure 1.18: ORF57 aa sequence, secondary structure and putative motifs.** Taken from (Majerciak and Zheng, 2009).

ORF57 is known to bind both viral and cellular mRNAs. Accordingly, sequence analysis identified two RGG-motifs, putative RNA-binding sites that are commonly found in RNA-binding proteins. While deletion of the first motif fails to cause a loss of function, mutation of the second motif results in a lack of mRNA binding and subsequently block in ORF57-mediated export of target mRNAs (Nekorчук et al., 2007). While it is presently still unclear, how ORF57 differentiates between cellular and viral mRNA, more recent findings seem to suggest an ORF57 responsive element (ORE) may be involved. The first ORE was identified in the KSHV polyadenylated nuclear (PAN) RNA, a non-coding RNA accounting for almost 80% of all KSHV lytic transcripts (Conrad et al., 2006). A 30 nucleotide ORF57-recognition sequence has since been identified containing a specific 9 nucleotide core required for ORF57-binding (Sei and Conrad, 2011). Transfer of the ORE ensured ORF57 responsiveness to a heterologous intronless reporter RNA. A very similar 9 nucleotide core was identified independently by a second group (Massimelli et al., 2011). Both sequences differ in a shift of one position. However, only 4 of these 9 nucleotides were conserved in a third study identifying an ORE within the KSHV vIL-6 mRNA (Kang et al., 2011). It still

remains to be elucidated if a similar ORE is found in other mRNAs targeted by ORF57 and if there is a conserved mechanism for RNA binding by this protein.

ORF57 contains four serine/arginine or arginine/serine dipeptides, which are typical of cellular splicing factors, so called SR proteins. It also contains an A/T hook motif, which is commonly found on chromosomal DNA binding proteins, as well as transcription factors (Aravind and Landsman, 1998), which has led to speculation that ORF57 may also function as a cofactor for RTA-mediated transactivation (Kirshner et al., 2000). Furthermore, the C-terminus contains a putative leucine zipper motif, a feature also commonly found in cellular transcription factors. While the leucine zipper domain is only found in KSHV ORF57 and not its homologues, a similar leucine rich region in HSV-1 ICP27 has been shown to contain a nuclear export signal (Sandri-Goldin, 1998) and might therefore contribute to ORF57 nucleo-cytoplasmic shuttling activity (Bello et al., 1999). Two other motifs are found in all gammaherpesvirus homologues of ORF57: a zinc-finger motif and a GLFF motif that appears to be involved in ORF57-mediated transactivation and repression activities (Cooper et al., 1999; Hardwicke and Sandri-Goldin, 1994; Ruvolo et al., 2004).

The high number of functional motifs encoded by ORF57 suggests that it is a multifunctional protein involved in all stages of viral mRNA processing. The crucial role of ORF57 in KSHV viral mRNA export, as well as other functions ensuring efficient expression of KSHV lytic genes, is discussed below.

### **1.5.1 ORF57-mediated mRNA export**

As mentioned above, KSHV expresses numerous intronless transcripts. However, host cells have an arsenal of mRNA surveillance and control mechanisms coupled to the mRNA export pathway, meaning intronless viral mRNAs would be retained in the nucleus, as they cannot recruit the hTREX complex via splicing. To circumvent this serious obstacle, KSHV expresses the immediate early protein ORF57, which itself is intron-containing and therefore expressed via the cellular pathway.

ORF57 was first shown to interact with the export adaptor Aly to form an export competent viral ribonucleoprotein particle (vRNP) (Malik et al., 2004b). Subsequently, the

complete hTREX complex was shown to be recruited onto viral mRNA through the interaction of Aly and ORF57 (Boyne et al., 2008). This is believed to be facilitated through the recruitment of UAP56 via Aly, which can then assemble the remaining members. Analogous to the mechanism of the endogenous hTREX complex, ORF57 recruitment of Aly allows the subsequent recruitment of the export receptor Nxf1, which then facilitates transport of the viral mRNA through the nuclear pore. Importantly, a study employing trans-dominant Aly mutants, which were able to interact with ORF57 and Nxf1, but unable to bind UAP56, failed to efficiently mediate viral mRNA export and led to a decrease in virus replication (Boyne et al., 2008). This confirms that recruitment of the complete hTREX complex is required for efficient viral mRNA export to take place, whereas the presence of Aly and Nxf1 alone is not sufficient.

While little detail is known of how ORF57 recruits Aly or facilitates subsequent UAP56 binding and assembly of the remaining hTREX components, structural data has recently been produced for the model gamma-herpesvirus, herpesvirus saimiri (HVS), describing a handover of viral mRNA from ORF57 to Aly (Tunncliffe et al., 2014). Upon interaction of the viral protein with the export adaptor, the RNA binding domain in ORF57 is partially occupied by Aly, causing a release of part of the viral RNA, which is then bound by Aly, forming a ternary complex.

As mentioned previously, ORF57 contains three nuclear localisation signals, two of which function together as a nucleolar localisation signal (Boyne and Whitehouse, 2006; Majerciak et al., 2006). Accordingly, ORF57 shuttles through the nucleolus, a process essential for viral mRNA export both in KSHV (Boyne and Whitehouse, 2009) and HVS (Boyne and Whitehouse, 2006) (Figure 1.19). ORF57 shuttling leads to all components of the hTREX complex to be re-localised to the nucleolus, where they co-localise with ORF57. It can be speculated that ORF57-mediated localisation to the nucleolus might protect viral mRNA from cellular mRNA surveillance and degradation. Alternatively, this could be the site where further viral mRNA modifications occur. This is concurrent with research suggesting that shuttling between the nucleus and nucleolus occurs before ORF57 facilitates exports viral mRNA into the cytoplasm and is then recycled back into the nucleus (Jackson et al., 2012). However, the precise mechanisms and reasons of ORF57 shuttling have to yet to be fully elucidated.

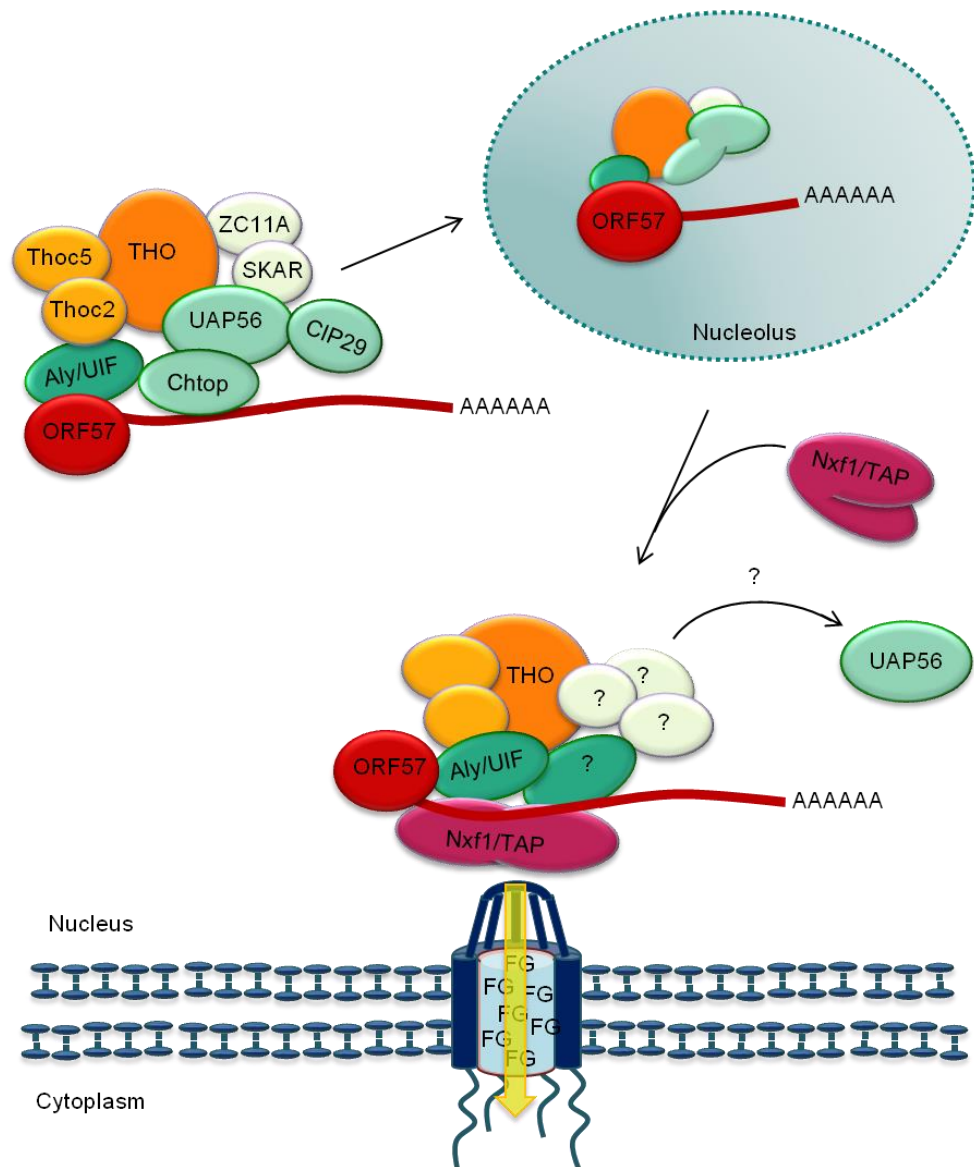


**Figure 1.19: ORF57 recruits the complete hTREX complex onto the viral mRNA.** ORF57-bound hTREX can be seen re-localising to the nucleolus of the host cell, a sub-nuclear structure through which ORF57 is known to shuttle prior to mRNA export. Modified from (Schumann et al., 2013).

ORF57 binds the mRNA export adaptor protein Aly to recruit hTREX. However, redundancy of Aly on a cellular level is reflected in viral mRNA export; ORF57 is also able to interact with UIF, enabling efficient viral mRNA export even if Aly is depleted (Jackson et al., 2011). Analogous to the mechanism in endogenous mRNA export, knock-down of just one of the two export adaptor results only in minor loss of ORF57-mediated mRNA export. However, siRNA knock-down of both Aly and UIF blocks viral RNA export and leads to a drastic decrease in viral protein expression. While UIF seems to be a compensatory export adaptor, with levels of mRNA export lowered upon Aly depletion and ORF57 preferentially

interacting with Aly, UIF is both able to bind viral mRNA, and facilitate binding of ORF57 and the viral transcripts to UAP56 (Jackson et al., 2011). Furthermore, interactions have also been shown with the cellular mRNA export factors OTT3 and RBM15, both of which seem to play a role in the expression of some viral transcripts (Majerciak et al., 2011).

Similar redundancy has been suspected for the HSV-1 homologue ICP27, which also facilitates export of viral mRNA (Koffa et al., 2001): Initial studies reported the interaction of the viral protein with Aly was not required for viral mRNA export, instead a direct interaction of ICP27 with Nxf1 was deemed essential (Johnson et al., 2009a). However, following studies based on structural data predicted direct binding of the two proteins and modelled an interface of the ICP27/Aly interaction (Tunnicliffe et al., 2011). Three key residues in the interaction of ICP27 and Aly were shown to be essential for HSV-1 ICP27-mediated mRNA export and virus replication.

As mentioned previously, ORF57 is highly conserved and several homologues have been shown to interact with all or some hTREX components. The EBV protein EB2 is also known to promote viral mRNA export via a direct interaction with Aly (Hiriart et al., 2003). VZV has also been reported to export viral mRNAs through the Nxf1/Nxt1 export pathway. Accordingly, the ORF57 homologue IE4 interacts with Aly and Nxf1, as well as other cellular export factors such as ASF/SF2, 9G8 and SRp20 (Boyne and Whitehouse, 2006). Interestingly though, not all herpesviruses require a direct interaction of their ORF57 homologue with Aly: the HCMV UL69 protein interacts directly with UAP56, which is sufficient to recruit all other hTREX components (Lischka et al., 2006). Together this data suggests that while the precise mechanisms of mRNA export may vary, the requirement to recruit the TREX complex, via an interaction with ORF57 or its homologues, onto viral mRNA is conserved between all herpesviruses.

### **1.5.2 Other roles of ORF57**

In addition to viral mRNA export, ORF57 is involved in all aspects of viral mRNA processing, as will be described in detail below.

#### 1.5.2.1 Transcriptional enhancement by ORF57

ORF57 interacts with the major transcriptional activating protein, RTA, to enhance efficiency of protein expression and thereby contributes to the expression cascade in KSHV lytic replication. As mentioned previously, ORF57 contains an A/T hook, which is able to bind DNA and has been shown to function as a co-transactivator for selected viral genes. Specifically, ORF57 enhances the effect of RTA upregulating activity of PAN/nut-1, Kaposin, *ori-Lyt* (L), K-bZIP, and TK promoters *in vitro* (Malik et al., 2004a; Kirshner et al., 2000; Palmeri et al., 2007). However, no ORF57-mediated transactivation was found on promoters that do not respond to RTA, such as ISRE and SV40 promoters (Malik et al., 2004a), making this an RTA-dependent effect.

Furthermore, ORF57 has been demonstrated to interact with a second KSHV transcription factor, K-bZIP. Here, ORF57 also binds the K-bZIP promoter in association with the K-bZIP protein, to autoregulate K-bZIP gene expression (Hunter et al., 2013).

#### 1.5.2.2 Stabilisation of mRNA by ORF57

As the original name of ORF57, mRNA transcription accumulation (MTA), suggests, ORF57 has long been known to enhance the accumulation and stability of viral transcripts (Nekorchuk et al., 2007; Stubbs et al., 2012). A prime example is the above mentioned polyadenylated nuclear (PAN) RNA, a transcript found in great abundance upon KSHV lytic replication. As stated above, studies employing PAN RNA led to advances in identifying the ORF57 response element (ORE) and mechanisms of ORF57-mediated transcript stability. It is speculated that recruitment of ORF57 and thereby recruitment of cellular mRNA processing proteins, allows masking of the viral mRNA against cellular aberrant RNA surveillance mechanisms. Specifically, ORF57 directly interacts with the cellular polyadenylate-binding protein cytoplasmic 1 (PABPC1), which is then recruited into the nucleus, where PAN is retained (Massimelli et al., 2011). The interaction with PABPC1 is essential for ORF57 to bind the PAN ORE and therefore it is believed to be an essential factor for ORF57-mediated PAN stability. A second ORF57-mediated mechanism was identified for the stabilisation of vIL-6. Here, binding of ORF57 to the vIL-6 mRNA was found to outcompete binding of a cellular miRNA and thus protect the transcript from

miRNA-mediated degradation (Kang et al., 2011). Moreover, ORF57 was found to protect the cellular IL-6 mRNA in a similar manner. This implies that ORF57 enhances transcript levels of both viral and cellular genes. Interestingly however, while a stabilising effect has been shown for many viral mRNAs (including ORF47, ORF59 and PAN), ORF57 binding does not necessarily convey enhanced stability, as is case for vGPCR and K5 mRNAs (Boyne et al., 2008; Kirshner et al., 2000). This mechanism of stability enhancement and the reasons for it are an ongoing area of research.

### 1.5.2.3 Translational enhancement by ORF57

The exon-junction complex (EJC) is a multi-protein complex deposited on the mRNA upon splicing, just upstream of every exon-exon junction. The EJC functions in translational enhancement, mRNA localisation and nonsense-mediated decay (NMD) (Giorgi and Moore, 2007; Nott et al., 2004; Chang et al., 2007). As marking of mRNA by the EJC is splicing dependent, KSHV faces a similar conundrum to the recruitment of hTREX. Interestingly though, ORF57 does not facilitate binding of the EJC onto unspliced viral mRNAs. Instead, ORF57 interacts directly with the translational enhancer PYM, which is endogenously recruited onto the mRNA by EJC components (Boyne et al., 2010a) (Figure 1.20). PYM is able to directly interact with the small ribosomal subunit, and as such the interaction of ORF57 and PYM is sufficient to facilitate assembly of the 48S pre-initiation complex onto viral intronless mRNAs (Boyne et al., 2010a; Boyne et al., 2010b; Diem et al., 2007). Furthermore, ORF57 has been shown to interact with SKAR, which has been shown to associate with both the EJC and the hTREX complex (Ma et al., 2008; Dufu et al., 2010). SKAR interacts with the 40S ribosomal protein S6 kinase 1 (S6K1), and hence regulates enhancement of translation in response to mTOR signalling. Together, binding of PYM and SKAR on mRNA leads to enhancement of the pioneer round of translation.

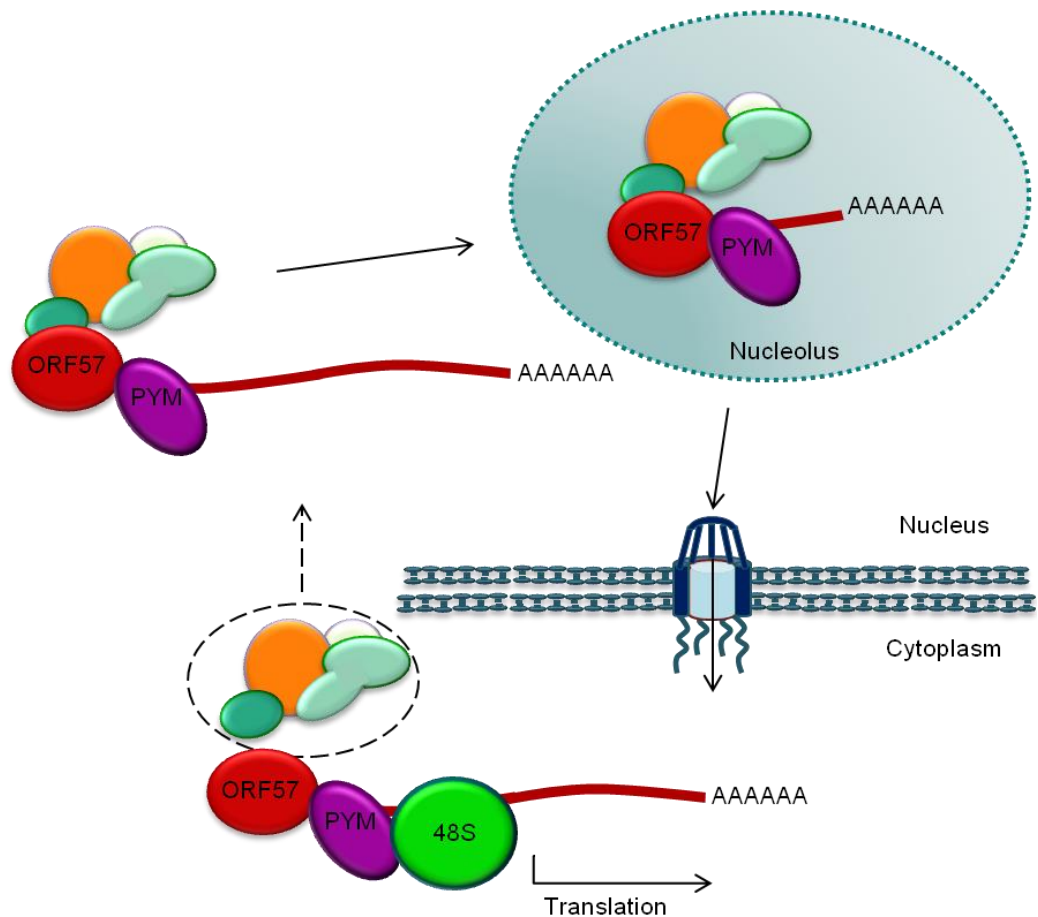


**Figure 1.20: ORF57 recruits the translational enhancer PYM onto viral mRNA.** This interaction is sufficient for recruitment of the 48S-preinitiation on viral target transcripts. It is speculated that hTREX components are recycled back into the nucleus at this stage. Modified from (Schumann et al., 2013).

#### 1.5.2.4 Regulation of splicing of viral transcripts by ORF57

Though the majority of KSHV genes are intronless, a small sub-set of genes do contain introns. The products of these genes are essential at all stages of the KSHV life cycle. It is therefore not surprising that, in contrast to its viral homologues, ORF57 can also act to enhance splicing of viral transcripts (Majerciak et al., 2008). While cellular genes usually contain small exons and large introns, KSHV genes feature a large exon upstream of a small intron. This unusual distribution leads to poor processing of the viral transcripts by the cellular splicing machinery. Surprisingly, ORF57 was found to specifically interact with, and enhance splicing of, both viral and non-viral constructs containing a large exon followed by a small intron. The viral protein was found to recruit the components of the spliceosome complex, such as small nuclear RNAs (snRNAs) U1, U2, U4, U5 and U6, as well

as splicing factors ASF/SF2 and U2AF. Interestingly, the interaction of ORF57 with inefficiently spliced pre-mRNA only takes place in the presence of whole nuclear extracts and not when using purified protein *in vitro*. This indicates that the interaction is not direct, with ORF57 requiring cellular components to modulate the normal splicing process. The EBV-homologue SM protein has also been shown to influence splicing, though opposed to ORF57, it mediates the selection of the splicing site (Verma and Swaminathan, 2008).

In contrast, other herpesvirus ORF57 homologues, such as HSV-1 ICP27 or HVS ORF57, are known to inhibit cellular splicing (Bryant et al., 2001; Whitehouse et al., 1998; Hardy and Sandri-Goldin, 1994). This process is part of the virus host shut-off (VHS), a mechanism closely associated with herpesvirus lytic replication (Fenwick and Clark, 1982). Unspliced pre-mRNAs are retained in the nucleus and subjected to mRNA surveillance and degradation, which leads to an overall downregulation in host gene expression (Fasken and Corbett, 2009).

## **1.6 KSHV drug discovery**

### **1.6.1 KSHV inhibitors**

#### **1.6.1.1 Current treatment options**

To date, no effective vaccines have been developed to prevent KSHV infections; however, a small number of anti-herpesvirus drugs have been shown to be efficacious against KSHV. As such, both prophylactic antiviral treatment, to prevent KSHV lytic replication and thus KS formation, as well as treatment of KS through general chemotherapeutic agents is advised.

Though in theory many aspects of the herpesviral life cycle present viable drug targets, all KSHV inhibitors (and in fact all general anti-herpesvirus drugs) in current clinical use are nucleoside analogues targeting the viral DNA polymerase. However, different efficacies are seen for herpesvirus subfamilies and a generally poor response is observed for KSHV for many of these drugs, compared to the alphaherpesvirus subfamily. Nucleoside analogues

are administered as pro-drugs, meaning they are provided as pharmacologically inactive compounds which are then converted into the active form through enzymatic processes. Pro-drugs are often used in drug development to enhance bioavailability, stability or target specificity. In case of anti-herpesvirus medication, nucleoside analogues require phosphorylation to be converted into triphosphates and subsequently present a target for the viral DNA polymerase. Many nucleoside analogues rely specifically on activation by a viral thymidine kinase and thus their active form is restricted to virus infected cells (Figure 1.21a). In KSHV, two viral encoded kinases were identified to phosphorylate nucleoside analogues and convey drug sensitivity: ORF21, a homologue of the conserved HSV-1 thymidine kinase, and ORF36, a homologue of the herpesvirus phosphotransferase (Cannon et al., 1999). However, some nucleoside analogues are activated by cellular kinases and function through their higher affinity for the viral DNA polymerase (Figure 1.21b). After activation, the triphosphate form of the inhibitor functions as guanosine analogue and is incorporated into the DNA template, by the viral DNA polymerase, as an alternative substrate, where it subsequently leads to chain termination.

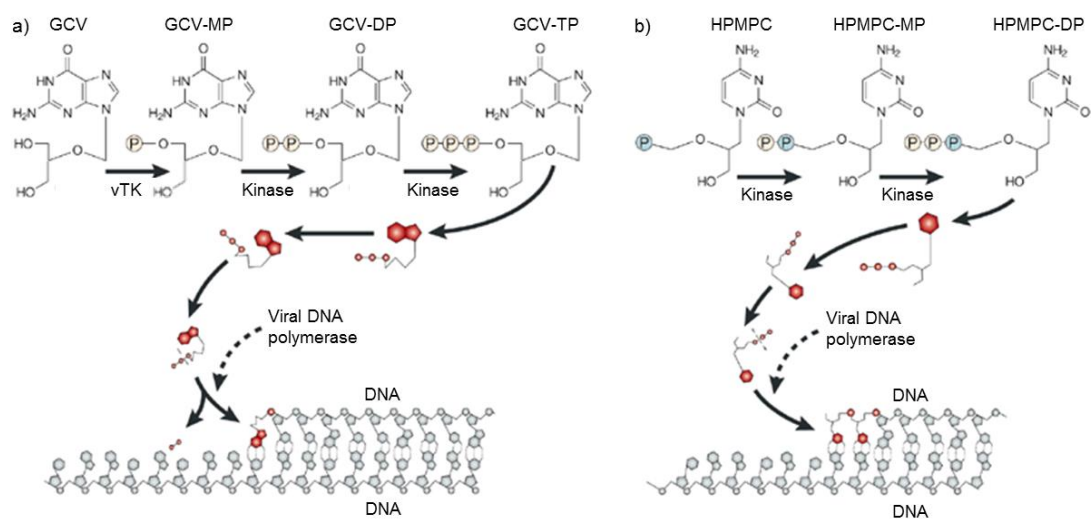


**Figure 1.21: Mechanism of action of ganciclovir and cidofovir.** a) ganciclovir (GCV), b) cidofovir (HPMPC). Both nucleoside analogues are delivered as pro-drugs that require activation through phosphorylation either by the viral thymidine kinase (vTK) or cellular kinases (Kinase). They are subsequently used as alternative substrates by the viral DNA polymerase, where they terminate chain elongation. MP = monophosphate, DP = diphosphate, TP = triphosphate. Modified from (De Clercq, 2002).

A number of studies have indicated ganciclovir has some efficacy against KS development, further implicating the lytic replication cycle in KS development (summarised in: (Gantt and Casper, 2011)). One study in particular included ganciclovir as an additional treatment of HCMV-mediated retinitis in HIV-patients, where the incidence rate of KS was found reduced by 75% if administered orally and by 93% if given intravenously, when compared to intraocular treatment alone (Martin et al., 1999). In contrast, other studies have shown little efficacy for DNA synthesis inhibitors in the treatment of KS. For example, some case reports indicated cidofovir and foscarnet could improve KS treatment, whereas other observational studies failed to report any clinical benefit of these drugs (Fife et al., 1999; Mazzi et al., 2001; Little et al., 2003). While continuous KSHV lytic replication is essential for the development and persistence of KS, DNA polymerase inhibitors may not be effective enough to prevent complete virus replication. Alternatively, the KSHV thymidine kinase does not process these pro-drugs as efficiently as the alphaherpesvirus enzymes. Furthermore, while these drugs target termination of DNA replication, expression of delayed early lytic proteins with tumourigenic activity (e.g. vIL-6 and vGPCR) might still occur (Lu et al., 2004; Klass et al., 2005). As such, new antiviral treatments against KSHV are needed.

Besides inhibition of KSHV, other approaches in the treatment of KS have focused on signal transduction pathways that are altered by the virus upon endothelial cell infection. While no therapies have been developed yet that target viral gene products directly, targeting cellular components within these pathways has been a promising approach. Specifically, inhibition of growth factor receptors c-kit and PDGF, which are activated by autocrine and paracrine mechanisms during KSHV endothelial cell infection, has proven successful in clinical trials (Koon et al., 2014). Promisingly, this c-kit/PDGF inhibitor imatinib mesylate (Gleevec) is already approved for the treatment of chronic myeloid leukemia. Another angiogenesis inhibitor, bevacizumab (trade name Avastin); a humanised anti-VEGF-A antibody, has also shown some efficacy in phase II clinical trials (Uldrick et al., 2012). Again, this inhibitor has previously been licensed to treat other cancers, such as kidney or ovarian cancer.

### 1.6.1.2 Novel approaches of herpesvirus therapy

After decades of use of viral DNA polymerase inhibitors, such as acyclovir, the first HSV-1 mutants have now evolved resistant to these drugs (Bacon et al., 2003). Therefore, novel approaches for herpesvirus inhibition are required. Current research has focussed on a series of helicase-primase inhibitors, which inhibit virus genome replication at the initial point of double strand unwinding (Katsumata et al., 2011). In addition, compounds targeting the terminase enzyme, which cleaves newly synthesised genomes prior to capsid packaging, were found to be promising against HCMV replication (Goldner et al., 2011). Other areas in herpesvirus treatment have explored drug targets in virus assembly and egress, protein expression, as well as attachment and entry. Promisingly, one inhibitor falling into the latter category was recently described for KSHV: natural ligands could inhibit the interaction of the viral gH/gL glycoprotein complex with the cellular ephrin receptor tyrosine kinase A2 (EphA2), which is utilised by the virus for cell entry (Hahn and Desrosiers, 2014). Though only described *in vitro*, the small molecule inhibitors could effectively prevent KSHV infection of target cells. This further highlights the little explored avenue of targeting cellular proteins as antiviral targets. Advantages of this are fewer occurrences of drug-resistance and potentially a broader activity against a range of viruses, although compounds targeting cellular pathways always bear the risk of cytotoxic side effects.

### 1.6.2 Drug development

Modern drug discovery and development is a very long, expensive and yet inefficient process. A recent estimate suggested a cost of US \$1.4 billion for developing a new drug, with the trend of the last 50 years being a doubling in (inflation-adjusted) cost every nine years (Lombardino and Lowe, 2004). The average time required for research and development (R&D) before approval of a first-in-class drug is 22 years (Eder et al., 2014). However, this estimation does not take into account the numerous trials that never yield an approved drug. Of all potential compounds taken into the development phase of R&D, only 4-7 % proceed through Phase I–III clinical trials, making drug development a highly risk associated process. Furthermore, none of these estimates take into account time and

cost of the fundamental research that lead to the discovery of the biological target, on which the drug development is based. Typical R&D starts after key discoveries have been made, which allow hypotheses on potential therapeutics. Following this, high-throughput screening (HTS) is commonly used in both target- and system-based approaches to identify suitable compound “hits”. These hits are compounds that display the relevant biological activity, which then undergo optimisation to generate more active lead compounds, a process known as hit-to-lead. The next phase, called lead optimisation, aims to generate new analogues with more extensive changes to chemical and physical properties of the compound, to improve potency, reduce off-target activity and enhance theoretical pharmacokinetics. Finally, the lead and several backup compounds will be taken into preclinical and clinical development; the “D” phase of R&D. Figure 1.22 displays the major stages of R&D and gives indications of compound numbers taken forward.

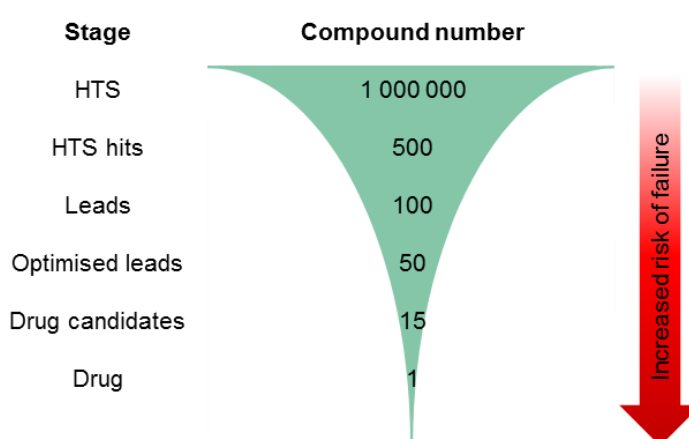


**Figure 1.22: Stages of research and development during a drug discovery cascade.** Numbers of HTS compounds and hits vary widely between screening and are for illustrative purposes only. One in 5–10 leads are taken forward as drug candidates. One in 15–25 candidates pass phase I–III clinical trials and are approved as drugs. Adapted from (Hann and Oprea, 2004).

Traditionally, development of a first-in-class drug focused heavily on system-based approaches (Figure 1.23a). These include phenotypic screening, based on a phenotype change *in vitro* or *in vivo*, and chemocentric approaches, which focus on known compounds or compound classes identified from “natural remedies” or through accidental findings (Eder et al., 2014). However, recent advances in research and emergence of more sophisticated techniques lead to more heavy investment in target-based approaches. Opposed to system-based drug discovery, these are hypothesis driven, focusing on a

known biological target. This can include development of synthetic small molecules, or naturally occurring, biologic compounds. Though this shift in R&D approach has taken place over three decades ago, results have only become visible: since 1999, target-based drug discovery started to yield more approved drugs than system-based approaches (Figure 1.23b and c). Promisingly, data suggests that drugs identified in target-based approaches take less time in their development, with a median of 20 instead of 25 years (Eder et al., 2014).

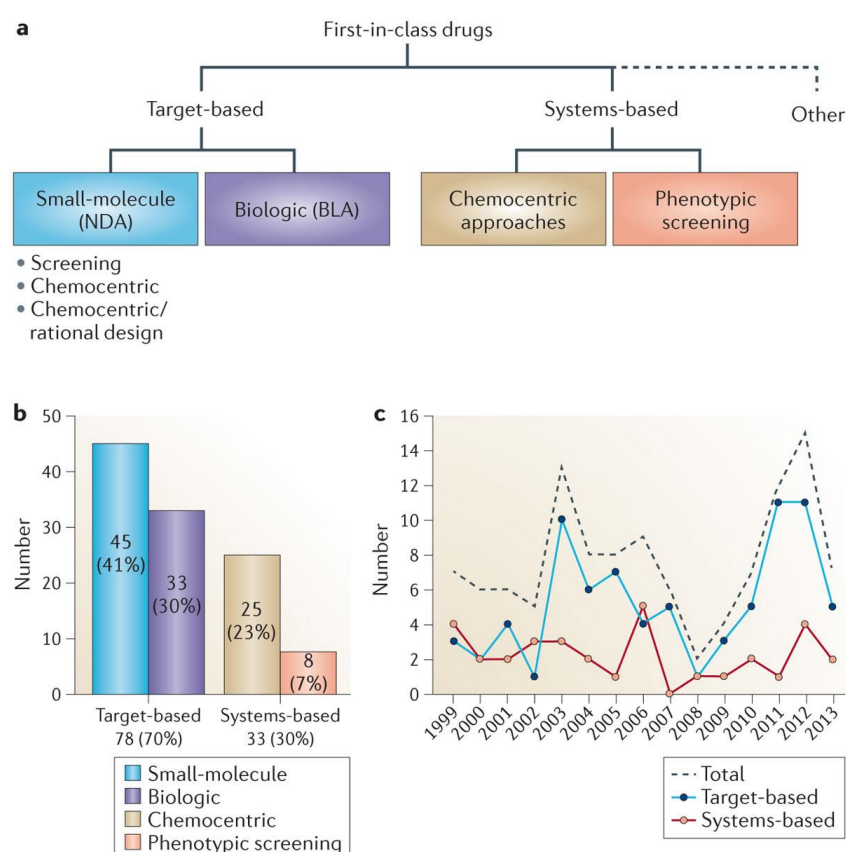


**Figure 1.23: Target-based vs. system-based approaches in drug discovery.** First-in-class drugs approved between 1999 and 2013 by the US Food and Drug Administration. a) Classification of approaches. NDA = New drug application, BLA = biologics license application. b) Total number of first-in-class compounds and their discovery approach. c) 15-year trend of discovery approach yielding new drugs, indicating an increase in target-based approaches. Taken from (Eder et al., 2014).

### 1.6.2.1 Rational-based drug design

While target-based drug development is often used synonymously to rational-based drug design, the latter describes a more focussed approach, in which existing knowledge about the target allows for a smaller and better selected set of candidate compounds during the

screening stage (Figure 1.24). In contrast, general target-based drug design might involve a known purified protein (the target) and HTS of several hundred-thousand compounds for “trial and error” testing. As illustrated in Figure 1.24, more detailed knowledge is inversely correlated with the diversity needed during the screening stage of drug discovery, yielding rational-based drug design.

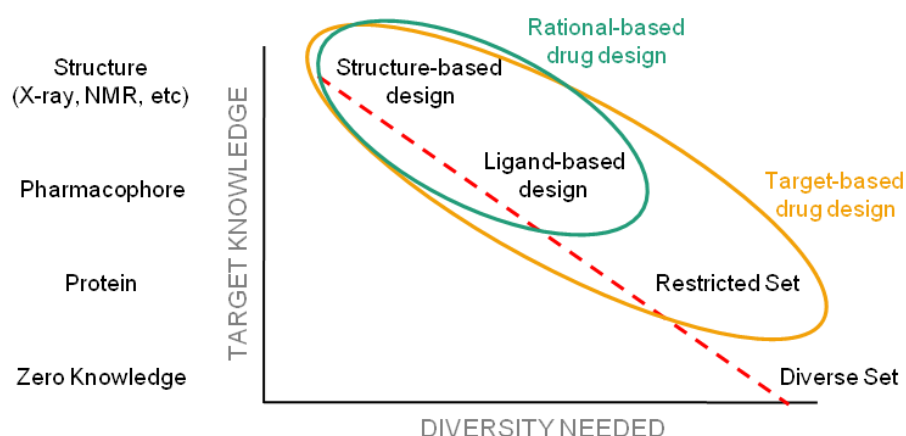


**Figure 1.24: Knowledge plot highlighting the approach of rational-based drug design.** Available knowledge of the target site is inversely proportional to the diversity in screening sets needed. Adapted from (Leach and Hann, 2007).

The aim of rational-based drug design is to identify a starting set of candidate compounds with “drug-like” properties. Common techniques used for rational-based drug design include, but are not limited to, structure-based drug design, ligand-based drug design and fragment-based drug design, all of which can be combined and overlapping when applied. Furthermore, any of these techniques can be combined with computational methods, such as *in silico* or virtual HTS (vHTS), docking studies or modelling tools, to yield an even more targeted set of potential drug candidates.

Ligand-based drug design relies on previously known molecules that bind to the target area. Knowledge from these ligands can then be used to generate a model of the target site, to subsequently produce a series of new and better binding molecules. A similar process can be found during lead discovery and optimisation, where known ligands are improved in their properties through generation of a quantitative structure-activity relationship (SAR). Opposed to this structure-based drug design relies heavily on knowledge of the three dimensional structure of the biological target site. Often combined

with vHTS, this allows quickly narrowing down a large number of molecules to those complementing the targets binding properties, using bioinformatics tools. These receptor-based screening softwares are based on docking and scoring algorithms, which allow prediction of the binding mode (docking) and affinity (scoring) (Ghosh et al., 2006). Structure-based drug design can also include *de novo* design of compounds, where these are virtually built or assembled within the constraints of the known binding pocket. This approach can easily be combined with fragment-based drug design, where molecules with low molecular mass are used for *in vitro* (and *in silico*) screening. Each fragment can be regarded as a binding epitope, which when combined amount to the entity of a drug molecule (Jencks, 1981; Farmer and Ariens, 1982). Fragment hits can be linked together (Figure 1.25a), or used for fragment evolution (Figure 1.25b) to generate a drug-like molecule.

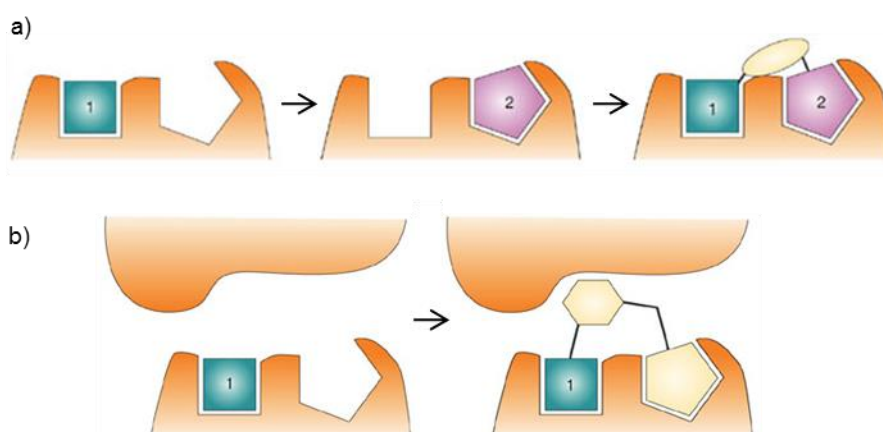


**Figure 1.25: Methods in fragment-based drug design: Fragment linking and fragment evolution.** a) Fragment linking describes the combination of several identified fragments into one drug molecule, whereas b) fragment evolution is based on one fragment hit, which is then expanded within the known constraints of the binding pocket. Modified from (Rees et al., 2004).

Advantages of fragment-based drug design include the comparatively smaller and simpler chemical structures, which need to be targeted against the known biological features. Less complex structures increase the probability of matching the target binding site. Furthermore, even a small number of screened fragments offer the possibility to be combined in numerous permutations, creating large diversity with little screening efforts. However, because of their lower affinities, fragment screening *in vitro* often requires different assay conditions to compound screening.

Cut-off values are often imposed on fragments and compounds during identification and screening, to ensure they display lead-likeness (i.e. they are likely to be suitable for lead generation). During *in vitro* screening fragments are usually expected to function in a range between 100  $\mu\text{M}$  to 1 mM, whereas suitable compounds identified by (v)HTS or structure-based drug design are expected to be potent at 100  $\mu\text{M}$  or lower, in order to be taken forward into optimisation. Another important requirement, beside affinity for the target structure, is the molecular weight (Figure 1.26). During lead optimisation, which is used to enhance the binding affinity amongst other properties, an increase in the relative molecular mass is almost always unavoidable. However, functioning drug molecules tend to have a relative molecular mass below 500, whereas larger molecules often display unfavourable binding, bioavailability or pharmacokinetics. It is therefore desirable to start off by screening compounds of low molecular mass, to achieve development a suitable drug candidate.

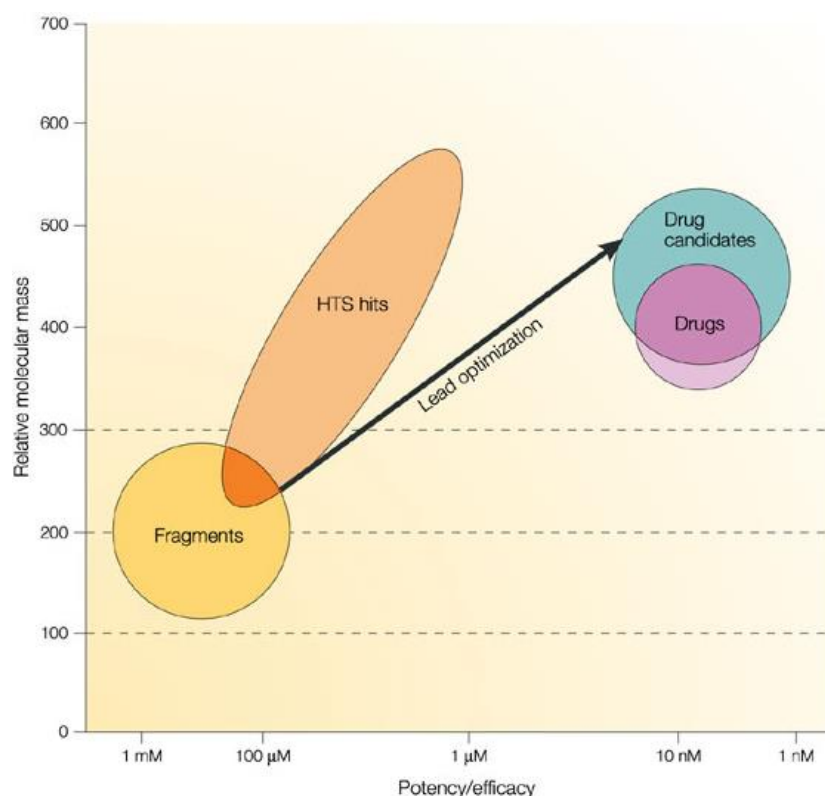


**Figure 1.26: Range of potency and molecular mass of fragments, HTS hits and drugs/drug candidates.** The schematics highlight average properties. While fragments have a lower molecular mass, their effective concentration range is usually one order of magnitude higher than HTS hits. Lead optimization will almost always increase the molecular weight of a compound, but also allow a much smaller effective concentration. Taken from (Rees et al., 2004).

## 1.7 Thesis aim

The KSHV ORF57 protein is involved in all steps of viral mRNA processing, in particular viral nuclear mRNA export. ORF57 recruits the complete hTREX complex to form an export-competent vRNP (Boyne et al., 2008). Disruption of the ORF57/hTREX complex interaction has been shown to significantly inhibit virus lytic replication, suggesting this is a viable antiviral target. Furthermore, KSHV lytic replication is essential for the development of KS tumours and as such disruption of the ORF57/hTREX interaction could have additional advantages for preventing KS development.

The aim of this thesis was to determine whether the ORF57/hTREX interaction provides a suitable antiviral target and subsequently identify lead compounds as a novel approach in KSHV drug development.

Chapter three arose from the recent finding that CIP29 is part of the hTREX complex (Dufu et al., 2010) and aimed to determine whether CIP29 is also part of the ORF57-induced vRNP. Following this, the functional significance of the CIP29/ORF57 interaction for viral mRNA export was explored. Finally, the ATP-dependency of the trimeric CIP29-UAP56-Aly complex in conjunction with the ORF57 mediated vRNP was investigated.

Chapter four further explored the ATP-dependency of ORF57-mediated vRNP formation. Showing not only ATP-dependency, but an ATP-cycle dependent remodelling of the hTREX complex, it was established that trapping the hTREX complex in one conformation could disrupt vRNP formation. Based on this, rational-based drug design was utilised to identify possible compounds targeted to a hTREX component, UAP56. *In vitro* screening subsequently identified a suitable inhibitor, which was shown to disrupt the ORF57/hTREX interaction in a concentration range where no cellular toxicity was observed. Furthermore, this compound could prevent viral mRNA export, viral late protein expression and virus replication in a physiologically relevant cell line.

Chapter five then investigated the effect of close structural analogues of the inhibitor, to confirm a structure-activity relationship. Furthermore, off-target effects of the inhibitor and its analogues were explored. Finally, the efficiency of the identified inhibitor was also tested against HSV-1, to examine pan-herpesviral activity.

## Chapter 2

~

## Material and Methods

## 2 Material and Methods

### 2.1 Materials

#### 2.1.1 Chemicals

All chemicals were purchased from Melford, Fisher Scientific, Sigma-Aldrich® and VWR International Inc., unless otherwise stated.

#### 2.1.2 Cell culture reagents

All reagents, media and selection antibiotics used in cell culture were supplied as shown in the table below (Table 2.1).

**Table 2.1: List of cell culture reagents and their suppliers.**

Reagent	Supplier
Dulbecco's Modified Eagle's Medium (DMEM)	Lonza
Phosphate buffered saline (PBS)	
RPMI1640	Life Technologies
Opti-MEM®	
Foetal bovine serum (FBS)	
Penicillin/streptomycin	
Trypsin-EDTA	
Hygromycin B	Invitrogen™
Lipofectamine® 2000	
Doxycycline hyclate	Sigma-Aldrich®
Agarose (low melt temperature)	Melford

#### 2.1.3 Antibodies

All primary antibodies, their working dilutions and suppliers are shown in Table 2.2. Horseradish peroxidase (HRP)-conjugated anti-mouse and anti-rabbit secondary IgG, used

for Western blotting at a 1:5000 dilution, were obtained from Dako. HRP-conjugated anti-sheep IgG, also used at a 1:5000 dilution for Western blotting, was purchased from Santa Cruz Biotech®. Alexa Fluor® 594- and 647-conjugated rabbit anti-mouse IgG and goat anti-rabbit IgG, used for immunofluorescence microscopy at a dilution of 1:500, were purchased from Life Technologies.

**Table 2.2: Primary antibodies, their working dilution and suppliers.**

Antibody	Origin	Working dilution		Supplier
		WB	IF	
Anti-GFP	Mouse	1:5000	-	Clontech
Anti-ORF57	Mouse	1:1000	-	Santa Cruz Biotech®
Anti-B23.1	Mouse	-	1:200	
Anti-HSP90	Mouse	1:1000	-	
Anti-FLAG	Rabbit	1:5000	1:200	Sigma-Aldrich®
Anti-Aly	Mouse	1:5000	1:200	
Anti-Myc	Mouse	1:5000	-	
Anti-HSP90	Mouse	1:5000	-	
Anti-UAP56	Rabbit	1:2500	-	Stuart Wilson, University of Sheffield
Anti-CIP29	Rabbit	1:2500	1:200	
Anti-Chtop	Rabbit	1:5000	-	Bethyl Laboratories, Inc.
Anti-mCP	Sheep	1:1000	-	Exalpa Biological, Inc.
Anti-GAPDH	Mouse	1:5000	-	Abcam®
Anti-CDC2	Mouse	1:5000	-	
Anti-ICP27	Mouse	1:1000	-	Rozanne Sandri-Goldin, University of California, Irvine

#### 2.1.4 Enzymes

All enzymes used and their suppliers are listed in Table 2.3.

**Table 2.3: List of enzymes and their suppliers.**

Enzyme	Supplier
M-MuLV Reverse Transcriptase	New England Biolabs, Inc.
DNA-free™ (DNase treatment kit)	Ambion®
Kinase Glo	Promega
DNase I	Invitrogen™
RNase OUT™	
RNase A	
Lysozyme	Sigma-Aldrich®
Proteinase K	Millipore

### 2.1.5 Oligonucleotides

Oligonucleotide primers for quantitative PCR (qPCR), as well as oligo(dT)<sub>15</sub> were obtained from Sigma-Aldrich®. Utilised primers and their sequences are shown in Table 2.4. CIP29-specific small interfering RNA (siRNA) was purchased from Thermo Scientific as siGENOME SMARTpool against human *CIP29*.

**Table 2.4: List of oligonucleotides and their sequences [Forward (F) and Reverse (R)].**

Gene name	Sequence (5'-3')
<i>GAPDH</i>	F - TGTGGTCATGAGTCCTCCACGAT
<i>GAPDH</i>	R - AGGGTCATCATCTCTGCCCCCTC
<i>ORF47</i>	F - CGCGGTCGTTCTGAAGATTGGG
<i>ORF47</i>	R - CGAGTCTGACTTCCGCTAACA
<i>ORF57</i>	F - GCCATAATCAAGCGTACTGG
<i>ORF57</i>	R - GCAGACAAATATTGCGGTGT

### 2.1.6 Plasmid expression constructs

All plasmid expression constructs were either present in the Whitehouse laboratory or kindly provided by collaborators, as shown in Table 2.5.

**Table 2.5: Plasmid expression constructs, their source and reference literature.**

Plasmid	Kindly provided by	Reference
GST (pGEX-4T.1)	GE Healthcare	Commercially available
GST-CIP29	Stuart Wilson, University of Sheffield	(Dufu et al., 2010)
GST-UAP56	Robin Reed, Harvard Medical School	(Masuda et al., 2005)
GST-Aly		
GFP (pEGFP-N1)	Clontech	Commercially available
ORF57-GFP	James Boyne (Whitehouse laboratory)	(Majerciak et al., 2006)
GFP-UAP56	Adam Taylor (Whitehouse laboratory)	-
UIF-GFP	Stuart Wilson, University of Sheffield	(Hautbergue et al., 2009)
FLAG-CIP29		(Dufu et al., 2010)
FLAG-PYM	Gideon Dreyfuss, University of Pennsylvania	(Diem et al., 2007)
FLAG- $\beta$ -catenin	Dave Griffith (Whitehouse laboratory)	-
mCherry-ORF57	James Boyne (Whitehouse laboratory)	(Boyne et al., 2010a)
ORF47		(Boyne et al., 2008)

### 2.1.7 Screening compounds

All screening compounds and fragments were part of an in-house compound library of the University of Leeds or purchased with a Tocriscreen Compound Library from Tocris Bioscience. Compounds used for further characterisation and their suppliers are listed below.

**Table 2.6: List of small molecule inhibitors and their suppliers.**

Compound	Supplier	Compound ID
C2	Tocris Bioscience	CCT 018159
An1	Sigma-Aldrich®	R910589
An3	Chembridge™	9284048
SKW032	Synthesised by S. Whitehead, University of Leeds	
SKW036		

## 2.2 Methods

### 2.2.1 Molecular cloning

#### 2.2.1.1 Transformation of *E. coli* BL21 and DH5 $\alpha$

Competent *E. coli* BL21 and DH5 $\alpha$  cells were thawed on ice. GST-expressing vectors were transformed into BL21 and the GFP- and FLAG-expressing fusion vectors were transformed into DH5 $\alpha$ . All constructs contained an ampicillin or kanamycin resistance gene. For each transformation 1  $\mu$ g DNA was mixed with 50  $\mu$ l competent cells and incubated on ice for 30 min. Cells underwent a heat-shock at 42°C for 30 sec before immediate cooling by ice. Following the addition of 200 ml S.O.C medium [0.5% (w/v) yeast extract, 2% (w/v) Tryptone, 10 mM NaCl, 2.5 mM KCl, 10 mM MgCl<sub>2</sub>, 10 mM MgSO<sub>4</sub>, 20 mM Glucose], the mixture was incubated at 37°C for 1 h while shaking. Afterwards, the cells were plated out onto lysogeny broth (LB) agar plates [1.5% (w/v) microagar in LB medium] containing 50  $\mu$ g/ml ampicillin or kanamycin. The plates were then incubated over night at 37°C.

Transformed *E. coli* BL21 cells were kept for long term storage as glycerol stock. For this, a single bacteria colony was picked from the agar plates and grown in 3 ml LB medium containing 50  $\mu$ g/ml ampicillin over night at 37°C with shaking. These starter cultures were then mixed in a 1:1 ratio with LB medium containing 40% glycerol and stored at -80°C.

#### 2.2.1.2 Plasmid purification

For isolation of large amounts of plasmid DNA the QIAGEN Plasmid Maxi kit was used according to the manufacturer's instructions. For each plasmid, a single bacteria colony of DH5 $\alpha$  was picked from the agar plates (section 2.2.1.1) and grown in 3 ml LB medium containing 50  $\mu$ g/ml ampicillin over night at 37°C with shaking. Of these starter cultures, 200  $\mu$ l were then used to inoculate 100 ml LB media containing 50  $\mu$ g/ml ampicillin and grown over night (approximately 16 h) at 37°C with shaking. The bacterial cultures were harvested at 4,500 x *g* for 10 min at 4°C and then resuspended in 10 ml buffer P1. Lysis buffer P2 (10 ml) was then added and the solution incubated for 5 min at room temperature. Neutralisation buffer P3 was added (10 ml) and the mix was left on ice for

20 min. Insoluble cell parts were spun down at 4,500 x *g* for 30 min at 4°C and the clear supernatant was added onto a pre-equilibrated QIAGEN-tip 500. After the supernatant had run through the column by gravity, the resin was washed using 2 x 30 ml washing buffer QC. The plasmid DNA was then eluted using 15 ml elution buffer QF. The DNA was precipitated by addition of 10.5 ml 100% isopropanol and immediately spun down at 16,000 x *g* for 20 min at 4°C. The supernatant was discarded and the DNA pellet washed with 5 ml 70 % (v/v) ethanol and left to air-dry. The DNA was dissolved in 500 µl dH<sub>2</sub>O. The DNA concentration and purity was assessed using the NanoDrop ND-1000 spectrophotometer (NanoDrop Technologies). The purified DNA was stored at -20°C.

## **2.2.2 Cell culture**

### **2.2.2.1 Cell lines**

Human embryonic kidney (HEK) 293T cells (referred to as 293T cells) were used for all experiments involving plasmid transfection (obtained from the Health Protection Agency Culture Collection). HFF cells, a human foreskin fibroblast cell line, were employed in all studies utilising HSV-1. HFF cells were a kind gift of John Sinclair, University of Cambridge. TReX BCBL1-Rta, a B lymphocyte cell line latently infected with KSHV and containing an inducible RTA-expression construct, was utilised for all experiments involving KSHV lytic replication, unless otherwise stated. These cells were a kind gift of Jae Jung, University of Southern California (Nakamura et al., 2003). Similar, 293 rKSHV.219 cells, a 293T cell line containing a recombinant bacterial artificial chromosome harbouring the KSHV genome, were utilised for protein knock-down studies during KSHV lytic replication (Vieira and O'Hearn, 2004).

### **2.2.2.2 Cell maintenance**

293T, HFF and 293 rKSHV.219 cells were grown in Dulbecco's Modified Eagle's Medium (DMEM), supplemented with 10% (v/v) heat inactivated foetal bovine serum (FBS) and 1% (v/v) penicillin/streptomycin (referred to hereafter as complete DMEM) at 37°C in the

presence of 5% CO<sub>2</sub>. TReX BCBL1-Rta cells were grown in RPMI1640 growth medium, also supplemented with 10% (v/v) FBS and 1% (v/v) penicillin/streptomycin (referred to as complete RPMI), under the same conditions. TReX BCBL1-Rta cells were kept under Hygromycin B selection (100 µg/ml) and 293 rKSHV.219 cells under puromycin selection (1 mg/ml).

Cell lines were split every 3-4 days when they reached approximately 80% confluence. All 293 derived cells were physically dislodged from the flask and split 1:20 into complete DMEM in a new flask. HFF cells were passaged by trypsinisation [0.05% (v/v) trypsin in PBS] for five minutes to dissociate adherent cells, before being resuspended in 10 ml complete DMEM to inactivate trypsin. A third of the resulting volume was subsequently transferred into a new flask containing complete media (1:3 split). HFF cells were subjected to a maximum of 20 passages. TReX BCBL1-Rta cells were grown in suspension and were diluted 1:6 into complete RPMI for passaging.

For long term storage, cells were cryopreserved in liquid nitrogen. For this, growing cells at 50% confluence were spun down at 500 x g for 3 min and the cell pellet was resuspended at 1 x 10<sup>6</sup> cells/ml in freezing medium [40% (v/v) complete medium, 50% (v/v) FBS, 10% (v/v) DMSO]. Cells were aliquoted into CryoTubes™ (NUNC™) and placed in a 5100 Cryo 1°C Freezing Container (NALGENE®) at -80°C for 24 hours. The tubes were then transferred to liquid nitrogen.

### 2.2.2.3 Transient transfection

For transient transfections, cells were seeded into a 6-well plate. After 20–24 h of cell growth, at approximately 80% confluence (or 50% confluence if used for immunofluorescence microscopy), transfections were performed using Lipofectamine® 2000, following the manufacturer's instructions. Typically, 1 µg of DNA per expression plasmid and 3 µl of Lipofectamine® were each diluted in 100 µl serum free DMEM and incubated for 5 min. Transfections for mRNA export assays were done with 2 µg of ORF57-GFP plasmid, 1 µg ORF47 reporter construct and 9 µl of Lipofectamine®. After the 5 min incubation, the Lipofectamine® 2000 solution was added to the DNA solution and incubated for an additional 20 min at room temperature. The cell medium was exchanged

with fresh complete medium and the Lipofectamine<sup>®</sup>/DNA mix was then added drop by drop into the wells. Cells were incubated typically for 24 h to allow efficient plasmid expression.

#### 2.2.2.4 siRNA knock-down

For siRNA-mediated gene knock-down, 293T and 293 rKSHV.219 cells were seeded into a 12-well plate (with 1 ml media per well). After 20–24 h of cell growth, at approximately 40–50% confluence, transfections were performed using Lipofectamine<sup>®</sup> 2000, following the manufacturer's instructions. Typically, 5  $\mu$ l of a 20  $\mu$ M siRNA stock (giving 100 nM final concentration per knock-down) and 5  $\mu$ l of Lipofectamine<sup>®</sup> were each diluted into 100  $\mu$ l of Opti-MEM<sup>®</sup> medium and incubated for 15 min at room temperature. The siRNA and Lipofectamine<sup>®</sup> 2000 dilutions were then combined and incubated another 15 min. Growth medium was replaced with fresh complete DMEM and the Lipofectamine<sup>®</sup>/siRNA mix was added drop by drop into the wells. Unless otherwise stated, this procedure was repeated after 24 h. Protein knock-down was usually detectable after 48–72 h.

#### 2.2.2.5 Treatment with small molecule inhibitors

Small molecule inhibitors were added to 293T cells 6 h post-transfection, to TReX BCBL1-Rta cells at the time of induction of virus lytic replication or to HFF cells directly after initial infection with HSV-1, unless otherwise indicated. All small molecule compounds were dissolved and diluted in DMSO. Cells were treated with 1  $\mu$ l of inhibitor per ml of media, with the concentration being 1000 x higher than the desired final dilution, giving a total of 0.1% (v/v) DMSO in all experiments.

#### 2.2.2.6 Cytotoxicity assays

Cytotoxicity of small molecule inhibitors was assessed using the MTS-based CellTiter 96<sup>®</sup> AQueous One Solution Cell Proliferation Assay (Promega). For this, 293T cells were seeded

into a 96-well plate and left to adhere for 20–24 h. When cells reached 80% confluence, they were treated with the small molecule inhibitors or DMSO control (section 2.2.2.5) and incubated for an additional 24 or 72 h. Growth medium was then removed and replaced with 100  $\mu$ l new complete medium per well, before addition of 20  $\mu$ l CellTiter 96<sup>®</sup> AQueous One Solution Reagent. After approximately 1 h at 37°C, the absorbance at 490 nm was measured using the Infinite<sup>®</sup> F50 Robotic microplate reader (Tecan).

Alternatively, 1 ml of TReX BCBL1-Rta cell suspension (approximately  $1 \times 10^6$  cells per ml) was seeded in a 12-well plate and treated directly with small molecule inhibitors. After 24 or 72 h, 100  $\mu$ l of the treated cells were transferred into a 96-well plate and 20  $\mu$ l CellTiter 96<sup>®</sup> AQueous One Solution Reagent was added. The absorbance was measured as described above.

### **2.2.3 Virus based assays**

#### **2.2.3.1 Induction of KSHV lytic replication**

Viral lytic replication in TReX BCBL1-Rta cells was induced by supplementing the media with 2  $\mu$ g/ml doxycycline hyclate. Viral mRNA export assays, protein expression studies or immunofluorescence experiments cells were performed 24 h post-induction, while viral load or production of new infectious virions was examined at 72 h after induction.

For induction of KSHV lytic replication in 293 rKSHV.219 cells media was supplemented with 3 mM sodium butyrate and 20 ng/ml 12-*O*-tetradecanoylphorbol-13-acetate (TPA).

#### **2.2.3.2 KSHV late protein expression**

To assess viral late protein expression in the absence or presence of small molecule inhibitors, 1 ml of TReX BCBL1-Rta cell suspension ( $1 \times 10^6$  cells/ml) were seeded into 12-well plates, induced and treated with compounds as described before (section 2.2.3.1 and 2.2.2.5). Cells were harvested 24 h post-induction and spun at 500 x *g* for 5 min at 4°C. The supernatant was removed and cell pellets were subsequently used for analysis of

protein expression by SDS-PAGE and Western blotting as described below in section 2.2.5.2 and 2.2.5.4.

#### 2.2.3.3 KSHV replication assay

To assess the changes in KSHV viral load within cells in the absence or presence of small molecule inhibitors,  $1 \times 10^6$  TReX BCBL1-Rta cells per ml were seeded into 12-well plates, induced and treated with small molecule inhibitors as described before (section 2.2.3.1 and 2.2.2.5). Cells were harvested 72 h post-induction and spun at  $500 \times g$  for 5 min at  $4^\circ\text{C}$ . Viral and cellular DNA was purified using a QIAamp DNA mini kit (QIAGEN), following the manufacturer's instructions. Briefly, the cell pellet was lysed using QIAGEN Protease and buffer AL, at  $56^\circ\text{C}$  for 10 min. Ethanol was added and the solution applied to a QIAquick spin column. Columns were centrifuged at  $6,000 \times g$  for 1 min at room temperature and the flow through discarded. This centrifugation step was repeated twice, with washes by buffer AW1 and AW2 in between, before a final spin at  $16,000 \times g$  for 3 min at room temperature. The column was then placed in a fresh microcentrifuge tube and DNA was eluted by addition of  $50 \mu\text{l}$   $\text{dH}_2\text{O}$  and centrifugation at  $13,000 \times g$  for 1 min at room temperature. Eluted DNA was stored at  $-20^\circ\text{C}$ . Viral and cellular DNA levels were quantified by qPCR as described below (section 2.2.8.6).

#### 2.2.3.4 HSV-1 primary infection

HSV-1 virus stocks were stored in aliquots at  $-80^\circ\text{C}$ . Typically, a low MOI of 0.001 was used for primary infection of HFF cells, unless otherwise stated. For this, the appropriate amount of virus stock was diluted in  $100 \mu\text{l}$  complete DMEM and then further diluted by a 1:10 dilution series, until the final concentration was reached. The medium was removed from HFF cells grown in a 6-well plate and 1 ml of medium containing HSV-1 at the desired MOI was added per well. Following 1 h incubation, virus containing media was removed and cells washed twice with PBS, followed by addition of 2 ml complete DMEM (for re-infection assays) or 2 ml plaque agar (for plaque assays of primary infection) per well. DMSO or small molecule inhibitors in DMSO were added at  $1 \mu\text{l}/\text{ml}$  to either the fresh

DMEM or the plaque agar and left on cells for either 72 h (re-infection assays) or 96–120 h (plaque assay), as described below.

#### 2.2.3.5 Viral re-infection assays

Re-infection assays were performed with KSHV and HSV-1. For KSHV re-infection assays, TReX BCBL1-Rta cells were induced and treated with small molecule inhibitors as described above (section 2.2.3.1 and 2.2.2.5). After 72 h, cells were spun down at 500 x *g* for 5 min at room temperature and the supernatant was mixed 1:1 with complete DMEM and added to confluent 293T cells. Following 24 h incubation, the 293T cells were washed once with PBS and total RNA was extracted using TRIzol (Invitrogen™) and subsequently used for quantitative reverse transcriptase PCR (qRT-PCR) (as described under 2.2.8.3–2.2.8.6). Viral mRNA was normalised against the housekeeping gene *GAPDH* and quantified using the comparative *C<sub>t</sub>* method.

For HSV-1 re-infection, primary infected HFF cells were incubated for 72 h. Cells were then harvested at 500 x *g* for 5 min at room temperature. The supernatant was collected and diluted 1:10–1:1,000 for re-infection of naive HFF cells, which were analysed by flow cytometry and Western blot, or 1:10–1:10,000 for re-infection assay analysed by plaque assay, as described below (section 2.2.3.6). Diluted virus-containing supernatants were added to confluent HFF cells, which had been seeded the previous day. For Western blot and flow cytometry based analysis, supernatants were incubated for 16 or 24 h, respectively, before cells were harvested at 500 x *g* for 5 min at 4°C and washed twice with PBS. Cellular and viral proteins were then analysed by SDS-PAGE and Western blotting as described below (section 2.2.5.2 and 2.2.5.4). Alternatively, cells were fixed with 4% (v/v) formaldehyde for 1 h at 4°C, before being again spun at 500 x *g* for 5 min at room temperature and washed twice with PBS. As a recombinant virus expressing GFP was used, all virus-infected cells were fluorescently marked, therefore resuspended cells were analysed for fluorescence using the BD LSRFortessa flow cytometer (BD Biosciences).

#### 2.2.3.6 HSV-1 plaque assay

Plaque assays were performed after primary infection or re-infection of HFF cells with HSV-1. Both, virus of a known titre for primary infection (2.2.3.4), or supernatant gained after 72 h of primary infection and used for a re-infection assay (2.2.3.5) were incubated on fully confluent HFF cells in a 6-well plate for 1 h. Plaque agar was prepared by 1:1 mixing of complete DMEM with a 2% (w/v) molten agarose solution, which was cooled to 42°C before use. The virus containing supernatant was removed, cells were washed twice with PBS and then overlaid with 2 ml of plaque agar, tempered to 37°C, and left at room temperature until the agarose had set. Cells were incubated at 37°C for 96–120 h until large viral plaques were visible under the microscope. The agarose was then carefully removed, cells washed once with PBS and fixed with 4% (v/v) formaldehyde at 4°C for 1 h. The cell monolayer was subsequently stained by the addition of 0.5% (w/v) crystal violet stain.

### 2.2.4 Large scale expression and purification of proteins

#### 2.2.4.1 Recombinant protein expression in *E. coli* BL21

Glycerol stocks of transformed *E. coli* BL21 bacteria cells were streaked out onto LB agar plates containing ampicillin, before a single clone was picked to generate a starter culture (described in section 2.2.1.1). These starter cultures were used 1:100 to inoculate LB medium, containing 50 µg/ml ampicillin, and left to grow for approximately 2 h (or until OD<sub>600</sub> reached 0.4–0.6) at 37 °C while shaking. Recombinant protein expression was induced with 1 mM isopropyl-β-D-thio-galactoside (IPTG). Bacteria samples were taken at 0 h, 1 h, 2 h, 3 h and 4 h post-induction, spun down at 5,000 x *g* for 10 min and the pellets stored at -20 °C. The remaining bacteria solution was likewise harvested at 4 h post-induction.

#### 2.2.4.2 Solubilisation of bacterially expressed protein

The pellet of 100 ml bacterial culture (section 2.2.4.1) was resuspended in 5 ml PBS supplemented with 1% Triton X-100 for GST-pulldowns or 5 ml lysis buffer [50 mM Tris, pH 7.6, 0.5 M NaCl, 2 mM MgCl, 50 mM KCl, 1% Triton] for biochemical assays. Resuspended cells were sonicated on ice with 6 x 20 sec bursts and 20 sec breaks in between. After sonication lysozyme (1 mg/ml) from chicken egg white (Sigma-Aldrich®), 1 µl/ml RNase A and 1 µl/ml DNase I were added and bacterial lysates incubated 20 min on ice. Cell debris was spun down at 16,000 x *g* for 30 min at 4°C. A sample of the pellet and the supernatant were stored separately on ice.

#### 2.2.4.3 Purification of GST-tagged proteins

GST-tagged protein was expressed in *E.coli* BL-21 and solubilised as described above (section 2.2.4.1 and 2.2.4.2). Per 100 ml culture 500 µl Glutathione Sepharose™ 4B beads (GE Healthcare) were primed by washing 3 x with 5 ml lysis buffer [50 mM Tris/HCl, pH 7.6, 0.5 M NaCl, 2mM MgCl, 50 mM KCl, 1% Triton ]. Bacteria lysates were then incubated with the GST-beads for 2 h at 4°C with end-over-end mixing. Lysates containing up to 1 ml of beads were added onto a 1 ml polypropylene column (Qiagen) and beads separated by gravity-flow chromatography. The columns were kept at 4°C and washed 4 x with 2ml ice cold wash buffer [50 mM Tris/HCl, pH 7.6, 0.5 M NaCl, 50 mM KCl, 2 mM MgCl<sub>2</sub>] without disturbing the top layer of the packed column. GST-tagged proteins were eluted from the beads with elution buffer [50 mM Tris, pH 7.6, 10 mM reduced Glutathione, 50 mM KCl, 2 mM MgCl<sub>2</sub>]. Fractions of 0.5 ml were collected and analysed for protein by SDS-PAGE and Coomassie blue staining, as described before (2.2.5.2–2.2.5.3). All protein containing fractions were combined and buffer exchange chromatography was performed using PD midiTrap™ G-25 columns (GE Healthcare), following the manufacturer's instructions. Briefly, G-25 columns were primed using 3 x 5 ml of ATPase assay buffer [50 mM Tris/HCl, pH 7.6, 50 mM KCl, 2 mM MgCl<sub>2</sub>], followed by addition of 1 ml of the combined fractions. Final protein was eluted using 1.5 ml ATPase assay buffer. Protein used for large scale compound screening was stored at -20°C; protein used for determination of binding

kinetics was prepared freshly and stored over night at 4°C. All work was performed on ice and all buffers were pre-chilled on ice prior to use.

## **2.2.5 Analysis of proteins**

### **2.2.5.1 Determination of protein concentration**

The concentration of protein samples was determined using the Bio-Rad *DC*<sup>TM</sup> protein assay. In a 96-well plate, 5 µl protein sample or pre-diluted bovine serum albumin (BSA) standards, obtained by 1:2 dilution series of 5 mg/ml BSA stock, were mixed with 25 µl reagent A (an alkaline copper tartrate solution) and 200 µl reagent B (a dilute Folin reagent). After 15 minutes incubation, absorbance was measured at 620 nm using the Infinite® F50 Robotic microplate reader (Tecan).

### **2.2.5.2 SDS-polyacrylamide gel electrophoresis**

Protein samples were separated by their molecular weight using sodium dodecyl sulphate (SDS)-polyacrylamide gel electrophoresis (PAGE). Protein samples were mixed 1:1 with 2 x SDS loading dye [100 mM Tris/HCl, pH 6.8, 4% (w/v) SDS, 20% (v/v) glycerol, 10 mM DTT, 0.25% (w/v) bromophenol blue], subsequently boiled at 95°C for 5 min and loaded alongside the BenchMark<sup>TM</sup> Pre-Stained Protein Ladder (Invitrogen<sup>TM</sup>) onto 10% polyacrylamide gels, composed of a resolving gel [10% (v/v) acrylamide/bis-acrylamide 37.5:1 (Severn Biotech Ltd), 375 mM Tris/HCl; pH 8.8, 0.1% (w/v) SDS, 0.12% (v/v) APS, 0.012% TEMED (v/v)] and stacking gel [5% (v/v) acrylamide/bis-acrylamide 37.5:1, 125 mM Tris/HCl; pH 6.8, 0.1% (w/v) SDS, 0.08% (v/v) APS, 0.008% (v/v) TEMED]. Gels were run at 180 V for 60 min or until the dye front reached the end of the resolving gel. The running buffer was 25 mM Tris, 192 mM Glycine and 0.1 % (w/v) SDS.

#### 2.2.5.3 Coomassie blue staining

Coomassie blue stain [50% (v/v) methanol, 10% (v/v) acetic acid, 0.05% (w/v) Brilliant Blue R-250] was used to permanently stain protein bands on SDS-PAGE gels (section 2.2.5.2). Gels were incubated for 30 min on a rocking platform at room temperature, before a destain solution [50% (v/v) methanol, 10% (v/v) acetic acid] was added and repeatedly exchanged until the desired degree of staining was reached.

#### 2.2.5.4 Western blotting

Protein samples separated by SDS-PAGE (section 2.2.5.2) were transferred to a nitrocellulose Hybond™-C (GE Healthcare) membrane by Western blotting. The set up for the transfer was: blotting pad, two pieces of Whatman filter paper, gel, nitrocellulose membrane, two pieces of Whatman filter paper and blotting pad. Before use, the membrane was pre-soaked alongside the blotting pads and filter paper in transfer buffer (20% (v/v) methanol, 25 mM Tris, 192 mM glycine). The transfer took place at 100 V for 60 min. Unspecific protein binding sites on the membrane were blocked for 1 h at room temperature with 5% (w/v) non-fat milk (Marvel) in Tris buffered saline and Tween-20 (TBS-T) [150 mM NaCl, 50 mM Tris/HCl pH 7.5, 1% (v/v) Tween-20] on a rocking platform. The membrane was then incubated with primary antibody in 2.5% (w/v) non-fat milk in TBS-T for 60 min at room temperature, followed by three 5 min washes in TBS-T. Secondary antibody (HRP-conjugated IgG) was applied in a similar manner as the primary antibody, again followed by washes with TBS-T. Chemiluminescence was developed adding the enhanced chemiluminescence (ECL) system (Geneflow) to the membrane for 1 min. A photographic Hyperfilm ECL™ (GE Healthcare) was then exposed to the membrane for the desired amount of time. The film was processed with a Konica SRX-101A developer.

## 2.2.6 Analysis of protein-protein interactions

### 2.2.6.1 GST-pulldown assay

*E. coli* BL21 lysates were prepared as previously described (section 2.2.4.2), added to 25  $\mu$ l of PBS primed Glutathione Sepharose 4B beads (GE Healthcare) per pulldown and incubated over night while shaking. HEK 293T cells were transfected as described in section 2.2.2.3. Cells were harvested 24 h after transfection at 500 x *g* for 5 min at 4°C, washed once in PBS and lysed for 20 min on ice with 1 ml modified RIPA buffer [150 mM NaCl, 50 mM Tris/HCl; pH 7.6, 1% NP-40] per well of a 6-well plate. Insoluble parts were pelleted at 12,000 x *g* for 10 min at 4°C and the supernatant kept on ice. Glutathione beads were centrifuged at 500 x *g* for 5 min at 4°C and the beads washed five times with washing buffer [250 mM NaCl, 50 mM Tris/HCl; pH 7.5]. After the final wash, a small amount of beads was taken aside to determine the GST protein amount bound to the beads by SDS-PAGE and subsequent Coomassie staining (section 2.2.5.2 and 2.2.5.3). The remaining GST-bound beads were added to the cell lysates and incubated for 4 h at 4°C while rotating. Following incubation, beads were pelleted at 500 x *g* for 5 min at 4°C and washed 5 x in modified RIPA buffer. The pelleted beads were resuspended in 75  $\mu$ l of SDS loading buffer for protein separation by SDS-PAGE and analysis by Western blotting (described under 2.2.5.2 and 2.2.5.4).

### 2.2.6.2 Co-immunoprecipitation assay

For co-immunoprecipitation assays, 293T cells were transfected as described in section 2.2.2.3. Transfected cells from a 6-well plate were harvested 24 h after transfection at 500 x *g* for 5 min at 4°C, washed once with PBS and lysed for 20 min on ice using 1 ml of modified RIPA buffer. The insoluble fraction was pelleted at 16,000 x *g* and the supernatant kept on ice, to which 1  $\mu$ l/ml RNase A was added to remove any protein/RNA interactions. Depending on whether the protein to be immunoprecipitated was GFP- or FLAG-tagged, 25  $\mu$ l slurry of anti-DDDDK tag (equivalent to FLAG) coupled agarose beads (Abcam®) or 20  $\mu$ l slurry of GFP-trap® beads (ChromoTek®) were used per immunoprecipitation. Before immunoprecipitation, beads were pelleted at 500 x *g* for 5 min at 4°C and washed 3 x with modified RIPA buffer to remove residual storage buffer. To remove

non-specific protein binding to the beads, the cell lysates were pre-cleared by incubation of 20  $\mu$ l of protein A-conjugated agarose beads (Roche) for 2 h at 4 °C with rotation. The beads were then pelleted at 500 x *g* for 5 min at 4°C and the pre-cleared supernatant transferred onto the prepared FLAG affinity or GFP-trap® beads. Where indicated, 1  $\mu$ l, 7.5  $\mu$ l, 12.5  $\mu$ l or 17.5  $\mu$ l ATP, ATP $\gamma$ S or ADP were added from a 100 mM stock (in 50 mM Tris/HCl, pH 7.6), to achieve 0.1 mM, 0.75 mM, 1.25 mM or 1.75 mM ATP, ATP $\gamma$ S or ADP per co-immunoprecipitation, as described for each experiment. Alternatively, 3.33  $\mu$ l DMSO control or small molecule inhibitor C2 (150 mM in DMSO) were added to the beads and lysate, as described. The beads were incubated for 2.5 h at 4°C under rotation and subsequently centrifuged at 500 x *g* for 5 min at 4°C and washed 5 x in ice cold modified RIPA buffer. The agarose-antibody-antigen complex was then taken up in 70  $\mu$ l SDS-loading buffer and eluted by heating to 95°C, to be analysed by SDS-gel and Western blotting.

#### 2.2.6.3 Immunofluorescence microscopy

293T cells were grown in 12-well plates containing sterile glass coverslips, which had been previously coated with poly-L lysine (Sigma-Aldrich®) for 5 min and washed with PBS. At 50% confluence, cells were transfected with expression plasmids as described in section 2.2.2.3. TREX BCBL1-Rta cells were seeded at a concentration of  $1 \times 10^6$  cells/ml on poly-L lysine treated glass coverslips. KSHV lytic replication was induced at the time of seeding, as described before (section 2.2.3.1). Before fixation, cells were washed with PBS and then fixed with 4% (v/v) paraformaldehyde for 10 min at room temperature, unless otherwise stated. Paraformaldehyde was removed and the cells washed twice in PBS, followed by permeabilisation with 1% (v/v) Triton X-100 in PBS for 15 min at room temperature. To block non-specific binding, 1% (w/v) BSA in PBS was added and the cells incubated for 60 min at 37°C. Cells were then incubated with primary antibodies in PBS and 1% BSA (w/v) for 60 min in a humidity chamber at 37°C. After three washes with PBS, Alexa Fluor®-conjugated secondary antibodies were incubated under the same conditions. Following three washes with PBS, coverslips were mounted onto microscope slides with DAPI containing mounting medium (VECTASHIELD®, Vector Laboratories) for detection of nuclei. The slides were stored in the dark at 4°C until visualised on an inverted LSM 700 Axio Observer Z1 confocal microscope (Zeiss).

## **2.2.7 Biochemical assays**

### **2.2.7.1 ATPase assay**

ATPase assays were performed in 96-well plates, with a total reaction volume of 50  $\mu$ l. ATP- and yeast tRNA-stocks were added to assay buffer to give the following assay conditions:

35  $\mu$ M ATP (unless otherwise indicated)

50  $\mu$ M yeast tRNA

50 mM Tris/HCl, pH 7.6

50 mM KCl

2 mM MgCl<sub>2</sub>

Where indicated, small molecules, fragments and ATP-analogues were diluted in DMSO or buffer as needed and 5  $\mu$ l of the inhibitor or control was added to each reaction (10% total DMSO). For IC<sub>50</sub> measurements, inhibitors were added in 0.25  $\mu$ l DMSO (giving a total of 0.5% DMSO in the assay). The ATPase reaction was started by the addition of purified UAP56 (section 2.2.4.3), with varying concentrations as described for each experiment, and incubated for 30 min at 37°C. Plates were cooled to room temperature for 2 min, before 50  $\mu$ l Kinase-Glo® Reagent (Promega) was added to each reaction and plates were incubated for a further 10 min at room temperature, in the dark. Luminescence was measured using the FLUOstar OPTIMA plate reader (BMG LABTECH), three times over a period of 15 min to ensure a stable signal. The signal intensity is directly correlated to the concentration of ATP remaining in each assay, which could be calculated using the control wells containing GST protein (0% enzyme activity) or UAP56 and no inhibitor (100% enzyme activity) and background measurements of GST protein in buffer (no ATP).

## **2.2.8 Analysis of mRNA**

### **2.2.8.1 Fluorescence *in situ* hybridisation (FISH)**

To detect polyadenylated (poly(A)) RNA in 293T cells, cells were transfected and fixed with 4% (v/v) paraformaldehyde as described under 2.2.2.3 and 2.2.6.3. Cells were

permeabilised with 0.5% Triton X-100 for 5 min and washed twice with PBS and once with 2 x saline-sodium citrate (SSC) buffer [300mM NaCl, 30 mM sodium citrate; pH 7.0] for 10 min at room temperature. A fluorescently labelled oligo(dT) probe was added at a final concentration of 1 µg/ml in ULTRAhyb® hybridization buffer (Ambion®) and incubated for 16–20 h at 42°C. Cells were washed twice with 2 x SSC, once with 0.5 x SSC and once with PBS. Coverslips were mounted using VECTASHIELD® + DAPI (Vector Laboratories) and visualised on an inverted LSM 700 Axio Observer Z1 confocal microscope (Zeiss).

#### 2.2.8.2 Nucleocytoplasmic fractionation for viral mRNA export assay

TREx BCBL1-Rta and 293T cells were grown and either induced or transfected as described in section 2.2.2.3 and 2.2.3.1. After 24 h, cells were washed off the plate with ice cold PBS and pelleted at 500 x *g* for 5 min at 4 °C. Cell pellets were resuspended in 600 µl of PBS with 1 % Triton (v/v) and 1 µl/ml RNase OUT (Invitrogen™) and lysed for 10 min on ice. Of this mixture, 250 µl were kept for analysis as whole cell fraction and the remaining 350 µl were centrifuged at 2000 x *g* for 5 min at 4 °C. The supernatant, containing the cytoplasmic fraction, was transferred to a new microcentrifuge tube for further processing, whereas the pelleted nuclei were washed in 1 ml of PBS and centrifuged again at 2000 x *g* for 5 min at 4 °C. The wash buffer was discarded and the nuclei resuspended in 200 µl PBS with 1 % Triton (v/v) and 1 µl/ml RNase OUT. A small sample was taken of each fraction to analyse protein by SDS-PAGE and Western blotting (section 2.2.5.2 and 2.2.5.4), before the fractions were immediately further processed for total RNA extraction and subsequent qRT-PCR, the steps of which are described below (section 2.2.8.3–2.2.8.6).

#### 2.2.8.3 Total RNA isolation

Total RNA was isolated from cells or cellular fractions with the use of TRIzol (Invitrogen™), according to the manufacturer's instruction. To each sample containing 2 x 10<sup>6</sup> TREx BCBL1-Rta or confluent 293T cells from one well of a 6-well plate, 1 ml TRIzol was added. Cells or cell fractions were homogenised in TRIzol for 5 min at room temperature, then 200 µl of chloroform were added and samples were vigorously shaken and incubated for

another 2 min at room temperature. Samples were centrifuged at 10,000 x *g* for 15 min at 4°C in order to separate the aqueous from the organic phenol phase. The 500 µl of the upper layer, the RNA-containing aqueous phase, was transferred into a new microcentrifuge tube containing 500 µl of isopropanol. Samples were mixed and incubated for 10 min at room temperature. Total RNA was precipitated by centrifugation of the samples at 10,000 x *g* for 10 min at 4°C. The supernatant was discarded, the RNA pellet washed in 70% ethanol and centrifuged at 10,000 x *g* for 5 min at 4°C. Again, the supernatant was discarded and the pellet air dried at room temperature for approximately 5 min. The RNA pellet was resuspended in 20 µl of DNase and RNase free H<sub>2</sub>O (Sigma-Aldrich®).

#### 2.2.8.4 DNase treatment

To remove contaminating DNA from RNA, samples were treated with the DNA-free™ DNA removal kit from Ambion® following the manufacturer's instructions. Briefly, 0.1 volumes of 10 x DNase I buffer and 1 µl of DNase I were added per sample and incubated for 30 min at 37 °C. Following DNA-digestion, each sample was treated with 0.1 volumes of DNase inactivating reagent and gently mixed for 2 min at room temperature. The DNase inactivating reagent was pelleted from the RNA solution by centrifugation at 7,500 x *g* for 1.5 min at 4 °C. The supernatant was transferred to a new microcentrifuge tube. Purified RNA was stored at -80°C.

#### 2.2.8.5 Reverse transcription

RNA concentration was measured using the NanoDrop ND-1000 spectrophotometer (NanoDrop Technologies) and diluted to 500 µg/ml before reverse transcription was carried out to synthesise cDNA. The following master mix was added to 2 µl of RNA (1 µg total RNA):

- 1 µl Oligo(dT)15 (500 µg/ml)
- 1 µl dNTP mix (2.5 mM/dNTP)
- 8 µl DNase/RNase free H<sub>2</sub>O

The mixture was incubated at 60°C for 5 min and then immediately cooled on ice and combined with the following master mix:

- 1 µl M-MuLV Reverse Transcriptase (RT)
- 4 µl 5x M-MuLV Reverse Transcriptase Reaction Buffer
- 2 µl 0.1 M DTT
- 1 µl RNase OUT™ (40 U/µl)

Samples were also prepared containing the same master mix, but omitting the reverse transcriptase, as negative RT control (-RT). The mixture was incubated at 42°C for 50 min, followed by inactivation of the reverse transcriptase at 90°C for 10 min. The cDNA was stored at -20°C.

#### 2.2.8.6 Quantitative real-time PCR (qPCR)

Levels of cDNA or DNA were quantified by qPCR using a Rotor-Gene 6000 Real-Time PCR machine (QIAGEN) and sequence-specific primers. For each sample 5 µl cDNA, as well as -RT samples as no-template control, were added to the following master-mix in 0.1 ml strip tubes (QIAGEN):

- 12.5 µl 2x SensiMix™*Plus* SYBR (Bioline)
- 2 µl (10 µM) forward primer
- 2 µl (10 µM) reverse primer
- 3.5 µl DNase/RNase free H<sub>2</sub>O

After an initial denaturation step of 95°C for 10 minutes, the cycling programme for qPCR was 35 cycles of a standard 3-step melt cycle, with the following parameters: denaturation at 95°C for 15 sec, annealing at 60°C for 30 sec and elongation at 72°C for 20 sec. Data was acquired during the elongation step of each cycle and analysed using the Rotor-Gene 6000 Series Software Version 1.7. After qPCR, a melting curve analysis was performed to confirm amplification of a single product. Samples were normalised against the housekeeping gene *GAPDH* and quantified using the comparative C<sub>t</sub> method.

## Chapter 3

~

A novel interaction of KSHV ORF57 with CIP29, a hTREX  
component

### 3 A novel interaction of ORF57 with CIP29, a hTREX component

#### 3.1 Introduction

The hTREX complex is a multiprotein complex that facilitates cellular bulk mRNA export, from the nucleus into the cytoplasm. It consists of the following core components: UAP56, a RNA-helicase, which is thought to bind to RNA in the early stages of spliceosome formation, the export adaptor Aly, as well as the hTHO complex proteins hTho1, hTho2, fSAP24, fSAP35 and fSAP79 (Luo et al., 2001; Masuda et al., 2005). Redundancy was shown for Aly, as UIF can replace the export adaptor in hTREX (Hautbergue et al., 2009). More recently, the proteins CIP29, Chtop, SKAR and ZC11A were also identified as hTREX components (Dufu et al., 2010; Chang et al., 2013; Folco et al., 2012). Complex assembly is strongly coupled to cellular mRNA maturation steps, ensuring export of only correctly processed mRNAs. Together, the hTREX complex then provides a binding platform for the nuclear export factor Nxf1 and its co-factor Nxt1, allowing transport of mRNA cargo through the well controlled NPC.

KSHV ORF57 is a multifunctional protein involved in all stages of viral mRNA processing. As many viral mRNAs are intronless, ORF57 recruits the hTREX complex, to form an export competent vRNP and facilitate efficient nuclear export of viral mRNAs. ORF57 is known to directly interact with the mRNA export adaptor proteins Aly and UIF (Boyne et al., 2008; Jackson et al., 2011), which facilitates subsequent recruitment of UAP56 and THO onto viral intronless transcripts. Furthermore, ORF57 interactions have also been shown for more recently identified hTREX proteins Chtop and SKAR (Baquero-Perez, unpublished data). We therefore speculated that CIP29 is also part of the ORF57-facilitated vRNP.

In this results chapter, the interaction of ORF57 with CIP29 was examined through a range of techniques, such as GST-pulldowns, co-immunoprecipitations and immunofluorescence. Moreover, the role of CIP29 in ORF57-mediated export of viral mRNA was investigated through depletion studies of CIP29. Similarly, the requirement of CIP29 for KSHV lytic replication was also assessed. Finally, as ATP-dependent formation of a trimeric complex consisting of UAP56, Aly and CIP29 was shown *in vitro* (Dufu et al., 2010), it was examined whether a similar effect could be seen in the presence of ORF57.

### 3.2 GST pulldowns show an interaction between CIP29 and ORF57

To examine if an interaction occurs between ORF57 and CIP29, GST-pulldowns were performed. Initially, bacterial expression vectors encoding GST and GST-tagged CIP29 were transformed into the *E. coli* strain BL21. Protein expression was induced by the addition of IPTG and samples were taken over a 4 h time period to monitor recombinant protein induction. The samples were then analysed by SDS-PAGE and Coomassie blue staining (Figure 3.1). Both proteins were seen to induce well over a 4 h period.

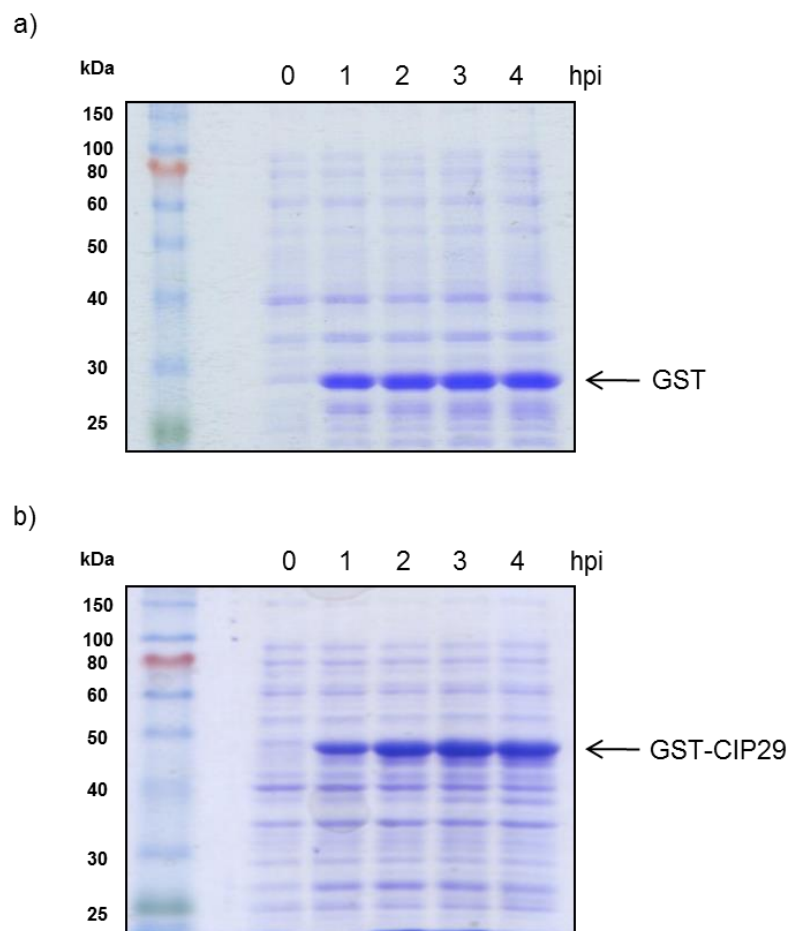


**Figure 3.1: Induction of bacterially expressed GST and GST-CIP29.** Protein samples were separated using SDS-PAGE and stained with Coomassie blue. The lanes contain a molecular weight marker and samples taken at indicated hours post induction (hpi).

The recombinant protein from the 4 h induction was solubilised and bound to glutathione-conjugated agarose beads. Prior to pulldown analysis, the amounts of protein bound to beads was again analysed by Coomassie blue staining (Figure 3.2), to ensure that an equal

amount of bound protein was thereafter used for each pulldown. Both proteins were observed to bind well to the beads. Although, CIP29 does show a number of smaller bands, it is unknown whether these are GST-CIP29 breakdown products or other bacterial proteins.

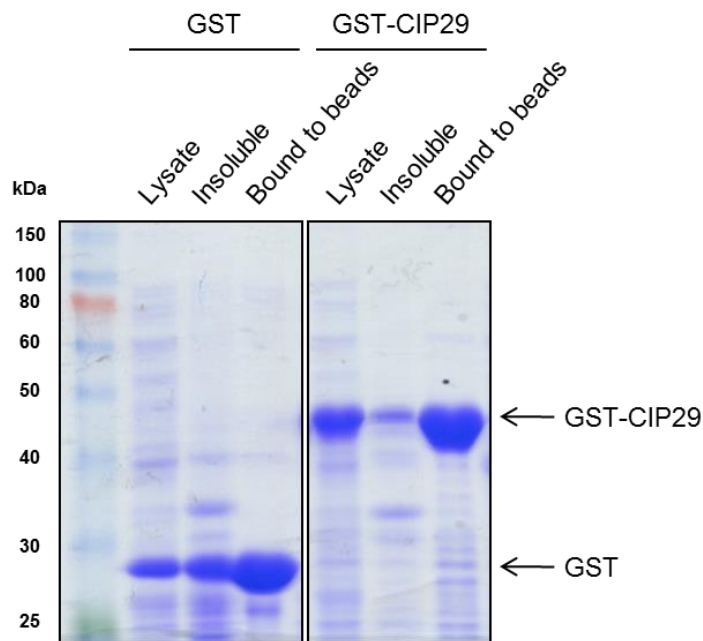


**Figure 3.2: Binding of GST and GST-CIP29 to glutathione-conjugated agarose beads.** Protein samples were separated using SDS-PAGE and stained with Coomassie blue. For each protein the following samples were loaded: Bacteria lysate obtained 4 h after induction, insoluble protein found in the pellet after centrifugation of the lysate and protein bound to agarose beads.

The bead-bound GST and GST-CIP29 proteins were then used for pulldowns to investigate ORF57 binding. For this, GFP, UIF-GFP or ORF57-GFP were expressed in 293T cells for 24 h and cell lysates then incubated with the protein-associated beads. As the beads were sedimented, proteins and protein complexes binding to GST or CIP29 would also be precipitated. Analysis of the sediment by SDS-PAGE and western blotting shows bands for all interacting proteins (Figure 3.3). GFP, which was used as a negative control, is shown to be strongly expressed in 293T cells (Lysate), but no interaction with GST or GST-CIP29 can be observed. GFP-tagged UIF, a known member of the hTREX complex, was used as a positive control. UIF is specifically pulled down with GST-CIP29, while no interaction is observed with GST alone. In a similar manner, ORF57 is shown to interact with CIP29, but not with GST. The observed bands for ORF57 represent full length ORF57-GFP and a caspase-7 cleavage product of the fusion protein, in which 33 amino acids are removed

from the N-terminus (Majerciak et al., 2010). This is the first time that CIP29 has been shown to interact with the viral ORF57 protein.

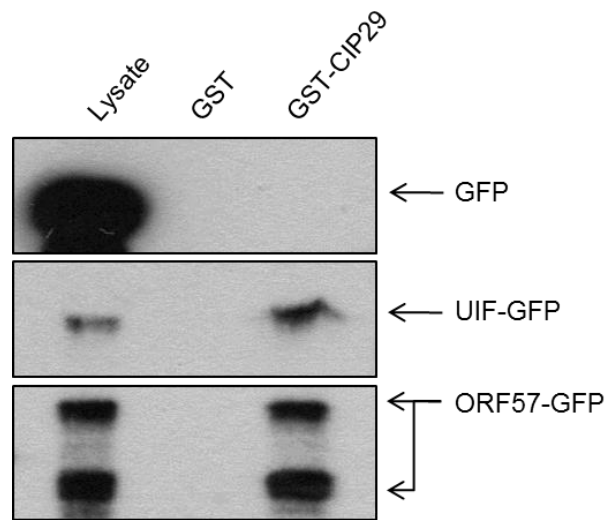


**Figure 3.3: GST-pulldown assay shows CIP29 interacting with ORF57 and UIF.** Eukaryotic cells were transfected with plasmids expressing GFP, UIF-GFP or ORF57-GFP and the lysates incubated with GST- or GST-CIP29-bound beads. Beads were precipitated and the sediment, as well as utilised cell lysates, were analysed using SDS-PAGE and Western blotting, which was probed using GFP-specific antibodies.

### 3.3 Co-Immunoprecipitation assays confirm an interaction between CIP29 and ORF57

To confirm the results of the pulldown assay and to study if the protein-protein interaction takes place in a cellular system, co-immunoprecipitations were employed. Here, 293T cells were co-transfected with FLAG-CIP29 and GFP, UIF-GFP or ORF57-GFP. As a negative control FLAG- $\beta$ -catenin was also co-transfected with GFP, UIF-GFP or ORF57-GFP. After 24 h, cell lysates were incubated with FLAG-affinity beads, in order to precipitate all protein complexes associating to CIP29 or  $\beta$ -catenin. RNase and DNase were added to the cell lysates prior to incubation with the beads. The precipitate was then analysed by SDS-PAGE and Western blotting, using GFP- and FLAG-specific antibodies (Figure 3.4). The co-immunoprecipitation assay confirmed the results of the GST-pulldowns, showing an interaction of CIP29 with ORF57, as well as UIF. Both proteins precipitate specifically alongside CIP29, in contrast to GFP-expressing cells. As RNase was added it is likely that this interaction is based on a protein-protein interaction. However, it still needs to be confirmed that all RNA, which can bridge two mRNA binding proteins, was degraded using

RNase. The control experiment using FLAG- $\beta$ -catenin shows no interactions with ORF57, confirming the above mentioned interactions are CIP29-specific.

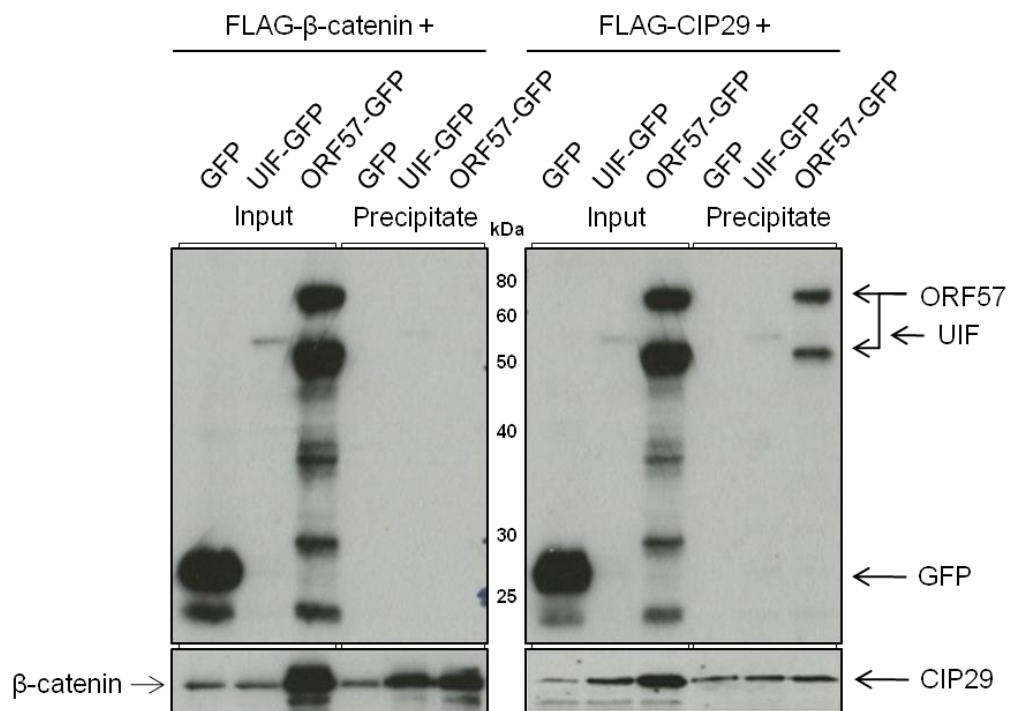


**Figure 3.4: Co-Immunoprecipitations confirm an interaction of CIP29 with ORF57 and UIF.** Cells were co-transfected with plasmids expressing FLAG-CIP29 and GFP, UIF-GFP or ORF57-GFP. Transfection of plasmids expressing FLAG- $\beta$ -catenin and GFP, UIF-GFP or ORF57-GFP was used as a negative control. Cell lysates were incubated with FLAG-affinity beads. Cell lysates (Input) and precipitated proteins (Precipitate) were analysed by SDS-PAGE and western blotting, probing with a GFP-specific antibody (top) and a FLAG-specific antibody (bottom).

### 3.4 Immunofluorescence microscopy shows ORF57 dependent relocalisation of CIP29

Immunofluorescence microscopy was employed to examine the subcellular localisation of CIP29 in the absence and presence of ORF57. For this, cells were transfected with GFP or ORF57-GFP alone. After fixation and permeabilisation, cells were immunostained using antibodies recognising endogenous CIP29 as well as B23.1, a nucleolar marker (Figure 3.5). Endogenous CIP29 can be observed predominantly in the nucleus of the cell in the presence of GFP. Specifically, CIP29 is excluded from the nucleolus (arrows), which is highlighted by the nucleolar marker B23.1, and instead appears in bright, punctuate speckles as has been described previously (Dufu et al., 2010). In contrast, ORF57 contains a

nucleolar localisation signal and is known to recruit hTREX components into the nucleolus. Accordingly, co-localisation of CIP29 and ORF57 was observed in the nucleolus, in ORF57-GFP transfected cells. Only minor amounts of CIP29 remain outside the nucleolus suggesting a redistribution of CIP29 from the nuclear speckles into the nucleolus by the ORF57 protein.

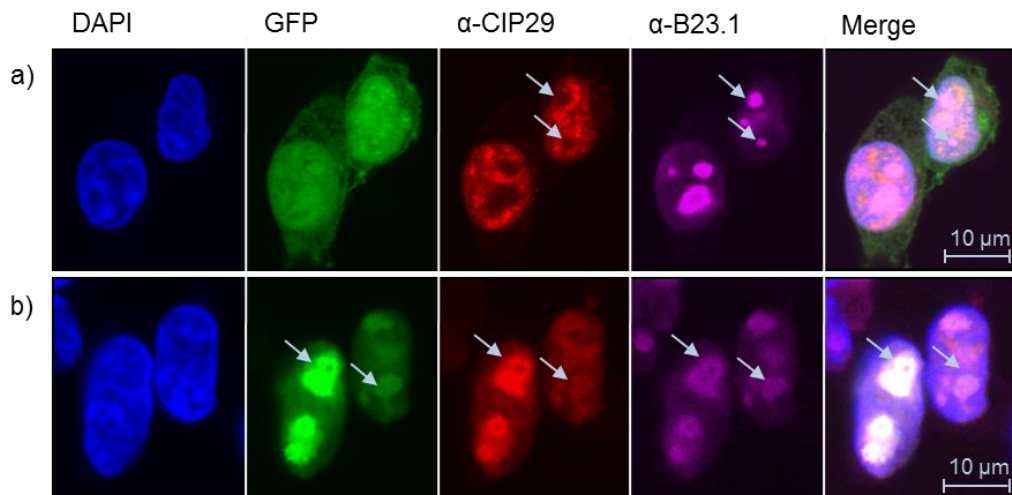


**Figure 3.5: Overexpression of ORF57 causes re-localisation of endogenous CIP29.** Cells were transfected with plasmids expressing GFP (a) or ORF57-GFP (b) for 24 h, cells were then fixed and permeabilised. Cells were stained using CIP29- (red) and B23.1-specific antibodies (pink). DAPI staining (blue) indicates the nucleus and ORF57 was visualised by GFP-fluorescence.

The same technique was employed using transfected FLAG-CIP29 and ORF57-GFP to examine if over-expressed and FLAG-tagged protein behaves in a similar manner. Cells were transfected with FLAG-CIP29 alone or co-transfected with ORF57-GFP and then immunostained using antibodies against the FLAG-tag (pink) and B23.1 (red) (Figure 3.6). Results show that FLAG-CIP29, like endogenous CIP29, localises to the nuclear speckles and is excluded from the nucleolus (arrows). Furthermore, when co-expressed with ORF57, re-localisation of FLAG-CIP29 to the nucleolus is observed. Both proteins are also present in the nuclear speckles, as can be seen on the merged image.

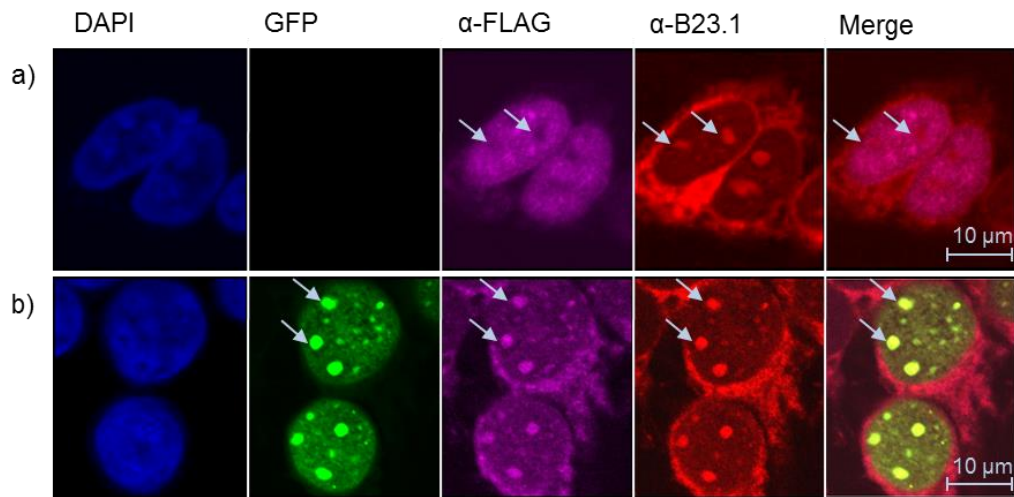


**Figure 3.6: Overexpression of ORF57 leads to a redistribution of recombinant CIP29.** Cells were transfected with a FLAG-CIP29 expression plasmid alone (a) or co-transfected with plasmids expressing FLAG-CIP29 and ORF57-GFP (b), fixed (1 h in ice-cold methanol) and permeabilised. Cells were stained using FLAG-specific antibodies to visualise CIP29 (pink), B23.1-specific antibodies (red) as a nucleolar marker and DAPI (blue), for staining the nucleus. ORF57 was detected by direct GFP fluorescence.

### 3.5 Role of CIP29 in UAP56-mediated ATP hydrolysis

UAP56, a central hTREX component is a RNA-helicase with reported ATPase activity (Shen et al., 2007). Recently, an ATP-dependent interaction has been shown for UAP56, binding to Aly and CIP29, to form a trimeric complex (Dufu et al., 2010). We therefore wanted to assess the role of CIP29 in UAP56-mediated ATP hydrolysis. To this end, bacterially expressed GST-Aly, GST-UAP56 and GST-CIP29 were bound and purified on Glutathione-beads and, after elution from the beads, run on a buffer exchange column. Samples of all stages of the purification were analysed by SDS-PAGE and visualised using Coomassie staining (Figure 3.7).

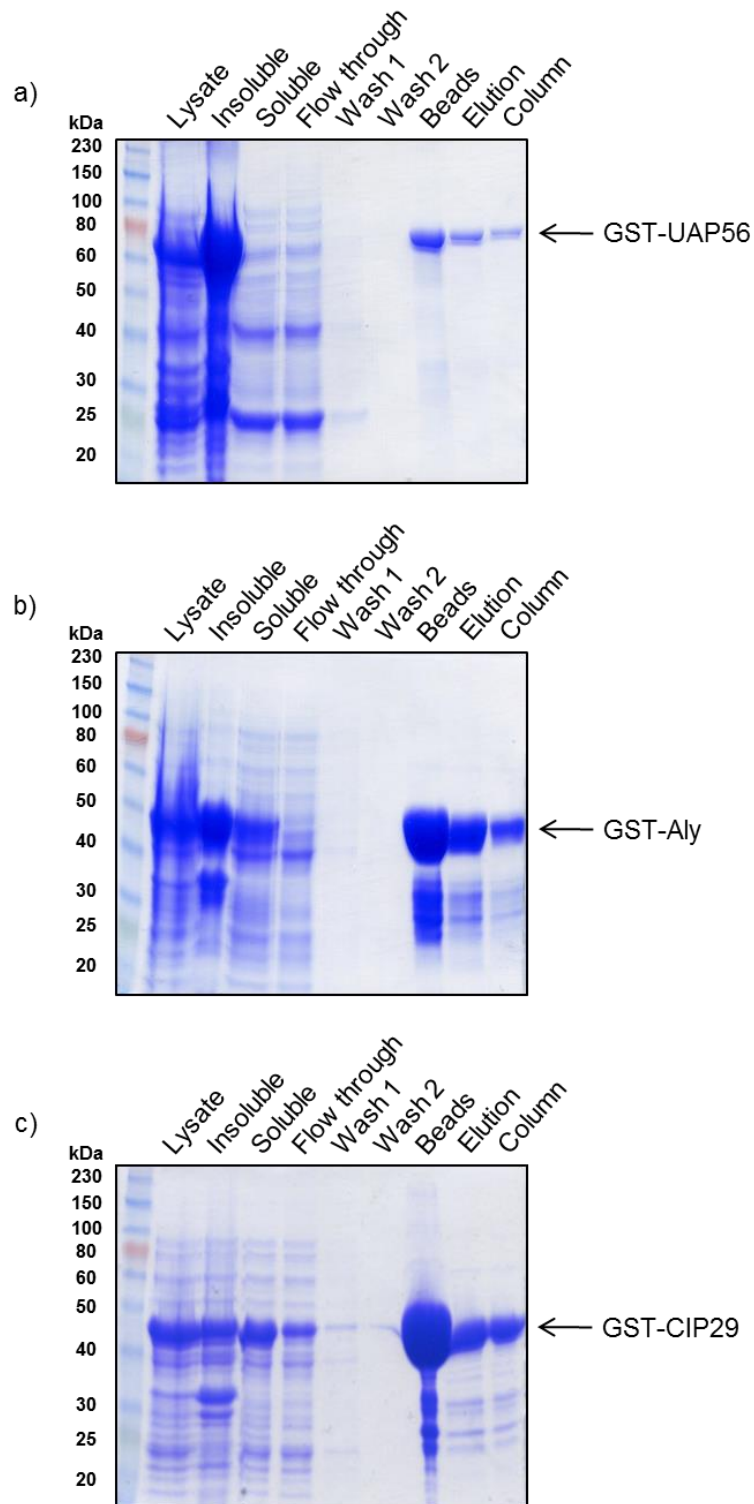


**Figure 3.7: Purification of GST-tagged hTREX components.** a) UAP56, b) Aly and c) CIP29 were expressed over 4 h in *E. coli* BL21 and analysed by SDS-PAGE and Coomassie blue staining. Samples are as follows: Whole cell lysate, insoluble fraction, soluble fraction, flow through after 2 h binding to Glutathione-beads, flow through of washing steps 1 and 2, all protein bound to Glutathione-beads after washing, protein eluted with Glutathione and protein after a buffer exchange column.

While GST-Aly and GST-CIP29 express to high levels and can be found in large parts in the soluble fraction, GST-UAP56 also expresses well, but remains mostly insoluble after lysis of the cells. Accordingly, the amount of protein bound to beads and eluted is notably less. Nonetheless, relatively pure protein samples were obtained for all three GST-tagged components of the hTREX complex. Both for GST-Aly and GST-CIP29 breakdown products can be seen binding to and being eluted from beads. However, the amounts of cleaved protein seem negligible in comparison to the quantity of full sized protein.

Purified proteins were then used at 1.5  $\mu\text{M}$  each in an ATPase assay. The ATPase activity of UAP56, Aly and CIP29 were assessed on their own and in combination. For this, proteins were mixed with a known concentration of ATP and yeast tRNA and left for 30 mins at 37°C. Remaining ATP was then quantified using a luciferase reaction, creating a luminescent signal, which directly correlated to the total ATP remaining. This amount was subtracted from the input, to get an overview of ATPase activity of the individual hTREX components (Figure 3.8). It is apparent that UAP56 hydrolyses ATP, whereas Aly and CIP29 did not display any ATPase activity on their own, or when both are combined. However, both proteins appear to stimulate the ATPase activity of UAP56 to about 2-fold, when present in the reaction. Interestingly, the presence of Aly and CIP29 together does not increase ATP hydrolysis of UAP56 further than the presence of just one protein.

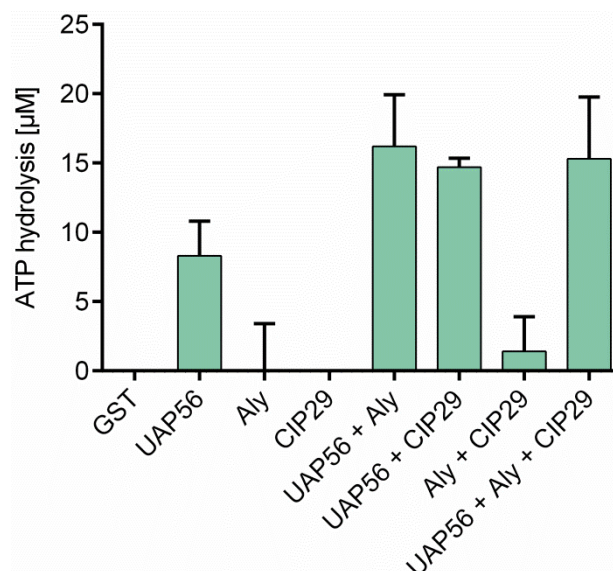


**Figure 3.8: CIP29 stimulates UAP56 ATPase activity *in vitro*.** Purified proteins were incubated at 1.5  $\mu\text{M}$  each with 50  $\mu\text{M}$  ATP for 30 min, before remaining ATP was quantified using a luminescent signal from a luciferase reaction.  $n = 3$ , error bars indicate the SD.

### **3.6 An ATP-dependent interaction of hTREX components affects the ability of ORF57 to interact with CIP29**

After establishing that CIP29 functions as a co-factor to UAP56-mediated ATP hydrolysis, the effect of the ATP-dependent interaction of Aly, UAP56 and CIP29, on the ability of ORF57 to interact with the hTREX proteins, was explored. For this co-immunoprecipitations were performed using FLAG-CIP29 and ORF57-GFP as described previously (section 3.3), but utilised FLAG-PYM as an ATP-independent positive control. The co-immunoprecipitations of FLAG-PYM and FLAG-CIP29 were performed in duplicate, once in the presence of ATP and once in the presence of Adenosine 5'-O-(3-thio)triphosphate (ATP $\gamma$ S), a non-hydrolysable ATP analogue. As ATP $\gamma$ S has a similar binding affinity to UAP56 as ATP (Taniguchi and Ohno, 2008), we speculated that any endogenous ATP present in the cell lysate would be efficiently displaced by the presence of 1.25 mM ATP $\gamma$ S. Similarly, we utilised 1.25 mM ATP for the ATP-positive immunoprecipitations. Proteins were sedimented using FLAG-affinity beads and analysed by Western blotting using GFP- and FLAG-specific antibodies (Figure 3.9a). ORF57 is seen to be specifically precipitated by FLAG-PYM and FLAG-CIP29 in the presence of ATP. In the presence of ATP $\gamma$ S, ORF57 still interacts with FLAG-PYM, however, the interaction with FLAG-CIP29 is virtually abolished. Quantification of the Western blots was performed for three individual experiments. Band intensity for each protein is displayed as a fold increase compared to the according precipitate in the presence of ATP (Figure 3.9b). This shows a significant loss of ORF57 precipitated by CIP29 in the presence of ATP $\gamma$ S. Compared to this, no significant difference is seen in the amount of ORF57 precipitated by PYM, in the presence of the non-hydrolysable ATP analogue. Furthermore, both FLAG-PYM and FLAG-CIP29 are found to bind to the beads equally in the presence of ATP and ATP $\gamma$ S, suggesting that the effect is specific for the interaction of ORF57 with hTREX component CIP29.

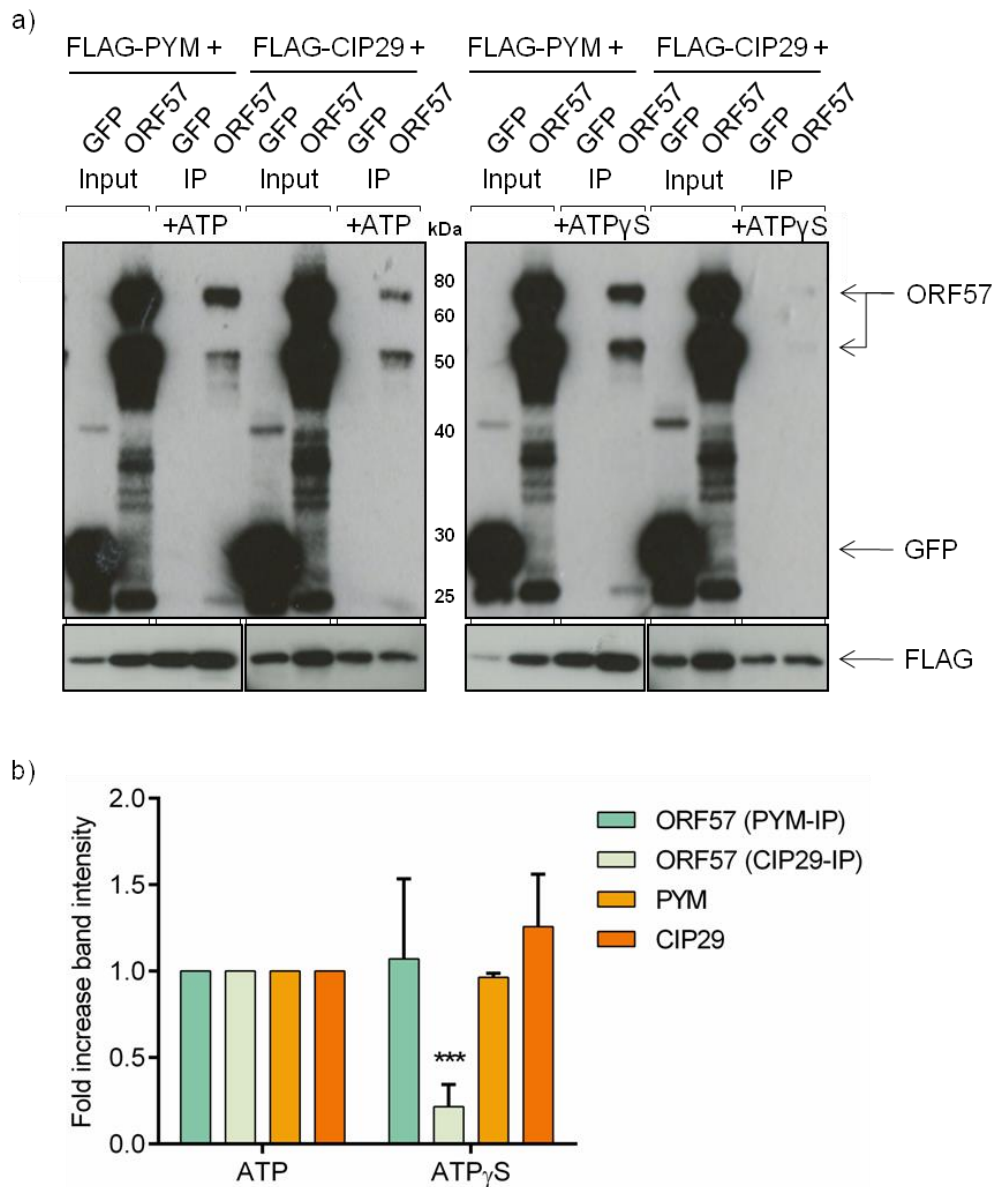


**Figure 3.9: ATP needs to be present for ORF57 to interact with CIP29.** a) Co-immunoprecipitations were performed as before (section 3.3) in the presence of 1.25 mM ATP or 1.25 mM ATP<sub>γ</sub>S. FLAG-PYM was utilised as a positive control not affected by ATP-dependency. b) Quantification of band intensities by ImageJ software. Values are average of 3 independent immunoprecipitations, error bars present the SD.  $p < 0.001$  effect of ATP<sub>γ</sub>S compared to ATP.

### 3.7 Role of CIP29 in ORF57-mediated export of viral intronless mRNAs

To assess the role of CIP29 in ORF57-mediated viral intronless mRNA export an mRNA export assay was performed in CIP29-depleted cells. The hTREC component can be efficiently knocked down by transfection of CIP29-specific siRNA for 72 h. Protein samples

were taken at 0, 24, 48 and 72 h and analysed by Western blotting using CIP29- and GAPDH-specific antibodies (Figure 3.10).

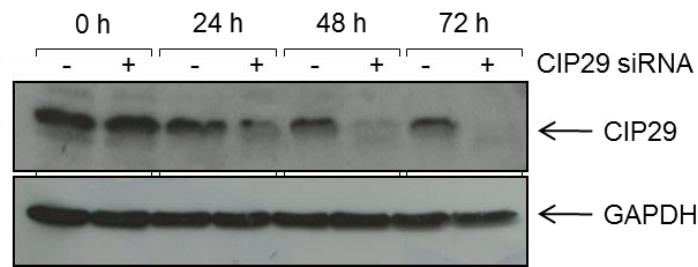


**Figure 3.10: Knock-down of CIP29 using siRNA in 293T cells.** Cells were transfected with CIP29-specific siRNA at 0 and 24 h. Cells were harvested at 0, 24, 48 and 72 h and protein expression analysed by SDS-PAGE and Western blotting using CIP29- and GAPDH-specific antibodies.

For the mRNA export assay, cells were transfected with CIP29 siRNA for 48 h, prior to transfection with GFP or ORF57-GFP expression plasmids, as well as an intronless ORF47 reporter plasmid. This intronless construct generates viral intronless transcripts that were used as reporter mRNA in this assay. At the 72 h time point, cells were fractionated in order to obtain a whole cell and a cytoplasmic fraction. Knock-down, protein expression and fractionation were controlled by Western blotting (Figure 3.11a). Effective knock-down of CIP29 can be seen in whole cell and cytoplasmic samples transfected with CIP29-specific siRNA. GAPDH was used as a loading control for all protein samples. RNA from fractionated samples was then extracted and DNase treated, before generation of cDNA and analysis by quantitative PCR (qPCR). Results are presented as the fold increase of ORF47 mRNA relative to ORF47 amounts in scrambled siRNA (siScr-) and GFP-transfected controls for each fraction (Figure 3.11b). Knock-down of CIP29 in GFP-transfected cells appears not to affect whole cell or cytoplasmic levels of ORF47 mRNA, whereas expression of ORF57 in scrambled control cells leads to a 4-fold increase in whole cell reporter mRNA. ORF57 is known to stabilise, protect and accumulate viral intronless transcripts, hence this effect is not unexpected (Kirshner et al., 2000; Stubbs et al., 2012; Nekorchuk et al., 2007). Moreover, cytoplasmic levels of ORF47 reporter mRNA are significantly increased in the presence of ORF57, compared to whole cell levels, confirming ORF57-mediated intronless ORF47 mRNA export, in addition to accumulation of the transcript. Surprisingly, in ORF57-transfected samples which have been depleted of CIP29 by siRNA, a further enhancement in whole cell ORF47 mRNA is observed. This effect of another 2-fold increase compared to

siScr samples is statistically significant. Similarly, cytoplasmic fractions of these samples again show a significant increase in mRNA export, indicating that loss of CIP29 does not affect the export function of ORF57. Interestingly, while total ORF47 amounts in cells with CIP29 knock-down are larger than in undepleted cells, mRNA export in relation to whole cell amounts remains similar: Both sets of samples show 1.5-fold increase in exported reporter mRNA compared to whole cell mRNA. This indicates that CIP29 knock-down does not affect specific mRNA export pathways.

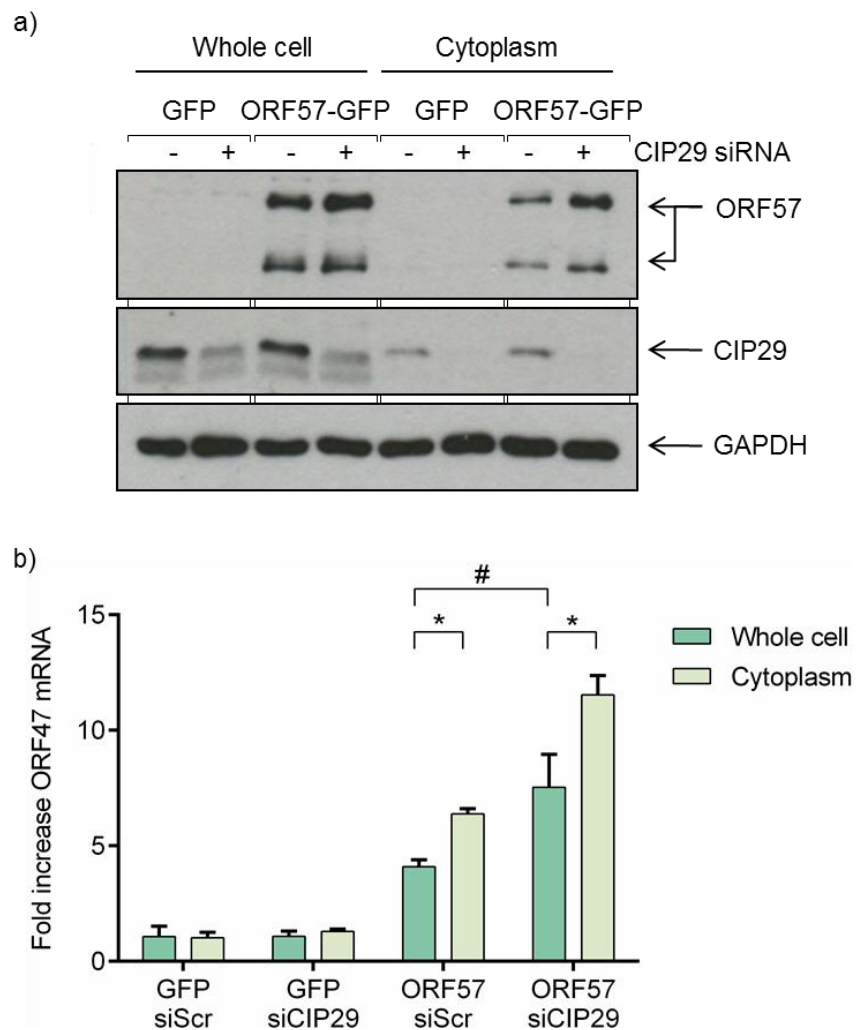


**Figure 3.11: CIP29 knock-down does not affect ORF57-mediated mRNA export.** 293T cells were transfected with scrambled or CIP29-specific siRNA at 0 and 24 h and then transfected with GFP or ORF57-GFP and an ORF47 reporter construct at 48 h. At 72 h cells were harvested and fractionated. a) Protein samples of fractions were analysed by SDS-PAGE and Western blotting, using ORF57-, CIP29- and GAPDH-specific antibodies. b) qRT-PCR results using ORF47- and GAPDH-specific primers. ORF47 CT values were normalised to GAPDH and the relative increase calculated using the  $\Delta\Delta\text{CT}$  method.  $n = 3$ , error bars display SD,  $p < 0.05$ .

### 3.8 Loss of CIP29 does not affect KSHV late protein expression

To examine effects of CIP29 knock-down on KSHV lytic replication, 293 rKSHV.219 cells were utilised, a 293T cell line containing a recombinant bacterial artificial chromosome containing a recombinant KSHV genome (Vieira et al., 2004). The recombinant virus rKSHV.219 establishes a latent infection in these cells and can be efficiently reactivated using TPA and sodium butyrate to undergo the lytic life cycle. Again, efficient knock-down of CIP29 was observed in these cells after 72 h, by transfecting CIP29-specific siRNA twice, at 0 and 24 h time points. Protein samples were then taken at 0, 24, 48 and 72 h after transfection and analysed by Western blotting using CIP29- and GAPDH-specific antibodies (Figure 3.12).

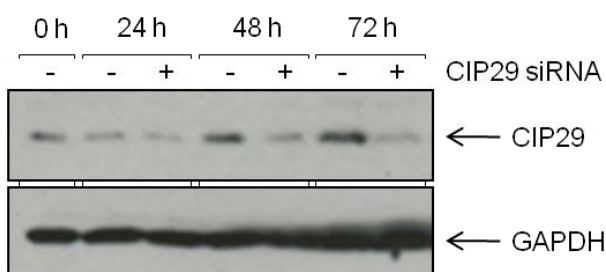


**Figure 3.12: Knock-down of CIP29 using siRNA in latent 293 rKSHV.219 cells.** Cells were transfected with CIP29-specific siRNA at 0 and 24 h. Protein samples were taken every 24 h for 72 h and subsequently analysed by SDS-PAGE and Western blotting (antibodies as indicated).

The effect of CIP29 knock-down on viral late protein expression was then examined. To this end, 293 rKSHV.219 cells were transfected with CIP29-specific or scrambled siRNA for 72 h, before lytic replication of KSHV was induced. After another 24 h, protein samples were analysed by Western blotting using a series of antibodies specific to viral and cellular proteins (Figure 3.13). ORF57 was probed as a control for induction of lytic replication, CIP29 was used to assess the level of knock-down in the cells and the KSHV minor capsid protein (mCP), a late viral protein translated from an intronless transcript, was used as a marker for lytic replication. Although good knock-down of CIP29 and successful induction of lytic replication is achieved, no difference was observed for mCP levels between cells expressing CIP29 and depleted for this protein. This result was expected, after viral mRNA export assays showed no decrease in viral mRNA export upon knock-down of CIP29. These

results suggest that CIP29 is not required for viral intronless mRNA export and efficient viral late protein expression.

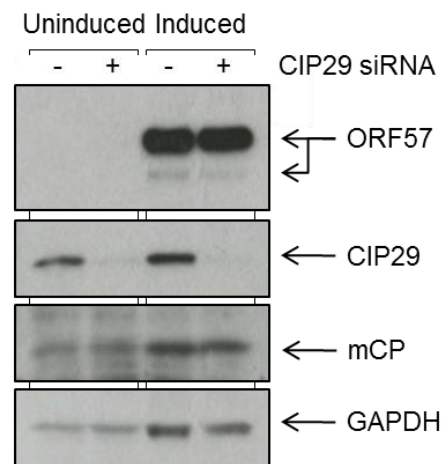


**Figure 3.13: CIP29 knock-down does not affect viral late protein expression.** Latent 293 rKSHV.219 cells were transfected at 0 and 24 h with CIP29 siRNA. KSHV lytic replication was induced at 48 h and cells harvested at 72 h. Protein samples were analysed by SDS-PAGE and Western blotting using specific antibodies as indicated (mCP = minor capsid protein).

### 3.9 Discussion

In this chapter an interaction between the viral mRNA export factor ORF57 and the hTREX component CIP29 was identified by GST-pulldowns, co-immunoprecipitation and subcellular co-localisation. CIP29 is one of several recently identified hTREX components (Dufu et al., 2010; Chang et al., 2013; Folco et al., 2012). No interaction with ORF57 has been shown previously; however, as ORF57 is believed to recruit the complete hTREX complex in order to form an export competent vRNP, this interaction was expected (Boyne et al., 2008). The formation of the trimeric complex of Aly-UAP56-CIP29 within the hTREX complex has been shown to be ATP-dependent (Dufu et al., 2010). Interestingly, UAP56 is a member of the RNA-helicase family with ATPase activity *in vitro*, which can be further stimulated by the presence of Aly (Shen et al., 2007; Taniguchi and Ohno, 2008). Other work has shown CIP29 associates with UAP56 to enhance its RNA-helicase activity (Sugiura et al., 2007). It has therefore been speculated that CIP29, as well as Aly, might function as co-factors for UAP56, potentially to unwind the 5' end of mRNA, in order to allow binding of the THO complex and TAP recruitment (Dufu et al., 2010). To establish the role of CIP29 in the ORF57-mediated export of viral mRNAs, GST-tagged CIP29, Aly and UAP56 were

purified and used in ATPase assays. Aly and CIP29 stimulated UAP56 ATPase activity *in vitro*, but the effect was not increased by the presence of both proteins together. Similar results have been recently described in the literature (Chang et al., 2013). It can therefore be speculated that Aly and CIP29 have overlapping and redundant functions with regard to UAP56 ATPase activity.

The ATP-dependency of the complex formation was then explored, with regard to ORF57-mediated recruitment of hTREX components. Co-immunoprecipitations in the presence of ATP and ATP $\gamma$ S confirmed that ORF57 binding is affected by the ATP-dependent formation of the trimeric complex and cannot override this effect: the viral protein did not co-precipitate with CIP29 in the presence of ATP $\gamma$ S. ORF57 is known to directly interact with Aly. Hence, it appears that if the Aly-UAP56-CIP29 complex is unable to form, ORF57 is not able to recruit either UAP56 or CIP29. It would be intriguing to see if ORF57 remains able to bind Aly in the presence of ATP $\gamma$ S and further co-immunoprecipitations should be conducted in the future to clarify this point. Interestingly, as ATP $\gamma$ S has a similar binding affinity to UAP56 as ATP, but cannot be hydrolysed, this highlights further that it is not ATP binding, but ATP hydrolysis (or a result thereof) that is necessary for formation of the Aly-UAP56-CIP29 interaction.

To clarify the role of CIP29 in KSHV lytic replication, the effect of CIP29 knock-down was examined on viral mRNA export and on expression of viral late proteins translated from intronless mRNAs. Intriguingly, enhanced viral intronless transcript levels were observed in CIP29 depleted cells, when ORF57 was present. It cannot be ruled out that this effect is due to experimental errors: Western blots indicate slightly increased protein bands for transfected ORF57 in cells with CIP29 knock-down. As ORF57 is known to stabilise viral transcripts, enhanced levels of the protein could lead to an increase in ORF47 whole cell mRNA. However, as mRNA export is not seen to rise accordingly in these cells, it is unlikely that this is the case. In both, CIP29 knock-down and mock transfected cells, cytoplasmic levels of the reporter mRNA are 1.5-fold higher than the according whole cell amounts. Compared to this, cells expressing more ORF57 would be expected to display a further relative increase in mRNA export. It therefore appears that CIP29 knock-down leads to increased mRNA stability in ORF57 expressing cells. To date, this effect cannot be explained and further experiments have to be conducted, looking at mRNA stability in the presence and absence of ORF57.

Interestingly, employing a KSHV infected cell line no change in expression of viral late proteins was seen in cells depleted of CIP29. Importantly, no effect of the knock-down could be observed on induction of lytic replication or expression of ORF57. This confirms the result of the mRNA export assay, showing that CIP29 does not affect ORF57-mediated export of viral intronless transcripts. Even though an increase in total cytoplasmic levels of ORF47 mRNA could be seen, no increase in protein expression is observed. It is possible that cellular regulatory mechanisms, such as protein degradation or post-transcriptional modifications, regulate any further downstream effects after mRNA export. Again, further research has to be conducted to investigate this effect. Moreover, additional research should clarify the role of CIP29 in hTREX, as well as cellular and viral mRNA export, as neither has been affected by CIP29 knock-down.

## Chapter 4

~

ATP-cycle dependent remodelling of hTREX complex  
affects ORF57-induced viral RNP formation and can be  
exploited as a therapeutic target

## **4 ATP-cycle dependent remodelling of hTREX complex affects ORF57-induced viral RNP formation and can be exploited as a therapeutic target**

### **4.1 Introduction**

The hTREX components UAP56, Aly and CIP29 form a trimeric complex in the presence of ATP, with UAP56 bridging the interaction of Aly and CIP29 (Dufu et al., 2010). This is perhaps not surprising, as UAP56, the core component essential for assembly of the hTREX complex and mRNA binding, belongs to the DExD-box family of RNA-helicases (Shen et al., 2007). RNA-binding, unwinding and release by members of this protein family is coupled to ATP binding and hydrolysis. As such, they have major roles in all stages of RNA metabolism, where their roles vary from rearranging RNA-structures, to remodelling protein or RNA-protein complexes (Cordin et al., 2006).

As shown in the previous chapter, ATPγS prevents the association of ORF57 with CIP29. Since ORF57 recruits the hTREX complex through a direct interaction with Aly, which in turn interacts with UAP56, it can be speculated that disrupting ATP hydrolysis will also abolish other ORF57/hTREX interactions. Recent research by Chang et al. has demonstrated dependency of hTREX function on UAP56-mediated ATP hydrolysis (Chang et al., 2013). Specifically, loading of Aly and Chtop onto RNA were prevented by a non-hydrolysable ATP-analogue. It was therefore proposed that an ATP-cycle dependent remodelling of hTREX, driven by UAP56, takes place.

After demonstrating the reliance of the ORF57/CIP29 interaction on ATP hydrolysis, we hypothesised that the ATP-cycle dependent remodelling of hTREX would affect the ability of ORF57 to form a vRNP and therefore present a novel antiviral target. The following chapter describes experiments performed in order to elucidate the mechanisms of ATP-dependent hTREX remodelling and its effects on ORF57. Experiments then show that targeting this process using small molecule inhibitors is a valid approach to inhibit KSHV lytic replication.

## 4.2 ATP-dependent formation of the ORF57-mediated vRNP

To assess the effect of ATP binding and ATP hydrolysis on vRNP formation, co-immunoprecipitation experiments were performed. For this, GFP or GFP-UAP56 expression vectors were transfected into 293T cells in the absence or presence of a mCherry-ORF57 construct. After 24 h, the cell lysates were incubated with GFP-trap® beads in the presence of mock, 1.25 mM ATP or ATP $\gamma$ S, which functions as an ATP-inhibitor. ATP $\gamma$ S can only be hydrolysed very slowly by UAP56, but having a similar binding affinity as ATP (Taniguchi and Ohno, 2008), we speculated that the presence of 1.25 mM would efficiently prevent hydrolysis of any present endogenous ATP. Precipitated proteins were then analysed by western blotting and detected with ORF57-, Aly-, CIP29- or GFP-specific antibodies (Figure 4.1a). Analysis of the precipitates revealed an ATP-dependent effect on the interaction of ORF57 with UAP56 and hence vRNP formation: ORF57, as well as the endogenous hTREX proteins Aly and CIP29, can be seen to specifically interact with UAP56. Binding of the viral and the endogenous proteins is clearly enhanced by the presence of ATP. In contrast, the presence of ATP $\gamma$ S significantly inhibits the interaction of ORF57 with UAP56, which highlights the necessity of ATP hydrolysis for formation of the vRNP. Interestingly, binding of Aly and CIP29 to UAP56 is not negatively affected by ATP $\gamma$ S, as densitometry suggest a slight increase in the formation of an Aly-UAP56-CIP29 complex (Figure 4.1b). A similar result is reflected in the precipitation of GFP-UAP56 in the absence of ORF57: The addition of ATP enhances binding of the endogenous hTREX components, whereas ATP $\gamma$ S does not have a negative effect on complex assembly. Interestingly, while the trend remains the same, the interaction of Aly and CIP29 with UAP56 is enhanced in the presence of ORF57, as less protein can be seen to co-precipitate in the absence of the viral protein. A GFP-specific antibody was used to confirm similar amounts of UAP56 have been pulled down in all samples, making the immunoprecipitations comparable.

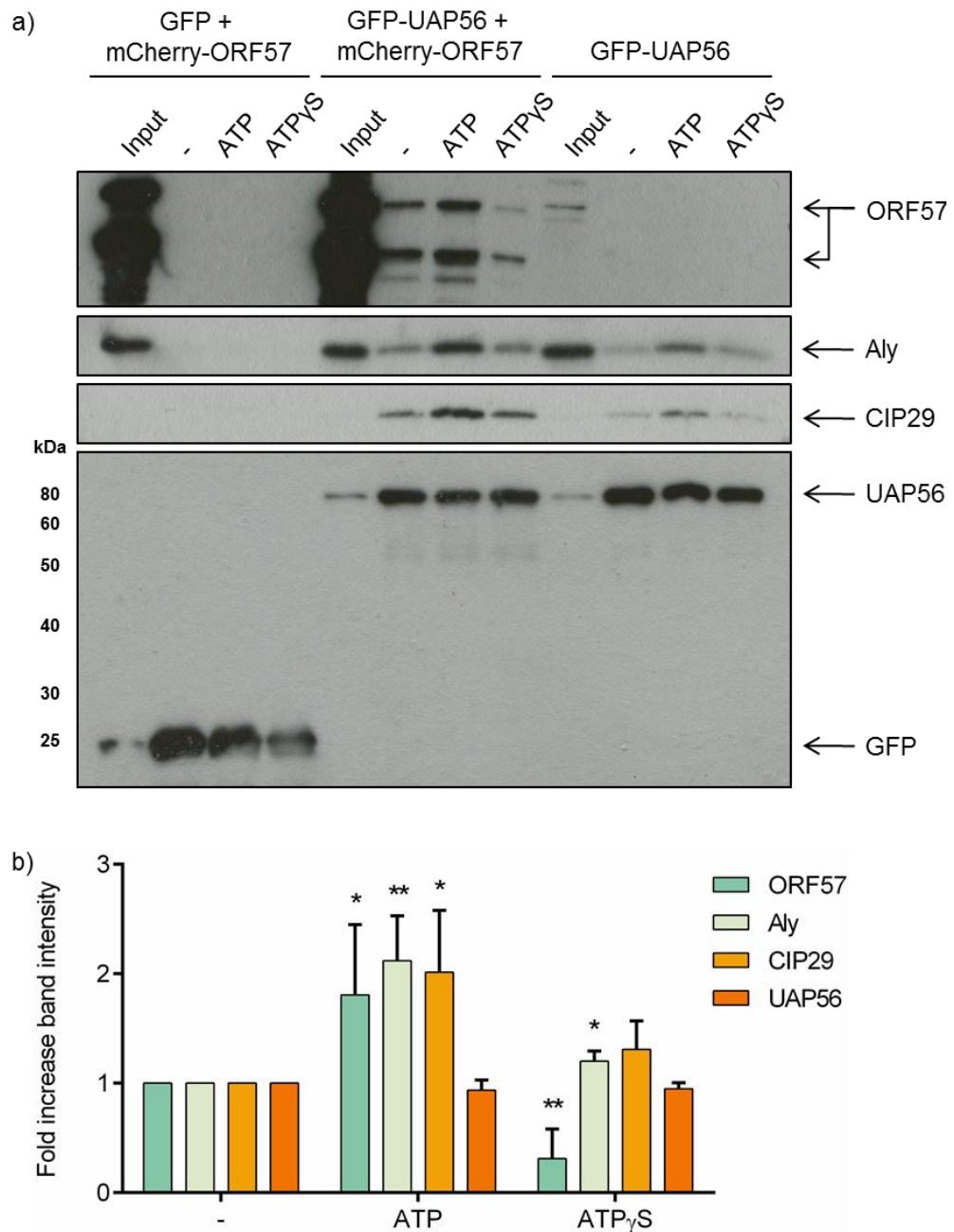


**Figure 4.1: ATP-dependent formation of the ORF57-mediated vRNP.** a) Co-immunoprecipitations were performed with cell lysates from 293T cells transfected with GFP or GFP-UAP56 and mCherry-ORF57 (Input), as indicated. Precipitations were performed with complete whole cell lysates or with the addition of 1.25 mM ATP or 1.25 mM ATP $\gamma$ S. Western blots were probed with ORF57-, Aly-, CIP29- and GFP-specific antibodies. b) Quantification of band intensities by ImageJ. Values are average of 4 independent immunoprecipitations (performed with mCherry-ORF57, as shown above, or Myc-ORF57). Error bars present the SD.  $p < 0.01$  (\*\*) or  $p < 0.05$  (\*), effect of ATP or ATP $\gamma$ S compared to untreated.

A dose-dependency effect of ATP and ATP $\gamma$ S would be expected, if the interactions of the hTREX complex and ORF57 could be dynamically remodelled by the presence of the

nucleotide or the non-hydrolysable analogue. Therefore the previous immunoprecipitation experiment was repeated in the presence of 0–1.75 mM ATP or ATP $\gamma$ S. Western blots were then probed with GFP-specific antibodies as a precipitation control for GFP-UAP56, or ORF57-specific antibodies to quantify precipitation of ORF57 (Figure 4.2). The experiment shows a dose-dependent effect for both ATP and ATP $\gamma$ S on the interaction of ORF57 with UAP56.

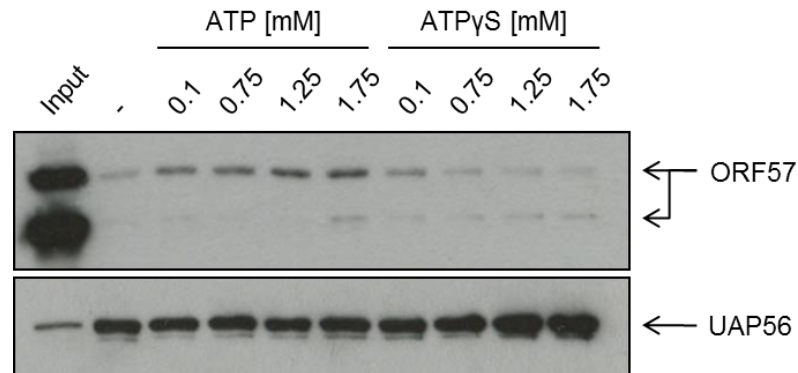


**Figure 4.2: Dose-dependent effect of ATP and ATP $\gamma$ S on ORF57-mediated vRNP formation.** Co-immunoprecipitations were performed as described before (Figure 4.1), with a series of ATP and ATP $\gamma$ S concentrations, as indicated.

### 4.3 ATP-cycle dependent remodelling of the ORF57-mediated vRNP

Since the ORF57 interaction with hTREX is specifically interrupted by the presence of ATP $\gamma$ S, it could be speculated that the ATPase-function of UAP56 is necessary for remodelling of hTREX, after the initial complex formation upon ATP binding. However, the previous experiment left unaddressed if the actual energy generating step of ATP hydrolysis is essential for a reorganisation of all involved hTREX proteins and possibly binding of Aly and Chtop to viral mRNA. Another mechanism could be a conformational change of the hTREX complex upon ADP binding to UAP56. This rearrangement might be necessary to accommodate the viral protein and would also be prevented by the presence of ATP $\gamma$ S. Therefore, further co-immunoprecipitation assays were performed in the presence of ATP, ATP $\gamma$ S and also ADP. As before, 293T cells were transfected with GFP or GFP-UAP56 and mCherry-ORF57, before cell lysates were incubated with GFP-trap<sup>®</sup> beads, either in the absence or in the presence of 1.25 mM ATP, ATP $\gamma$ S or ADP. Precipitates were analysed by Western blotting using GFP- and ORF57-specific antibodies (Figure 4.3).

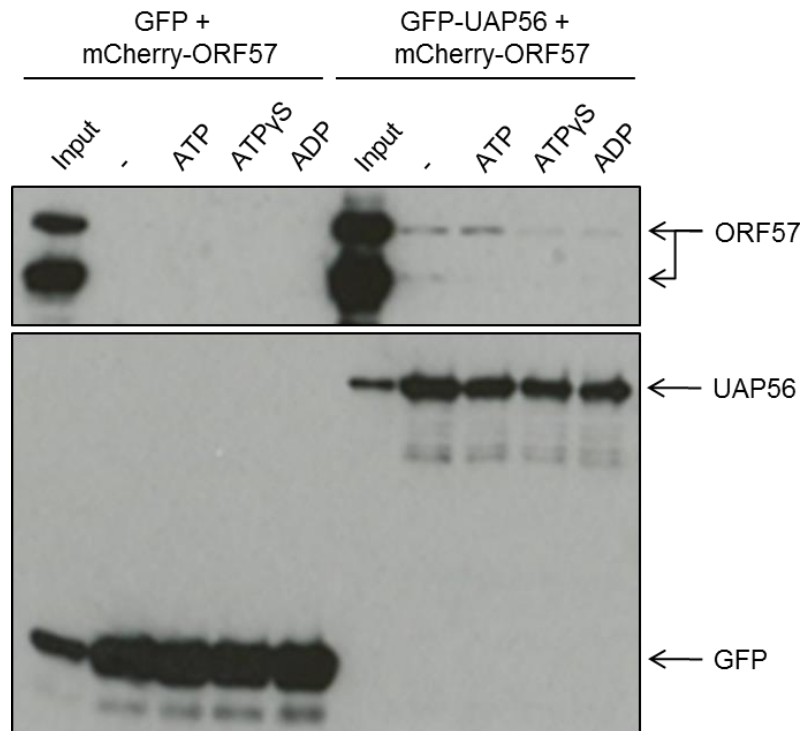


**Figure 4.3: ATP-cycle dependent remodelling of the ORF57-mediated vRNP.** Co-immunoprecipitations were performed as before (Figure 4.1), in the presence of 1.25 mM ATP, ATP $\gamma$ S or ADP, as indicated.

As before, ATP can be seen to enhance the interaction of UAP56 and ORF57, whereas it is reduced with ATP $\gamma$ S. Interestingly, ADP also disrupts the interaction of UAP56 and ORF57, indicating that the presence of hydrolysable ATP is the essential factor for ORF57-mediated binding of the hTREX complex. To confirm these results, co-immunoprecipitations were performed in a dose-dependent manner. The experiment was conducted as before, using a concentration range from 0.1 to 1.75 mM ATP, ATP $\gamma$ S or ADP. Western blots were probed using ORF57-, Aly-, CIP29- or GFP-specific antibodies, to determine the effect of ATP-cycle dependent complex remodelling on both the viral protein and endogenous hTREX components (Figure 4.4a). Again, ADP can be seen to disrupt the interaction of ORF57 with UAP56 in a dose-dependent manner, in a similar fashion to ATP $\gamma$ S. Densitometry of 3 individual experiments shows for both ATP $\gamma$ S and ADP a significant decrease in precipitated ORF57 at concentrations between 1.25 and 1.75 mM (Figure 4.4b). Interestingly, ADP is also found to significantly disrupt the interaction of the endogenous hTREX components Aly and CIP29 with UAP56. This is in contrast to the effect observed in the presence of ATP $\gamma$ S, where again a stabilising effect can be seen on the formation of the Aly-UAP56-CIP29 complex, similar to that of ATP.

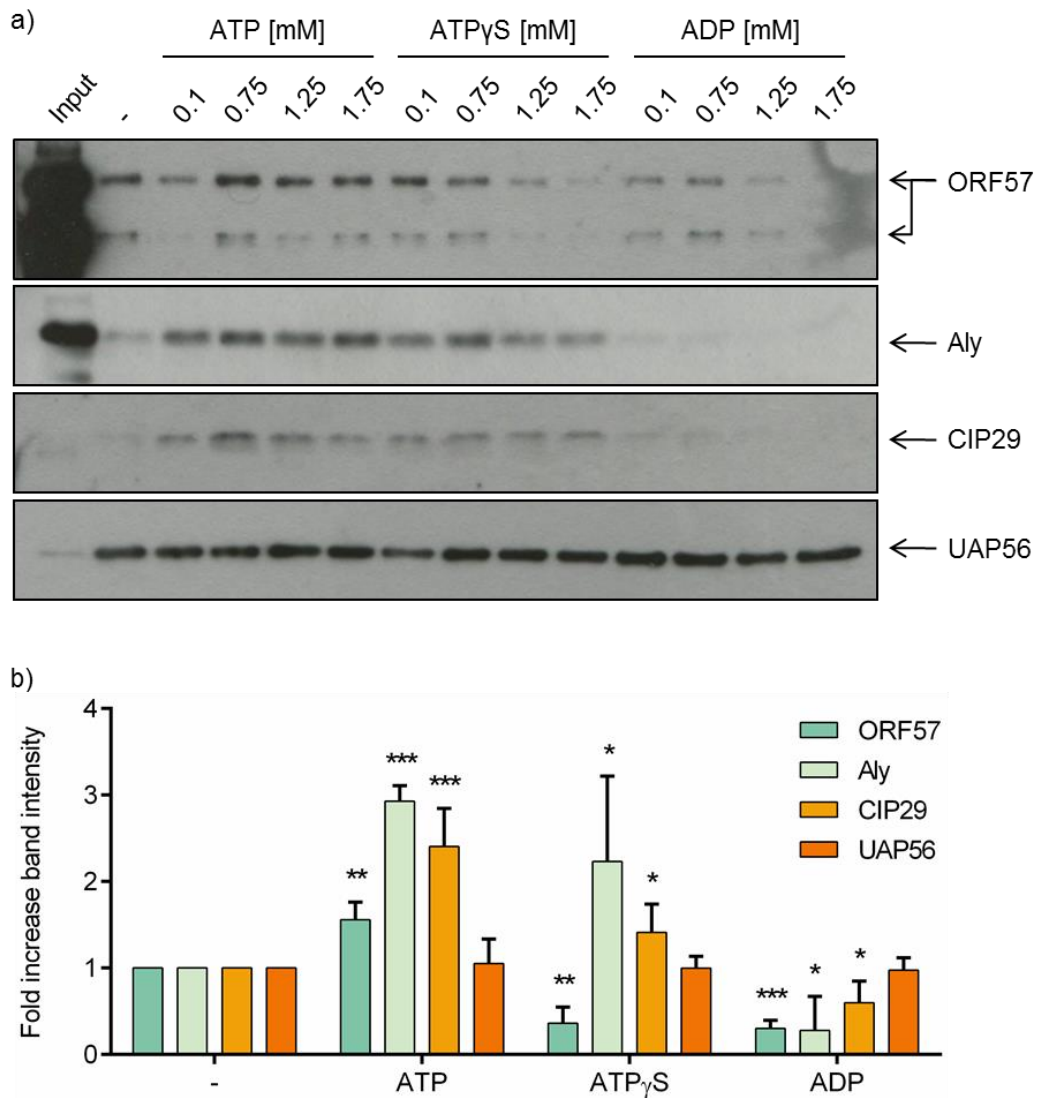


**Figure 4.4: Dose-dependency of ATP-cycle dependent remodelling of the ORF57-mediated vRNP.** a) Co-immunoprecipitations were performed as described before (Figure 4.1) with a series of ATP, ATP $\gamma$ S and ADP concentrations, as indicated. b) Quantification of bands at 1.25 and 1.75mM ATP, ATP $\gamma$ S or ADP by ImageJ. Values are average of 3 independent immunoprecipitations. Error bars present the SD.  $p < 0.05$  (\*),  $p < 0.01$  (\*\*) or  $p < 0.001$  (\*\*\*) effect of ATP, ATP $\gamma$ S or ADP compared to untreated.

Together, this data indicates an ATP-cycle dependent remodelling of the hTREX that affects the ability of ORF57 to interact with the complex and form a vRNP (Figure 4.5). Upon ATP binding (simulated by the presence of ATP $\gamma$ S) the endogenous trimeric complex Aly-UAP56-CIP29 is able to form. It can be further speculated that ATP hydrolysis (in the presence of ATP) allows a conformational change within hTREX, which enables ORF57 to interact with Aly and recruit the hTREX complex. Whereas after release of inorganic phosphate, bound ADP causes the protein complex to dissociate.

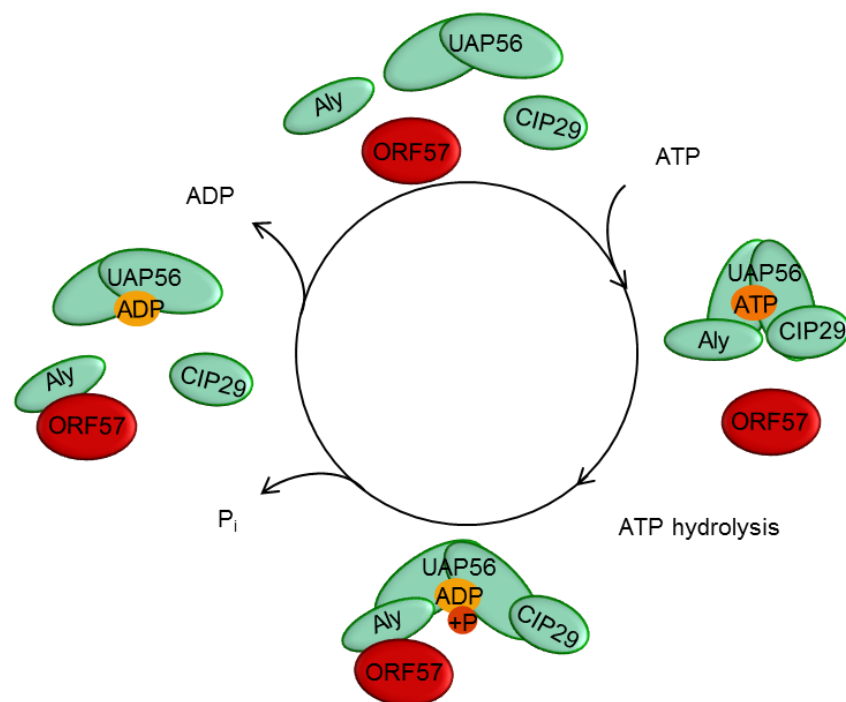


**Figure 4.5: Schematics of ATP-cycle dependent remodelling of central hTREX components and the ORF57-mediated vRNP.** Proposed model based on co-immunoprecipitations in the presence of ATP, ATP $\gamma$ S and ADP, as shown above (Figure 4.3 and Figure 4.4).

#### 4.4 High-throughput screening for UAP56 ATPase inhibitors

We speculated that inhibitors targeted against UAP56 ATPase-activity would function to prevent formation of the vRNP, while allowing the interaction of hTREX components, as could be seen for ATP $\gamma$ S. *In silico* high-throughput screening (HTS) was therefore utilised to identify small molecules capable of binding in the UAP56 ATP binding site, based on the known crystal structure (Shi et al., 2004). Furthermore, a series of compounds were manually chosen from the Tocriscreen Compound Library, a screening library of known bioactive compounds suitable for HTS. Finally, a small number of fragments were also selected. Following selection of 400 compounds/fragments giving the highest score using the virtual docking programme eHiTS (SymBioSys), these were tested against *in vitro* ATPase activity of UAP56. Conditions for the *in vitro* screening were established using several preparations of GST-UAP56, which was purified as shown before (Figure 3.7). While all batches of purified protein showed RNA-dependent ATPase activity, the rates of hydrolysis were found to vary between preparations (Figure 4.6a). Therefore, to obtain comparable results with several protein preparations during the screening process, no

fixed protein concentration was used, but rather a specific concentration for each batch (between 1 and 3  $\mu\text{M}$  UAP56), that resulted in hydrolysis of 30% ATP used in the assay. This would yield the best assay window, giving a high signal-to-background ratio and maintaining velocity of ATP hydrolysis in the linear range with enzyme concentration. The ATP concentration for the screen was set as 35  $\mu\text{M}$ , which was equivalent to the average  $K_M$  experimentally determined for three individual protein preparations (Figure 4.6b). Using a substrate concentration  $[S] = K_M$  is recommended as “balanced assay conditions”, as this provides equal opportunities for all inhibitor types (Copeland, 2005).

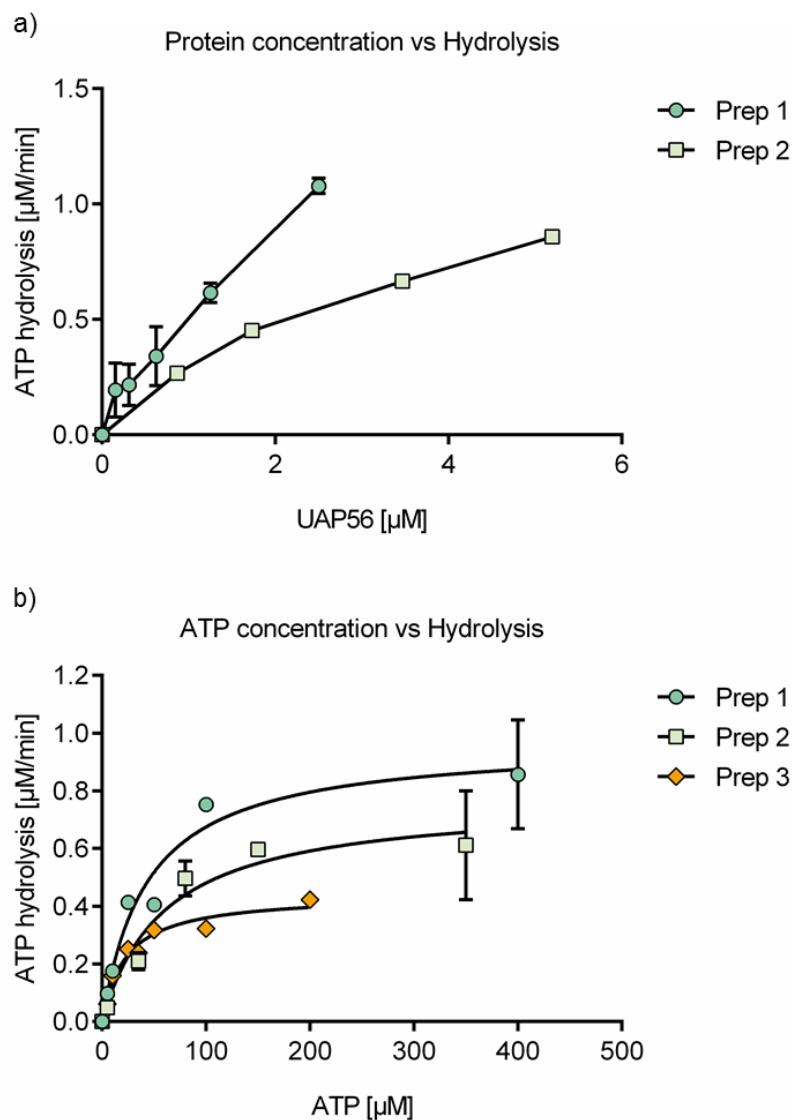


**Figure 4.6: Determination of assay conditions for UAP56-ATPase assay.** Purified GST-UAP56 was incubated with a known concentration of ATP for 30 min at 37° C, before remaining amounts of ATP were determined using a luminescent signal from a luciferase reaction. a) A fixed substrate concentration of 50  $\mu\text{M}$  ATP was used. Error bars present the SD,  $n = 3$ . b) A fixed protein concentration of 1.5  $\mu\text{M}$  UAP56 was used. Michaelis-Menten curve was fitted using Graphpad Prism software. Error bars present the SD,  $n = 2$ .

Under these conditions, ATP $\gamma$ S was used as a control inhibitor and was found to display a typical sigmoidal inhibition curve (Figure 4.7).

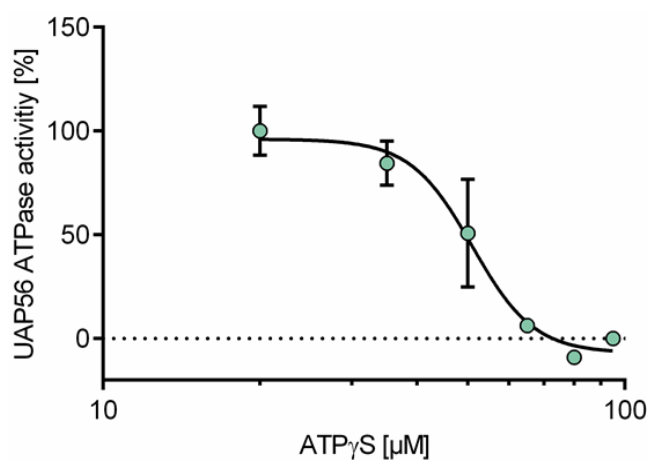


**Figure 4.7: Inhibition of UAP56 ATPase activity by ATP $\gamma$ S.** Assay conditions were tested using increasing concentrations of a known inhibitor of UAP56, ATP $\gamma$ S. n = 3, error bars display SD.

*In vitro* screening of the pre-chosen 400 small molecules/fragments identified four compounds, all from the Tocriscreen Compound Library, which had the ability to inhibit UAP56 enzyme activity to below 80% (Figure 4.8). Excitingly, none of the “hits” are adenosine-based structures, enhancing enzyme specificity and making them suitable for further characterisation.

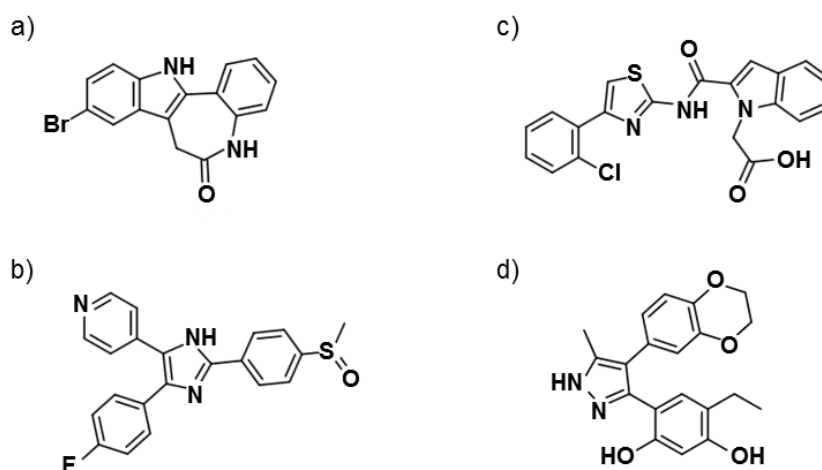
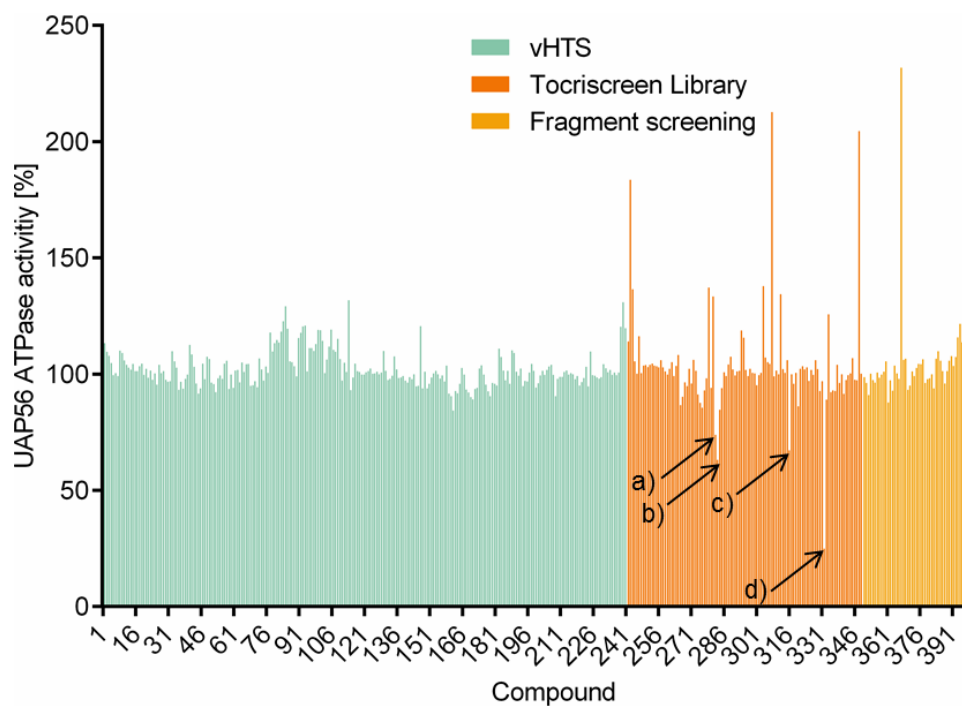


**Figure 4.8: Screening of small molecules and fragments against UAP56 ATPase activity identified four potential inhibitors.** Compounds selected by vHTS are in teal, compounds manually chosen from the Tocriscreen library are in dark orange and screened fragments are in light orange. Screening was performed under conditions described above with 100  $\mu$ M of each compound and 1 mM of each fragment. UAP56 ATPase activity in the presence of inhibitor: a) 74%, b) 63%, c) 67% and d) 25%.

The most potent compound (d), C2, reduced enzyme activity by 75%. AutoDoc, a software for calculating binding energies of small molecules to proteins, predicted C2 to bind to the ATP binding pocket of UAP56, suggesting an ATP competitive inhibitor (Figure 4.9). C2 is expected to form the indicated hydrogen-bonding interactions,  $\pi$ -stacking interactions with Phe-65 and hydrophobic interactions with Met-93.

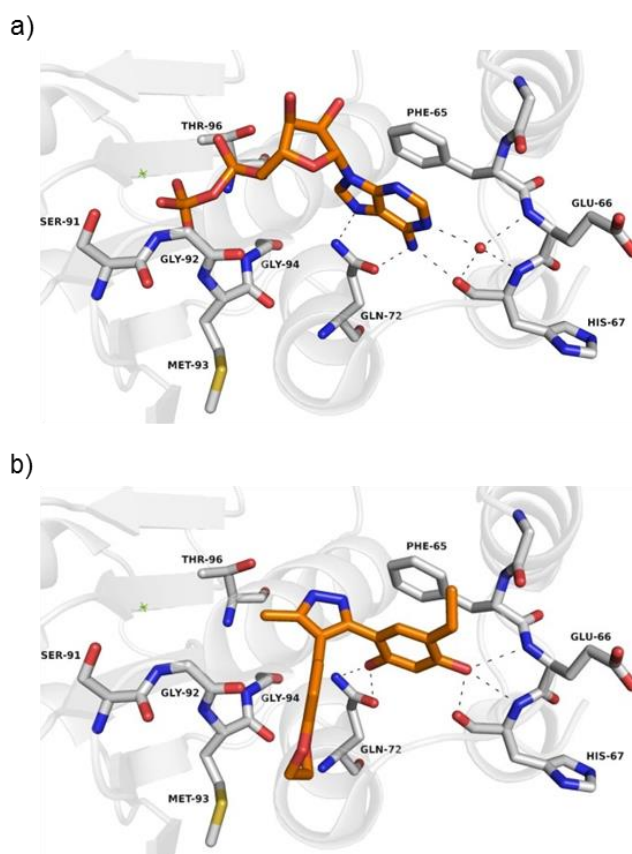


**Figure 4.9: Compound C2 is predicted to bind to the ATP binding pocket of UAP56.** a) Crystal structure of UAP56 ATP binding site as solved in the presence of ADP. b) Suggested binding of C2 by AutoDock software is within the UAP56 ATP binding pocket (images kindly provided by Dr Ian Yule and Dr Richard Foster).

#### 4.5 Confirmation of UAP56 inhibition by small molecule inhibitor C2

To confirm a dose-dependent inhibition of UAP56, the enzymes ATPase activity was measured over a wide concentration range of compound C2. Non-linear regression could then be used to determine the half maximal inhibitory concentration ( $IC_{50}$ ) of C2 for UAP56 ATPase activity. Because of the observed variation in activity of different protein batches, this was done with GST-UAP56 protein from three individual purifications at set concentrations. Two measurements, both at a concentration of 5  $\mu$ M protein, resulted in an averaged  $IC_{50} = 63.5 \mu$ M  $\pm$  3.5  $\mu$ M (Figure 4.10a). This indicates that while absolute activity between batches may vary, normalised activity of each batch yields comparable inhibition by C2. Since the  $IC_{50}$  is directly dependent on the protein concentration used in the assay, we also repeated the experiment with 700 nM GST-UAP56. Due to a smaller

signal-to-background ratio, variation between replicates is larger; however, we were still able to determine an  $IC_{50}$  of 7.6  $\mu\text{M}$  at this concentration (Figure 4.10b).

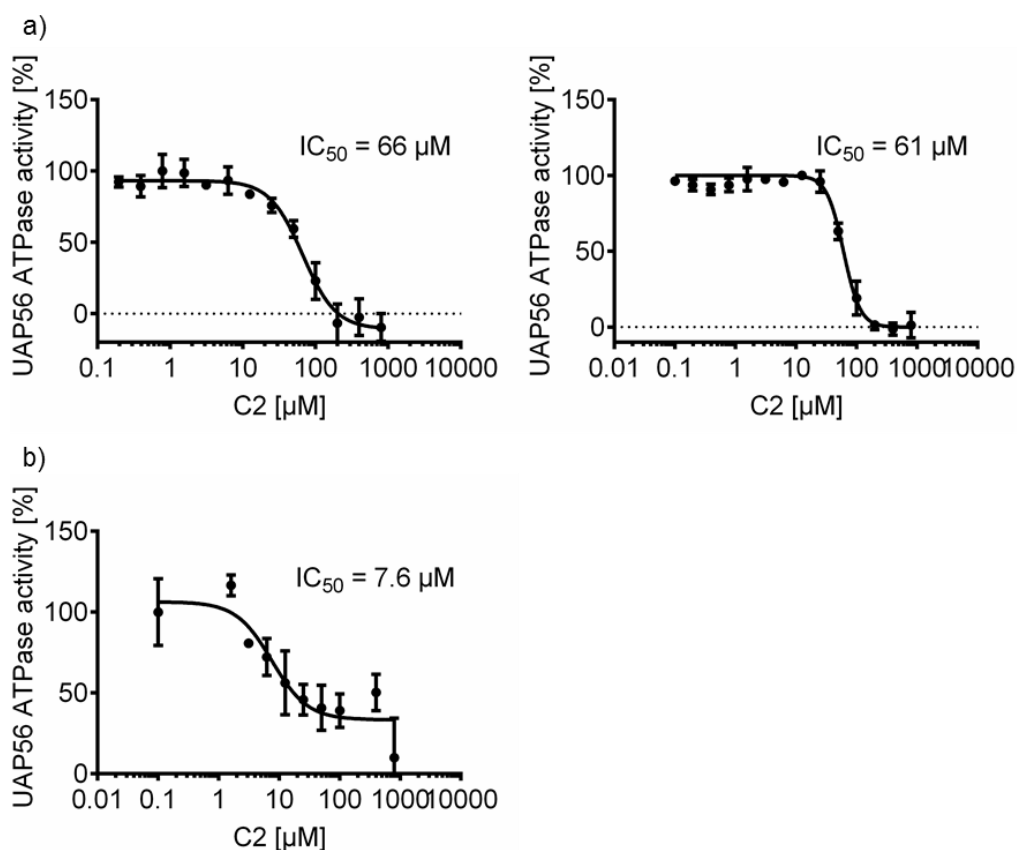


**Figure 4.10:  $IC_{50}$  measurements of C2 for UAP56.** Assays were performed with recombinant protein from three individual protein purifications. a) Two measurements using 5  $\mu\text{M}$  UAP56 from individual protein purifications each. b) Measurement employing 700 nM UAP56 from a separate protein purification. UAP56 was incubated with increasing amounts of C2 in the presence of 0.5% DMSO and 35  $\mu\text{M}$  ATP for 30 min.  $n = 3$ , error bars display the SD.  $IC_{50}$  was determined using non-linear regression.

In addition to  $IC_{50}$  measurements, microscale thermophoresis was performed to determine the dissociation constant,  $K_D$ . For this, GST-UAP56 was purified as described before (Figure 3.7) and fluorescently labelled with FITC on amine groups. Thermophoretic movement measured via normalised fluorescence in the presence of increasing amounts of C2 (Figure 4.11) (assay performed by Dr Brian Jackson). A  $K_D$  of 12.8  $\mu\text{M}$  was calculated for the thermophoresis binding curve.

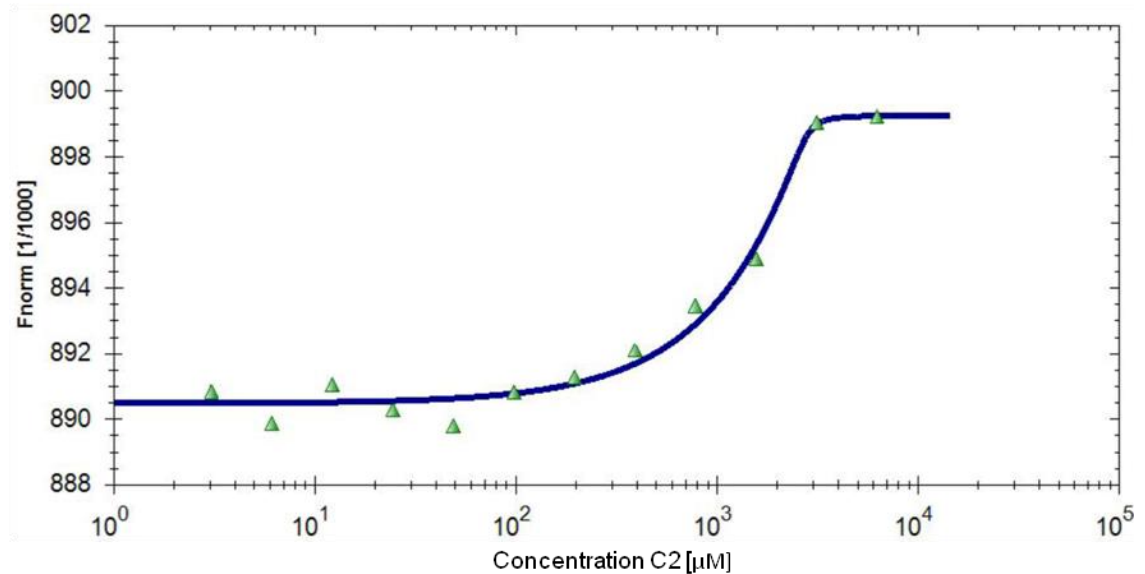


**Figure 4.11: Thermophoresis binding curve for UAP56 and C2.** The binding curve shows normalised fluorescence ( $F_{norm}$ ) in the presence of increasing amounts of C2.  $K_D = 12.8 \mu M$ , calculated using the following formula:  $f(c) = \text{unbound} + (\text{bound} - \text{unbound}) / 2 * (\text{FluoConc} + c + K_D - \text{Sqrt}((\text{FluoConc} + c + K_D)^2 - 4 * \text{FluoConc} * c))$ , with  $\text{FluoConc} = 2830$ ,  $\text{bound} = 899.29$  and  $\text{unbound} = 890.49$ , square root ( $\text{Sqrt}$ ), concentration C2 ( $c$ ). Assay performed by Dr Brian Jackson (Schumann, S., Yule, I., Jackson, B. R., Foster, R. and Whitehouse, A.; Manuscript in preparation).

#### 4.6 Disruption of vRNP formation *in vitro* by ATPase inhibitor C2

After successful identification of an UAP56-targeted ATPase inhibitor, the effect of the compound on vRNP formation *in vitro* was tested. Because the compound has to be delivered in a solvent, co-immunoprecipitations were carried out in duplicate using either 3.3% DMSO or 5% EtOH as delivering vehicles or mock control. Co-immunoprecipitations were performed as before, adding the compound and solvent to GFP or GFP-UAP56 and mCherry-ORF57 transfected cell lysates for 2 h during binding to GFP-trap® beads. Precipitates were analysed using ORF57-, Aly-, CIP29-, Chtop- and GFP-specific antibodies (Figure 4.12). Intriguingly, the presence of 0.5 mM C2 specifically disrupts binding of ORF57 to the hTREX complex, whereas no effect is seen on the interaction of endogenous hTREX components with UAP56. The same result is seen regardless of solvent used. This confirms the hypothesis that disruption of UAP56-mediated ATP hydrolysis prevents ORF57 from recruiting the hTREX complex, while allowing assembly of the endogenous complex.

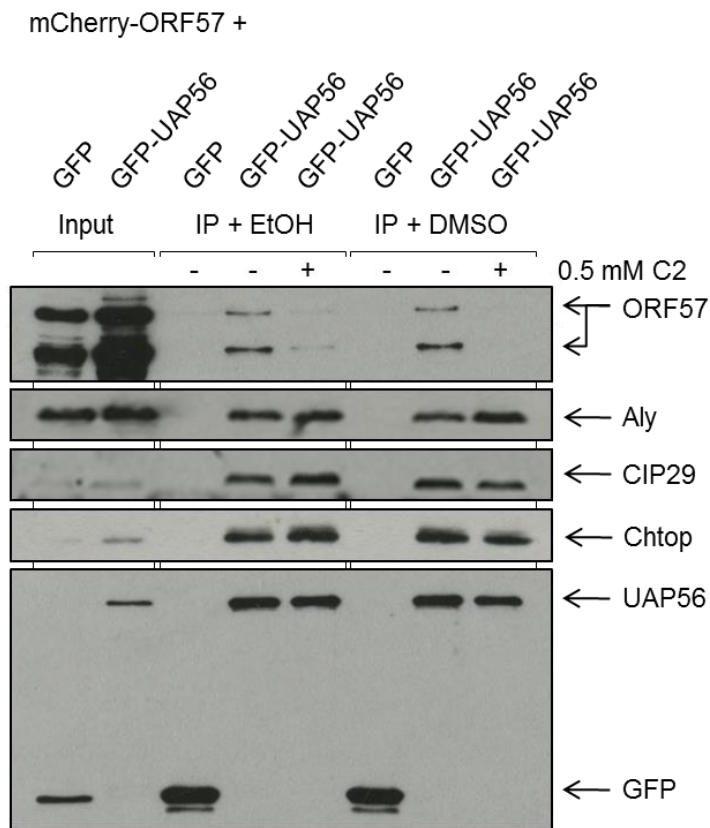


**Figure 4.12: Disruption of vRNP formation by UAP56 ATPase inhibitor C2.** Co-immunoprecipitations were performed as described before (Figure 4.1), in the absence or presence of 0.5 mM C2 and 3.3% DMSO or 5% EtOH, as indicated. Western blots were analysed using ORF57-, Aly-, CIP29-, Chtop- and GFP-specific antibodies.

To assess the effect of C2 on vRNP formation in cell culture, MTS assays were first performed to identify a non-toxic working concentration of C2. Cells were treated with increasing amounts of the compound delivered in 0.1% total DMSO for 24 h, before cell viability was assessed using the calorimetric MTS assay (Figure 4.13). Up to 15  $\mu$ M C2 could be used on 293T cells without a loss in metabolic activity, indicating 100% viable cells.

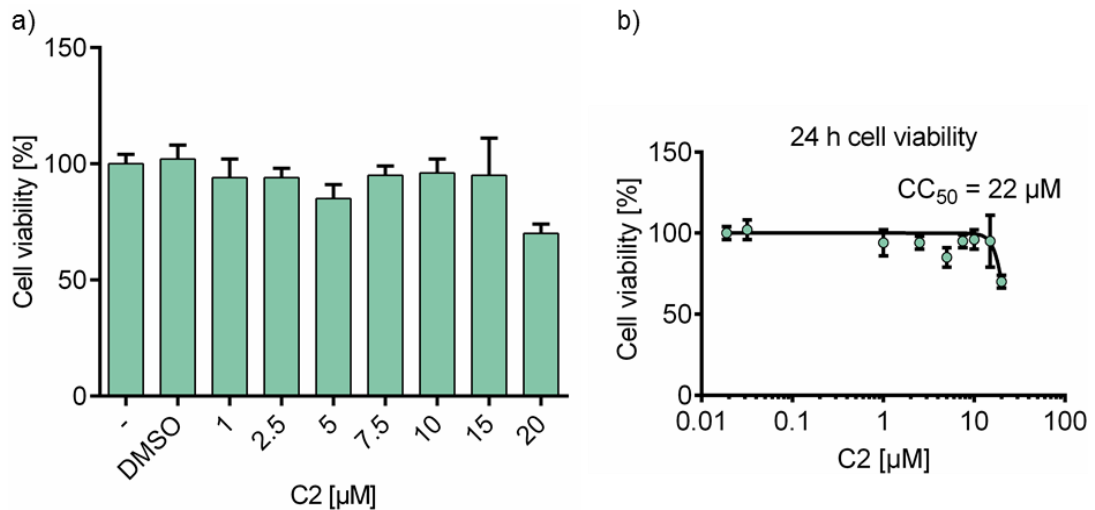


**Figure 4.13: Cell viability of 293T cells in the presence of C2.** Cells were incubated with increasing concentrations of C2 and a total of 0.1% DMSO for 24 h. Cell viability was assessed by MTS assay and normalised to untreated cells.  $n = 5$ , error bars present SD. Results are displayed as a) column graph, b) on a xy-graph using a log-scale and non-linear regression to determine the  $\text{CC}_{50}$ .

As previously described, ORF57 localises to the nucleolus of the cells and can be seen co-localising with hTREX components in this subcellular compartment (Boyne and Whitehouse, 2009). Using immunofluorescence microscopy the localisation of ORF57 and hTREX components was explored in the absence and presence of compound C2. For this, cells were transfected with GFP-UAP56 in the absence or presence of mCherry-ORF57 and treated 6 h after transfection with DMSO or C2. Cells were fixed 24 h after transfection (Figure 4.14). GFP-UAP56 localised to the nucleus as bright, punctuate speckles, excluding the nucleolus (arrows) in the absence of ORF57. In cells expressing ORF57 both proteins are found to co-localise in the cell nucleolus, with UAP56 losing its punctuate appearance. However, in cells treated with 2.5  $\mu\text{M}$  C2, mCherry-ORF57 is unable to sequester GFP-UAP56 to the nucleolus and no co-localisation is detected between the two proteins. UAP56 is again seen localising in punctuate speckles excluding the nucleolus, whereas ORF57 remains in the nucleolus (arrows).

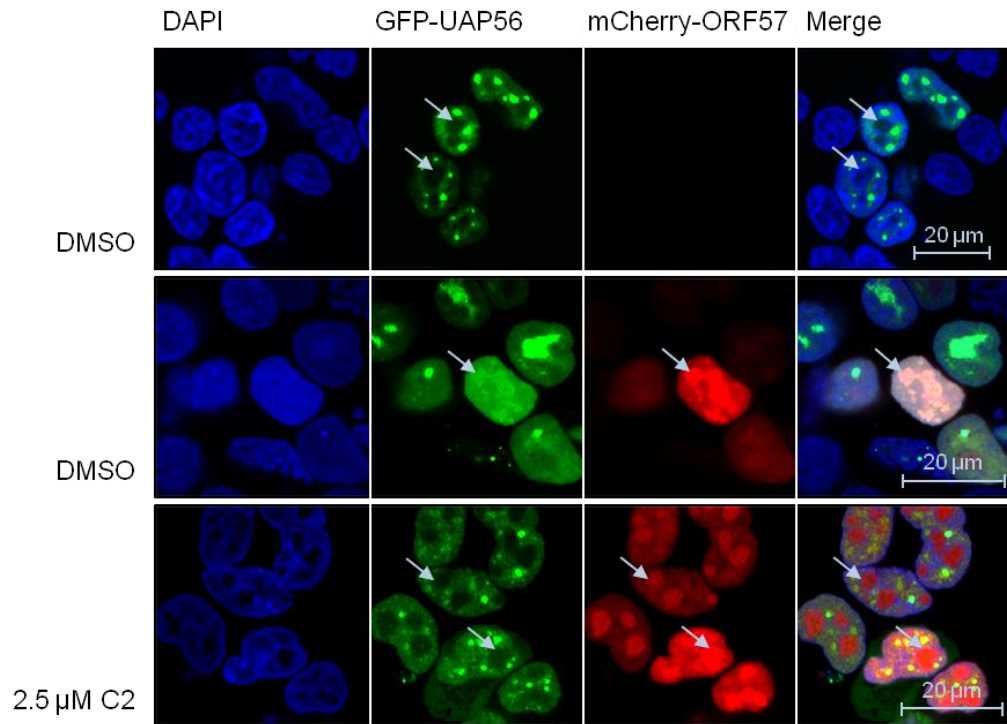


**Figure 4.14: Disruption of UAP56 co-localisation with ORF57 in the presence of C2.** 293T cells were transfected with plasmids expressing GFP-UAP56 in the absence or presence of mCherry-ORF57. After 6 h transfection, cells were treated with DMSO or C2, as indicated, for another 18 h, before they were fixed and permeabilised. DAPI staining (blue) indicates the nucleus, UAP56 was visualised by direct GFP-fluorescence (green) and ORF57 by direct mCherry-fluorescence (red).

Immunofluorescence microscopy was also employed to assess co-localisation of ORF57 and endogenous hTREX proteins. For this, GFP or ORF57-GFP transfected cells were incubated with DMSO or 2.5  $\mu$ M C2, as indicated. After fixation and permeabilisation, cells were immunostained using CIP29-specific antibodies (Figure 4.15). As described in chapter 3 (Figure 3.5), CIP29 localises to nuclear speckles and is seen excluding the nucleolus (arrows), but can be recruited into this compartment by ORF57, where the two proteins co-localise. Treatment of cells with compound C2 prevents the interaction of ORF57 and endogenous CIP29, stopping the viral protein from sequestering CIP29 to the nucleolus. These results support the hypothesis that C2 prevents the interaction of ORF57 and hTREX proteins.

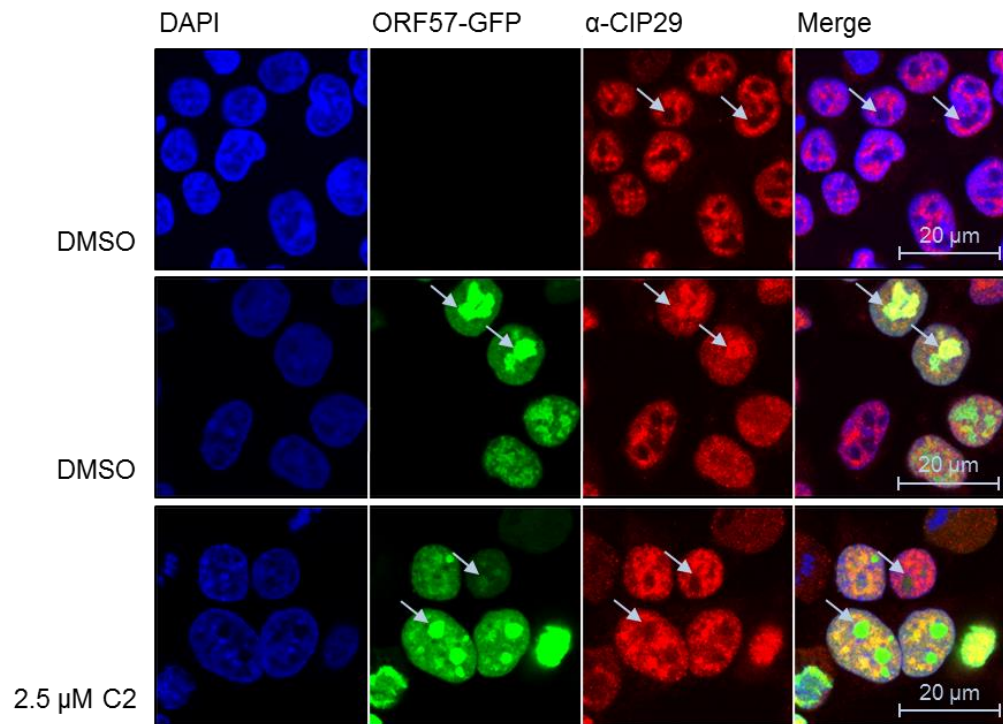


**Figure 4.15: Disruption of CIP29 co-localisation with ORF57 in the presence of C2.** 293T cells were transfected with mock or a plasmid expressing ORF57-GFP. After 6 h transfection, cells were treated with DMSO or C2, as indicated, for another 18 h, before they were fixed and permeabilised. Cells were stained using a CIP29-specific antibody (red). DAPI staining (blue) indicates the nucleus, ORF57 was visualised by direct GFP-fluorescence (green).

#### **4.7 ATPase inhibitor C2 prevents recruitment of hTREX by ORF57 but does not inhibit cellular bulk mRNA export**

Compound C2 prevents ATP hydrolysis by UAP56 and subsequently ATP-cycle dependent remodelling of the hTREX complex, potentially rendering a dysfunctional complex. Therefore, to test the effect of the inhibitor on endogenous mRNA export, fluorescence *in situ* hybridisation (FISH) was employed to monitor cellular mRNA export in the absence and presence of both ORF57 and C2. Cells were transfected with GFP or ORF57-GFP and 6 h later treated with DMSO or C2. After another 18 h cells were fixed, permeabilised and incubated with a fluorescently labelled oligo(dT) probe to detect polyadenylated (poly(A)) RNA (Figure 4.16). In the presence of GFP, poly(A) RNA is detected in large quantities in the cytoplasm of the cell (arrows) and only minor amounts remain in the nucleus within nuclear speckles. However, functional ORF57 recruits the complete hTREX complex and during this process ORF57 sequesters hTREX from endogenous mRNA, leading to a marked

reduction of poly(A) RNA in the cytoplasm and retention in the nucleus (arrows), when compared to GFP transfected cells. Excitingly, when ORF57-GFP transfected cells are treated with compound C2, a loss of nuclear retention can be observed (arrows) and an increased amount of poly(A) RNA is again found in the cytoplasm. Some co-localisation of ORF57 and poly(A) RNA can be observed in nuclear speckles, which is expected as both the viral protein and endogenous RNAs are known to localise to this subnuclear structure independently of each other. However, all C2 treated cells in the presence of GFP exhibit normal mRNA export with large amounts of poly(A) RNA being found in the cytoplasm (arrows). This confirms that the interaction of ORF57 and the hTREX complex is efficiently disrupted in the presence of C2 and, importantly, that the presence of C2 does not inhibit endogenous cellular bulk mRNA export.

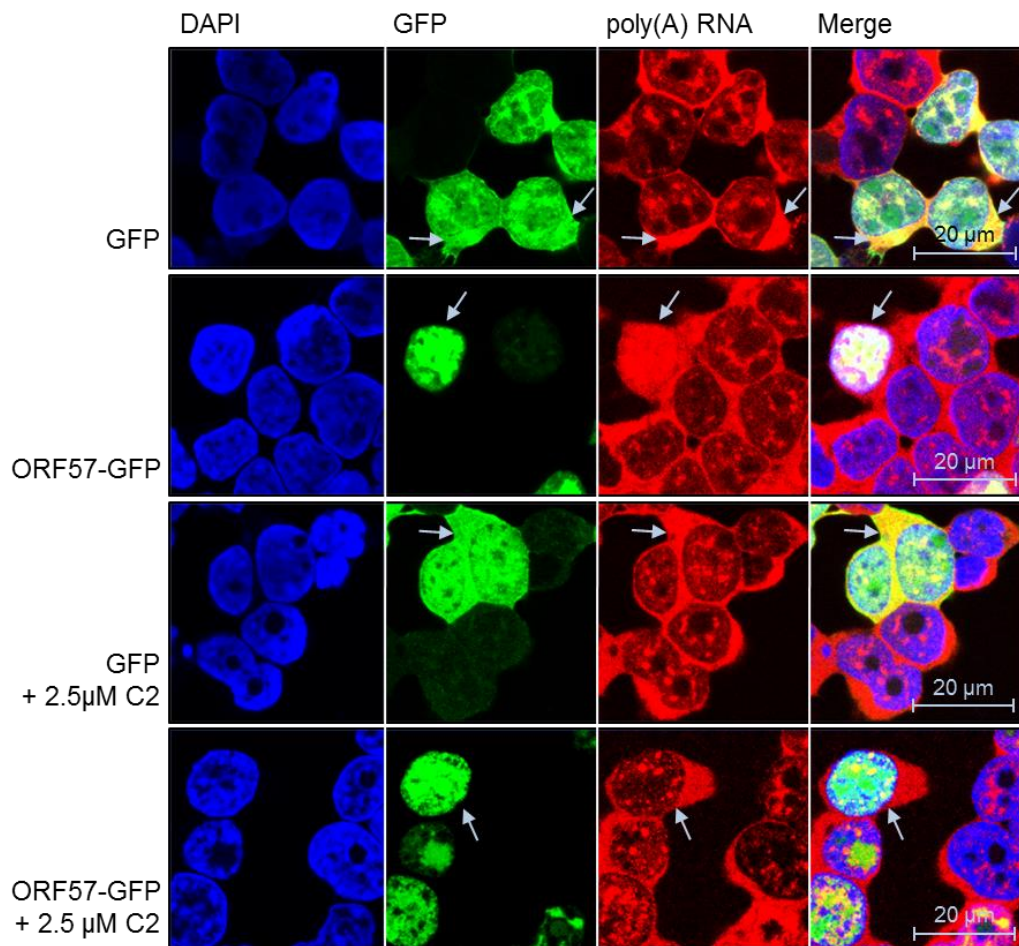


**Figure 4.16: Fluorescence *in situ* hybridisation (FISH) demonstrates C2 prevents hTREX sequestration by ORF57, but does not inhibit cellular bulk mRNA export.** HEK 293T cells were transfected with plasmids expressing GFP or ORF57-GFP and treated after 6 h with DMSO or C2, as indicated, for another 18 h. Cells were fixed and permeabilised, before they were incubated with a fluorescently labelled oligo(dT) probe. DAPI staining (blue) indicates the nucleus, ORF57 was visualised by direct GFP-fluorescence (green) and poly(A) RNA is shown in red.

#### 4.8 C2 prevents ORF57-mediated export of viral mRNAs

After observing no change in cellular mRNA export upon C2 treatment, viral mRNA nuclear export was assessed. To perform a viral mRNA export assay, cells were transfected with GFP or ORF57-GFP, as well as an intronless construct coding for ORF47, generating viral intronless transcripts that function as a reporter RNA. After 6 h, cells were treated with DMSO or C2, 18 h later cells were fractionated in order to obtain whole cell and cytoplasmic fractions, before generation of cDNA and analysis by quantitative PCR (qPCR). Figure 4.17 presents the fold increase of ORF47 mRNA in the respective fractions compared to the GFP control. In the presence of ORF57, a 4-fold increase in whole cell reporter mRNA can be observed. This is expected, as ORF57 recruits the hTREX complex onto viral mRNA and thereby stabilises viral intronless transcripts, protecting them from cellular RNA decay mechanisms (Stubbs et al., 2012). Furthermore, ORF57 expressing cells show a significant increase in cytoplasmic levels of ORF47 mRNA, compared to whole cell levels, confirming that ORF57 enhances export of viral transcripts, in addition to protecting them. However, a significant decrease in whole cell ORF47 transcripts is detected in C2 treated cells, compared to DMSO treated cells. As C2 efficiently disrupts the interaction of ORF57 and hTREX components, a loss in viral mRNA stability is expected. Importantly though, no significant export of viral mRNA can be seen in the presence of C2, as cytoplasmic levels do not exceed whole cell amounts.

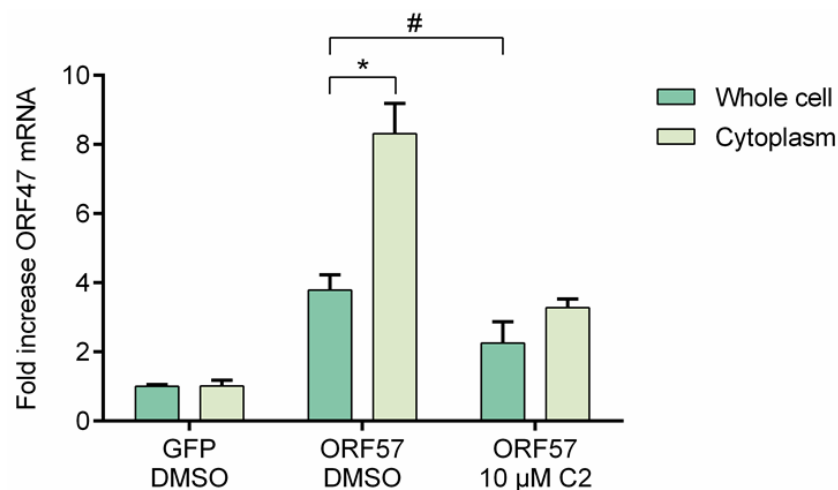


**Figure 4.17: Inhibitor C2 reduces ORF57-mediated mRNA export.** 293T cells were transfected with GFP or ORF57-GFP expressing plasmids, as well as an ORF47 reporter construct. After 6 h, cells were treated with DMSO or C2 as indicated and after another 16 h fractionated. qRT-PCR was performed using ORF47 and GAPDH specific primers. ORF47 CT values were normalised to GAPDH and the relative increase calculated using the  $\Delta\Delta\text{CT}$  method.  $n = 3$ , error bars display SD,  $p < 0.05$ .

#### 4.9 Cytotoxicity of C2 in TReX BCBL-1 Rta cells

To confirm the previous mRNA export results obtained in transfected 293T cells, a well characterised KSHV infected cell line, TReX BCBL1-Rta, was also employed. This cell line is a derivative of a BCBL-1 cell line (B-cell lymphoma cells latently infected with KSHV), containing a Myc-tagged version of RTA under the control of a tetracycline-inducible promoter. TReX BCBL1-Rta cells were shown to undergo the full lytic replication cycle and produce infectious viral progeny after induction by doxycycline (Nakamura et al., 2003). The viability of TReX BCBL1-Rta cells was assessed in the presence of C2 at 24 and 72 h by MTS assay (Figure 4.18). The half maximal cytotoxic concentration ( $CC_{50}$ ) was determined using non-linear regression (Figure 4.18b). No cytotoxicity was observed up to 2.5  $\mu$ M C2 at both 24 and 72 h. A small decrease in  $CC_{50}$  can be observed between 24 and 72 h, indicating that the effect of C2 within the cell is stable over the observed time.

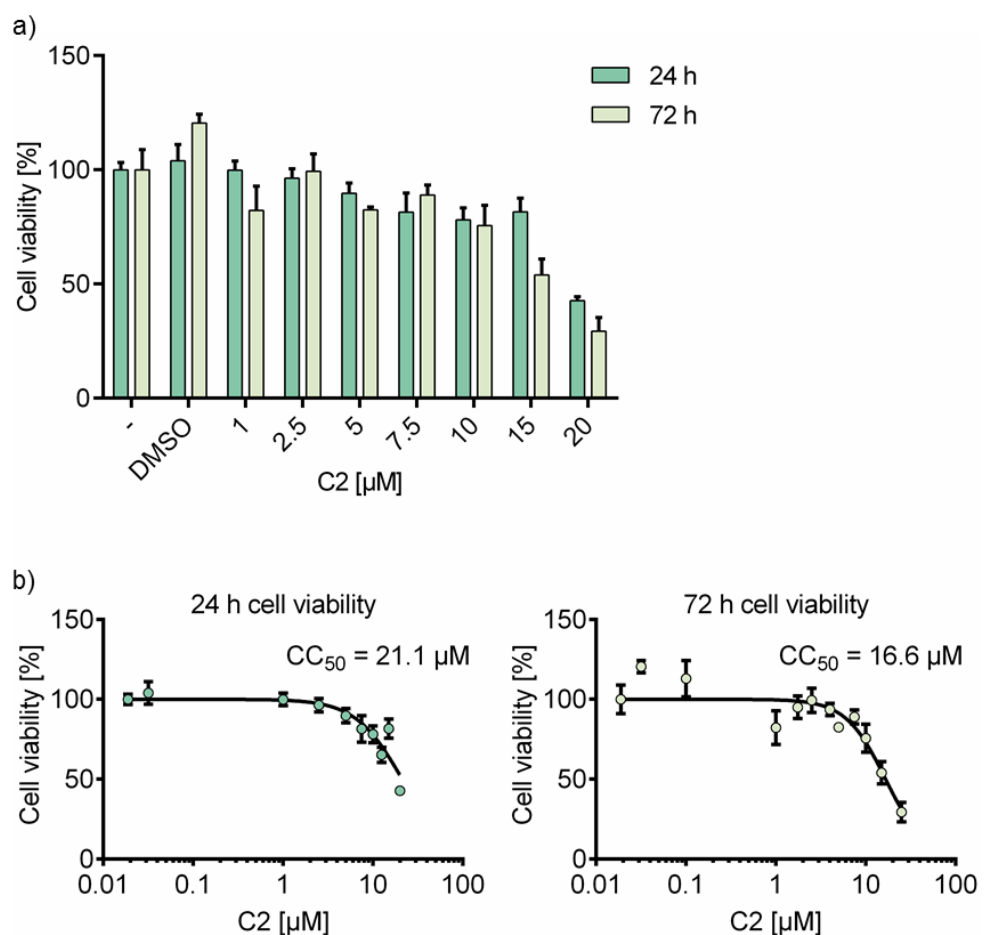


**Figure 4.18: Cell viability of TReX BCBL1-Rta cells in the presence of C2.** Cells were incubated with increasing concentrations of C2 and a total of 0.1% DMSO for 24 and 72 h. Cell viability was assessed by MTS assay and normalised to untreated cells.  $n = 5$ , error bars present SD. Results are displayed as a) column graph, b) on a xy-graph using a log-scale and non-linear regression to determine the  $CC_{50}$ .

#### 4.10 Disruption of vRNP formation by C2 in KSHV infected cells

Immunofluorescence microscopy was employed to assess co-localisation of ORF57 and hTREF components in KSHV infected TREF BCBL1-Rta cells. For this, cells were treated with DMSO or 2.5  $\mu$ M C2 at the time of induction. After 24 h, cells were fixed, permeabilised and immunostained with CIP29- and ORF57-specific antibodies. Cells were visualised using confocal microscopy (Figure 4.19). As was described earlier, CIP29 localises in nuclear speckles of the cell nucleus and is also found here in latently infected TREF BCBL1-Rta cells. The protein is visible in bright nuclear speckles and appears to be excluded from the nucleolus (arrows). Upon induction of KSHV lytic replication and expression of ORF57, CIP29 can be seen co-localising with the viral protein and appears to lose its bright, punctuate appearance. However, in induced cells that were treated with C2, CIP29 and ORF57 fail to co-localise. Furthermore, CIP29 appears again in punctuate speckles. Together this data confirms our previous immunofluorescence in a physiologically relevant KSHV-infected cell line.

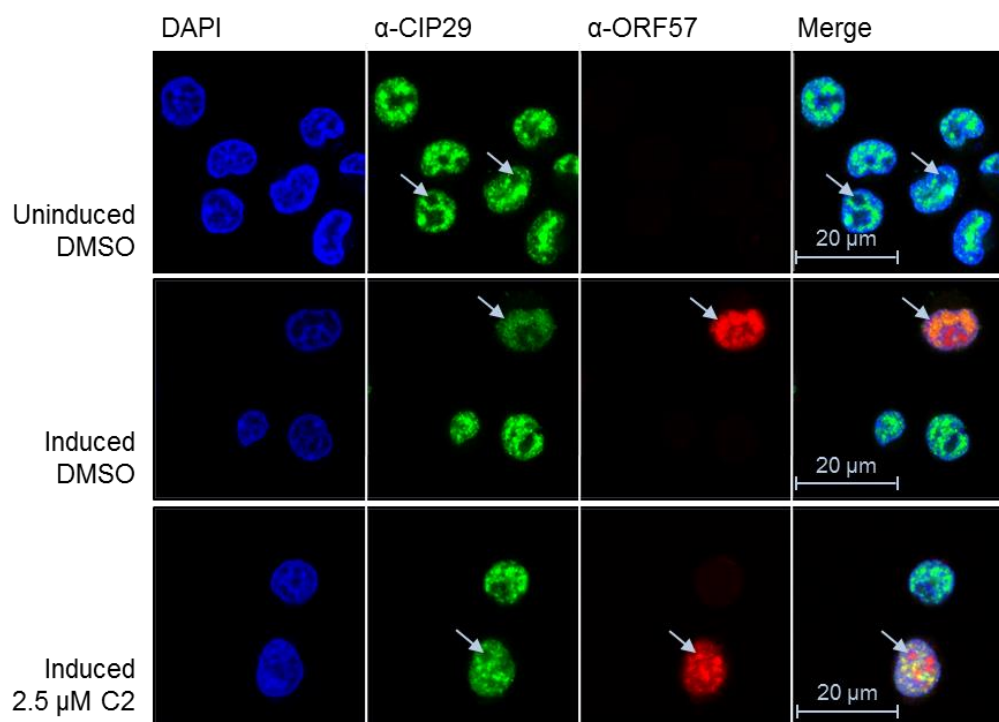


**Figure 4.19: Disruption of CIP29 co-localisation with ORF57 in the presence of C2.** TREF BCBL1-Rta cells were either left uninduced or induced with doxocycline, and then treated with DMSO or C2, as indicated, for 24 h, before they were fixed and permeabilised. Cells were stained using a CIP29- (green) or ORF57-specific antibody (red). DAPI staining (blue) indicates the nucleus.

#### **4.11 Treatment of TReX BCBL1-Rta cells with C2 prevents export of viral intronless mRNA**

To assess the effect of C2 on viral intronless mRNA export in lytic KSHV infected cells, TReX BCBL1-Rta cells were used for a viral RNA export assay. Cells were induced with doxycycline or mock induced and treated with DMSO or 2.5  $\mu$ M C2 for 24 h. Cells were then harvested and fractionated in order to obtain whole cell, cytoplasmic and nuclear fractions. Protein samples of all fractions were also obtained and analysed by SDS-PAGE and Western blotting (Figure 4.20a). Treatment of cells with 2.5  $\mu$ M C2 does not impede induction of lytic replication or ORF57 expression, as similar amounts of protein were present in all induced samples.

The mRNA of each fraction was analysed by reverse transcriptase quantitative PCR (qRT-PCR). We examined ORF47 and ORF57 mRNA to contrast both viral intronless and intron-containing mRNA. Figure 4.20b presents the fold increase of ORF47 and ORF57 mRNA in each fraction, normalised to induced cell samples in the presence of DMSO. Comparing whole cell mRNA levels between DMSO and C2 treated induced cells, a significant reduction can be observed for both ORF47 and ORF57. However, this effect is not a general effect on viral transcripts; instead there is a significant difference between the two types of mRNA. While ORF47 mRNA levels are reduced by more than half, only a 0.25 fold decrease is detected for ORF57 transcripts. It is likely that intronless viral transcripts are less stable in the presence of C2, as observed before for 293T cells. Furthermore, the lytic expression cascade of KSHV might be less efficient in the presence of C2, causing an additional general deficit in viral gene transcription seen for both types of mRNA. Interestingly, even though a decrease in whole cell ORF57 mRNA was noted, this is not reflected in the cytoplasmic levels of the mRNA, where no difference to untreated cells can be detected. This indicates efficient export of viral intron-containing transcripts, in the presence of the inhibitor. In contrast, ORF47 intronless mRNA is only poorly exported into the cytoplasm and a significant loss can be observed compared to DMSO treated cells. Interestingly, no significant decrease in nuclear ORF47 transcripts is detected, although whole cell levels were halved. This indicates retention of the intronless mRNA in the nucleus. Opposed to this, a further loss of nuclear ORF57 transcripts compared to whole cell levels suggests further depletion by efficient export into the cytoplasm.

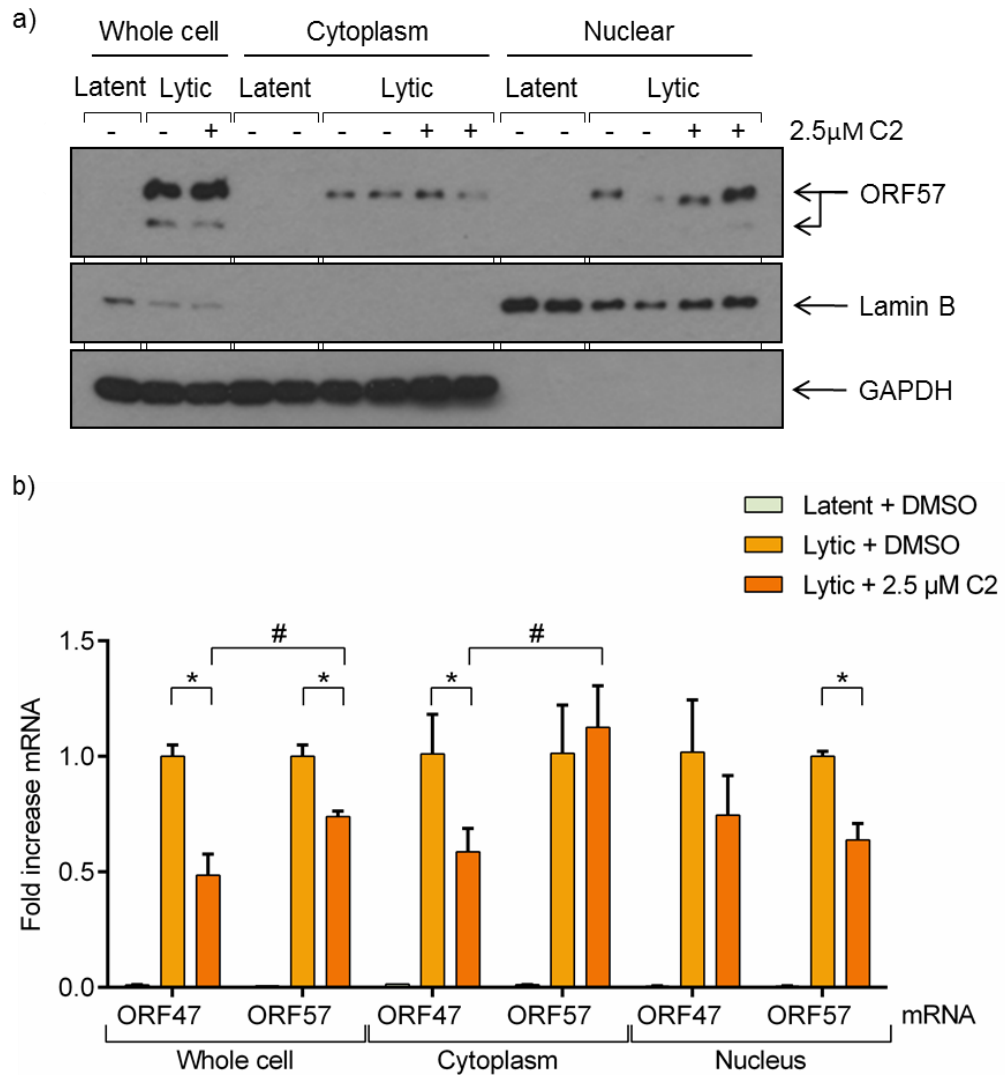


**Figure 4.20: Inhibitor C2 reduces ORF57-mediated mRNA export in KSHV infected cells.** TReX BCBL1-Rta cells were induced and treated with DMSO or C2, as indicated. After 24 h, cells were harvested and fractionated. a) Protein samples were analysed by SDS-PAGE and Western blotting, using ORF57-, Lamin B- and GAPDH-specific antibodies, to detect the indicated proteins. b) qRT-PCR was performed using ORF47, ORF57 and GAPDH specific primers. ORF47 and ORF57 CT values were normalised to GAPDH and the relative increase calculated using the  $\Delta\Delta CT$  method.  $n = 3$ , error bars display SD,  $p < 0.05$ .

#### 4.12 Small molecule inhibitor C2 prevents expression of viral late proteins in KSHV infected cells

After showing a marked reduction in nuclear export of viral intronless transcripts in the presence of C2, it would be plausible if this is mirrored in decreased expression of late proteins translated from the mRNAs. To test this hypothesis KSHV lytic replication in TReX BCBL1-Rta cells was induced and cells treated with increasing amounts of C2. After 24 h,

protein samples were analysed by Western blotting (Figure 4.21a). Myc- and ORF57-specific antibodies were employed to test for the presence of RTA, the viral transcriptional activator, and ORF57 as markers for induction of lytic replication. Antibodies specific to the KSHV minor capsid protein (mCP) were used to assess the levels of viral late protein translated from intronless mRNA. At 2.5  $\mu$ M C2, a concentration where cell viability was 100%, a marked reduction in expression of the mCP is visible compared to untreated or DMSO treated samples. No decrease in ORF57 expression is noted at this concentration, confirming that a decrease in mCP expression is not due to loss of ORF57 or reduction in lytic replication. Both ORF57 and RTA are translated from intron-containing transcripts and hence indicate a functional hTREX complex. All Western blots were quantified and levels of protein expression presented as fold increase in relation to induced, DMSO treated control samples (Figure 4.21b). Plotting of the mCP expression levels allowed for non-linear regression to obtain a half maximal effective concentration ( $EC_{50}$ ) for viral late protein expression (Figure 4.21c). Intriguingly, the  $EC_{50}$  of 0.6  $\mu$ M is far lower than the  $CC_{50}$  of 21  $\mu$ M at the same time point. Comparing both curves, a large “therapeutic window” can be observed, showing that cytotoxicity occurs at higher concentrations than inhibition of viral protein expression.



### **4.13 Inhibition of viral replication and production of infectious virus particles in the presence of C2**

Having shown a loss in viral intronless mRNA export and subsequent decrease in viral late protein expression, it was speculated that this would lead to a decrease in viral replication within C2 treated cells. To this end, TREx BCBL1-Rta cells were induced and treated with increasing amounts of C2. After 72 h, cells were harvested and complete genomic and viral DNA isolated before being analysed by quantitative PCR using primer pairs for GAPDH and the viral genes ORF47 and ORF57. Viral DNA levels were normalised to cellular DNA to account for cytotoxicity at higher concentrations of C2. Figure 4.22a shows the viral load within cells as a percentage of induced, DMSO treated cells. A steep decrease in viral load is visible at 1 and 2.5  $\mu\text{M}$  C2, showing a reduction to 55 and 15%, respectively. Using non-linear regression we plotted an inhibition curve for C2, calculating an  $\text{EC}_{50}$  on viral replication of 1.1  $\mu\text{M}$  (Figure 4.22b). Again, when comparing this to the 72 h  $\text{CC}_{50}$  of 16.6  $\mu\text{M}$  and plotting the curves next to each other, a large “therapeutic window” can be observed. This range of concentrations allows for almost a complete inhibition of viral replication at a concentration range that does not cause cytotoxicity.

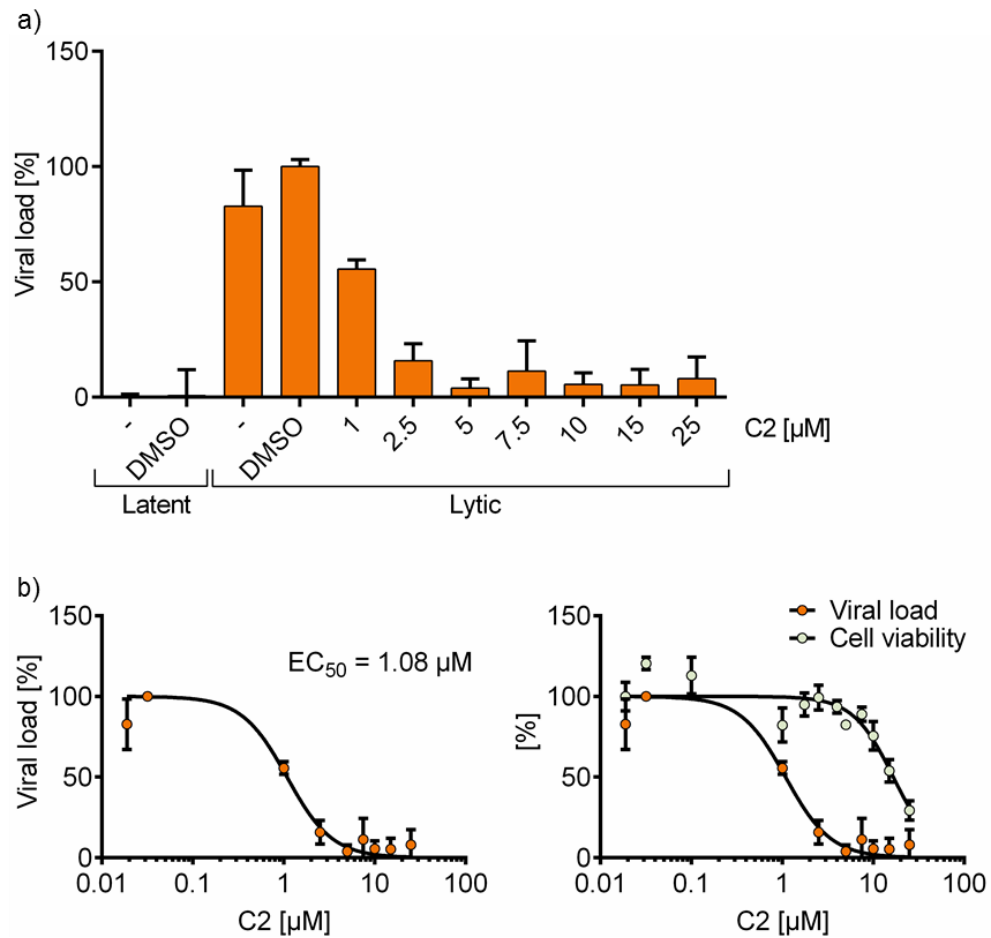


**Figure 4.22: Reduction of viral load in KSHV-infected cells treated with C2.** TREx BCBL1-Rta cells were induced and treated with DMSO or increasing amounts C2, as indicated, for 72 h. Viral DNA load was quantified using qPCR with ORF47, ORF57 and GAPDH specific primers. ORF47 and ORF57 CT values were normalised to GAPDH and the relative increase calculated using the  $\Delta\Delta\text{CT}$  method. Results display the average of two individual experiments, with each  $n = 2$ , error bars display SD. Results are displayed as a) column graph, b) on a xy-graph using a log-scale and non-linear regression to determine the  $\text{CC}_{50}$  and in combination with cell viability data at 72 h.

The production of infectious virus particles was also examined in the presence of 2.5  $\mu\text{M}$  C2. For this, TREx BCBL1-Rta cells were induced for 72 h, before taking the supernatant and adding it in a 1:1 dilution onto confluent 293T cells for 24 h, to allow infection. RNA was then extracted and qRT-PCR was performed. Viral transcripts were normalised to GAPDH and presented as fold increase of induced, DMSO treated samples (Figure 4.23). Results show that 293T cells incubated with supernatant from C2 treated TREx BCBL1-Rta cells contain 80% less viral mRNA, than cells that were re-infected with supernatant from DMSO treated lytic TREx BCBL1-Rta cells. This demonstrates a clear decrease in the production of infectious virions in KSHV infected cells upon treatment with C2. Cells that

were infected with the supernatant of latent TReX BCBL1-Rta cells show minor levels of viral mRNA. This is due to a small degree of spontaneous lytic replication occurring at all times in BCLB-1 cells as described before (Taylor and Blackburn, 2011).

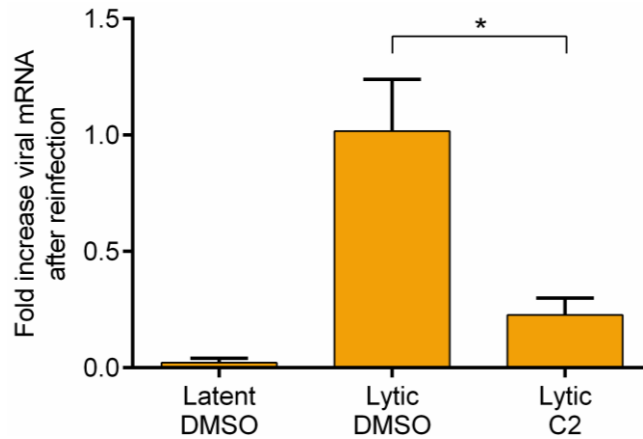


**Figure 4.23: Inhibition of infectious virion production by C2.** TReX BCBL1-Rta cells were induced and treated with DMSO or 2.5  $\mu$ M C2, as indicated, for 24 h. Cell supernatant was added 1:1 to uninfected 293T cells for a further 24 h. qRT-PCR was performed using ORF57- and GAPDH-specific primers. ORF57 CT values were normalised to GAPDH and the relative increase calculated using the  $\Delta\Delta$ CT method.  $n = 3$ , error bars display SD,  $p < 0.05$ .

#### 4.14 Discussion

UAP56 belongs to the family of DExD-box RNA-helicases and shows RNA-stimulated ATPase activity (Shen et al., 2007). Both RNA-helicase and ATPase activity of DExD-box proteins are known to contribute to remodelling of intramolecular RNA-, RNA-protein and protein-protein interactions (Cordin et al., 2006).

In this chapter, an ATP-cycle dependent remodelling of the ORF57/hTReX complex interaction has been described. Results show formation of the endogenous, trimeric Aly-UAP56-CIP29 complex upon ATP binding of UAP56 and a subsequent remodelling upon ATP hydrolysis. This was illustrated by ORF57, which was found to interact with hTReX components in the presence of ATP, but was specifically disrupted after the addition of the non-hydrolysable ATP analogue ATP $\gamma$ S. Importantly, endogenous hTReX interactions were retained in the presence of ATP $\gamma$ S, suggesting that the complex is remodelled after initial binding of Aly and CIP29 to UAP56, into a conformation which can then accommodate the ORF57 protein. This extremely exciting observation indicates that ORF57 interacts with

proteins that are part of an already formed complex, instead of recruiting one or more individual hTREX components and then facilitating recruitment of the remaining proteins. Whether this is the complete or a partial complex is unknown. Results further highlight a dissociation of UAP56 from hTREX components and ORF57 upon ADP binding, which completes the hTREX cycle. While no structural data has confirmed this to date, an ATP-cycle dependent remodelling of hTREX has recently been suggested (Chang et al., 2013). Intriguingly, it was reported that ATP hydrolysis is necessary for loading of Aly onto the mRNA, as the presence of the non-hydrolysable AMP-PNP was found to prevent this transfer.

Data herein indicates that inhibition of ATP hydrolysis by UAP56 would trap the hTREX complex in a conformation, preventing ORF57 recruitment. It was furthermore speculated that this disruption of ORF57/hTREX interaction would efficiently inhibit virus lytic replication. This is especially exciting since redundancy has been shown for the direct interaction of ORF57 and the mRNA adaptor Aly, through UIF, and hence this interaction cannot be targeted efficiently (Jackson et al., 2011). A similar approach has been described in the literature, where a series of small molecule inhibitors (ring expanded nucleosides) were shown to suppress replication of human immune deficiency virus type 1 (HIV-1) by inhibition of the ATP dependent activity of human helicase DDX3 (Yedavalli et al., 2008). At low concentrations these drugs were found to prevent virus replication without affecting cell viability. It was therefore speculated that a small molecule inhibitor designed for high affinity binding to the ATP binding site in UAP56 would prove to efficiently disrupt the ORF57/hTREX interaction.

To this end, structure-based drug design was employed and 400 selected compounds and fragments were screened *in vitro* against UAP56 ATPase activity. Four novel inhibitors with a diverse structural background were identified. All hit compounds were sourced from a Tocriscreen Library, a compound library of known bioactive compounds. This is not surprising, as screening approaches utilising known bioactive compounds or inhibitors for novel targets tend to generate a higher hit rate than vHTS. Furthermore, while fragments were screened at a higher concentration, it is possible that assay conditions were not optimal for identification of fragment hits. The most potent hit, compound C2, disrupted vRNP formation in immunoprecipitation assays, while allowing the interaction of UAP56 with hTREX components Aly, CIP29 and Chtop. Subsequently, disruption of co-localisation

of ORF57 with hTREX components in the presence of C2 was observed, both in transfected 293T cells and in KSHV infected TReX BCBL1-Rta cells, at concentrations where no cytotoxicity could be observed. Importantly, using a FISH assay, it was demonstrated that endogenous bulk mRNA export is not disrupted in the presence of the inhibitor. Furthermore, ORF57 was unable to block bulk cellular mRNA export by sequestration of hTREX after addition of C2. Moreover, a disruption of viral intronless mRNA export was shown in both transfected 293T cells and in KSHV infected BCBL-1 cells. In both experiments, a loss in whole cell amounts of viral mRNA was observed. This effect was specific for viral intronless transcripts, and is likely due to the loss of ORF57-mediated hTREX binding to these nucleic acids. ORF57 has been shown in the past to cause accumulation and stabilisation of viral transcripts (Stubbs et al., 2012; Nekorchuk et al., 2007). Unbound viral RNAs can be detected by cellular surveillance mechanisms and hence are more prone to RNA decay. Importantly, using a physiologically relevant cell culture model, results also demonstrated a loss in late viral protein production upon treatment of cells infected with lytic replicating KSHV. Almost a complete loss of protein was observed at a concentration where no loss in cytotoxicity and normal expression of RTA and ORF57, two proteins translated from intron-containing mRNAs, was detected. Furthermore, an 85% reduction in viral load and an 80% reduction in the production of infectious virions was achieved at a non-cytotoxic concentration. For a first generation compound, this presents a very encouraging “therapeutic window”, in which a concentration range proves effective against the virus induced RNP, but does not affect cellular hTREX.

Together, work identifying and testing this first-generation compound has provided positive results and future work will aim to explore this novel antiviral target further by elucidating a structure-activity-relationship, followed by optimisation of the structure to reduce cytotoxic side effects and improve virus inhibition. Other interesting questions include the effect on other herpesviruses and viruses that utilise the hTREX complex to allow viral mRNA export.

## Chapter 5

~

Structural analogues of UAP56 ATPase inhibitor C2 and  
the inhibitory effect on HSV-1

## 5 Structural analogues of UAP56 ATPase inhibitor C2 and the inhibitory effect on HSV-1

### 5.1 Introduction

In the previous chapter, an ATP-cycle dependent remodelling of the ORF57-mediated vRNP was described. Intriguingly, results showed that during the ATP-cycle, hTREX enters a conformation in which ORF57 is unable to recruit the complex onto viral mRNA. Prevention of ATP-hydrolysis by UAP56 allowed the endogenous hTREX components Aly and CIP29 to bind to UAP56, but inhibited ORF57 binding. These findings presented a novel antiviral target for inhibition of lytic virus replication. Using virtual high-throughput screening compounds were identified, which specifically inhibited UAP56 ATPase function and showed subsequent disruption of vRNP formation. As a consequence the best hit was able to prevent viral mRNA export, lytic protein production and hence disrupted lytic virus replication. In this chapter, the identification of novel inhibitors was followed up by examining close structural analogues, to identify a structure-activity-relationship (SAR). Furthermore, as compound C2 has previously been described as an HSP90 inhibitor, the effect on HSP90 and HSP90 client proteins was assessed, in comparison with the effect on the hTREX complex and KSHV protein expression.

ORF57 is conserved across all families of *Herpesviridae*; ICP27 in HSV-1, UL69 in HCMV, ORF4 in VZV and EB2 in EBV are all essential for virus replication. While these proteins are distinct in size and differ in large parts of their sequence, they all interact with the hTREX complex in order to allow viral intronless mRNA export. As this approach is targeting a component of the hTREX complex and not ORF57 directly, it was speculated that the inhibitor should also efficiently prevent replication of other herpesviruses. Therefore, the effect of inhibitor C2 was examined on primary infection and production of infectious HSV-1 virions in re-infection assays.

## 5.2 Effect of close structural analogue An1 on KSHV late protein expression and viral load in KSHV lytic replication

Four structural analogues were selected, to assess a SAR and confirm the previously observed effects of C2 on viral protein expression and viral load.

The first tested analogue (An1) had the dioxane ring removed (Figure 5.1a). As this functional group potentially forms an interaction within the UAP56 binding site, this compound was utilised to examine if removal could change the inhibitors properties. The compound was first examined for cellular toxicity (Figure 5.1b). As previously described, TReX BCBL1-Rta cells were treated with increasing amounts of An1, before MTS assays were performed after 24 and 72 h. Plotting of results and non-linear regression were further used to determine a  $CC_{50}$  for both time points (Figure 5.1c). At 24 h, the cytotoxic effect of An1 is reduced compared to C2. No cytotoxicity occurs at concentrations up to 7.5  $\mu$ M An1 and the  $CC_{50}$  is increased from 21.1 to 28.9  $\mu$ M compared to C2. However, after 72 h the effect is reversed: concentrations above 2.5  $\mu$ M An1 decrease cell viability noticeably and the  $CC_{50}$  drops to 7.6  $\mu$ M, compared to 16  $\mu$ M C2.

The effect of An1 was then examined on expression of the viral late protein mCP. As described in chapter 4 (Figure 4.21), increasing amounts of the inhibitor were added to TReX BCBL1-Rta cells, before cell lysates were analysed by Western blotting (Figure 5.2a). Densitometry of blots was performed for all proteins (Figure 5.2b). At 5  $\mu$ M An1, a concentration with 100% cell viability, an 82% reduction of mCP is observed, without any loss in expression of the viral proteins RTA and ORF57. This demonstrates a specific decrease in expression for viral proteins translated from intronless mRNAs, while viral proteins from intron-containing mRNAs remain expressed at 5  $\mu$ M. This effect is comparable with C2 at its maximal non-cytotoxic concentration. Using non-linear regression, an  $EC_{50} = 3.1$   $\mu$ M An1 on mCP expression was determined (Figure 5.2c). This is larger than for C2, however as An1 also displays a larger  $CC_{50}$ , a similar therapeutic window can be seen for both inhibitors.

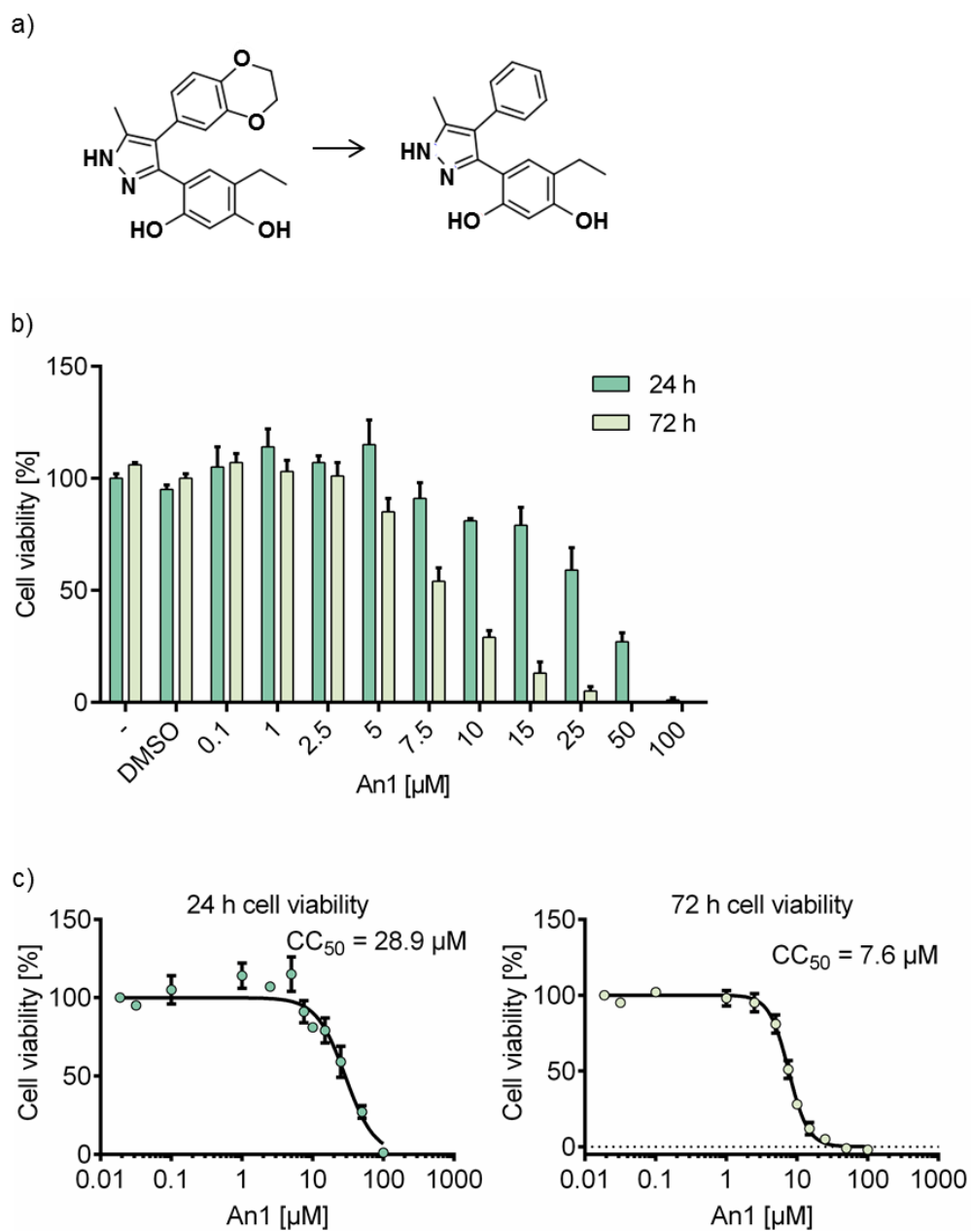


**Figure 5.1: Cell viability of TREx BCBL1-Rta cells in the presence of An1.** The assay was performed as previously described (Figure 4.18).  $n = 5$ , error bars present SD. a) Chemical modifications from C2 to An1. Results are displayed as b) column graph, c) on a xy-graph using a log-scale and non-linear regression to determine the  $CC_{50}$ .

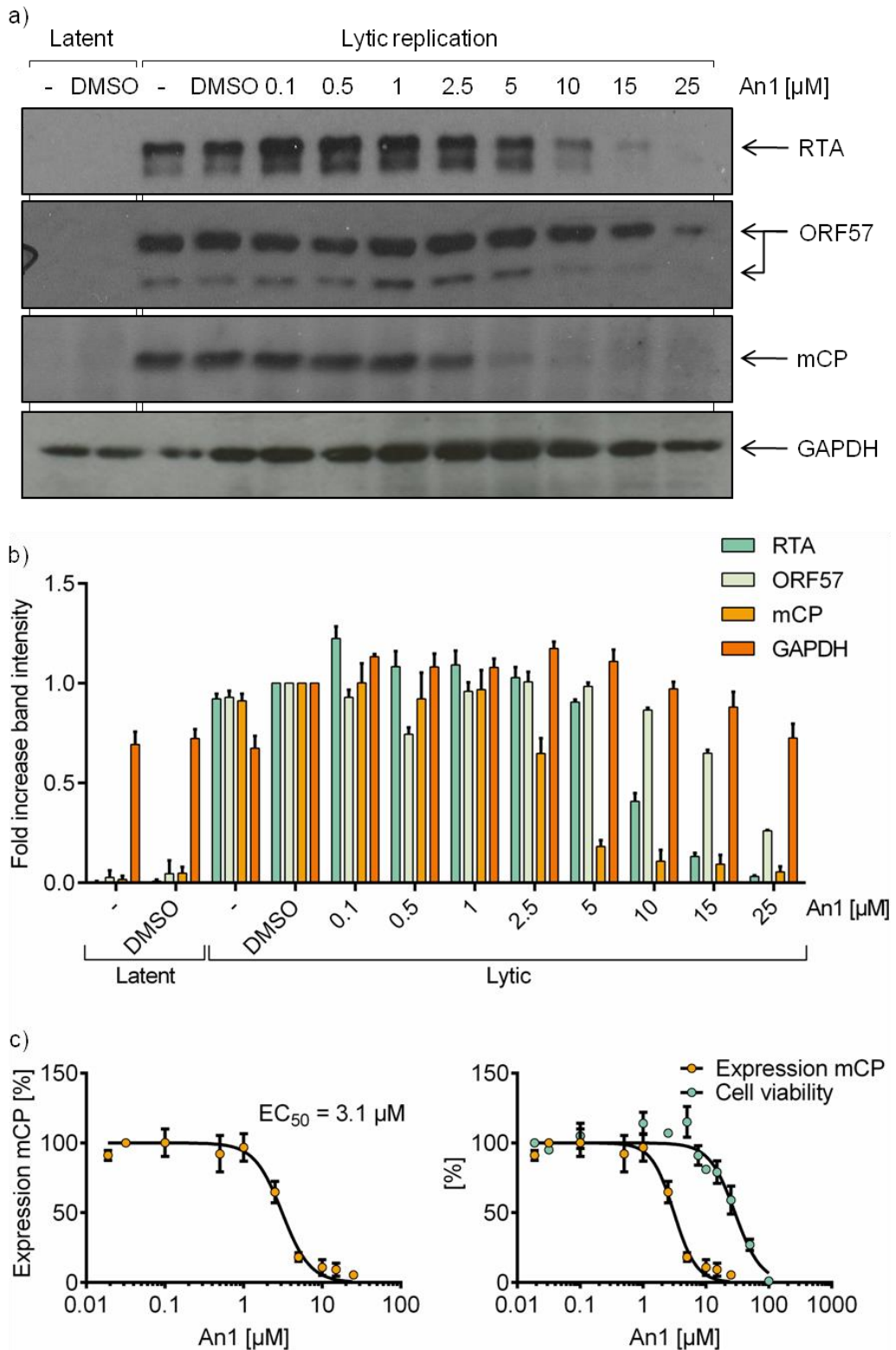


**Figure 5.2: Viral late protein expression is disrupted by An1.** The experiment was performed and analysed as previously described (Figure 4.21).

The effect of An1 on KSHV genome load was also assessed. TREx BCBL1-Rta cells were treated with increasing amounts of An1 upon reactivation of virus lytic replication. Viral DNA was quantified 72 h after treatment and normalised to cellular DNA levels (Figure 5.3a). Viral load is seen to decrease from 0.5  $\mu\text{M}$  An1 upwards and an  $\text{EC}_{50} = 1.54 \mu\text{M}$  was determined (Figure 5.3b). While this is equal to the original inhibitor C2, cytotoxicity of An1 is increased compared to C2, leaving a smaller concentration range before cell death occurs. As both cell viability as well as the effective concentration on viral protein expression or DNA load, seem to decrease between 24 and 72 h, it can be speculated that An1 is less efficient in reaching the protein target within the cell. This could be due to slower uptake into the cell and the nucleus or potentially changed binding affinities to UAP56.

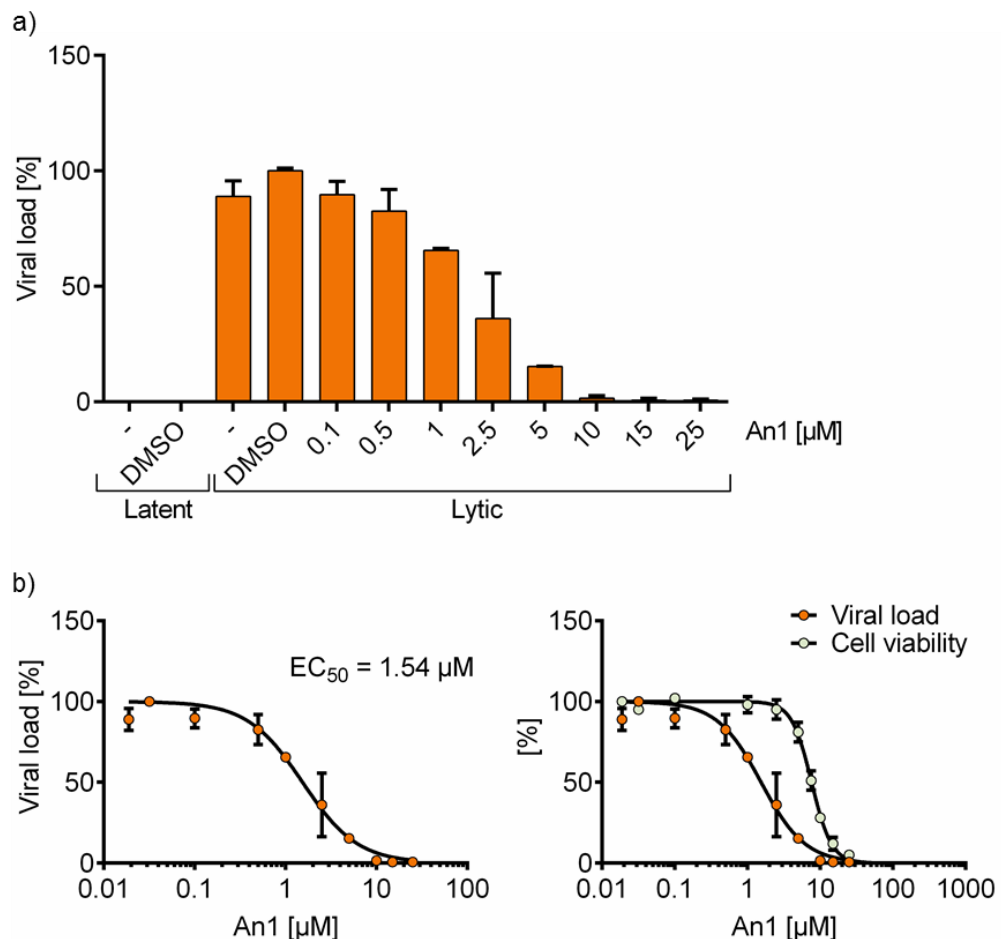


**Figure 5.3: Reduction of viral load in cells treated with An1.** The assay was performed as previously described (Figure 4.22).  $n = 2$ , error bars display SD.

### **5.3 Effect of close structural analogue An3 on KSHV late protein expression and viral load in KSHV lytic replication**

An3 is another close structural analogue of C2, where the ethyl group is removed from the diphenol ring (Figure 5.4a). Again, the effect of An3 was assessed on cytotoxicity, viral late protein expression and viral load. As with both C2 and An1 before, a decrease in  $CC_{50}$  can be observed between 24 and 72 h (Figure 5.4b and Figure 5.4c). However, at both time points, cytotoxicity of An3 occurs at higher concentrations than with other inhibitors. Interestingly, below 15  $\mu$ M, no difference is seen between 24 and 72 h. Only at concentrations of 25 and 50  $\mu$ M is a reduction in cell viability visible between the two time points, causing the apparent drop in  $CC_{50}$ . This means that An3 is the least cytotoxic of the three tested compounds.

Nonetheless, when investigating the effect of An3 on viral late protein expression (as described before), a marked decrease in mCP was seen between 1 and 2.5  $\mu$ M An3 (Figure 5.5). Intriguingly, ORF57 and RTA expression was not reduced at concentrations up to 15  $\mu$ M, much higher than for any other compound, which is in accordance with the high cell viability.

An3 also decreased the viral load in TReX BCBL1-Rta cells, similar to the two other tested compounds (Figure 5.6). The  $EC_{50}$  is detected at 5.1  $\mu$ M, larger than for C2 and An1, but equally still yielding a concentration range where a reduction of 60% in viral load is observed, without a decrease in cell viability. It appears that while removing the ethyl group made the compound less cytotoxic, it has also made it slightly less effective at later time points. It is therefore possible that removing the ethyl group decreased the binding affinity of the compound to UAP56 or that it allows for faster removal from the cell, for example through xenobiotic metabolism of the compound.

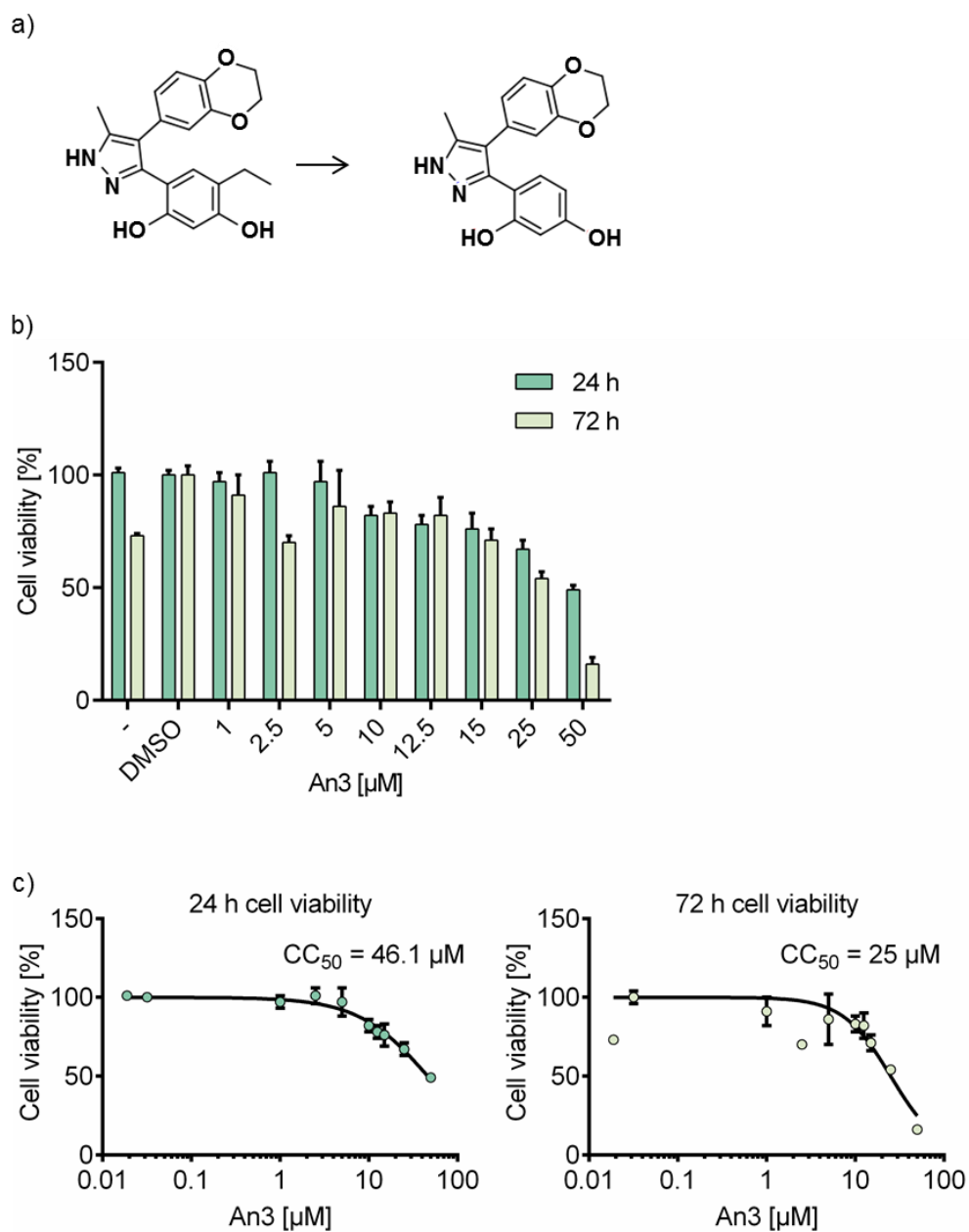


**Figure 5.4: Cell viability of TREx BCBL1-Rta cells in the presence of An3.** The assay was performed as previously described (Figure 4.18).  $n = 5$ , error bars present SD. a) Chemical modifications from C2 to An3. Results are displayed as b) column graph, c) on a xy-graph using a log-scale and non-linear regression to determine the  $CC_{50}$ .

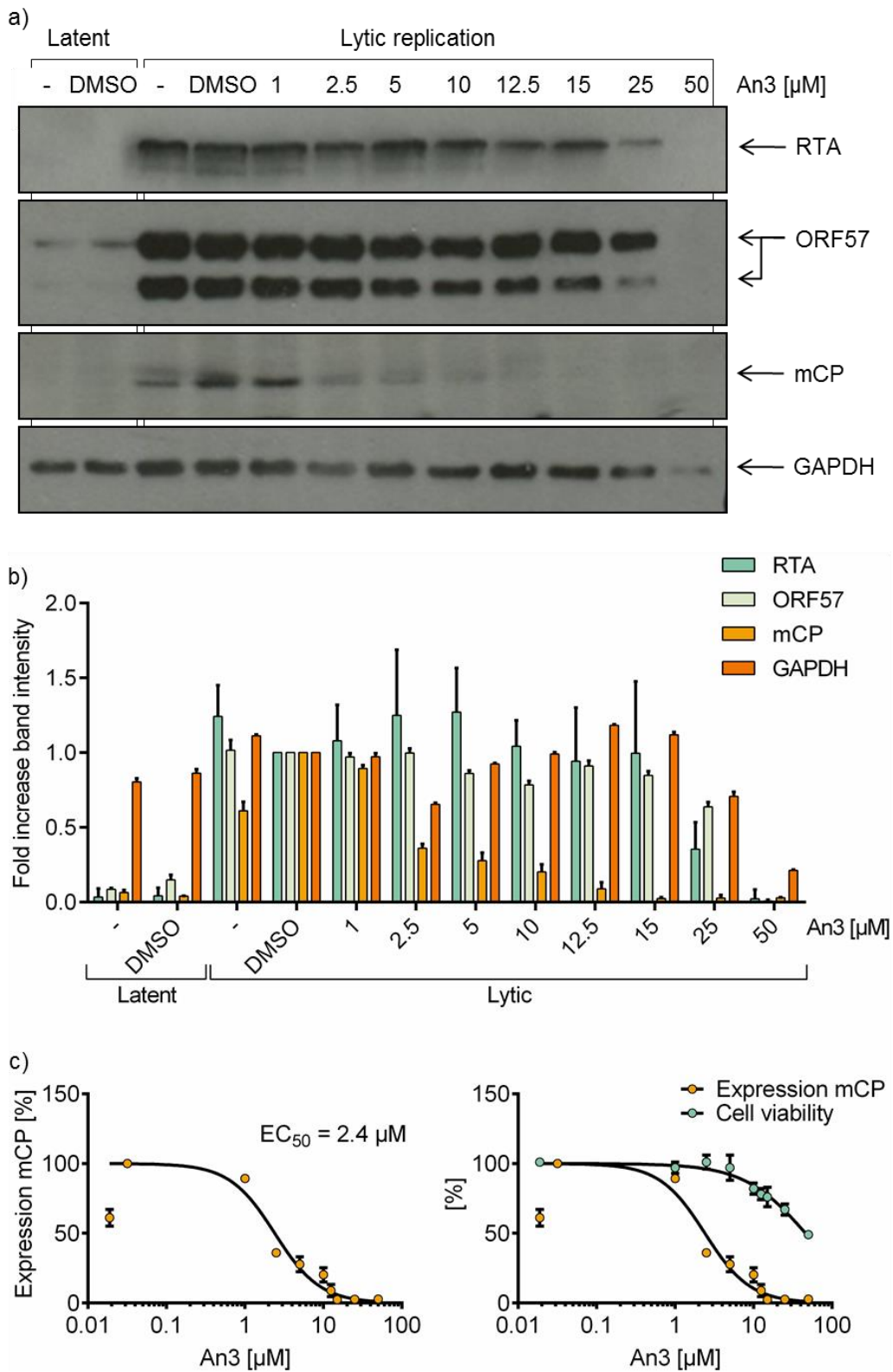


**Figure 5.5: Viral late protein expression is disrupted by An3.** The experiment was performed and analysed as previously described (Figure 4.21).

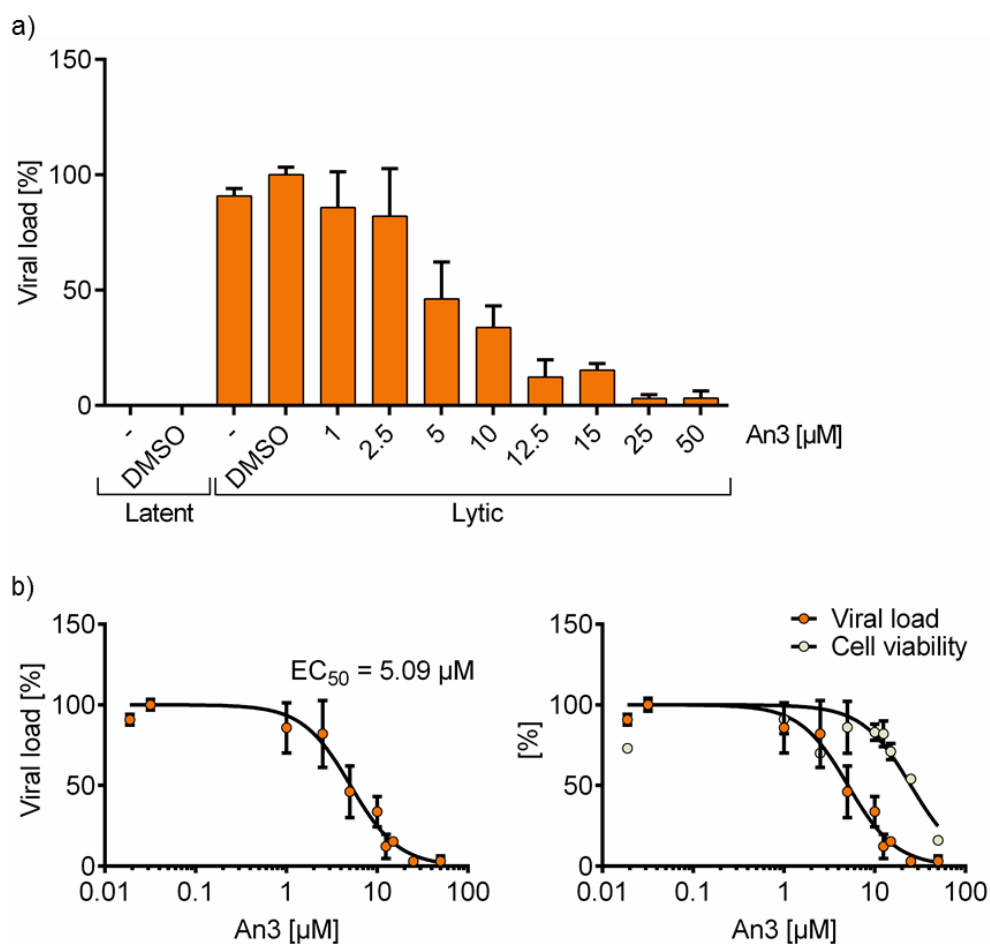


**Figure 5.6: Reduction of viral load in cells treated with An3.** The assay was performed as previously described (Figure 4.22). Results display the average of 2 individual experiments, with each  $n = 2$ , error bars display SD.

#### 5.4 Effect of close structural analogue SKW032 on KSHV late protein expression and viral load in KSHV lytic replication

SKW032 displays changes to the same functional group as An1, but with the dioxane ring substituted with a 4-methoxy group (Figure 5.7a). As with An1, the change in this area lead to an initial increase in cell viability at 24 h, but then a more marked decrease at 72 h, compared to the initial inhibitor hit C2 (Figure 5.7b). The 24 h  $CC_{50} = 27.9 \mu\text{M}$  of SKW032 is very similar to An1, however the cell viability at 72 h appears less strongly decreased, with  $CC_{50} = 14.7 \mu\text{M}$  (Figure 5.7c).

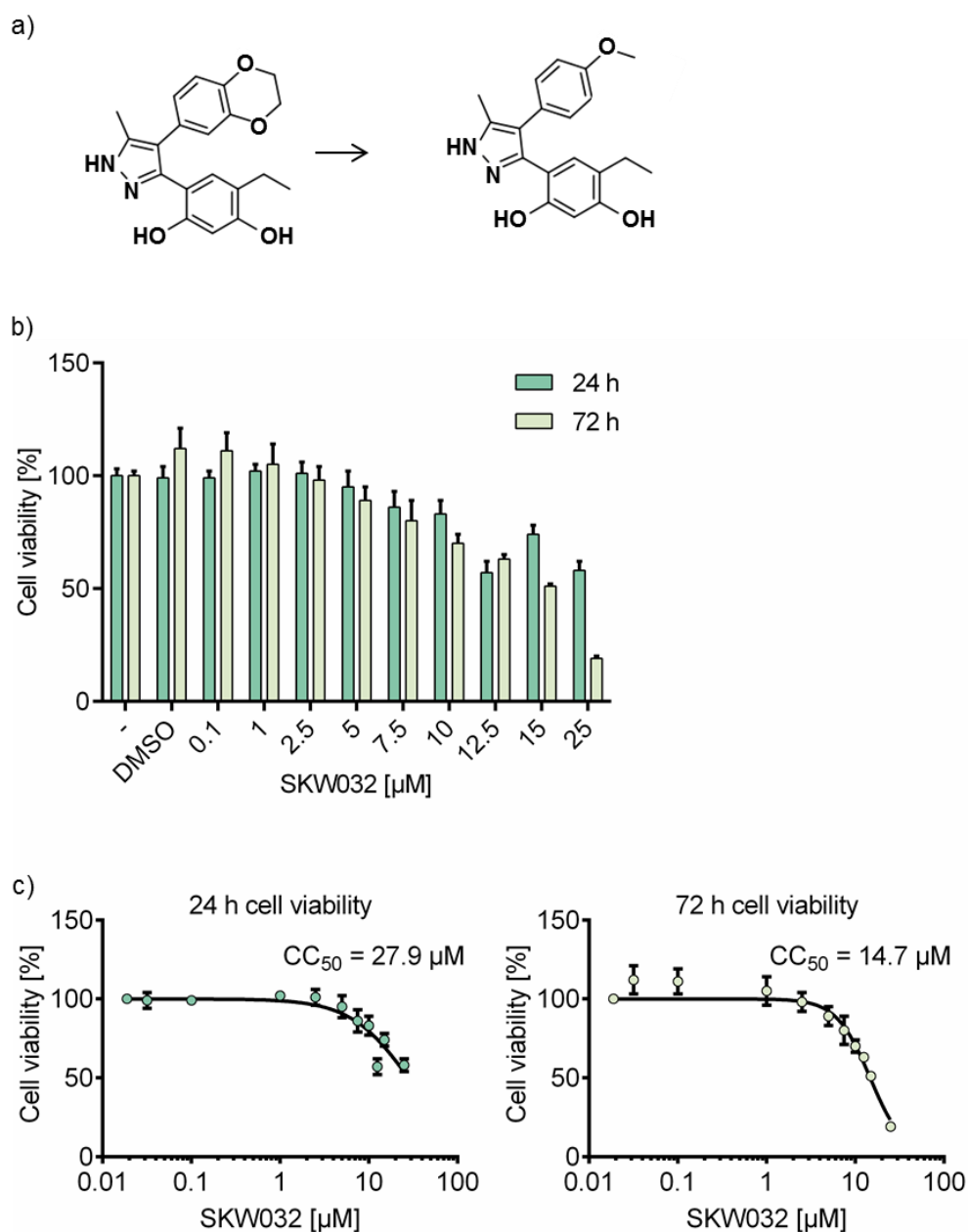


**Figure 5.7: Cell viability of TREx BCBL1-Rta cells in the presence of SKW032.** The assay was performed as previously described (Figure 4.18).  $n = 5$ , error bars present SD. a) Chemical modifications from C2 to SKW032. Results are displayed as b) column graph, c) on a xy-graph using a log-scale and non-linear regression to determine the  $CC_{50}$ .

As all tested analogues before, SKW032 decreases expression of the minor capsid protein in a concentration range where neither cytotoxicity, nor a decrease of ORF57 or RTA expression is detected (Figure 5.8a and Figure 5.8b). Even though the  $EC_{50}$  is more than doubled, compared to C2 (2.5  $\mu\text{M}$  compared to 1.1  $\mu\text{M}$ ), due to lower cytotoxicity of

SKW032 the compound also achieves 80% reduction in viral protein expression, at a concentration where 100% cell viability occurs (Figure 5.8c).

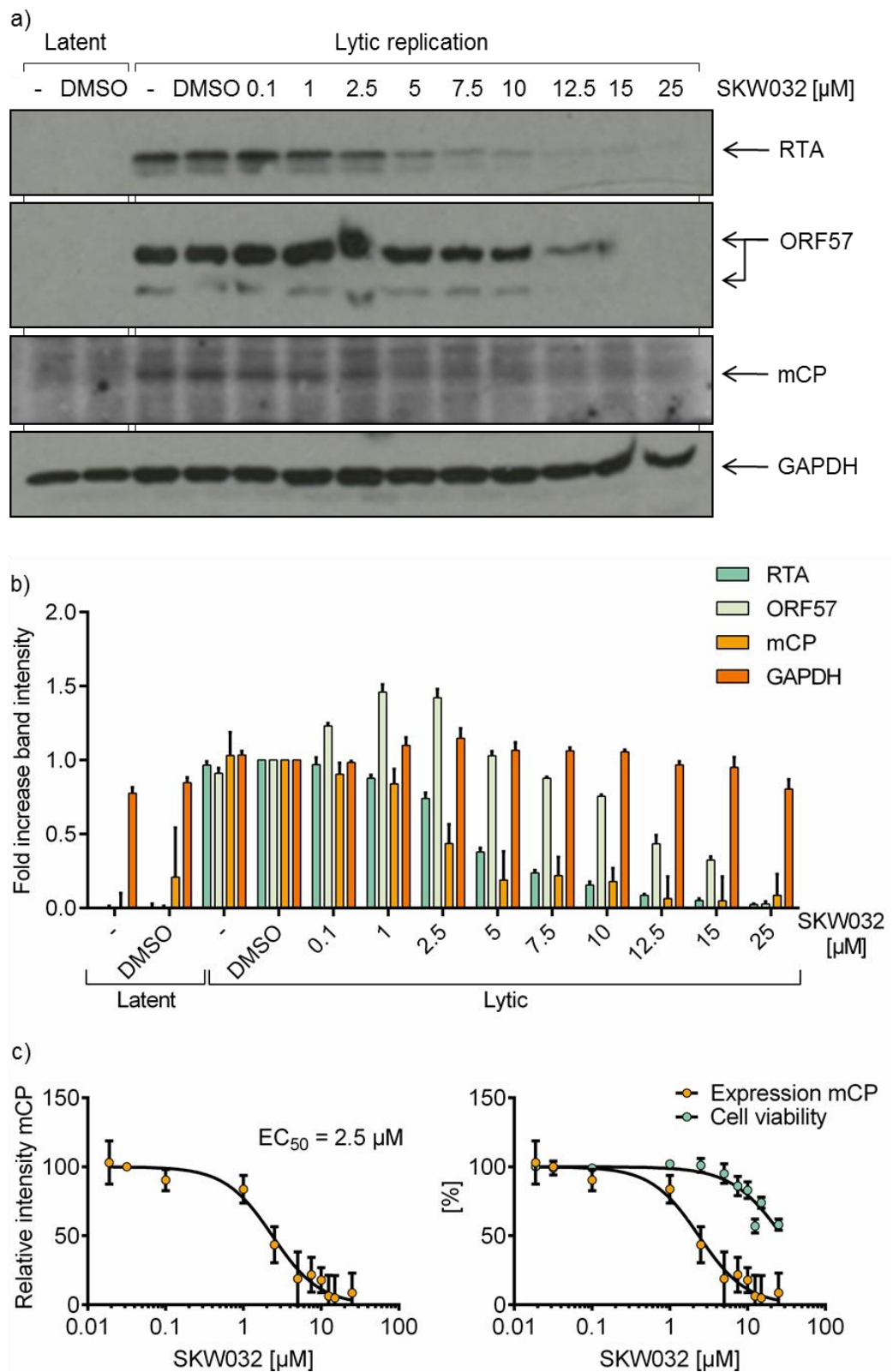


**Figure 5.8: Viral late protein expression is disrupted by SKW032.** The experiment was performed and analysed as previously described (Figure 4.21).

The presence of SKW032 results in almost identical inhibition of virus replication, as is seen for expression of mCP (Figure 5.9). With an  $EC_{50} = 2.75 \mu\text{M}$  and  $CC_{50} = 14.7 \mu\text{M}$  a therapeutic window can also be detected for this analogue. With either complete removal of the dioxane ring (An1) or substitution of this group by a methoxy group (SKW032) we found an initial decrease in cell viability but a stronger toxic effect at 72 h. The polar dioxane ring therefore seems to facilitate a faster response within the cell. This effect is dampened if replaced by a less polar methoxy group and further reduced by a complete loss of functional group in this area.

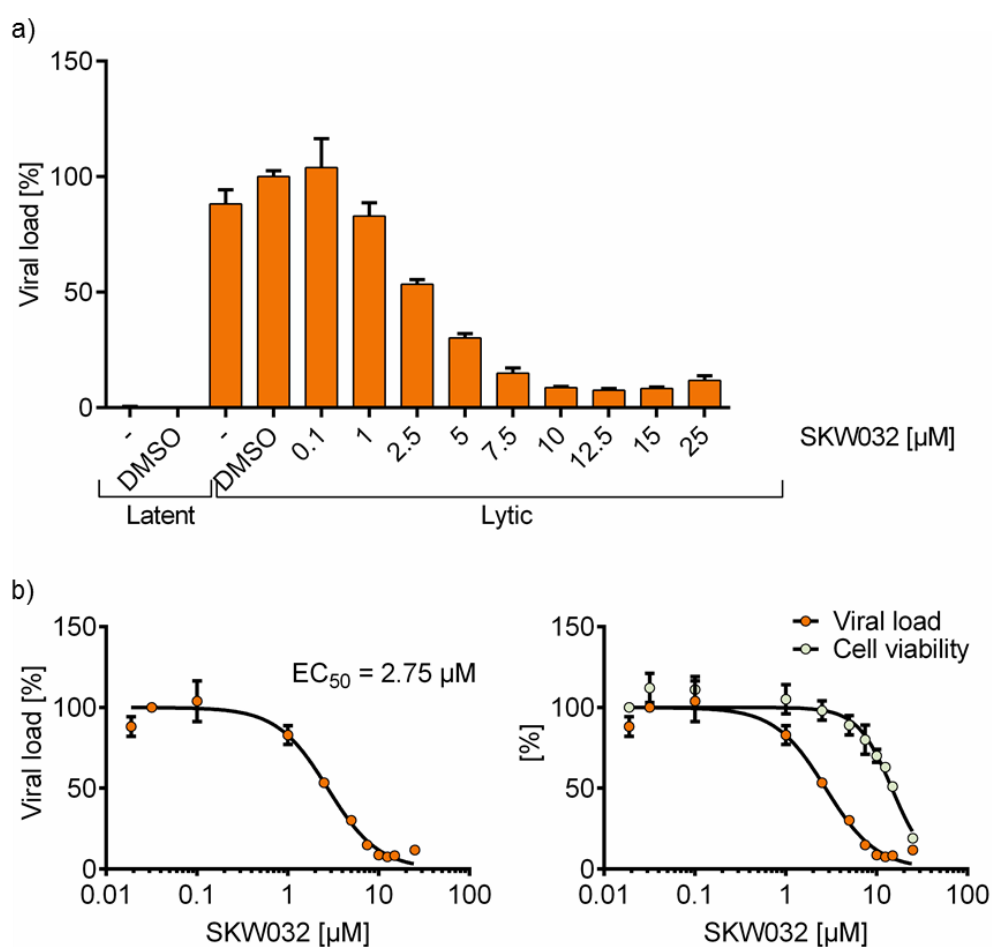


**Figure 5.9: Reduction of viral load in cells treated with SKW032.** The assay was performed as previously described (Figure 4.22).  $n = 2$ , error bars display SD.

## 5.5 Effect of close structural analogue SKW036 on KSHV late protein expression and viral load in KSHV lytic replication

SKW036 is based on structure SKW032, but has a carboxyl group substituting the methyl group (Figure 5.10a). Addition of this polar group is expected to decrease the membrane crossing ability of the compound, as it is less favourable to enter a lipid bilayer.

The effect of SKW036 was first tested on cytotoxicity at 24 and 72 h (Figure 5.10b). At both time points almost no decrease of cell viability is seen; even at a maximum tested concentration of 100  $\mu\text{M}$  cell viability does not drop below 80%. A  $\text{CC}_{50} = 824 \mu\text{M}$  was calculated at 24 h, but no curve could be fitted to the 72 h values, using non-linear regression.

These results were confirmed by the expression levels of KSHV proteins in reactivated TReX BCBL1-Rta cells (Figure 5.11). Even with the addition of 100  $\mu\text{M}$  SKW036, no reduction was observed. Quantification of mCP shows a slight drop of protein levels at higher concentrations, however, this minor change is also visible for ORF57 expression and could just be due to a general reduction in cell viability that has been described above (Figure 5.10b and c). An  $\text{EC}_{50}$  of 1.2 mM could be calculated, which is no feasible concentration for an inhibitor, and has to be seen as an unspecific effect from a loss in cell viability.

As expected, the effect of SKW036 on viral load in cells infected with lytic replicating KSHV was similarly weak (Figure 5.12). A minimal decrease is visible above 25  $\mu\text{M}$  and a reduction of 50% is detected at 100  $\mu\text{M}$ . However, with an  $\text{EC}_{50} = 138 \mu\text{M}$  and a cell viability curve that falls at the same rate until 50  $\mu\text{M}$  this analogue cannot be seen as an inhibitor of KSHV lytic replication. However, the decrease in viral load at higher concentrations is encouraging. Modification of this side chain to a less polar group will enhance uptake into the cell and bring the compound into lower effective concentration range, where it might demonstrate good inhibition while causing less cytotoxicity.

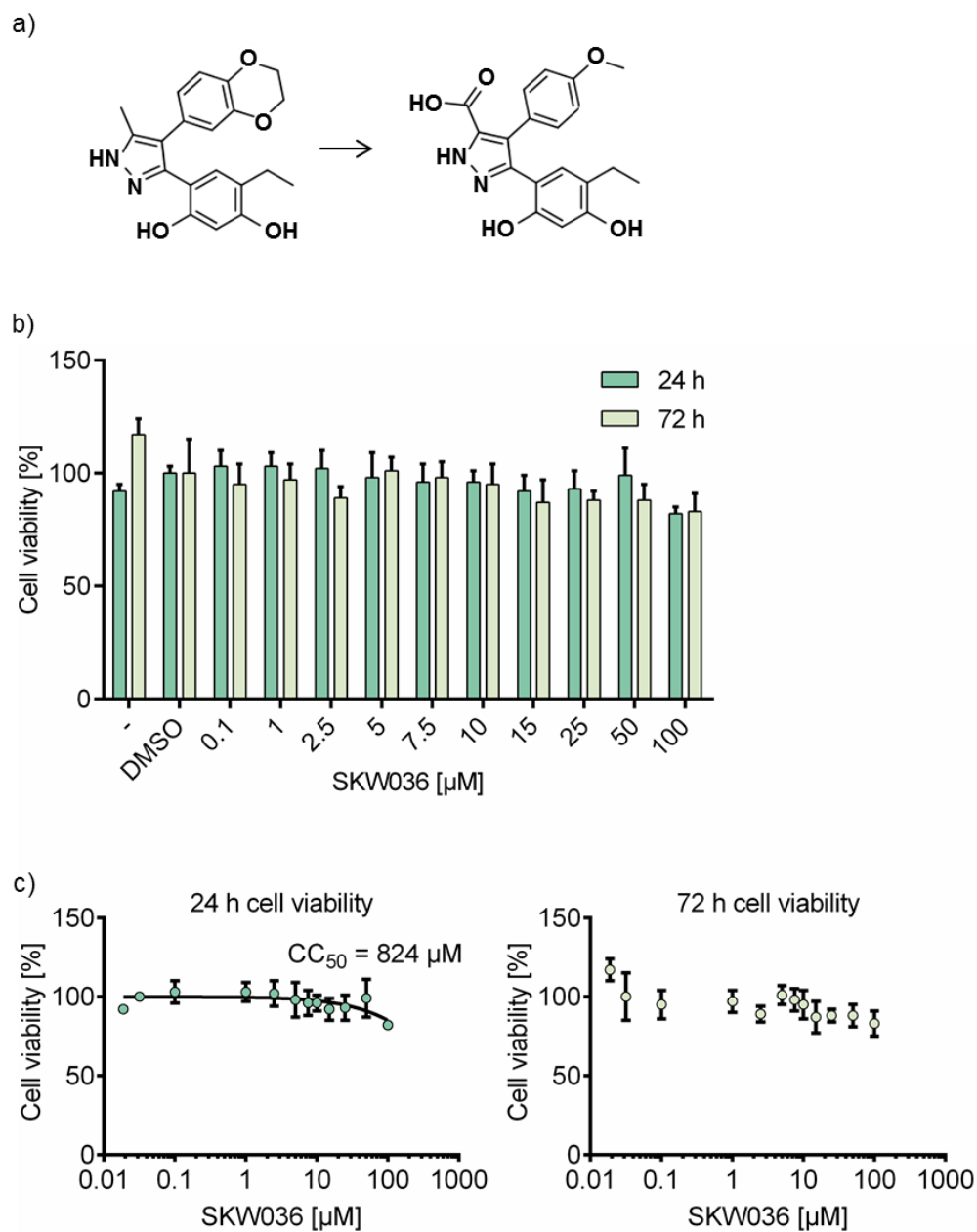


**Figure 5.10: Cell viability of TREx BCBL1-Rta cells in the presence of SKW036.** The assay was performed as previously described (Figure 4.18).  $n = 5$ , error bars present SD. a) Chemical modifications from C2 to SKW036. Results are displayed as b) column graph, c) on a xy-graph using a log-scale and non-linear regression to determine the  $CC_{50}$ . No curve could be fitted to the 72 h values using non-linear regression.

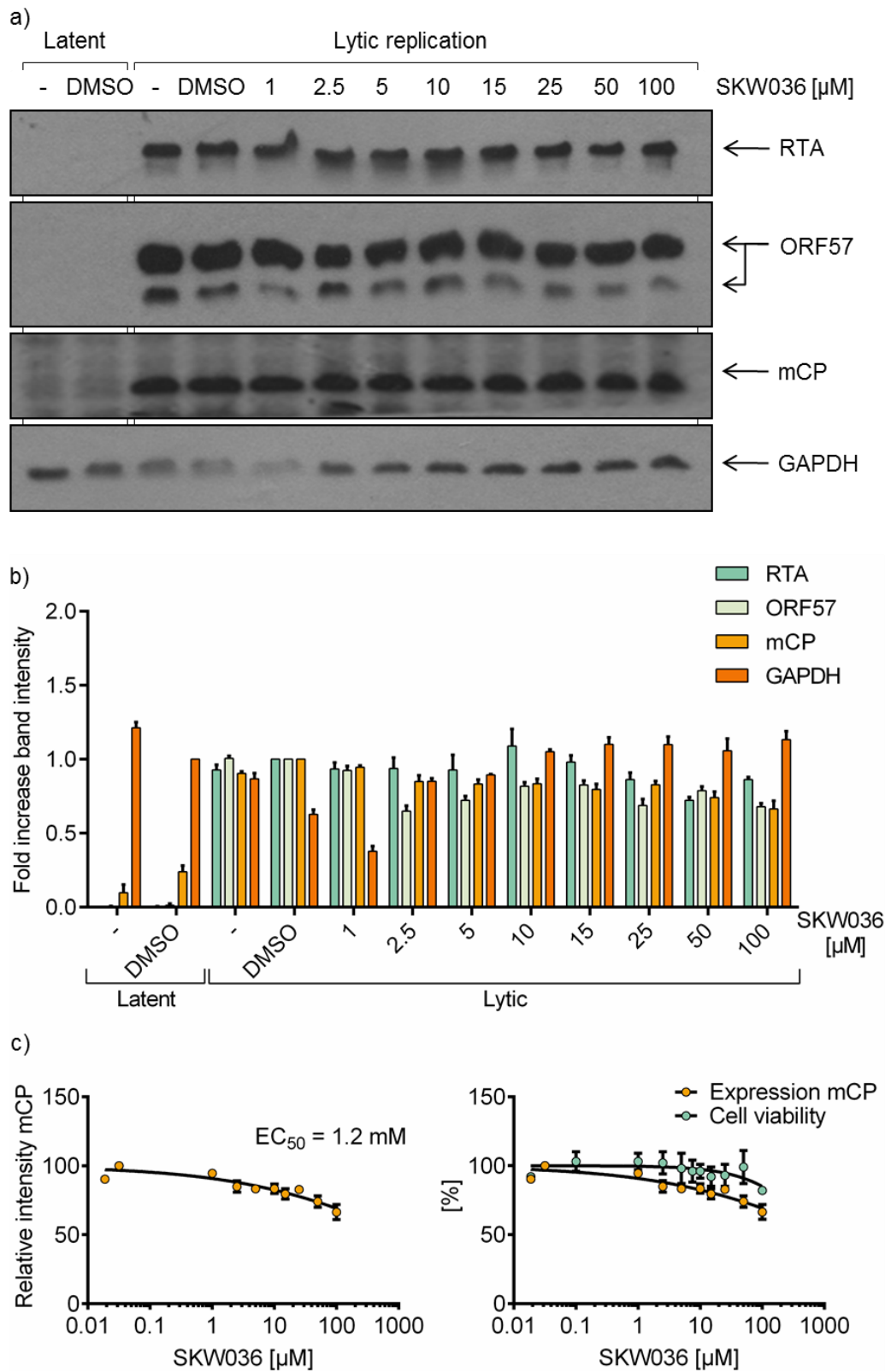


**Figure 5.11: SKW036 does not have an effect on viral late protein expression.** The experiment was performed and analysed as previously described (Figure 4.21).

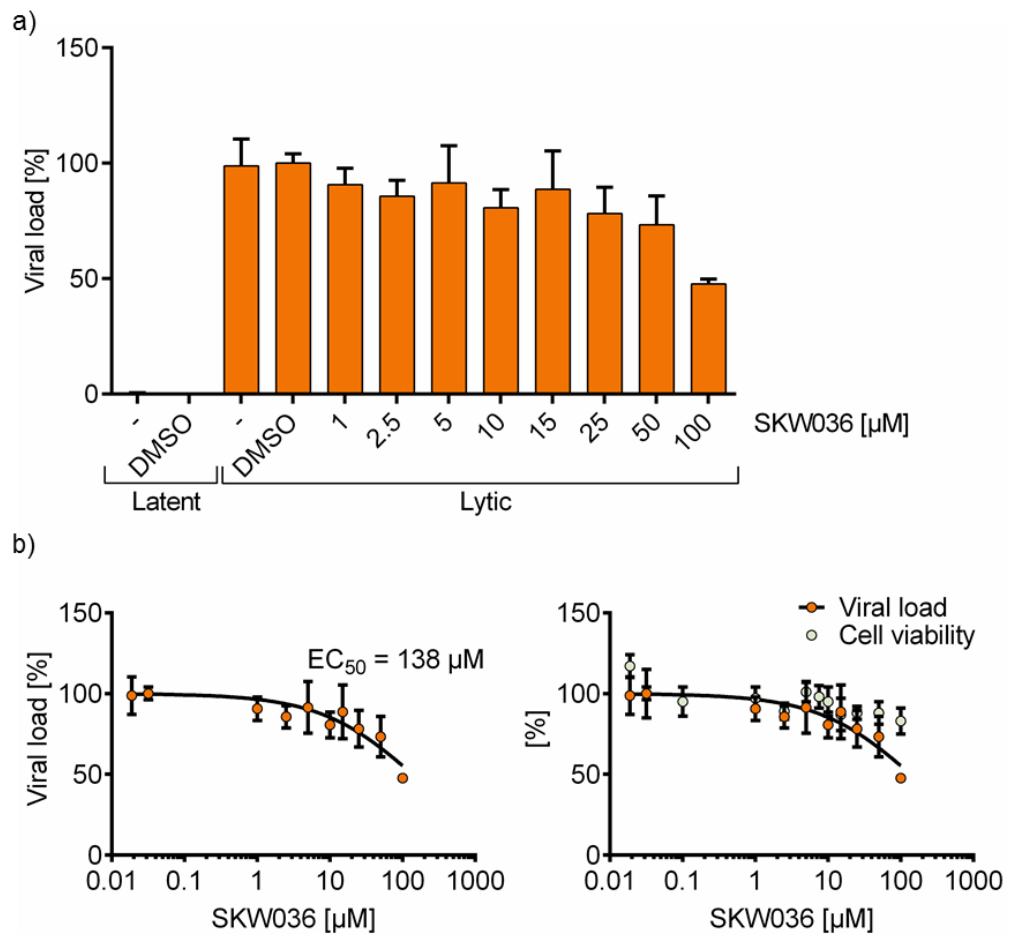


**Figure 5.12: Reduction of viral load in cells treated with SKW036.** The assay was performed as previously described (Figure 4.22). n = 2, error bars display SD.

## 5.6 Effect of C2 on HSP90 and HSP90 client proteins

Compound C2 has previously been published as a HSP90 (heat shock protein 90) inhibitor, identified by high-throughput screening (Sharp et al., 2007). HSP90 is a molecular chaperone that is responsible for maturation, stability and activity of selected client proteins.

While experiments in chapter 4 were designed to provide evidence for inhibition of UAP56, and subsequent disruption of the ORF57/hTREX interaction, the effect of the inhibitor C2 and some selected analogues were also examined on HSP90 and HSP90 client proteins, to assess whether this might play an additional role in KSHV inhibition. To this end, Western blotting was performed on samples previously used in Figure 4.21, taken 24 h after induction of KSHV lytic replication and treatment with the inhibitor, using

HSP90- or CDC2-specific antibodies. CDC2 is a HSP90 client protein with a half-life of 7.5–18 h (depending on cell cycle phase) (Welch and Wang, 1992) and therefore a suitable control for HSP90 inhibition.

Figure 5.13a shows Western blots from Figure 4.21, now also probed for expression of CDC2 and HSP90. A marked decrease in CDC2 protein expression can be seen at 5  $\mu$ M C2; quantification shows a reduction from almost 100% expression to below 30% (Figure 5.13b). Higher concentrations of the inhibitor do not decrease CDC2 protein levels further, so these can be considered background protein levels, expressed before inhibition of HSP90 took place. At the same concentration threshold, an increase in HSP90 expression can be seen. This over-expression could be a cellular counter action to inhibition of HSP90. It can therefore be speculated that efficient inhibition of HSP90 occurs between 2.5 and 5  $\mu$ M C2 in TReX BCBL1-Rta cells after 24 h. Intriguingly, inhibition of mCP expression already occurs at concentrations of 1 and 2.5  $\mu$ M C2, where normal expression of CDC2 is observed. Comparing inhibition curves for expression of both proteins, a different trend can be noticed (Figure 5.13c), highlighting a specific inhibitory effect on KSHV replication, not mediated by HSP90 inhibition.

The same analysis of HSP90 and CDC2 was performed in the presence of An1 (Figure 5.14a). Interestingly, an increase in HSP90 expression can be observed from 0.5  $\mu$ M An1. Again this could be a cellular response to the presence of an inhibitor. However, CDC2 expression seems constant up to 15  $\mu$ M An1 and at this concentration only a minor loss in protein expression can be observed (Figure 5.14b). Conversely, the major decrease in mCP expression occurs between 2.5 and 5  $\mu$ M An1. This 10  $\mu$ M difference in concentration, between the effect on the viral mCP and the effect on the HSP90 client protein CDC2 (Figure 5.14c), is much greater than what is observed for C2.



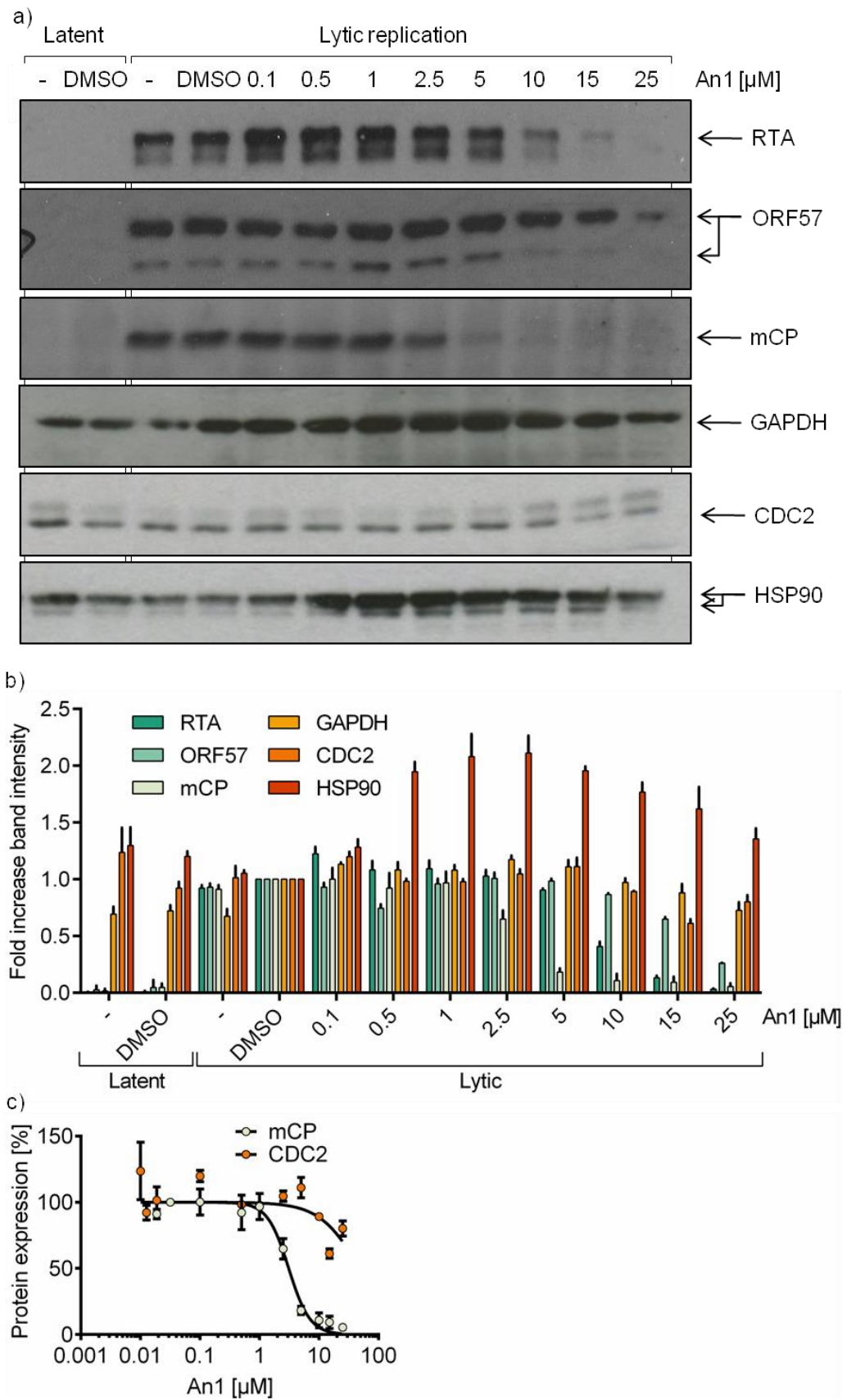


**Figure 5.14: Comparison of viral late protein and of HSP90 client protein expression in the presence of An1.** The experiment was performed and analysed as previously described (Figure 5.13).

The activity of HSP90 and CDC2 was also examined in the presence of An3. Western blots of HSP90 and the client protein present contrasting observations, compared to the other compounds: both the viral protein mCP and the HSP90 client protein CDC2 show a marked decrease in expression at 2.5  $\mu$ M An3 (Figure 5.15a). Comparing expression of mCP and CDC2 a very similar inhibition profile is seen (Figure 5.15a and b). Interestingly, quantification of Western blots failed to determine an increase in HSP90 expression. Based on CDC2 protein expression it appears that An3 is the most efficient HSP90 inhibitor of the three tested compounds.

While all three compounds were found to affect expression of HSP90 client protein CDC2, very different responses were observed for all inhibitors. No clear trend is apparent between inhibition of viral late protein expression and HSP90 protein expression. While further tests have to be performed to rule out an involvement of HSP90-inhibition, this encouraging data indicates no direct connection between inhibition of HSP90 and loss of viral late protein expression.

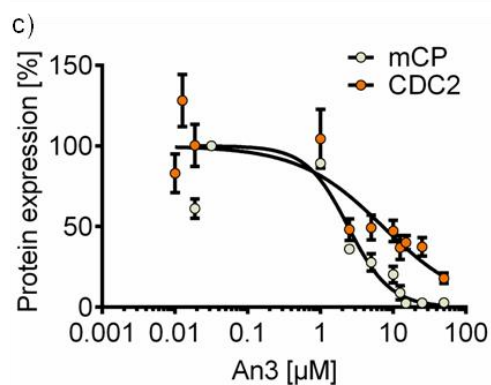
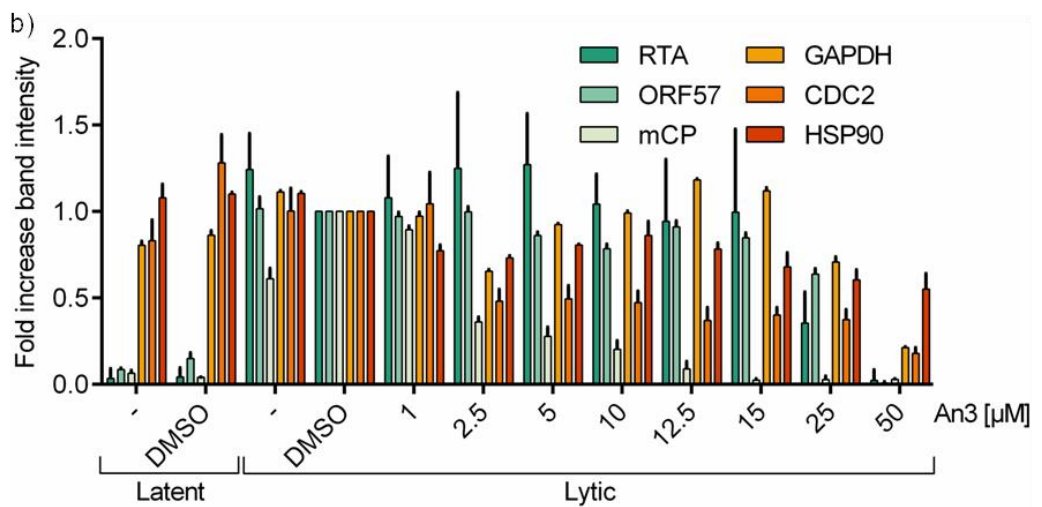
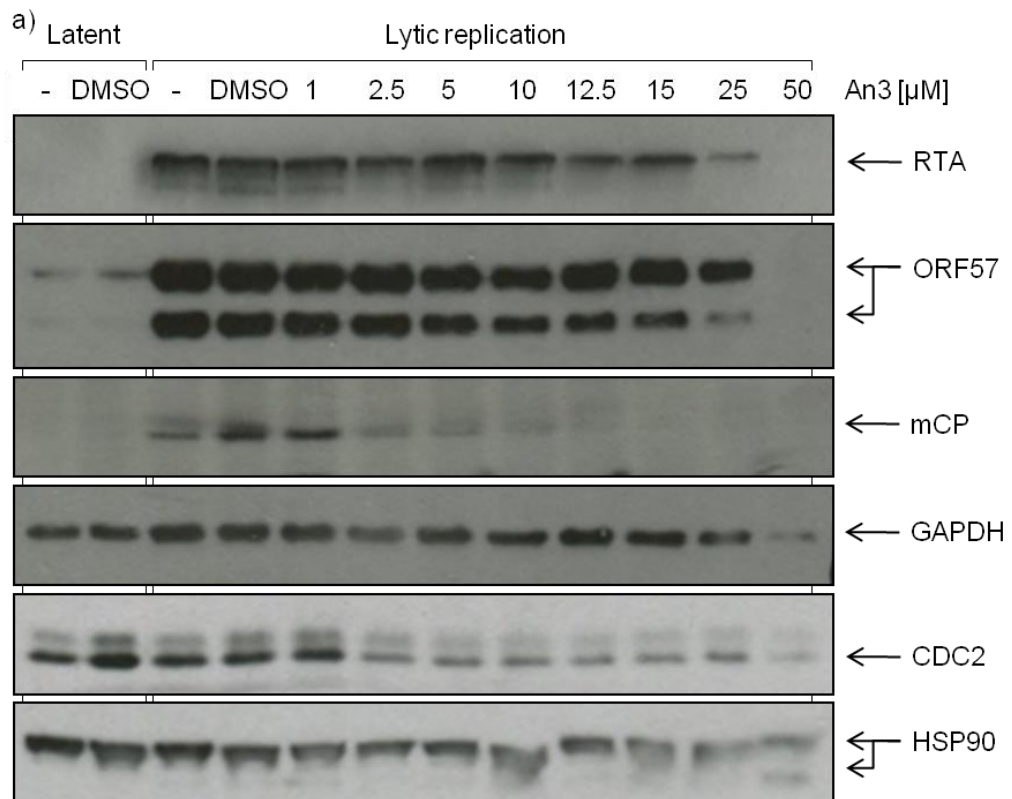


**Figure 5.15: Comparison of viral late protein and of HSP90 client protein expression in the presence of An3.** The experiment was performed and analysed as previously described (Figure 5.13).

## 5.7 Effect of inhibitor C2 on HSV-1 replication

All herpesviruses express an essential ORF57 protein homologue, which utilises the hTREX complex to export viral intronless mRNA. It was therefore speculated that the inhibitor identified against the KSHV ORF57/hTREX interaction would also efficiently serve to disrupt replication of other human herpesviruses.

To examine this, the replication of HSV-1 in a HFF (human foreskin fibroblasts) cell line was examined. As before, a non-cytotoxic working concentration of C2 in HFF cells was initially determined using a MTS assay (Figure 5.16). Concentrations up to 25  $\mu\text{M}$  could be used in HFF cells before a marked decrease in cell viability was observed.

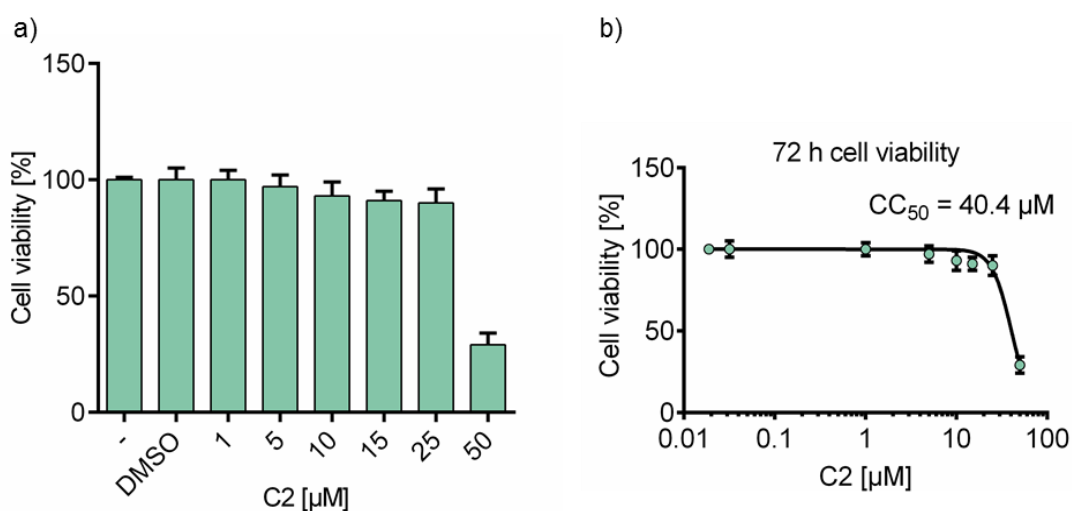


**Figure 5.16: Cell viability of HFF cells in the presence of C2.** The experiment was performed and analysed as previously described (Figure 4.13).

HFF cells were infected with HSV-1 for 1 h, before cells were washed, to remove excess virus, and treated with increasing amounts of C2 or DMSO. Figure 5.17 presents images of HFF cells 72 h post infection with HSV-1 and treatment with C2 or DMSO. It can be seen that virus lytic replication causes cell death in infected, DMSO treated cells after 72 h, compared to uninfected cells. However, with increasing amounts of compound C2, cells appear viable and protected from virus-mediated lysis.

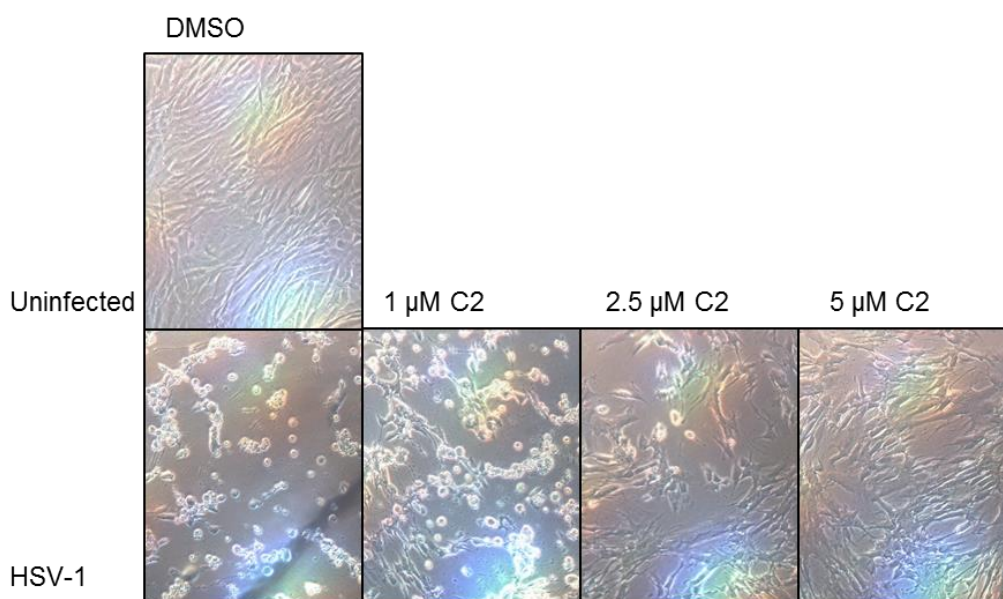


**Figure 5.17: Compound C2 protects HFF cells from HSV-1 mediated cell lysis after primary infection.** Confluent HFF cells were infected with HSV-1 (MOI = 0.001), treated with DMSO or increasing amounts of C2 and left for 72 h. Images of cells were taken at 40x magnification.

The effect of C2 on HSV-1 lytic replication after primary infection was also assessed using plaque assays. A confluent layer of HFF cells was infected with HSV-1 for 1 h, before cells were washed and overlaid with a viscous layer of media containing 1% molten agarose and the indicated concentration of inhibitor C2. Development of primary infection was assessed 120 h later, after the top layer was removed (Figure 5.18). Virus lytic replication can be detected by plaque formation within the monolayer of stained cells. Intriguingly, with increasing concentrations of C2, plaque size and plaque number can be seen to decrease dramatically, demonstrating efficient inhibition of virus lytic replication.



detection limit of this assay. However, infectious virions from cells treated with 5  $\mu\text{M}$  C2 infected less than 50% of the new cell population, indicating a strong decrease in virus production in the presence of the inhibitor. Furthermore, at the tested concentrations of 7.5 and 10  $\mu\text{M}$  C2, no re-infection can be seen, demonstrating that these concentrations sufficiently blocked HSV-1 replication and production of infectious virus particles in HFF cells. Re-infection at the higher dilutions (1:100 and 1:1000) was more suitable for assessing low concentrations of inhibitor. At a 1:100 dilution, DMSO and 1  $\mu\text{M}$  C2 treated samples caused re-infection rates of 82% and 71%, respectively, and it is therefore likely that these samples were “maxing out”, too. However, treatment with 2.5  $\mu\text{M}$  C2 reduced re-infection to 50% of cells, before a drop to 5% is seen at 5  $\mu\text{M}$  C2. Both re-infection with a 1:100 dilution, as well as comparison to the 1:10 dilution confirm a 10-fold decrease in virus production between 2.5 and 5  $\mu\text{M}$  C2. Again, these values are confirmed by the highest dilution (1:1000) which shows 5% infection rate at 2.5  $\mu\text{M}$  C2. At this dilution, 12% infected cells were detected from DMSO treated samples and a loss of approximately half the virus in cells treated with 1  $\mu\text{M}$  C2. Together, this data indicates a dose dependent reduction in HSV-1 lytic replication in the presence of inhibitor C2. An effect could be detected from 1  $\mu\text{M}$  C2, and no infectious virus production was detected at 7.5  $\mu\text{M}$  C2 and above.

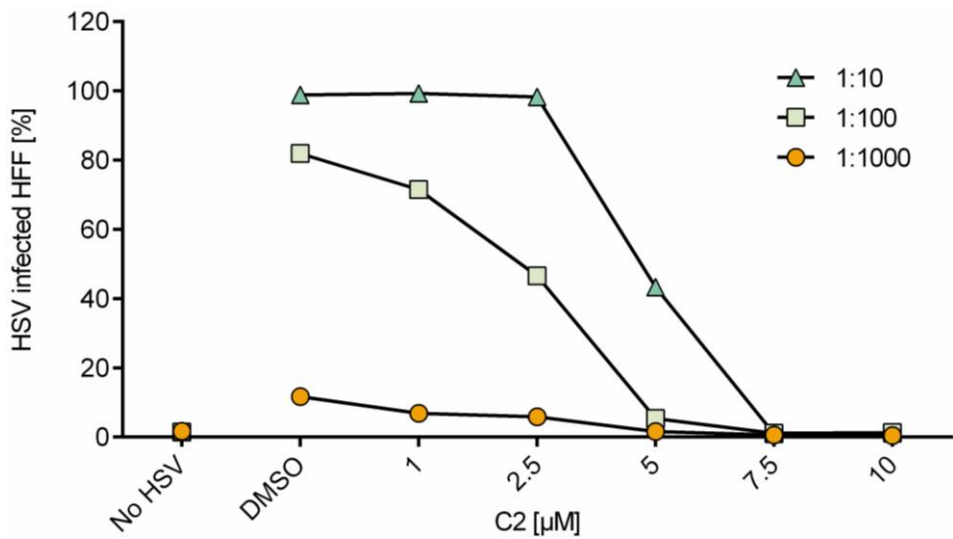


**Figure 5.19: Flow cytometry analysis shows inhibition of HSV-1 infectious virion production by C2.** HFF cells were infected with HSV-1 (MOI = 0.001) and treated with DMSO or increasing concentrations of C2 for 72 h. Supernatants were then added to uninfected HFF cells in 1:10–1:1000 dilutions and left without further treatment for 24 h. Cells were fixed with formaldehyde and HSV-1 positive cells quantified using flow cytometry.

Moreover, to complement analysis of infectious virus particles by flow cytometry, plaque assays were used to quantify the reduction of plaque forming units upon treatment with C2. Again, primary infection took place for 72 h in the absence and presence of C2, before the supernatant was harvested and HFF cells re-infected with 1 ml supernatant diluted 1:10–1:10,000. After 1 h re-infection, cells were washed and again overlaid with DMEM containing 1% agarose to prevent spread of infectious virus particles. After 96 h cells were fixed and stained using crystal violet stain. The number of plaque forming units (pfu) was determined by counting of viral plaques and multiplication by the dilution factor. The dose-dependent decrease in pfu over the range of effective concentrations can best be observed on a log scale (Figure 5.20a), whereas the linear scale (Figure 5.20b) highlights the large initial drop in pfu achieved by a concentration 10-times below the maximum non-toxic concentration of 25  $\mu$ M C2.

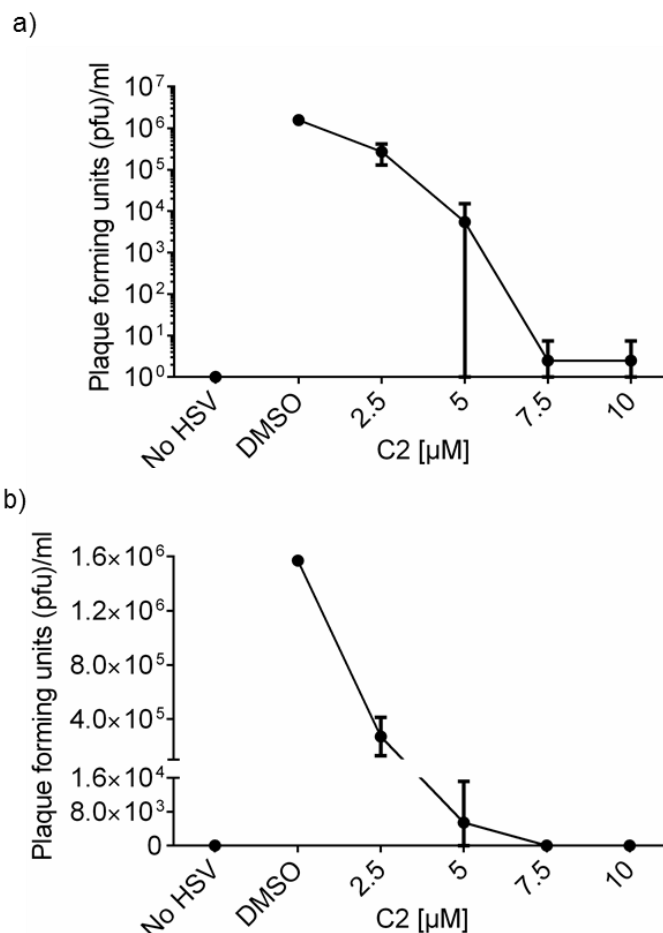


**Figure 5.20: Viral plaque assays show inhibition of HSV-1 infectious virion production by C2.** HFF cells were infected with HSV-1 (MOI = 0.001) and treated with DMSO or increasing concentrations of C2 for 72 h. Supernatants were then added to uninfected HFF cells in 1:10–1:10,000 dilutions. Viral plaques were analysed after 96 h using formaldehyde fixation and crystal violet stain. Results are displayed a) on a log-scale and b) a linear scale.

Finally, these results were confirmed by Western blotting, to assess viral protein production after infection of a new cell population. All samples were obtained as described above, before dilution and re-infection of new HFF cells for 16 h. After this time, protein samples were obtained and analysed by Western blotting using ICP27- and GAPDH-specific antibodies (Figure 5.21). Again, a dose-dependent reduction in HSV-1 ICP27 is visible in re-infected cells, indicating inhibition of lytic replication and virus production by C2. Interestingly, neither flow cytometry analysis nor western blotting detected HSV-1 re-infection in cells treated with 7.5 or 10  $\mu$ M C2.

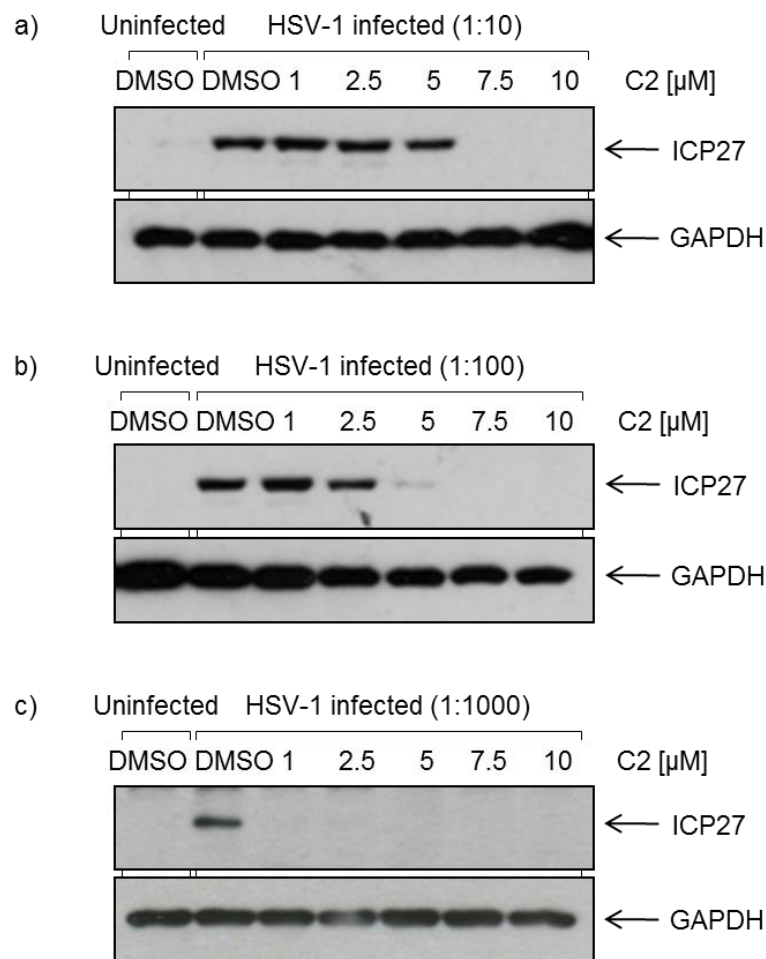


**Figure 5.21: Western blotting confirms inhibition of HSV-1 infectious virion production by C2.** HFF cells were infected with HSV-1 (MOI = 0.001) and treated with DMSO or increasing concentrations of C2 for 72 h. Supernatants were then added to uninfected HFF cells in 1:10–1:1000 dilutions. Protein samples were taken after 16 h and analysed by SDS-PAGE and Western blotting using ICP27 and GAPDH specific antibodies.

## 5.8 Effect of inhibitor C2 on HSP90 and HSP90-client proteins in HFF cells

The HSP90 function in the presence of C2 was also examined in HFF cells, to determine if a HSP90-dependent effect resulted in the inhibition of HSV-1 replication. Confluent HFF cells were treated with increasing amounts of C2 for 72 h, before cell lysates were analysed by Western blotting using HSP90- and CDC2-specific antibodies (Figure 5.22a). Western blots were also quantified and an inhibition curve for CDC2-expression calculated using non-linear regression (Figure 5.22b and c). Together, a marked decrease in CDC2-expression can be observed between 5 and 7.5  $\mu\text{M}$  C2. It can therefore be concluded that effective inhibition of HSP90 takes place in this concentration range. Interestingly, a 90% reduction (by flow cytometry) or a 99% reduction (by plaque assay) was determined at a concentration of 5  $\mu\text{M}$  C2, where no inhibition of HSP90 occurs. While an effect of HSP90 on virus replication cannot be ruled out, this data indicates no immediate connection.

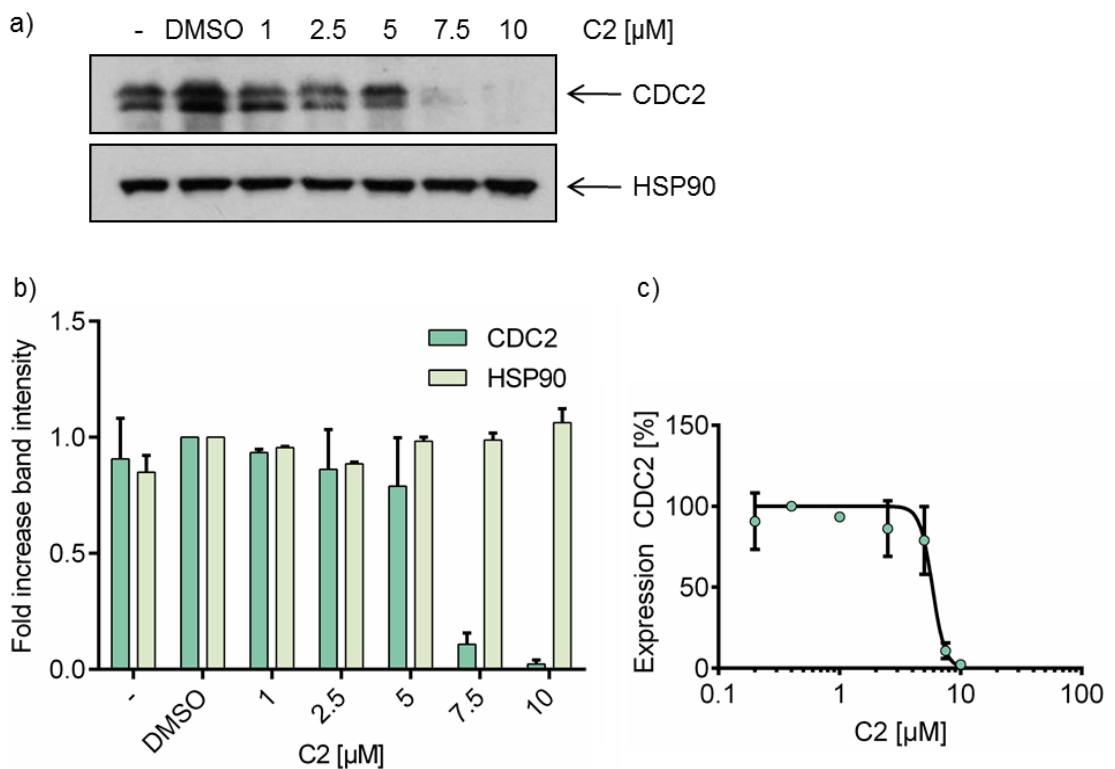


**Figure 5.22: Expression of HSP90 client protein CDC2 by HFF cells in the presence of C2.** Confluent HFF cells were treated with DMSO or increasing concentrations of C2 for 72 h. a) Protein samples were analysed by Western blotting using CDC2 and HSP90 specific antibodies. b) Western blots were quantified using ImageJ.  $n = 3$ , error bars present the SD. c) CDC2 expression levels are displayed on a log scale. The inhibition curve was calculated using non-linear regression.

## 5.9 Discussion

After identifying a UAP56-ATPase inhibitor by virtual high-throughput screening and subsequent *in vitro* screening, the activity of close structural analogues that had minor changes to functional groups of compound C2 were explored. Together the analogues demonstrated a structure activity relationship, with three compounds having the ability to inhibit KSHV lytic replication. Functional groups were identified, which could be manipulated to allow changes in activity and cytotoxicity. Interestingly, modifications to the dioxane group lead to an initial increase in cell viability and EC<sub>50</sub> value at 24 h but a decrease in cell viability at later time points. Results showed one inhibitor that was unable to inhibit KSHV lytic replication, due to the presence of a polar carboxyl group. Again, this provides valuable insight into the uptake and function of the inhibitor, highlighting the fact that the compounds are probably taken up by passive diffusion through the cell membrane.

While targeting a cellular protein carries greater risks, such as inhibition of essential cellular functions and subsequent cytotoxicity, it can also be advantageous: Inhibiting a cellular protein allows targeting several pathogens that utilise this pathway, using the same compound. We speculated that C2 should have the ability to act as a generic herpesvirus inhibitor, given the common pathway for viral mRNA export between all *Herpesvirinae* (Schumann et al., 2013). Results showed concentrations as low as 1 µM significantly reduced HSV-1 lytic replication. Furthermore, 5 µM of C2 prevented production of 90-99% of virions. Intriguingly, this concentration was still 5-fold below the maximum concentration at which no cytotoxicity occurred. Together, the data herein showed that indeed compound C2 is able to prevent replication of both herpesviruses KSHV and HSV-1, and indicates potential pan-viral activity across the *Herpesviridae* family. Further testing of other herpesviruses and influenza viruses would be useful to determine the extent of this pan-viral activity.

Finally, we addressed previously published reports of compound C2 as a HSP90 inhibitor (Cheung et al., 2005; Dymock et al., 2005; Sharp et al., 2007). An IC<sub>50</sub> against yeast Hsp90 ATPase activity was reported as 6.6 µM, or in a second study as 8.9 µM, whereas purified, recombinant HSP90β showed an IC<sub>50</sub> of 3.2 µM (Dymock et al., 2005; Sharp et al., 2007). However, these values are not ideal for direct comparison to the data reported in

chapter 4. While the  $IC_{50}$  is a useful tool for comparing several inhibitors for one protein against each other, values are dependent on the enzyme, assay and assay conditions used: More sensitive assays or highly active enzymes allow for lower enzyme concentration in the screening, which in turn gives way to lower  $IC_{50}$  values.

While data conclusively showed inhibition of UAP56 and disruption of ORF57 interaction with hTREC by C2, an additional effect through inhibition of HSP90 cannot be excluded. We used the cellular HSP90 client protein CDC2, to assess inhibition of HSP90. Specifically, we compared protein levels of CDC2 expression with expression of the viral late protein mCP. Interestingly, inhibition of KSHV and HSV-1 replication was evident at concentrations where no inhibition of CDC2 expression occurred. Furthermore, inhibition of HSP90 by the analogues An1 and An3 was compared with inhibition by C2. Intriguingly, while both analogues acted against HSP90, the effect did not follow an obvious trend. While An1 showed a 6-fold difference in concentration (over 10  $\mu$ M) between inhibition of the viral and cellular protein, An3 inhibited both proteins at a similar concentration. This indicates that the effect seen on viral mCP expression originates in a different upstream event than inhibition of CDC2. However, further testing should be done to clarify this issue. To this end, established HSP90 inhibitors, such as Geldanamycin, could be used to compare the effect on expression of viral late proteins and HSP90 client proteins. Furthermore, knock-down of HSP90 could be attempted, followed by treatment with C2. Any effect seen by C2 could be contributed to factors other than HSP90 inhibition.

To summarise, results herein presented three close structural analogues, which inhibit KSHV late protein expression and virus replication. Furthermore, one analogue failed to have an inhibitory effect, due to changes in the structure. Moreover, inhibition of HSV-1 was demonstrated, showing that C2 functions as a novel inhibitor against herpesviruses. Finally, the effect of HSP90 inhibition was examined for KSHV replication, where no clear trend could be detected. Similarly, HSV-1 replication was inhibited at concentrations where no effect on HSP90 could be observed.

## Chapter 6

~

## Final Discussion and Future Perspectives

## 6 Discussion

The oncogenic herpesvirus KSHV replicates in the nucleus of the host cell and relies on cellular mRNA export factors to efficiently export viral transcripts into the cytoplasm, where translation occurs. Cellular mRNA export, however, is a complex and highly regulated process that is directly coupled to splicing. This poses a problem for KSHV and other herpesviruses, who express numerous intronless mRNAs. In order to circumvent the splicing requirement, as well as other cellular mRNA processing steps, KSHV expresses the conserved protein ORF57, which facilitates viral mRNA export. ORF57 is able to recruit components of the hTREX complex onto viral transcripts, which in turn recruits the cellular export receptor Nxf1, allowing export through the nuclear pore complex. Dysfunctional ORF57 is associated with nuclear retention of viral transcripts and inhibition of viral lytic replication.

This is of significant importance, as lytic replication has been shown essential for KS development, the most common malignancy associated with KSHV infection. Lytic replication enables the virus to disseminate from its B-cell reservoir and infect endothelial cells, where cancer manifests. Furthermore, reoccurring lytic replication allows persistence of infection within these cells, and therefore enables constant expression of viral oncogenic proteins which drive tumourigenesis. Accordingly, disruption of lytic replication is associated with remission of cancer. However, clinical studies show that available antiherpevirus drugs are ineffective against KSHV after the onset of KS and only preventative use of ganciclovir showed some moderate clinical success (Gantt and Casper, 2011). Considering the high burden of KS in sub-Saharan Africa, new, KSHV-targeted drugs are desperately needed.

As detailed above, due to its essential nature, ORF57 is an attractive target for novel anti-KSHV drug discovery. ORF57 recruits the hTREX complex via an interaction with the export adaptor Aly. However, this interaction cannot be targeted directly, as UIF can also be recruited by ORF57 to export viral mRNAs and therefore provides redundancy in the system.

In 2010, a then novel hTREX component called CIP29 was identified and with it the idea of ATP-dependency of the hTREX complex (Dufu et al., 2010). The interaction between the

export adaptor Aly, the RNA-helicase UAP56 and CIP29 was shown to occur only in the presence of ATP. Later, UAP56 was shown to load hTREX components onto the mRNA in what is thought to be an ATP-cycle dependent manner (Chang et al., 2013).

We therefore speculated that ATP-dependency would also be found to affect the formation of the ORF57-mediated vRNP and aimed to explore this option as a novel drug target.

## **6.1 ORF57 and CIP29**

Chapter 3 first investigated the involvement of CIP29 in the KSHV-mediated vRNP. Using a range of methods, CIP29 was shown to be part of the hTREX complex associated with the ORF57-mediated vRNP. This was expected, as ORF57 has previously been shown to recruit all known hTREX components onto viral mRNA (Boyne et al., 2008). While no clear function of CIP29 in the hTREX complex is to date known, the role of this component in the vRNP was explored using siRNA approaches. However, even though efficient CIP29 depletion was achieved, no effect of CIP29 knock-down could be observed on viral mRNA export or on viral late protein expression. Similar, Dufu and co-workers found no loss in cellular bulk mRNA or reporter mRNA export after knock-down of CIP29 (Dufu et al., 2010). However, they described a block of cellular mRNA export upon over-expression of CIP29, which is commonly seen for hTREX components. It is therefore possible that redundancy exists for CIP29 and other cellular proteins are able to take over the role upon loss of the protein, as is seen for Aly and UIF (Hautbergue et al., 2009). Surprisingly though, an increase in viral intronless transcript levels was observed after CIP29 knock-down, however, this effect was only visible in ORF57-expressing cells and not in control-transfected cells. No such effect has been previously described in the literature and further studies are required to clarify if this is an experimental artefact, or if depletion of CIP29 indeed leads to a greater abundance of viral intronless transcripts in the cell. If the latter is confirmed, this could have interesting implications, such as a role of CIP29 in transcription or transcriptional control, which should be explored in detail.

We further investigated if ATP-dependency of the hTREX complex formation also affects the interaction of ORF57 with the hTREX complex. First, results were confirmed showing

that CIP29 and Aly stimulate UAP56 ATPase activity *in vitro*. Immunoprecipitations were performed using CIP29 in the presence of either ATP or the non-hydrolysable ATP-analogue ATP $\gamma$ S. Interestingly, an interaction between ORF57 and CIP29 is only visible in the presence of ATP and not in the presence of ATP $\gamma$ S. CIP29 has been shown to interact directly with UAP56, which in turn bridges the interaction to Aly, to form a trimeric complex in the presence of ATP (Dufu et al., 2010). A disrupted interaction of CIP29 and ORF57 therefore indicates an inhibition of the trimeric complex. ORF57 might still be able to recruit Aly, but cannot override the ATP-dependency or interact with CIP29 directly. However, to explore the interaction of ORF57 with other hTREX components, namely Aly or UAP56 in the absence of ATP, further experiments were needed.

## **6.2 ORF57 and hTREX: ATP-dependency and complex remodelling**

In chapter four, the ATP-dependency of the ORF57-mediated vRNP was further investigated. The presence of the non-hydrolysable ATP analogue ATP $\gamma$ S was found to specifically disrupt the interaction of ORF57 with UAP56 and hence the hTREX complex. Importantly, the formation of the endogenous trimeric Aly-UAP56-CIP29 complex was not prevented by the non-hydrolysable analogue. Furthermore, results show that the presence of ADP caused disruption of both the endogenous and the viral complex. Together these data lead to a proposed model of ATP-cycle dependent remodelling of hTREX which affects the ability of ORF57 to interact with the complex (Figure 6.1).

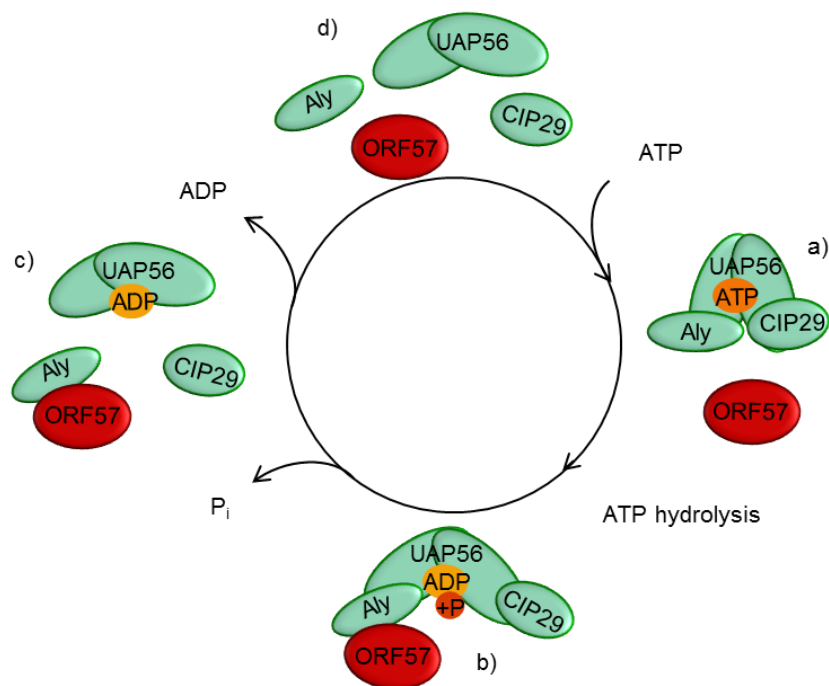


**Figure 6.1: Schematics of ATP-cycle dependent remodelling of central hTREX components and the ORF57-mediated vRNP.** a) Binding of ATP to UAP56 is believed to induce a closed conformation in the ATPase, which allows binding of Aly and CIP29. b) Hydrolysis of ATP mediates a further conformational change of UAP56 and rearrangement of hTREX components, which allows ORF57 binding. c) Exclusion of inorganic phosphate and subsequent ADP binding facilitates a dissociation of UAP56 from Aly and CIP29. d) After dissociation of ADP, UAP56 can enter the ATP-cycle again, possibly to load other ATP-dependent hTREX components onto the mRNA.

This remodelling process is most likely mediated by UAP56, an ATP-dependent RNA helicase with RNA-stimulated ATPase activity (Shen et al., 2007). Like other DExD-box proteins, UAP56 contains an ATP binding motif, called the ‘Q-motif’, responsible for total ATP specificity, rather than allow binding of other nucleoside triphosphates (Cordin et al., 2006). It is not completely understood how RNA helicases facilitate RNA unwinding, however two models have been proposed and seem widely accepted. Both mechanisms are based on a coupling of one ATPase cycle to one RNA unwinding step (Tanner and Linder, 2001; Rocak and Linder, 2004; Tuteja and Tuteja, 2004). In accordance, studies have shown RNA helicases entering several different conformational states during their ATPase cycle (Lorsch and Herschlag, 1998). These conformational changes are thought to be necessary for the progression of the protein along the RNA *in vivo*, but they also commonly confer remodelling of associated protein complexes (Pyle, 2011). The underlying mechanism for the conformational changes seem to be found in the ATP binding pocket of UAP56 and other DExD-box helicases, which is found in a cleft between

two loosely connected helicase domains, each assuming a RecA-like fold (Shi et al., 2004; Zhao et al., 2004) (Figure 6.2). Binding of ATP is believed to induce a structural reorganisation in the nucleotide binding site, causing a positional change of the two subunits relative to each other. This brings the two domains closer together and enables a so called closed conformation, in a similar fashion to the HCV NS3 protein (Appleby et al., 2011). It is not clear if the energy for the structural changes is derived from ATP hydrolysis or from ATP binding alone. In the latter case, hydrolysis could be used to facilitate the release of the protein from the RNA, as has been shown for the yeast helicase and UAP56 ortholog, Sub2 (Kistler and Guthrie, 2001).

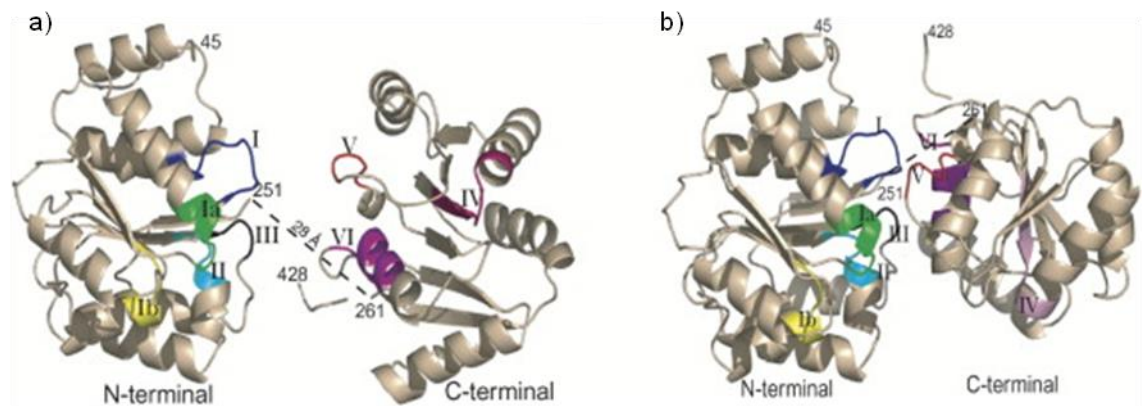


**Figure 6.2: Crystal structure of UAP56 N-terminal and C-terminal domains.** a) Model of UAP56 in an open conformation, generated by superimposing the domains onto to corresponding domains of full-length eIF4A. b) Model of UAP56 in a closed conformation, generated by superimposing the two  $\alpha/\beta$  domains of hepatitis C virus (HCV) NS3 protein. Conserved helicase motifs are mapped onto the structure in different colours and labelled I-VI. The black dashed line represents the flexible linker between both domains. Taken from (Zhao et al., 2004).

UAP56 was stabilised in the ATP-bound state by ATP $\gamma$ S, a non-hydrolysable ATP-analogue. Results showed that this conformation confers binding of the endogenous proteins Aly and CIP29 (Figure 6.1, step a). Importantly however, ORF57 could not interact with ATP $\gamma$ S-bound UAP56. This extremely exciting observation suggests that the complex will be remodelled after initial binding of Aly and CIP29 to UAP56, into a conformation which can accommodate ORF57. It is possible that binding of ATP-loaded UAP56 by Aly occupies the ORF57 binding site and further hTREX remodelling is needed before ORF57 can interact with Aly.

While no structural data has confirmed this to date, it has been previously proposed that ATP hydrolysis induces further conformational changes in DExD-box proteins, which could function as an essential destabilisation step of base pairs in the duplex region during RNA unwinding (Cordin et al., 2006). It has also been reported that members of the exon junction complex (EJC) specifically stabilise the post-hydrolysis state of the helicase eIF4AIII, preventing release of inorganic phosphate, in order to inhibit ATP turnover and thereby trapping the protein complex onto the RNA (Nielsen et al., 2009). This also suggests that the helicase and protein complex enter a distinct conformation after ATP hydrolysis, in order for components of the EJC to differentiate the pre- and post-hydrolysis state. Similarly, here another reorganisation of hTREX was observed, which is driven by UAP56-facilitated hydrolysis of ATP. While this hydrolysis event was previously shown essential for the loading of Aly onto mRNA (Chang et al., 2013), our results indicate that Aly is able to remain in a protein-protein interaction with UAP56 post-hydrolysis and after the transfer of mRNA has taken place. It can therefore easily be imagined that a structural change and remodelling of the complex, which facilitates binding of mRNA by Aly, also allows ORF57 to interact with the export adaptor and hence recruit UAP56 and the remaining hTREX onto viral mRNA (Figure 6.1, step b).

Finally, results suggest that binding of ADP confers another structural change in UAP56, disrupting endogenous hTREX. As an example, the RNA helicase DbpA has been shown to adopt a significantly different conformation in an ADP-bound state, when compared to ATP- or RNA-bound states, independently of ATP hydrolysis (Henn et al., 2002). For many RNA helicases this step has been found associated with release of the protein from the RNA (Henn et al., 2008; Cao et al., 2011; Iost et al., 1999). Here, results show that ADP binding disrupts the interaction of core components of the endogenous hTREX and the vRNP (Figure 6.1, step c). It is possible that UAP56 shuttles through this conformation to enable consecutive loading of Aly and the more recently identified Chtop protein onto the mRNA, as has been suggested before (Chang et al., 2013). As both proteins interact with the N-terminal region of UAP56, this might mean that one protein is recruited to hTREX and loaded onto the mRNA during one ATP-cycle, before the interaction to UAP56 is disrupted by ADP and the second protein is loaded during another ATP-cycle. Fitting with this hypothesis is data reported for Sub2, which shows release of the RNA from the helicase upon ATP-hydrolysis (Kistler and Guthrie, 2001). While subsequent binding of ADP

is often found to disrupt protein-RNA interactions in other helicases, here this could be utilised to disrupt protein-protein interactions to enable recruitment of another protein. To extend this idea, as ATP-dependency has also been shown for the hTREX components CIP29, pDIP3 and ZC11A, this loading mechanism might also be applied to them, though they are not associated with mRNA binding during the export process. As the THO complex is not associated with any ATP-dependency, but has been reported to bind the cap-binding complex and UAP56 or Aly (Dufu et al., 2010; Chi et al., 2013), this could be speculated to act as a molecular anchor throughout this process, keeping UAP56 in close proximity of the mRNA and the partly assembled hTREX. Finally, UAP56 has been shown to leave the hTREX before mRNA export occurs (Viphakone et al., 2012), which could be facilitated by nucleotide free UAP56.

As previous results have shown ORF57 to bind Aly directly (Boyne et al., 2008), it is likely that both proteins would remain bound to the viral mRNA during the stages of hTREX and vRNP assembly. However, we cannot clearly determine if ORF57 recruits Aly before an interaction with UAP56 takes place, or if UAP56-bound Aly is recruited onto viral mRNA. Based on the immunoprecipitation data, it appears that ORF57 interacts with proteins that are part of an already formed complex, whether this is the complete or a partial complex. In contrast, if Aly is recruited by ORF57 before any interactions with UAP56 take place, then ORF57 would require the lone ability to load Aly onto viral mRNA. Such a mechanism has been recently suggested for the HVS ORF57 protein, where a strong affinity for Aly caused formation of a ternary complex and cooperative binding of viral mRNA by both ORF57 and Aly (Tunncliffe et al., 2014). In this case, upon interaction of Aly with ATP-bound UAP56, the adaptor protein might lose the direct interaction with ORF57, but remain within the ternary complex via binding of the RNA *in vivo*. However, considering the interlinked nature of ORF57 and viral mRNA binding by Aly shown in HVS, this seems questionable. Further experiments therefore need to be performed to address the mechanism of ORF57-mediated complex assembly *in vivo*.

### 6.3 Identification of a novel KSHV-inhibitor

As it has previously been shown that ORF57-mediated recruitment of Aly and Nxf1 alone are not sufficient for viral mRNA export and that the remaining hTREX complex is also needed for functional vRNP formation, it is exciting to see that the above mentioned model suggests potential options for the inhibition of the ORF57/hTREX interaction. Our data indicates that by stabilising the ATP bound conformation of UAP56, ORF57 is prevented from interacting with hTREX, without disruption of the endogenously formed trimeric complex of Aly, UAP56 and CIP29. Furthermore, as the ORF57-mediated vRNP was disrupted in the absence of ATP hydrolysis by UAP56, the most promising approach was to identify compounds inhibiting UAP56 ATPase activity. While recent findings have indicated that UAP56 might have to shuttle through one or several ATP-cycles to load hTREX components onto mRNA, this approach might not be feasible without disrupting the endogenous complex and causing cytotoxicity (Chang et al., 2013). However, a similar approach has been described in the literature, where a series of small molecule inhibitors (ring expanded nucleosides) were shown to suppress replication of human immune deficiency virus type 1 (HIV-1) by targeting the ATPase activity of human helicase DDX3 (Yedavalli et al., 2008). At low concentrations these drugs were found to prevent virus replication without affecting cell viability. We therefore speculated that a small molecule inhibitor designed for high affinity binding to the ATP binding site of UAP56 would prove to efficiently disrupt the ORF57/hTREX interaction.

A combined approach of structure-based drug design, virtual HTS and fragment-based drug design was used to identify four novel inhibitors of UAP56 ATPase function, all with a diverse structural background. The most potent inhibitor of UAP56, C2, was taken forward to assess the validity of our hypothesis and its potential as anti-KSHV inhibitor. Binding of C2 to UAP56 was confirmed by determination of an  $IC_{50}$  and also through direct study of binding kinetics by microscale thermophoresis, which showed a  $K_D$  of 12.8  $\mu$ M. Chapter 4 contains consequential evidence for a disruption of ORF57-mediated vRNP formation in a concentration range where neither cytotoxicity nor endogenous bulk mRNA export was affected. Results also show that C2 significantly reduced export of intronless viral mRNAs, expression of late intronless proteins and KSHV replication.

For all of the above mentioned experiments it was shown that a “therapeutic window” exists, in which a concentration range proves effective against the virus induced RNP, but did not affect either hTRES formation *in vitro*, cellular bulk mRNA export or cytotoxicity. There are several possibilities for this: While C2 has been shown to inhibit the ATPase function of UAP56, the inhibitor has not been tested against DDX39. DDX39 has recently been more heavily implicated in mRNA export, either with a redundant function of UAP56 or in an alternative pathway (Sugiura et al., 2007; Yamazaki et al., 2010; Kapadia et al., 2006; Thomas et al., 2011). While DDX39 shares a high degree of sequence similarity, it is likely that both proteins have different binding affinities for the small molecule inhibitor. Therefore, cells might compensate partially inhibited UAP56 by up-regulating DDX39 expression, which could provide redundancy and facilitate bulk mRNA export in the presence of C2, as observed in the FISH experiment. Furthermore, it is feasible that KSHV is more sensitive to disruption of viral mRNA export, whereas the cell is able to compensate for these events more efficiently. As such, inhibitor concentrations that disrupt a certain degree of viral and cellular mRNA export might block KSHV replication but could allow persistence of the cell. Finally, it is possible that different affinities, association or dissociation rates for the compound are found in the ORF57-bound protein complex, compared to the endogenous complex, i.e. the inhibitor might dissociate faster from UAP56 in the endogenous complex, than in an ORF57-stabilised complex. None of these hypothetical options have been identified as mechanism of action, but remain an ongoing focus of our study. However, the general concept of targeting cellular enzymes to prevent viral or bacterial toxicity is not a novel notion; several drugs have been successfully studied in animal trials indicating that a therapeutic window can also be used in fully developed drugs (Kibler et al., 2004; Sarac et al., 2002).

Chapter five explored further aspects of the novel inhibitor, such as the effect of close structural analogues, to elucidate a structure activity relationship. As such, a further three compounds were identified, which were able to inhibit virus late protein production and replication within a therapeutic window. Data generated here can be used to indicate future directions in the development of an anti-KSHV drug and will be discussed in more detail below.

One advantage of targeting cellular proteins for the treatment of viral infections is that one drug could theoretically have a very broad antiviral spectrum and target multiple

viruses that are dependent on this host factor. As such, targeting cellular helicases is a novel but very attractive antiviral target (Kwong et al., 2005). ORF57 is conserved amongst all herpesviruses and several of these homologues are known to interact with the hTREX complex. It was therefore speculated that C2 would also have inhibitory effects against other human herpesviruses. This hypothesis was tested in chapter five using HSV-1 and results showed specific disruption of HSV-1 lytic replication in the presence of C2. Furthermore, having used a physiologically relevant cell line, we could show a broad therapeutic window, with cytotoxicity occurring at concentrations ten times higher than inhibition of the virus. This is especially encouraging, as both structures for the binding of HSV-1 ICP27 protein and model-gammapherpesvirus HVS ORF57 with hTREX adaptor protein Aly, have highlighted significant differences in their interaction with the hTREX complex (Tunncliffe et al., 2011; Tunncliffe et al., 2014). The results, showing that inhibition of the ATP-cycle dependent remodelling of hTREX disrupts both an alpha- and a gamma-herpesvirus, are therefore exciting and suggest that inhibition of other human herpesviruses, such as HCMV, VZV, or potentially even influenza viruses, which also utilise parts of hTREX (Read and Digard, 2010), might also be possible. Similar, inhibition of West Nile Virus and HIV-1 has been shown using the same ring-expanded nucleoside inhibitors, which were found to inhibit both cellular and viral helicases (Zhang et al., 2003; Yedavalli et al., 2008).

#### **6.4 Implication of the inhibitor as anti-KSHV drug**

Together, the data generated in chapter four suggests a very promising, novel approach to disrupt KSHV lytic replication and treat KS. Of special interest is also a potentially novel mechanism recently identified in KSHV-mediated tumourigenesis: ORF57-sequestration of hTREX has been shown to induce the formation of RNA:DNA hybrids, so called R-loops (Jackson et al., 2014). These R-loops often result in DNA double-strand breaks and genome instability, both of which potentially contribute to the formation of KS. As such, a treatment directly disrupting the interaction of ORF57 and hTREX and thereby preventing R-loop formation, could not only disrupt KSHV lytic replication but also prevent a direct pathway in KSHV tumourigenesis, strengthening the therapeutic potential of our inhibitor.

Two possible therapeutic scenarios can subsequently be envisaged with this type of inhibitor: As prophylactic treatment in high-risk transplant patients or as part of a combined therapy in HIV-patients. To provide preventative systemic treatment, oral dosing of a drug would be advantageous, though depending on the final pharmacokinetic properties of the drug, intravenous therapy might be necessary. As treatment of existing KS, a topical application could also be considered. This would allow increased local concentrations of the drug, while having a lower risk of systemic side effects.

Successful preventative treatment has been suggested for the anti-HCMV drug and herpesvirus inhibitor ganciclovir in some clinically studies, even though ganciclovir does not generally provide very good activity against lytically replicating KSHV (Gantt and Casper, 2011). It would therefore be exciting to see the effect of a very potent anti-KSHV drug in preventative treatment. Patients at risk of developing KS could be identified through screening of KSHV-seropositivity in both the transplant recipient and donor. Furthermore, quantitative measurements by PCR of KSHV lytic replication have shown a close correlation between viral load and the risk and progression of subsequent KS (Engels et al., 2003; Campbell et al., 2005). This would therefore allow a personalised treatment approach and could prevent progression of KSHV infection from an asymptomatic infection to development of KS and as such increase the success of organ transplants. A similar approach is already used for EBV and HCMV in transplant patients (Kotton et al., 2013; Allen et al., 2009)

To date, the most effective treatment of AIDS-related KS is anti-retroviral therapy (ART). The availability of ART has previously led to a dramatic decline in occurrence of KS, mostly through restoration of the patient's immune functions. However, KS is still found in many cases of individuals treated with ART and well controlled HIV. As such, combination of these two treatment strategies would promise a much more enhanced efficacy.

## **6.5 Inhibition of HSP90 and off-target effects**

Compound C2 has previously been described as an inhibitor for the molecular chaperone HSP90 (Dymock et al., 2005), which is responsible for correct folding and subsequent function of client proteins.

HSP90 has previously been mentioned in the context of KSHV infection in the literature: The latency associated nuclear antigen (LANA), responsible for maintenance of the viral episome during latency, has been identified as HSP90 client protein (Chen et al., 2012). The study showed inhibition of HSP90 lead to a loss in LANA and as such a decrease in latent KSHV reservoirs. Furthermore, HSP90 inhibitors had a negative effect on progression of KS and proliferation of latency-associated PEL tumour cells. However, it was speculated that anti-tumour effects on KS and PEL were also promoted through other cellular targets of HSP90, such as CDC2 and Akt, both of which transduce paracrine and autocrine growth signals during KSHV malignancies.

Another study also identified HSP90 inhibitors for their therapeutic potential against PEL. Here, the viral protein K1, a transmembrane glycoprotein able to inhibit apoptosis and transform rodent fibroblasts, was shown to bind HSP90 and subsequently suggested as novel client protein (Wen and Damania, 2010). While K1 is expressed at low levels during latency, but also at higher levels during lytic replication, treatment with the HSP90 inhibitors 17-AAG and 17-DMAG showed reduction of K1 expression and subsequent suppression of PEL cell line growth.

Finally, the involvement of HSP90 on signal transduction in hijacked cell signalling pathways has been implied in KSHV pathogenesis: The viral oncoprotein vFLIP complexes with the IKK complex and HSP90 to activate the NF- $\kappa$ B pathway (Field et al., 2003). Again, HSP90 inhibitors have shown to reduce proliferation of KSHV infected PEL cell lines and induce apoptosis in KSHV-associated tumour cells.

While all studies connected KSHV infection and pathogenesis with HSP90, the molecular chaperone was either implicated in viral latency, or transformation and proliferation of cancer cells. No association between HSP90 and ORF57 or viral lytic replication has been previously suggested.

Interestingly, the effect of inhibitors on HSP90 activity and chaperone function was assessed using the client protein CDC2. As such, a decrease in CDC2 expression was associated with the loss of viral target proteins, such as LANA (Chen et al., 2012). Here, experiments for viral lytic protein expression were also controlled with CDC2. Interestingly

though, inhibition of cellular HSP90 and loss of CDC2 expression occurred at a higher concentrations of the inhibitors, than observed effects on virus lytic replication.

Published data of HSP90 inhibition by C2 shows a half maximal growth-inhibitory concentration ( $GI_{50}$ , 50% inhibition of cell proliferation) of 5.3  $\mu$ M across a panel of tumour cell lines, however the effect ranged from 0.8–23  $\mu$ M for individual cell lines (Cheung et al., 2005; Dymock et al., 2005; Sharp et al., 2007). This concentration range is comparably low to other pharmacological inhibitors of HSP90. As way of comparison, the geldanamycin-derived HSP90 inhibitors, 17-AAG and 17-DMAG, were found to suppress growth of KSHV-associated PEL cells at 50 nM (Wen and Damania, 2010). Furthermore, inhibition of HSP90 by C2 was shown on a cellular level by depletion of client proteins c-Raf and Cdk4 in HCT116 cells, a human colon cancer cell line, after 8–24 h at a concentration of 20.5  $\mu$ M (Dymock et al., 2005). Similarly, SKMEL 28 cells (a human melanoma cell line) showed a loss in HSP90 client proteins c-Raf, CDK4, ERBB2 and Phospho-ERK1/2 after 24 h incubation with 14.5  $\mu$ M C2 (Sharp et al., 2007). In contrast, we showed inhibition of ORF57-associated protein expression and viral replication around 1  $\mu$ M of the same compound, again highlighting the higher affinity of C2 for this cellular pathway.

The above listed findings further strengthen our hypothesis that C2 and its analogues specifically inhibit the hTREX complex pathway in viral replication and not the molecular chaperone HSP90. However, future work will aim at reducing off target effects on HSP90 and possibly other cellular ATPases, as discussed below. This will also serve to reduce cytotoxic side effects further.

## **6.6 Hit to lead development and future work**

Present work has identified a hit compound for an UAP56 ATPase inhibitor. This compound has not yet been involved in hit to lead development; but nonetheless displays considerably good potency, which is extremely encouraging. Furthermore, the low to average molecular weight of C2 allows further optimisations and additions to the structure to increase affinity and specificity.

To advance the hit-to-lead development of C2 by rationale-based drug design, more analogues need to be tested in the future. As part of this, the known structural analogues already utilised in this work should be assessed for their biochemical properties, through determination of  $IC_{50}$ , as well as binding kinetics to UAP56 by microscale thermophoresis. Optimally, a complete structure-activity-relationship (SAR) for C2 should first be determined by strategic changes to all functional groups of C2. Furthermore, lead-like properties need to be incorporated by focusing on improvement of physicochemical and pharmacological properties. Chemical changes for this could include substitutions which probe presently unoccupied sites or add solvent exposed groups, as predicted by the modelling of C2 binding to UAP56.

For development of a SAR, the resorcinol group should first be maintained, as essential hydrogen-bonding interactions are believed to be formed here. However, this could be tested through a series of compounds with substitutions to the hydroxyl groups. An overview of possible changes is shown in Figure 6.3. For example, the pyrazole ring could be explored for isosteric replacement (Figure 6.3a), which is a commonly used technique in drug design that describes exchange of one substituent or group for another, with similar chemical properties. While maintaining the chemical structure, this allows change of physical or biological properties, such as reduced toxicity, enhanced activity or changed metabolism of the compound. Other chemical sub-structures of C2 could be extended to explore unoccupied pockets of the ATP binding site (Figure 6.3b and c), such as the phosphate channel. Furthermore, a substitution of the dioxane region could be used to exploit a free amino acid side chain of UAP56 (Figure 6.3e). All of these changes would aim to improve affinity for UAP56 and potentially decrease off-target activity, by enhancing the enzyme specificity. Another substitution could also explore the potential of adding a solvent exposed vector (Figure 6.3d). This could help incorporate a solubilising group and therefore increase bioavailability of the next generation compound. Finally, the potential of isosteric replacement for the resorcinol group could also be investigated (Figure 6.3f). Previous reports of HSP90 inhibitors with the same scaffold showed glucuronidation of resorcinol hydroxyl-groups, which limited the bioavailability (Biamonte et al., 2009; Eccles et al., 2008). As such, using resorcinol mimetics might improve lead-likeness and could limit this unwanted side effect.

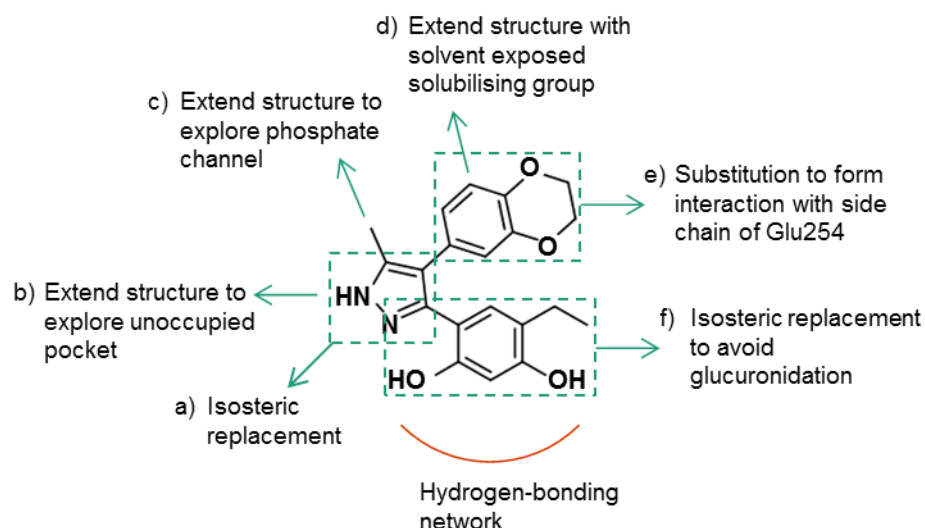


**Figure 6.3: Initial strategy for advancing hit compound C2.** Possible chemical changes are indicated as teal arrows, the existing structure involved in hydrogen-bond formation is indicated in red.

All changes should be assessed by biochemical *in vitro* evaluation, namely through determination of  $IC_{50}$  and binding kinetics by microscale thermophoresis. In a second step of the evaluation strategy, cellular toxicity and off-target effects could be investigated. Finally, the efficacy of the lead compounds should be tested regarding their inhibition of vRNP formation and KSHV lytic replication.

In addition to the biochemical and cell based evaluation mentioned above, hit-to-lead advances could be guided and supported by computational techniques, which would provide quantitative SAR (QSAR) models. These regression-based models help summarise the relationship between chemical structures and biological activity and predict changes in activity through further chemical substitutions. Furthermore, generation of an X-ray crystal structure of UAP56 bound to C2 could confirm current docking models and advance the structure-based design. Once optimal crystallisation conditions were found, the aim would be to generate further crystal structures with advanced lead compounds.

Finally, all compounds with lead-likeness featuring the desired potency should then be evaluated regarding their off-target activity. The above proposed structural changes are aiming to increase selectivity for UAP56, which would help increase binding affinity and simultaneously minimise inhibition of other ATPases and kinases. To test this, a panel of cellular kinases including, but not limited to, the closely related and structurally similar

RNA helicase DDX39 and HSP90 should be used for biochemical assessments alongside UAP56. If the above proposed changes were effective, the new lead compounds could then be tested in a recently developed humanised bone marrow, liver and thymus mouse model for KSHV (Wang et al., 2014).

## References

- Aguilera, A. (2005). Cotranscriptional mRNP assembly: from the DNA to the nuclear pore. *Current Opinion in Cell Biology* **17**, 242-250.
- Akula, S. M., Pramod, N. P., Wang, F. Z. & Chandran, B. (2002). Integrin alpha3beta1 (CD 49c/29) is a cellular receptor for Kaposi's sarcoma-associated herpesvirus (KSHV/HHV-8) entry into the target cells. *Cell* **108**, 407-419.
- Albrecht, J. C. & Fleckenstein, B. (1990). Structural organization of the conserved gene block of Herpesvirus saimiri coding for DNA polymerase, glycoprotein B, and major DNA binding protein. *Virology Journal* **174**, 533-542.
- Allen, U., Preiksaitis, J. & the AST Infectious Diseases Community of Practice (2009). Epstein-Barr Virus and Posttransplant Lymphoproliferative Disorder in Solid Organ Transplant Recipients. *American Journal of Transplantation* **9**, S87-S96.
- Alt, J. R., Cleveland, J. L., Hannink, M. & Diehl, J. A. (2000). Phosphorylation-dependent regulation of cyclin D1 nuclear export and cyclin D1-dependent cellular transformation. *Genes and Development* **14**, 3102-3114.
- Ambroziak, J. A., Blackbourn, D. J., Herndier, B. G., Glogau, R. G., Gullett, J. H., McDonald, A. R., Lennette, E. T. & Levy, J. A. (1995). Herpes-like sequences in HIV-infected and uninfected Kaposi's sarcoma patients. *Science* **268**, 582-583.
- Appleby, T. C., Anderson, R., Fedorova, O., Pyle, A. M., Wang, R., Liu, X., Brendza, K. M. & Somoza, J. R. (2011). Visualizing ATP-dependent RNA translocation by the NS3 helicase from HCV. *Journal of Molecular Biology* **405**, 1139-1153.
- Aravind, L. & Landsman, D. (1998). AT-hook motifs identified in a wide variety of DNA-binding proteins. *Nucleic Acids Research* **26**, 4413-4421.
- Arias, C., Weisburd, B., Stern-Ginossar, N., Mercier, A., Madrid, A. S., Bellare, P., Holdorf, M., Weissman, J. S. & Ganem, D. (2014). KSHV 2.0: a comprehensive annotation of the Kaposi's sarcoma-associated herpesvirus genome using next-generation sequencing reveals novel genomic and functional features. *PLoS Pathogens* **10**.
- AuCoin, D. P., Colletti, K. S., Xu, Y., Cei, S. A. & Pari, G. S. (2002). Kaposi's sarcoma-associated herpesvirus (human herpesvirus 8) contains two functional lytic origins of DNA replication. *Journal of Virology* **76**, 7890-7896.
- Babcock, G. J., Decker, L. L., Volk, M. & Thorley-Lawson, D. A. (1998). EBV persistence in memory B cells in vivo. *Immunity* **9**, 395-404.
- Bacon, T. H., Levin, M. J., Leary, J. J., Sarisky, R. T. & Sutton, D. (2003). Herpes simplex virus resistance to acyclovir and penciclovir after two decades of antiviral therapy. *Clinical Microbiology Reviews* **16**, 114-128.
- Bagni, R. & Whitby, D. (2009). Kaposi's sarcoma-associated herpesvirus transmission and primary infection. *Current Opinion in HIV and AIDS* **4**, 22-26.
- Balasubramaniam, V. R. M. T., Wai, T. H., Tejo, B. A., Omar, A. R. & Hassan, S. S. (2013). Highly pathogenic avian influenza virus nucleoprotein interacts with TREX complex adaptor protein Aly/REF. *PLoS ONE* **8**.

- Ballestas, M. E., Chatis, P. A. & Kaye, K. M. (1999). Efficient persistence of extrachromosomal KSHV DNA mediated by latency-associated nuclear antigen. *Science* **284**, 641-644.
- Ballon, G., Chen, K., Perez, R., Tam, W. & Cesarman, E. (2011). Kaposi sarcoma herpesvirus (KSHV) vFLIP oncoprotein induces B cell transdifferentiation and tumorigenesis in mice. *Journal of Clinical Investigation* **121**, 1141-1153.
- Bello, L. J., Davison, A. J., Glenn, M. A., Whitehouse, A., Rethmeier, N., Schulz, T. F. & Barklie Clements, J. (1999). The human herpesvirus-8 ORF 57 gene and its properties. *Journal of General Virology* **80** 3207-3215.
- Beral, V., Peterman, T. A., Berkelman, R. L. & Jaffe, H. W. (1990). Kaposi's sarcoma among persons with AIDS: a sexually transmitted infection? *The Lancet* **335**, 123-128.
- Biamonte, M. A., Van de Water, R., Arndt, J. W., Scannevin, R. H., Perret, D. & Lee, W.-C. (2009). Heat shock protein 90: inhibitors in clinical trials. *Journal of Medicinal Chemistry* **53**, 3-17.
- Birkmann, A., Mahr, K., Ensser, A., Yağuboğlu, S., Titgemeyer, F., Fleckenstein, B. & Neipel, F. (2001). Cell surface heparan sulfate is a receptor for human herpesvirus 8 and interacts with envelope glycoprotein K8.1. *Journal of Virology* **75**, 11583-11593.
- Blackbourn, D. J., Fujimura, S., Kutzkey, T. & Levy, J. A. (2000). Induction of human herpesvirus-8 gene expression by recombinant interferon gamma. *AIDS* **14**, 98-99.
- Blackbourn, D. J., Lennette, E. T., Ambroziak, J., Mourich, D. V. & Levy, J. A. (1998). Human herpesvirus 8 detection in nasal secretions and saliva. *Journal of Infectious Diseases* **177**, 213-216.
- Borza, C. M. & Hutt-Fletcher, L. M. (2002). Alternate replication in B cells and epithelial cells switches tropism of Epstein-Barr virus. *Nature Medicine* **8**, 594-599.
- Bottero, V., Kerur, N., Sadagopan, S., Patel, K., Sharma-Walia, N. & Chandran, B. (2011). Phosphorylation and polyubiquitination of transforming growth factor  $\beta$ -activated kinase 1 are necessary for activation of NF- $\kappa$ B by the Kaposi's sarcoma-associated herpesvirus G protein-coupled receptor. *Journal of Virology* **85**, 1980-1993.
- Boulanger, E., Gérard, L., Gabarre, J., Molina, J.-M., Rapp, C., Abino, J.-F., Cadranet, J., Chevret, S. & Oksenhendler, E. (2005). Prognostic factors and outcome of human herpesvirus 8-associated primary effusion lymphoma in patients with AIDS. *Journal of Clinical Oncology* **23**, 4372-4380.
- Boyne, J. R., Colgan, K. J. & Whitehouse, A. (2008). Recruitment of the complete hTREX complex is required for Kaposi's sarcoma-associated herpesvirus intronless mRNA nuclear export and virus replication. *PLoS Pathogens* **4**, e1000194.
- Boyne, J. R., Jackson, B. R., Taylor, A., Macnab, S. A. & Whitehouse, A. (2010a). Kaposi's sarcoma-associated herpesvirus ORF57 protein interacts with PYM to enhance translation of viral intronless mRNAs. *EMBO Journal* **29**, 1851-1864.
- Boyne, J. R., Jackson, B. R. & Whitehouse, A. (2010b). ORF57: Master regulator of KSHV mRNA biogenesis. *Cell Cycle* **9**, 2702-2703.
- Boyne, J. R. & Whitehouse, A. (2006). Nucleolar trafficking is essential for nuclear export of intronless herpesvirus mRNA. *Proceedings of the National Academy of Sciences of the United States of America* **103**, 15190-15195.

- Boyne, J. R. & Whitehouse, A. (2009). Nucleolar disruption impairs Kaposi's sarcoma-associated herpesvirus ORF57-mediated nuclear export of intronless viral mRNAs. *FEBS Letters* **583**, 3549-3556.
- Bray, M., Prasad, S., Dubay, J. W., Hunter, E., Jeang, K. T., Rekosh, D. & Hammariskjöld, M. L. (1994). A small element from the Mason-Pfizer monkey virus genome makes human immunodeficiency virus type 1 expression and replication Rev-independent. *Proceedings of the National Academy of Sciences of the United States of America* **91**, 1256-1260.
- Brennan, C. M., Gallouzi, I.-E. & Steitz, J. A. (2000). Protein ligands to HuR modulate its interaction with target mRNAs *in vivo*. *Journal of Cell Biology* **151**, 1-14.
- Brodsky, A. S. & Silver, P. A. (2000). Pre-mRNA processing factors are required for nuclear export. *RNA* **6**, 1737-1749.
- Bryant, H. E., Wadd, S. E., Lamond, A. I., Silverstein, S. J. & Clements, J. B. (2001). Herpes simplex virus IE63 (ICP27) protein interacts with spliceosome-associated protein 145 and inhibits splicing prior to the first catalytic step. *Journal of Virology* **75**, 4376-4385.
- Burke, B. & Stewart, C. L. (2002). Life at the edge: the nuclear envelope and human disease. *Nature Reviews. Molecular Cell Biology* **3**, 575-585.
- Burysek, L., Yeow, W. S. & Pitha, P. M. (1999). Unique properties of a second human herpesvirus 8-encoded interferon regulatory factor (vIRF-2). *Journal of Human Virology* **2**, 19-32.
- Cai, Q., Verma, S. C., Choi, J. Y., Ma, M. & Robertson, E. S. (2010). Kaposi's sarcoma-associated herpesvirus inhibits interleukin-4-mediated STAT6 phosphorylation to regulate apoptosis and maintain latency. *Journal of Virology* **84**, 11134-11144.
- Cai, X., Lu, S., Zhang, Z., Gonzalez, C. M., Damania, B. & Cullen, B. R. (2005). Kaposi's sarcoma-associated herpesvirus expresses an array of viral microRNAs in latently infected cells. *Proceedings of the National Academy of Sciences of the United States of America* **102**, 5570-5575.
- Caldwell, R. G., Wilson, J. B., Anderson, S. J. & Longnecker, R. (1998). Epstein-Barr virus LMP2A drives B cell development and survival in the absence of normal B cell receptor signals. *Immunity* **9**, 405-411.
- Callan, M. F., Steven, N., Krausa, P., Wilson, J. D., Moss, P. A., Gillespie, G. M., Bell, J. I., Rickonson, A. B. & McMichael, A. J. (1996). Large clonal expansions of CD8+ T cells in acute infectious mononucleosis. *Nature Medicine* **2**, 906-911.
- Campbell, T. B., Staskus, K. A., Folkvord, J., White, I. E., Neid, J., Zhang, X. Q. & Connick, E. (2005). Persistence of Kaposi sarcoma associated herpesvirus (KSHV) infected cells in KSHV/HIV-1 coinfecting subjects without KSHV-associated diseases. *Journal of Infectious Diseases* **191**, 367-371.
- Cannon, J. S., Hamzeh, F., Moore, S., Nicholas, J. & Ambinder, R. F. (1999). Human herpesvirus 8-encoded thymidine kinase and phosphotransferase homologues confer sensitivity to ganciclovir. *Journal of Virology* **73**, 4786-4793.
- Cao, W., Coman, M. M., Ding, S., Henn, A., Middleton, E. R., Bradley, M. J., Rhoades, E., Hackney, D. D., Pyle, A. M. & De La Cruz, E. M. (2011). Mechanism of Mss116 ATPase reveals functional diversity of DEAD-box proteins. *Journal of Molecular Biology* **409**, 399-414.

- Cardone, G., Winkler, D. C., Trus, B. L., Cheng, N., Heuser, J. E., Newcomb, W. W., Brown, J. C. & Steven, A. C. (2007). Visualization of the herpes simplex virus portal *in situ* by cryo-electron tomography. *Virology* **361**, 426-434.
- Cesarman, E., Chang, Y., Moore, P. S., Said, J. W. & Knowles, D. M. (1995). Kaposi's sarcoma-associated herpesvirus-like DNA sequences in AIDS-related body-cavity-based lymphomas. *New England Journal of Medicine* **332**, 1186-1191.
- Chang, C. T., Hautbergue, G. M., Walsh, M. J., Viphakone, N., van Dijk, T. B., Philipsen, S. & Wilson, S. A. (2013). Chtop is a component of the dynamic TREX mRNA export complex. *EMBO Journal* **32**, 473-486.
- Chang, Y.-F., Imam, J. S. & Wilkinson, M. F. (2007). The nonsense-mediated decay RNA surveillance pathway. *Annual Review of Biochemistry* **76**, 51-74.
- Chang, Y., Cesarman, E., Pessin, M. S., Lee, F., Culpepper, J., Knowles, D. M. & Moore, P. S. (1994). Identification of herpesvirus-like DNA sequences in AIDS-associated Kaposi's sarcoma. *Science* **266**, 1865-1869.
- Chen, W., Sin, S.-H., Wen, K. W., Damania, B. & Dittmer, D. P. (2012). Hsp90 inhibitors are efficacious against Kaposi Sarcoma by enhancing the degradation of the essential viral gene LANA, of the viral co-receptor EphA2 as well as other client proteins. *PLoS Pathogens* **8**.
- Chen, Y. B., Rahemtullah, A. & Hochberg, E. (2007). Primary effusion lymphoma. *Oncologist* **12**, 569-576.
- Cheng, H., Dufu, K., Lee, C. S., Hsu, J. L., Dias, A. & Reed, R. (2006). Human mRNA export machinery recruited to the 5' end of mRNA. *Cell* **127**, 1389-1400.
- Cheung, K. M. J., Matthews, T. P., James, K., Rowlands, M. G., Boxall, K. J., Sharp, S. Y., Maloney, A., Roe, S. M., Prodromou, C., Pearl, L. H., Aherne, G. W., McDonald, E. & Workman, P. (2005). The identification, synthesis, protein crystal structure and in vitro biochemical evaluation of a new 3,4-diarylpyrazole class of Hsp90 inhibitors. *Bioorganic and Medicinal Chemistry Letters* **15**, 3338-3343.
- Chi, B., Wang, K., Du, Y., Gui, B., Chang, X., Wang, L., Fan, J., Chen, S., Wu, X., Li, G. & Cheng, H. (2014). A Sub-Element in PRE enhances nuclear export of intronless mRNAs by recruiting the TREX complex via ZC3H18. *Nucleic Acids Research* **42**, 7305-7318.
- Chi, B., Wang, Q., Wu, G., Tan, M., Wang, L., Shi, M., Chang, X. & Cheng, H. (2013). Aly and THO are required for assembly of the human TREX complex and association of TREX components with the spliced mRNA. *Nucleic Acids Research* **41**, 1294-1306.
- Choong, M. L., Tan, L. K., Lo, S. L., Ren, E.-C., Ou, K., Ong, S.-E., Liang, R. C. M. Y., Seow, T. K. & Chung, M. C. M. (2001). An integrated approach in the discovery and characterization of a novel nuclear protein over-expressed in liver and pancreatic tumors. *FEBS Letters* **496**, 109-116.
- Collins, C. M. & Medveczky, P. G. (2002). Genetic requirements for the episomal maintenance of oncogenic herpesvirus genomes. *Advances in Cancer Research* **84**, 155-174.
- Conrad, N. K., Mili, S., Marshall, E. L., Shu, M. D. & Steitz, J. A. (2006). Identification of a rapid mammalian deadenylation-dependent decay pathway and its inhibition by a viral RNA element. *Molecular Cell* **24**, 943-953.

- Cooper, M., Goodwin, D. J., Hall, K. T., Stevenson, A. J., Meredith, D. M., Markham, A. F. & Whitehouse, A. (1999). The gene product encoded by ORF 57 of herpesvirus saimiri regulates the redistribution of the splicing factor SC-35. *Journal of General Virology* **80**, 1311-1316.
- Copeland, R. A. (2005). *Evaluation of Enzyme Inhibitors in Drug Discovery: A Guide for Medicinal Chemists and Pharmacologists*, New Jersey: John Wiley & Sons, Inc.
- Cordin, O., Banroques, J., Tanner, N. K. & Linder, P. (2006). The DEAD-box protein family of RNA helicases. *Gene* **367**, 17-37.
- Coscoy, L. (2007). Immune evasion by Kaposi's sarcoma-associated herpesvirus. *Nature Reviews. Immunology* **7**, 391-401.
- Cotter, M. A., 2nd & Robertson, E. S. (1999). The latency-associated nuclear antigen tethers the Kaposi's sarcoma-associated herpesvirus genome to host chromosomes in body cavity-based lymphoma cells. *Virology* **264**, 254-264.
- Croen, K. D. (1991). Latency of the human herpesviruses. *Annual Review of Medicine* **42**, 61-67.
- Cullen, B. R. (2003). Nuclear mRNA export: insights from virology. *Trends in Biochemical Sciences* **28**, 419-424.
- Dalton-Griffin, L., Wilson, S. J. & Kellam, P. (2009). X-box binding protein 1 contributes to induction of the Kaposi's sarcoma-associated herpesvirus lytic cycle under hypoxic conditions. *Journal of Virology* **83**, 7202-7209.
- Damania, B. (2004). Oncogenic gamma-herpesviruses: comparison of viral proteins involved in tumorigenesis. *Nature Reviews. Microbiology* **2**, 656-668.
- Davis, D. A., Rinderknecht, A. S., Zoetewij, J. P., Aoki, Y., Read-Connole, E. L., Tosato, G., Blauvelt, A. & Yarchoan, R. (2001). Hypoxia induces lytic replication of Kaposi sarcoma-associated herpesvirus. *Blood* **97**, 3244-3250.
- Davison, A. J. (2007). Comparative analysis of the genomes. In: Arvin A, Campadelli-Fiume G, Mocarski E, Moore PS, Roizman B, Whitley R & K, Y. (eds.) *Human Herpesviruses: Biology, Therapy, and Immunoprophylaxis*. Cambridge: Cambridge University Press.
- Davison, A. J. (2010). Herpesvirus systematics. *Veterinary Microbiology* **143**, 52-69.
- Davison, A. J., Eberle, R., Ehlers, B., Hayward, G. S., McGeoch, D. J., Minson, A. C., Pellett, P. E., Roizman, B., Studdert, M. J. & Thiry, E. (2009). The order Herpesvirales. *Archives of Virology* **154**, 171-177.
- De Clercq, E. (2002). Strategies in the design of antiviral drugs. *Nature Reviews. Drug Discovery* **1**, 13-25.
- Deng, H., Young, A. & Sun, R. (2000). Auto-activation of the rta gene of human herpesvirus-8/Kaposi's sarcoma-associated herpesvirus. *Journal of General Virology* **81**, 3043-3048.
- Diem, M. D., Chan, C. C., Younis, I. & Dreyfuss, G. (2007). PYM binds the cytoplasmic exon-junction complex and ribosomes to enhance translation of spliced mRNAs. *Nature Structural and Molecular Biology* **14**, 1173-1179.
- Dittmer, D., Lagunoff, M., Renne, R., Staskus, K., Haase, A. & Ganem, D. (1998). A cluster of latently expressed genes in Kaposi's sarcoma-associated herpesvirus. *Journal of Virology* **72**, 8309-8315.

- Doma, M. K. & Parker, R. (2007). RNA quality control in eukaryotes. *Cell* **131**, 660-668.
- Dufu, K., Livingstone, M. J., Seebacher, J., Gygi, S. P., Wilson, S. A. & Reed, R. (2010). ATP is required for interactions between UAP56 and two conserved mRNA export proteins, Aly and CIP29, to assemble the TREX complex. *Genes and Development* **24**, 2043-2053.
- Dymock, B. W., Barril, X., Brough, P. A., Cansfield, J. E., Massey, A., McDonald, E., Hubbard, R. E., Surgenor, A., Roughley, S. D., Webb, P., Workman, P., Wright, L. & Drysdale, M. J. (2005). Novel, potent small-molecule inhibitors of the molecular chaperone Hsp90 discovered through structure-based design. *Journal of Medicinal Chemistry* **48**, 4212-4215.
- Eccles, S. A., Massey, A., Raynaud, F. I., Sharp, S. Y., Box, G., Valenti, M., Patterson, L., Brandon, A. d. H., Gowan, S., Boxall, F., Aherne, W., Rowlands, M., Hayes, A., Martins, V., Urban, F., Boxall, K., Prodromou, C., Pearl, L., James, K., Matthews, T. P., Cheung, K.-M., Kalusa, A., Jones, K., McDonald, E., Barril, X., Brough, P. A., Cansfield, J. E., Dymock, B., Drysdale, M. J., Finch, H., Howes, R., Hubbard, R. E., Surgenor, A., Webb, P., Wood, M., Wright, L. & Workman, P. (2008). NVP-AUY922: A novel heat shock protein 90 inhibitor active against xenograft tumor growth, angiogenesis, and metastasis. *Cancer Research* **68**, 2850-2860.
- Eder, J., Sedrani, R. & Wiesmann, C. (2014). The discovery of first-in-class drugs: origins and evolution. *Nature Reviews Drug Discovery* **13**, 577-587.
- Engels, E. A., Atkinson, J. O., Graubard, B. I., McQuillan, G. M., Gamache, C., Mbisa, G., Cohn, S., Whitby, D. & Goedert, J. J. (2007). Risk factors for human herpesvirus 8 infection among adults in the United States and evidence for sexual transmission. *Journal of Infectious Diseases* **196**, 199-207.
- Engels, E. A., Biggar, R. J., Marshall, V. A., Walters, M., Gamache, C. J., Whitby, D. & Goedert, J. J. (2003). Detection and quantification of Kaposi's sarcoma-associated herpesvirus to predict AIDS-associated Kaposi's sarcoma. *AIDS* **17**, 1847-1851.
- Epstein, M. A., Achong, B. G. & Barr, Y. M. (1964). Virus particles in cultured lymphoblasts from Burkitt's lymphoma. *Lancet* **1**, 702-703.
- Farmer, P. S. & Ariens, E. J. (1982). Speculations on the design of nonpeptidic peptidomimetics. *Trends in Pharmacological Sciences* **3**, 362-365.
- Fasken, M. B. & Corbett, A. H. (2009). Mechanisms of nuclear mRNA quality control. *RNA Biology* **6**, 237-241.
- Fenwick, M. L. & Clark, J. (1982). Early and delayed shut-off of host protein-synthesis in cells infected with herpes simplex virus. *Journal of General Virology* **61**, 121-125.
- Field, N., Low, W., Daniels, M., Howell, S., Daviet, L., Boshoff, C. & Collins, M. (2003). KSHV vFLIP binds to IKK-gamma to activate IKK. *Journal of Cell Science* **116**, 3721-3728.
- Fife, K., Gill, J., Bourbouli, D., Gazzard, B., Nelson, M. & Bower, M. (1999). Cidofovir for the treatment of Kaposi's sarcoma in an HIV-negative homosexual man. *British Journal of Dermatology* **141**, 1148-1150.
- Fingerroth, J. D., Weis, J. J., Tedder, T. F., Strominger, J. L., Biro, P. A. & Fearon, D. T. (1984). Epstein-Barr virus receptor of human B lymphocytes is the C3d receptor CR2. *Proceedings of the National Academy of Sciences of the United States of America* **81**, 4510-4514.

- Fischer, U., Huber, J., Boelens, W. C., Mattajt, L. W. & Lührmann, R. (1995). The HIV-1 Rev activation domain is a nuclear export signal that accesses an export pathway used by specific cellular RNAs. *Cell* **82**, 475-483.
- Folco, E. G., Lee, C. S., Dufu, K., Yamazaki, T. & Reed, R. (2012). The proteins PDIP3 and ZC11A associate with the human TREX complex in an ATP-dependent manner and function in mRNA export. *PLoS ONE* **7**, e43804.
- Fornerod, M., Ohno, M., Yoshida, M. & Mattaj, I. W. (1997). CRM1 is an export receptor for leucine-rich nuclear export signals. *Cell* **90**, 1051-1060.
- Friberg, J., Jr., Kong, W., Hottiger, M. O. & Nabel, G. J. (1999). p53 inhibition by the LANA protein of KSHV protects against cell death. *Nature* **402**, 889-894.
- Fukuda, S., Wu, D. W., Stark, K. & Pelus, L. M. (2002). Cloning and characterization of a proliferation-associated cytokine-inducible protein, CIP29. *Biochemical and Biophysical Research Communications* **292**, 593-600.
- Furlong, D., Roizman, B. & Swift, H. (1972). Arrangement of herpesvirus deoxyribonucleic acid in core. *Journal of Virology* **10**, 1071-1074.
- Ganem, D. (2007). Kaposi's Sarcoma-associated Herpesvirus. In: Knipe, D. M. & Howley, P. M. (eds.) *Fields Virology*. Philadelphia: Lippincott-Williams & Wilkins.
- Ganem, D. (2010). KSHV and the pathogenesis of Kaposi sarcoma: listening to human biology and medicine. *Journal of Clinical Investigation* **120**, 939-949.
- Gantt, S. & Casper, C. (2011). Human herpesvirus 8-associated neoplasms: the roles of viral replication and antiviral treatment. *Current Opinion in Infectious Diseases* **24**, 295-301.
- Garrigues, H. J., Rubinchikova, Y. E., Dipersio, C. M. & Rose, T. M. (2008). Integrin  $\alpha_v\beta_3$  binds to the RGD motif of glycoprotein B of Kaposi's sarcoma-associated herpesvirus and functions as an RGD-dependent entry receptor. *Journal of Virology* **82**, 1570-1580.
- Ghosh, S., Nie, A., An, J. & Huang, Z. (2006). Structure-based virtual screening of chemical libraries for drug discovery. *Current Opinion in Chemical Biology* **10**, 194-202.
- Giorgi, C. & Moore, M. J. (2007). The nuclear nurture and cytoplasmic nature of localized mRNPs. *Seminars in Cell and Developmental Biology* **18**, 186-193.
- Godden-Kent, D., Talbot, S. J., Boshoff, C., Chang, Y., Moore, P., Weiss, R. A. & Mitnacht, S. (1997). The cyclin encoded by Kaposi's sarcoma-associated herpesvirus stimulates cdk6 to phosphorylate the retinoblastoma protein and histone H1. *Journal of Virology* **71**, 4193-4198.
- Goldner, T., Hewlett, G., Ettischer, N., Ruebsamen-Schaeff, H., Zimmermann, H. & Lischka, P. (2011). The novel anticytomegalovirus compound AIC246 (Letermovir) inhibits human cytomegalovirus replication through a specific antiviral mechanism that involves the viral terminase. *Journal of Virology* **85**, 10884-10893.
- Golovanov, A. P., Hautbergue, G. M., Tintaru, A. M., Lian, L.-Y. & Wilson, S. A. (2006). The solution structure of REF2-I reveals interdomain interactions and regions involved in binding mRNA export factors and RNA. *RNA* **12**, 1933-1948.
- Goodwin, D. J. & Whitehouse, A. (2001). A gamma-2 herpesvirus nucleocytoplasmic shuttle protein interacts with importin alpha 1 and alpha 5. *Journal of Biological Chemistry* **276**, 19905-19912.

- Görlich, D. & Kutay, U. (1999). Transport between the cell nucleus and the cytoplasm. *Annual Review of Cell and Developmental Biology* **15**, 607-660.
- Gould, F., Harrison, S. M., Hewitt, E. W. & Whitehouse, A. (2009). Kaposi's sarcoma-associated herpesvirus RTA promotes degradation of the Hey1 repressor protein through the ubiquitin proteasome pathway. *Journal of Virology* **83**, 6727-6738.
- Gregory, S. M., West, J. A., Dillon, P. J., Hilscher, C., Dittmer, D. P. & Damania, B. (2009). Toll-like receptor signaling controls reactivation of KSHV from latency. *Proceedings of the National Academy of Sciences of the United States of America* **106**, 11725-11730.
- Griffiths, R. & Whitehouse, A. (2007). Herpesvirus saimiri episomal persistence is maintained via interaction between open reading frame 73 and the cellular chromosome-associated protein MeCP2. *Journal of Virology* **81**, 4021-4032.
- Grolich, A. E., Li, Y., McDonald, A. M., Correll, P. K., Law, M. G. & Kaldor, J. M. (2001). Decreasing rates of Kaposi's sarcoma and non-Hodgkin's lymphoma in the era of potent combination anti-retroviral therapy. *AIDS* **15**, 629-633.
- Grundhoff, A., Sullivan, C. S. & Ganem, D. (2006). A combined computational and microarray-based approach identifies novel microRNAs encoded by human gamma-herpesviruses. *RNA* **12**, 733-750.
- Grüter, P., Taberner, C., von Kobbe, C., Schmitt, C., Saavedra, C., Bachi, A., Wilm, M., Felber, B. K. & Izaurralde, E. (1998). TAP, the human homolog of Mex67p, mediates CTE-dependent RNA export from the nucleus. *Molecular Cell* **1**, 649-659.
- Gu, M. & Lima, C. D. (2005). Processing the message: structural insights into capping and decapping mRNA. *Current Opinion in Structural Biology* **15**, 99-106.
- Hahn, A. S. & Desrosiers, R. C. (2014). Binding of the Kaposi's sarcoma-associated herpesvirus to the ephrin binding surface of the EphA2 receptor and its inhibition by a small molecule. *Journal of Virology* **88**, 8724-8734.
- Han, Z. & Swaminathan, S. (2006). Kaposi's sarcoma-associated herpesvirus lytic gene ORF57 is essential for infectious virion production. *Journal of Virology* **80**, 5251-5260.
- Hann, M. M. & Oprea, T. I. (2004). Pursuing the leadlikeness concept in pharmaceutical research. *Current Opinion in Chemical Biology* **8**, 255-263.
- Haque, M., Davis, D. A., Wang, V., Widmer, I. & Yarchoan, R. (2003). Kaposi's sarcoma-associated herpesvirus (human herpesvirus 8) contains hypoxia response elements: relevance to lytic induction by hypoxia. *Journal of Virology* **77**, 6761-6768.
- Hardwicke, M. A. & Sandri-Goldin, R. M. (1994). The herpes simplex virus regulatory protein ICP27 contributes to the decrease in cellular mRNA levels during infection. *Journal of Virology* **68**, 4797-4810.
- Hardy, W. R. & Sandri-Goldin, R. M. (1994). Herpes simplex virus inhibits host cell splicing, and regulatory protein ICP27 is required for this effect. *Journal of Virology* **68**, 7790-7799.
- Hargous, Y., Hautbergue, G. M., Tintaru, A. M., Skrisovska, L., Golovanov, A. P., Stevenin, J., Lian, L. Y., Wilson, S. A. & Allain, F. H.-T. (2006). Molecular basis of RNA recognition and TAP binding by the SR proteins SRp20 and 9G8. *EMBO Journal* **25**, 5126-5137.

- Hashii, Y., Kim, J. Y., Sawada, A., Tokimasa, S., Hiroyuki, F., Ohta, H., Makiko, K., Takihara, Y., Ozono, K. & Hara, J. (2004). A novel partner gene CIP29 containing a SAP domain with MLL identified in infantile myelomonocytic leukemia. *Leukemia* **18**, 1546-1548.
- Hatch, E. M. & Hetzer, M. W. (2012). RNP export by nuclear envelope budding. *Cell* **149**, 733-735.
- Hautbergue, G. M., Hung, M. L., Golovanov, A. P., Lian, L. Y. & Wilson, S. A. (2008). Mutually exclusive interactions drive handover of mRNA from export adaptors to TAP. *Proceedings of the National Academy of Sciences of the United States of America* **105**, 5154-5159.
- Hautbergue, G. M., Hung, M. L., Walsh, M. J., Snijders, A. P., Chang, C. T., Jones, R., Ponting, C. P., Dickman, M. J. & Wilson, S. A. (2009). UIF, a new mRNA export adaptor that works together with REF/ALY, requires FACT for recruitment to mRNA. *Current Biology* **19**, 1918-1924.
- Hengge, U. R., Ruzicka, T., Tying, S. K., Stuschke, M., Roggendorf, M., Schwartz, R. A. & Seeber, S. (2002). Update on Kaposi's sarcoma and other HHV8 associated diseases. Part 2: pathogenesis, Castleman's disease, and pleural effusion lymphoma. *The Lancet Infectious Diseases* **2**, 344-352.
- Henn, A., Cao, W., Hackney, D. D. & De La Cruz, E. M. (2008). The ATPase cycle mechanism of the DEAD-box rRNA helicase, DbpA. *Journal of Molecular Biology* **377**, 193-205.
- Henn, A., Shi, S.-P., Zarivach, R., Ben-Zeev, E. & Sagi, I. (2002). The RNA helicase DbpA exhibits a markedly different conformation in the ADP-bound state when compared with the ATP- or RNA-bound states. *Journal of Biological Chemistry* **277**, 46559-46565.
- Hilleren, P., McCarthy, T., Rosbash, M., Parker, R. & Jensen, T. H. (2001). Quality control of mRNA 3'-end processing is linked to the nuclear exosome. *Nature* **413**, 538-542.
- Hiriart, E., Farjot, G., Gruffat, H., Nguyen, M. V. C., Sergeant, A. & Manet, E. (2003). A novel nuclear export signal and a REF interaction domain both promote mRNA export by the Epstein-Barr virus EB2 protein. *Journal of Biological Chemistry* **278**, 335-342.
- Hladik, W., Dollard, S. C., Mermin, J., Fowlkes, A. L., Downing, R., Amin, M. M., Banage, F., Nzaro, E., Kataaha, P., Dondero, T. J., Pellett, P. E. & Lackritz, E. M. (2006). Transmission of human herpesvirus 8 by blood transfusion. *New England Journal of Medicine* **355**, 1331-1338.
- Hocine, S., Singer, R. H. & Grunwald, D. (2010). RNA processing and export. *Cold Spring Harbor Perspectives in Biology* **2**, a000752.
- Hollinshead, M., Johns, H. L., Sayers, C. L., Gonzalez-Lopez, C., Smith, G. L. & Elliott, G. (2012). Endocytic tubules regulated by Rab GTPases 5 and 11 are used for envelopment of herpes simplex virus. *EMBO Journal* **31**, 4204-4220.
- Huang, J. & Liang, T. J. (1993). A novel hepatitis B virus (HBV) genetic element with Rev response element-like properties that is essential for expression of HBV gene products. *Molecular and Cellular Biology* **13**, 7476-7486.
- Huang, Y. & Carmichael, G. G. (1997). The mouse histone H2a gene contains a small element that facilitates cytoplasmic accumulation of intronless gene transcripts and of unspliced HIV-1-related mRNAs. *Proceedings of the National Academy of Sciences of the United States of America* **94**, 10104-10109.

- Huang, Y., Gattoni, R., Stevenin, J. & Steitz, J. A. (2003). SR splicing factors serve as adapter proteins for TAP-dependent mRNA export. *Molecular Cell* **11**, 837-843.
- Huen, D. S., Henderson, S. A., Croom-Carter, D. & Rowe, M. (1995). The Epstein-Barr virus latent membrane protein-1 (LMP1) mediates activation of NF-kappa B and cell surface phenotype via two effector regions in its carboxy-terminal cytoplasmic domain. *Oncogene* **10**, 549-560.
- Hunter, O. V., Sei, E., Richardson, R. B. & Conrad, N. K. (2013). Chromatin immunoprecipitation and microarray analysis suggest functional cooperation between Kaposi's sarcoma-associated herpesvirus ORF57 and K-bZIP. *Journal of Virology* **87**, 4005-4016.
- Iost, I., Dreyfus, M. & Linder, P. (1999). Ded1p, a DEAD-box protein required for translation initiation in *Saccharomyces cerevisiae*, is an RNA helicase. *Journal of Biological Chemistry* **274**, 17677-17683.
- Jackson, B. R., Boyne, J. R., Noerenberg, M., Taylor, A., Hautbergue, G. M., Walsh, M. J., Wheat, R., Blackbourn, D. J., Wilson, S. A. & Whitehouse, A. (2011). An interaction between KSHV ORF57 and UIF provides mRNA-adaptor redundancy in herpesvirus intronless mRNA export. *PLoS Pathogens* **7**, e1002138.
- Jackson, B. R., Noerenberg, M. & Whitehouse, A. (2012). The Kaposi's sarcoma-associated herpesvirus ORF57 protein and its multiple roles in mRNA biogenesis. *Frontiers in Microbiology* **3**, 59.
- Jackson, B. R., Noerenberg, M. & Whitehouse, A. (2014). A novel mechanism inducing genome instability in Kaposi's sarcoma-associated herpesvirus infected cells. *PLoS Pathogens* **10**.
- Jencks, W. P. (1981). On the attribution and additivity of binding-energies. *Proceedings of the National Academy of Sciences of the United States of America-Biological Sciences* **78**, 4046-4050.
- Jeong, J. H., Orvis, J., Kim, J. W., McMurtrey, C. P., Renne, R. & Dittmer, D. P. (2004). Regulation and autoregulation of the promoter for the latency-associated nuclear antigen of Kaposi's sarcoma-associated herpesvirus. *Journal of Biological Chemistry* **279**, 16822-16831.
- Johnson, L. A., Li, L. & Sandri-Goldin, R. M. (2009a). The cellular RNA export receptor TAP/NXF1 is required for ICP27-mediated export of herpes simplex virus 1 RNA, but the TREX complex adaptor protein Aly/REF appears to be dispensable. *Journal of Virology* **83**, 6335-6346.
- Johnson, S. A., Cubberley, G. & Bentley, D. L. (2009b). Cotranscriptional recruitment of the mRNA export factor Yra1 by direct interaction with the 3' end processing factor Pcf11. *Molecular Cell* **33**, 215-226.
- Johnson, S. A., Kim, H., Erickson, B. & Bentley, D. L. (2011). The export factor Yra1 modulates mRNA 3' end processing. *Nature Structural and Molecular Biology* **18**, 1164-1171.
- Jokhi, V., Ashley, J., Nunnari, J., Noma, A., Ito, N., Wakabayashi-Ito, N., Moore, Melissa J. & Budnik, V. (2013). Torsin mediates primary envelopment of large ribonucleoprotein granules at the nuclear envelope. *Cell Reports* **3**, 988-995.
- Kaleeba, J. A. R. & Berger, E. A. (2006). Kaposi's sarcoma-associated herpesvirus fusion-entry receptor: cystine transporter xCT. *Science* **311**, 1921-1924.

- Kang, J. G., Pripuzova, N., Majerciak, V., Kruhlak, M., Le, S. Y. & Zheng, Z. M. (2011). Kaposi sarcoma-associated herpesvirus ORF57 promotes escape of viral and human interleukin-6 from microRNA-mediated suppression. *Journal of Virology* **85**, 2620-2630.
- Kapadia, F., Pryor, A., Chang, T.-H. & Johnson, L. F. (2006). Nuclear localization of poly(A)<sup>+</sup> mRNA following siRNA reduction of expression of the mammalian RNA helicases UAP56 and URH49. *Gene* **384**, 37-44.
- Kaposi, M. (1872). Idiopathisches multiples Pigmentsarkom der Haut. *Archiv für Dermatologie und Syphilis* **4**, 265-273.
- Kaschka-Dierich, C., Werner, F. J., Bauer, I. & Fleckenstein, B. (1982). Structure of nonintegrated, circular Herpesvirus saimiri and Herpesvirus ateles genomes in tumor cell lines and in vitro-transformed cells. *Journal of Virology* **44**, 295-310.
- Katahira, J., Inoue, H., Hurt, E. & Yoneda, Y. (2009). Adaptor Aly and co-adaptor Thoc5 function in the Tap-p15-mediated nuclear export of HSP70 mRNA. *EMBO Journal* **28**, 556-567.
- Katsumata, K., Chono, K., Sudo, K., Shimizu, Y., Kontani, T. & Suzuki, H. (2011). Effect of ASP2151, a herpesvirus helicase-primase inhibitor, in a guinea pig model of genital herpes. *Molecules* **16**, 7210-7223.
- Kelly, B. J., Fraefel, C., Cunningham, A. L. & Diefenbach, R. J. (2009). Functional roles of the tegument proteins of herpes simplex virus type 1. *Virus Research* **145**, 173-186.
- Kibler, K. V., Miyazato, A., Yedavalli, V. S. R. K., Dayton, A. I., Jacobs, B. L., Dapolito, G., Kim, S.-j. & Jeang, K.-T. (2004). Polyarginine inhibits gp160 processing by furin and suppresses productive human immunodeficiency virus type 1 infection. *Journal of Biological Chemistry* **279**, 49055-49063.
- King, C. A. (2013). Kaposi's sarcoma-associated herpesvirus kaposin B induces unique monophosphorylation of STAT3 at serine 727 and MK2-mediated inactivation of the STAT3 transcriptional repressor TRIM28. *Journal of Virology* **87**, 8779-8791.
- Kirshner, J. R., Lukac, D. M., Chang, J. & Ganem, D. (2000). Kaposi's sarcoma-associated herpesvirus open reading frame 57 encodes a posttranscriptional regulator with multiple distinct activities. *Journal of Virology* **74**, 3586-3597.
- Kistler, A. L. & Guthrie, C. (2001). Deletion of MUD2, the yeast homolog of U2AF65, can bypass the requirement for Sub2, an essential spliceosomal ATPase. *Genes and Development* **15**, 42-49.
- Klass, C. M., Krug, L. T., Pozharskaya, V. P. & Offermann, M. K. (2005). The targeting of primary effusion lymphoma cells for apoptosis by inducing lytic replication of human herpesvirus 8 while blocking virus production. *Blood* **105**, 4028-4034.
- Klein, E., Kis, L. L. & Klein, G. (2007). Epstein-Barr virus infection in humans: from harmless to life endangering virus-lymphocyte interactions. *Oncogene* **26**, 1297-1305.
- Knipe, D. M. & Cliffe, A. (2008). Chromatin control of herpes simplex virus lytic and latent infection. *Nature Reviews. Microbiology* **6**, 211-221.
- Koffa, M. D., Clements, J. B., Izaurralde, E., Wadd, S., Wilson, S. A., Mattaj, I. W. & Kuersten, S. (2001). *Herpes simplex virus ICP27 protein provides viral mRNAs with access to the cellular mRNA export pathway.*

- Kohler, A. & Hurt, E. (2007). Exporting RNA from the nucleus to the cytoplasm. *Nature Reviews. Molecular Cell Biology* **8**, 761-773.
- Koon, H. B., Krown, S. E., Lee, J. Y., Honda, K., Rapisuwon, S., Wang, Z., Aboulafia, D., Reid, E. G., Rudek, M. A., Dezube, B. J. & Noy, A. (2014). Phase II trial of Imatinib in AIDS-associated Kaposi's sarcoma: AIDS malignancy consortium protocol 042. *Journal of Clinical Oncology* **32**, 402-U441.
- Kotton, C. N., Kumar, D., Caliendo, A. M., Asberg, A., Chou, S., Danziger-Isakov, L., Humar, A. & Transplantation Soc Int, C. M. V. (2013). Updated international consensus guidelines on the management of cytomegalovirus in solid-organ transplantation. *Transplantation* **96**, 333-360.
- Kudo, N., Khochbin, S., Nishi, K., Kitano, K., Yanagida, M., Yoshida, M. & Horinouchi, S. (1997). Molecular cloning and cell cycle-dependent expression of mammalian CRM1, a protein involved in nuclear export of proteins. *Journal of Biological Chemistry* **272**, 29742-29751.
- Kurth, J., Spieker, T., Wustrow, J., Strickler, J. G., Hansmann, M. L., Rajewsky, K. & Kuppers, R. (2000). EBV-infected B cells in infectious mononucleosis: Viral strategies for spreading in the B cell compartment and establishing latency. *Immunity* **13**, 485-495.
- Kwong, A. D., Rao, B. G. & Jeang, K. T. (2005). Viral and cellular RNA helicases as antiviral targets. *Nature Reviews Drug Discovery* **4**, 845-853.
- Le Hir, H. & Andersen, G. R. (2008). Structural insights into the exon junction complex. *Current Opinion in Structural Biology* **18**, 112.
- Le Hir, H., Izaurralde, E., Maquat, L. E. & Moore, M. J. (2000). The spliceosome deposits multiple proteins 20-24 nucleotides upstream of mRNA exon-exon junctions. *EMBO Journal* **19**, 6860-6869.
- Leach, A. R. & Hann, M. M. (2007). Constructing a fragment-set for screening. In: Jhoti, H. & Leach, A. R. (eds.) *Structure-based Drug Discovery*. 1st ed. Dordrecht, The Netherlands: Springer.
- Lee, C.-P. & Chen, M.-R. (2010). Escape of herpesviruses from the nucleus. *Reviews in Medical Virology* **20**, 214-230.
- Lei, E. P. & Silver, P. A. (2002). Intron status and 3'-end formation control cotranscriptional export of mRNA. *Genes and Development* **16**, 2761-2766.
- Lei, H., Dias, A. P. & Reed, R. (2011). Export and stability of naturally intronless mRNAs require specific coding region sequences and the TREX mRNA export complex. *Proceedings of the National Academy of Sciences of the United States of America* **108**, 17985-17990.
- Lei, H., Zhai, B., Yin, S., Gygi, S. & Reed, R. (2013). Evidence that a consensus element found in naturally intronless mRNAs promotes mRNA export. *Nucleic Acids Research* **41**, 2517-2525.
- Lejeune, F., Ishigaki, Y., Li, X. & Maquat, L. E. (2002). The exon junction complex is detected on CBP80-bound but not eIF4E-bound mRNA in mammalian cells: dynamics of mRNP remodeling. *EMBO Journal* **21**, 3536-3545.

- Li, M., Lee, H., Yoon, D. W., Albrecht, J. C., Fleckenstein, B., Neipel, F. & Jung, J. U. (1997). Kaposi's sarcoma-associated herpesvirus encodes a functional cyclin. *Journal of Virology* **71**, 1984-1991.
- Liang, Y., Chang, J., Lynch, S. J., Lukac, D. M. & Ganem, D. (2002). The lytic switch protein of KSHV activates gene expression via functional interaction with RBP-Jkappa (CSL), the target of the Notch signaling pathway. *Genes and Development* **16**, 1977-1989.
- Libri, D., Dower, K., Boulay, J., Thomsen, R., Rosbash, M. & Jensen, T. H. (2002). Interactions between mRNA export commitment, 3'-end quality control, and nuclear degradation. *Molecular and Cellular Biology* **22**, 8254-8266.
- Lischka, P., Toth, Z., Thomas, M., Mueller, R. & Stamminger, T. (2006). The UL69 transactivator protein of human cytomegalovirus interacts with DEXD/H-box RNA helicase UAP56 to promote cytoplasmic accumulation of unspliced RNA. *Molecular and Cellular Biology* **26**, 1631-1643.
- Little, R. F., Mercad-Galindez, F., Staskus, K., Whitby, D., Aoki, Y., Humphrey, R., Pluda, J. M., Marshall, V., Walters, M., Welles, L., Rodriguez-Chavez, I. R., Pittaluga, S., Tosato, G. & Yarchoan, R. (2003). A pilot study of cidofovir in patients with Kaposi sarcoma. *Journal of Infectious Diseases* **187**, 149-153.
- Liu, L., Eby, M. T., Rathore, N., Sinha, S. K., Kumar, A. & Chaudhary, P. M. (2002). The human herpes virus 8-encoded viral FLICE inhibitory protein physically associates with and persistently activates the I $\kappa$ B kinase complex. *Journal of Biological Chemistry* **277**, 13745-13751.
- Lombardino, J. G. & Lowe, J. A. (2004). The role of the medicinal chemist in drug discovery - Then and now. *Nature Reviews Drug Discovery* **3**, 853-862.
- Long, J. C. & Caceres, J. F. (2009). The SR protein family of splicing factors: master regulators of gene expression. *Biochemical Journal* **417**, 15-27.
- Lorsch, J. R. & Herschlag, D. (1998). The DEAD box protein eIF4A. 2. A cycle of nucleotide and RNA-dependent conformational changes. *Biochemistry* **37**, 2194-2206.
- Lu, M., Suen, J., Frias, C., Pfeiffer, R., Tsai, M. H., Chuang, E. & Zeichner, S. L. (2004). Dissection of the Kaposi's sarcoma-associated herpesvirus gene expression program by using the viral DNA replication inhibitor cidofovir. *Journal of Virology* **78**, 13637-13652.
- Lukac, D. M., Kirshner, J. R. & Ganem, D. (1999). Transcriptional activation by the product of open reading frame 50 of Kaposi's sarcoma-associated herpesvirus is required for lytic viral reactivation in B cells. *Journal of Virology* **73**, 9348-9361.
- Lukac, D. M., Renne, R., Kirshner, J. R. & Ganem, D. (1998). Reactivation of Kaposi's sarcoma-associated herpesvirus infection from latency by expression of the ORF 50 transactivator, a homolog of the EBV R protein. *Virology* **252**, 304-312.
- Luo, M.-J. & Reed, R. (1999). Splicing is required for rapid and efficient mRNA export in metazoans. *Proceedings of the National Academy of Sciences of the United States of America* **96**, 14937-14942.
- Luo, M.-J., Zhou, Z., Magni, K., Christoforides, C., Rappsilber, J., Mann, M. & Reed, R. (2001). Pre-mRNA splicing and mRNA export linked by direct interactions between UAP56 and Aly. *Nature* **413**, 644-647.

- Ma, X. M., Yoon, S. O., Richardson, C. J., Julich, K. & Blenis, J. (2008). SKAR links pre-mRNA splicing to mTOR/S6K1-mediated enhanced translation efficiency of spliced mRNAs. *Cell* **133**, 303-313.
- Mabit, H., Nakano, M. Y., Prank, U., Saam, B., Dohner, K., Sodeik, B. & Greber, U. F. (2002). Intact microtubules support adenovirus and herpes simplex virus infections. *Journal of Virology* **76**, 9962-9971.
- Majerciak, V., Kruhlak, M., Dagur, P. K., McCoy, J. P., Jr. & Zheng, Z. M. (2010). Caspase-7 cleavage of Kaposi sarcoma-associated herpesvirus ORF57 confers a cellular function against viral lytic gene expression. *Journal of Biological Chemistry* **285**, 11297-11307.
- Majerciak, V., Uranishi, H., Kruhlak, M., Pilkington, G. R., Massimelli, M. J., Bear, J., Pavlakis, G. N., Felber, B. K. & Zheng, Z.-M. (2011). Kaposi's sarcoma-associated herpesvirus ORF57 interacts with cellular RNA export cofactors RBM15 and OTT3 to promote expression of viral ORF59. *Journal of Virology* **85**, 1528-1540.
- Majerciak, V., Yamanegi, K., Allemand, E., Kruhlak, M., Krainer, A. R. & Zheng, Z. M. (2008). Kaposi's sarcoma-associated herpesvirus ORF57 functions as a viral splicing factor and promotes expression of intron-containing viral lytic genes in spliceosome-mediated RNA splicing. *Journal of Virology* **82**, 2792-2801.
- Majerciak, V., Yamanegi, K., Nie, S. H. & Zheng, Z. M. (2006). Structural and functional analyses of Kaposi sarcoma-associated herpesvirus ORF57 nuclear localization signals in living cells. *Journal of Biological Chemistry* **281**, 28365-28378.
- Majerciak, V. & Zheng, Z. M. (2009). Kaposi's sarcoma-associated herpesvirus ORF57 in viral RNA processing. *Frontiers in Bioscience* **14**, 1516-1528.
- Malik, P., Blackbourn, D. J., Cheng, M. F., Hayward, G. S. & Clements, J. B. (2004a). Functional co-operation between the Kaposi's sarcoma-associated herpesvirus ORF57 and ORF50 regulatory proteins. *Journal of General Virology* **85**, 2155-2166.
- Malik, P., Blackbourn, D. J. & Clements, J. B. (2004b). The evolutionarily conserved Kaposi's sarcoma-associated herpesvirus ORF57 protein interacts with REF protein and acts as an RNA export factor. *Journal of Biological Chemistry* **279**, 33001-33011.
- Malim, M. H. & Cullen, B. R. (1991). HIV-1 structural gene expression requires the binding of multiple Rev monomers to the viral RRE: Implications for HIV-1 latency. *Cell* **65**, 241-248.
- Martin, D. F., Kuppermann, B. D., Wolitz, R. A., Palestine, A. G., Li, H., Robinson, C. A. & Roche Ganciclovir Study, G. (1999). Oral ganciclovir for patients with cytomegalovirus retinitis treated with a ganciclovir implant. *New England Journal of Medicine* **340**, 1063-1070.
- Martin, J. N., Ganem, D. E., Osmond, D. H., Page-Shafer, K. A., Macrae, D. & Kedes, D. H. (1998). Sexual transmission and the natural history of human herpesvirus 8 infection. *New England Journal of Medicine* **338**, 948-954.
- Martin, J. N. & Osmond, D. H. (2000). Invited commentary: determining specific sexual practices associated with human herpesvirus 8 transmission. *American Journal of Epidemiology* **151**, 225-229.
- Massimelli, M. J., Kang, J.-G., Majerciak, V., Le, S.-Y., Liewehr, D., Steinberg, S. & Zheng, Z. M. (2011). Stability of a long noncoding viral RNA depends on a 9-nt core element

- at the RNA 5' end to interact with viral ORF57 and cellular PABPC1. *International Journal of Biological Sciences* **7**, 1145-1160.
- Masuda, S., Das, R., Cheng, H., Hurt, E., Dorman, N. & Reed, R. (2005). Recruitment of the human TREX complex to mRNA during splicing. *Genes and Development* **19**, 1512-1517.
- Matta, H., Sun, Q., Moses, G. & Chaudhary, P. M. (2003). Molecular Genetic Analysis of Human Herpes Virus 8-encoded Viral FLICE Inhibitory Protein-induced NF- $\kappa$ B Activation. *Journal of Biological Chemistry* **278**, 52406-52411.
- Matthews, R. E. F. (1979). Classification and nomenclature of viruses. . *Intervirolgy* **12**, 129-296.
- Maurer, T., Ponte, M. & Leslie, K. (2007). HIV-associated Kaposi's sarcoma with a high CD4 count and a low viral load. *New England Journal of Medicine* **357**, 1352-1353.
- Mazzi, R., Parisi, S. G., Sarmati, L., Uccella, I., Nicastrì, E., Carolo, G., Gatti, F., Concia, E. & Andreoni, M. (2001). Efficacy of cidofovir on human herpesvirus 8 viraemia and Kaposi's sarcoma progression in two patients with AIDS. *AIDS* **15**, 2061-2062.
- McCormick, C. & Ganem, D. (2005). The kaposin B protein of KSHV activates the p38/MK2 pathway and stabilizes cytokine mRNAs. *Science* **307**, 739-741.
- McGeoch, D. J., Davison, A. J., Dolan, A., Gatherer, D. & Sevilla-Reyes, E. E. (2008). Molecular Evolution of the *Herpesvirales*. In: Domingo, E., Parrish, C. R. & Holland, J. J. (eds.) *Origin and Evolution of Viruses*. Second ed.: Academic Press.
- Méjat, A., Decostre, V., Li, J., Renou, L., Kesari, A., Hantaï, D., Stewart, C. L., Xiao, X., Hoffman, E., Bonne, G. & Misteli, T. (2009). Lamin A/C-mediated neuromuscular junction defects in Emery-Dreifuss muscular dystrophy. *Journal of Cell Biology* **184**, 31-44.
- Mesri, E. A., Cesarman, E. & Boshoff, C. (2010). Kaposi's sarcoma and its associated herpesvirus. *Nature Reviews. Cancer* **10**, 707-719.
- Mettenleiter, T. C. (2002). Herpesvirus assembly and egress. *Journal of Virology* **76**, 1537-1547.
- Mettenleiter, T. C. (2004). Budding events in herpesvirus morphogenesis. *Virus Research* **106**, 167-180.
- Mettenleiter, T. C., Klupp, B. G. & Granzow, H. (2009). Herpesvirus assembly: an update. *Virus Research* **143**, 222-234.
- Moore, M. S. (1998). Ran and nuclear transport. *Journal of Biological Chemistry* **273**, 22857-22860.
- Moore, M. S. & Blobel, G. (1993). The GTP-binding protein Ran/TC4 is required for protein import into the nucleus. *Nature* **365**, 661-663.
- Muralidhar, S., Pumfery, A. M., Hassani, M., Sadaie, M. R., Kishishita, M., Brady, J. N., Doniger, J., Medveczky, P. & Rosenthal, L. J. (1998). Identification of kaposin (open reading frame K12) as a human herpesvirus 8 (Kaposi's sarcoma-associated herpesvirus) transforming gene. *Journal of Virology* **72**, 4980-4988.
- Nakamura, H., Lu, M., Gwack, Y., Souvlis, J., Zeichner, S. L. & Jung, J. U. (2003). Global changes in Kaposi's sarcoma-associated virus gene expression patterns following expression of a tetracycline-inducible Rta transactivator. *Journal of Virology* **77**, 4205-4220.

- Naranatt, P. P., Krishnan, H. H., Smith, M. S. & Chandran, B. (2005). Kaposi's sarcoma-associated herpesvirus modulates microtubule dynamics via RhoA-GTP-diphospho signaling and utilizes the dynein motors to deliver its DNA to the nucleus. *Journal of Virology* **79**, 1191-1206.
- Nekorchuk, M., Han, Z., Hsieh, T. T. & Swaminathan, S. (2007). Kaposi's sarcoma-associated herpesvirus ORF57 protein enhances mRNA accumulation independently of effects on nuclear RNA export. *Journal of Virology* **81**, 9990-9998.
- Nicholas, J., Cameron, K. R., Coleman, H., Newman, C. & Honess, R. W. (1992). Analysis of nucleotide sequence of the rightmost 43 kbp of herpesvirus saimiri (HVS) L-DNA: general conservation of genetic organization between HVS and Epstein-Barr virus. *Virology Journal* **188**, 296-310.
- Nielsen, K. H., Chamieh, H., Andersen, C. B. F., Fredslund, F., Hamborg, K., Le Hir, H. & Andersen, G. R. (2009). Mechanism of ATP turnover inhibition in the EJC. *RNA* **15**, 67-75.
- Nott, A., Le Hir, H. & Moore, M. J. (2004). Splicing enhances translation in mammalian cells: an additional function of the exon junction complex. *Genes and Development* **18**, 210-222.
- Oettle, A. G. (1962). Geographical and racial differences in the frequency of Kaposi's Sarcoma as evidence of environmental or genetic causes. *Acta Unio Internationalis Contra Cancrum* **18**, 330-363.
- Ohno, M., Segref, A., Bachi, A., Wilm, M. & Mattaj, I. W. (2000). PHAX, a mediator of U snRNA nuclear export whose activity is regulated by phosphorylation. *Cell* **101**, 187-198.
- Ohsaki, E., Suzuki, T., Karayama, M. & Ueda, K. (2009). Accumulation of LANA at nuclear matrix fraction is important for Kaposi's sarcoma-associated herpesvirus replication in latency. *Virus Research* **139**, 74-84.
- Ohsaki, E. & Ueda, K. (2012). Kaposi's sarcoma-associated herpesvirus genome replication, partitioning, and maintenance in latency. *Frontiers in Microbiology* **3**.
- Oksenhendler, E., Carcelain, G., Aoki, Y., Boulanger, E., Maillard, A., Clauvel, J.-P. & Agbalika, F. (2000). High levels of human herpesvirus 8 viral load, human interleukin-6, interleukin-10, and C reactive protein correlate with exacerbation of multicentric Castleman disease in HIV-infected patients. *Blood* **96**, 2069-2073.
- Ote, I., Lebrun, M., Vandevenne, P., Bontems, S., Medina-Palazon, C., Manet, E., Piette, J. & Sadzot-Delvaux, C. (2009). Varicella-Zoster virus IE4 protein interacts with SR proteins and exports mRNAs through the TAP/NXF1 pathway. *PLoS ONE* **4**, e7882.
- Pagano, J. S. (2008). Epstein-Barr Virus Diseases. In: Damania, B. & Pipas, J. M. (eds.) *DNA Tumor Viruses*. New York: Springer Science & Business Media.
- Palmeri, D., Spadavecchia, S., Carroll, K. D. & Lukac, D. M. (2007). Promoter- and cell-specific transcriptional transactivation by the Kaposi's sarcoma-associated herpesvirus ORF57/Mta protein. *Journal of Virology* **81**, 13299-13314.
- Parkin, D. M., Sitas, F., Chirenje, M., Stein, L., Abratt, R. & Wabinga, H. (2008). Part I: Cancer in indigenous Africans - burden, distribution, and trends. *Lancet Oncology* **9**, 683-692.

- Pauk, J., Huang, M. L., Brodie, S. J., Wald, A., Koelle, D. M., Schacker, T., Celum, C., Selke, S. & Corey, L. (2000). Mucosal shedding of human herpesvirus 8 in men. *New England Journal of Medicine* **343**, 1369-1377.
- Paulose-Murphy, M., Ha, N.-K., Xiang, C., Chen, Y., Gillim, L., Yarchoan, R., Meltzer, P., Bittner, M., Trent, J. & Zeichner, S. (2001). Transcription program of human herpesvirus 8 (Kaposi's sarcoma-associated herpesvirus). *Journal of Virology* **75**, 4843-4853.
- Penn, I. (1978). Development of cancer in transplantation patients. *Advances in Surgery* **12**, 155-191.
- Pfeffer, S., Sewer, A., Lagos-Quintana, M., Sheridan, R., Sander, C., Grasser, F. A., van Dyk, L. F., Ho, C. K., Shuman, S., Chien, M., Russo, J. J., Ju, J., Randall, G., Lindenbach, B. D., Rice, C. M., Simon, V., Ho, D. D., Zavolan, M. & Tuschl, T. (2005). Identification of microRNAs of the herpesvirus family. *Nature Methods* **2**, 269-276.
- Pietrek, M., Brinkmann, M. M., Glowacka, I., Enlund, A., Havemeier, A., Dittrich-Breiholz, O., Kracht, M., Lewitzky, M., Saksela, K., Feller, S. M. & Schulz, T. F. (2010). Role of the Kaposi's sarcoma-associated herpesvirus K15 SH3 binding site in inflammatory signaling and B-cell activation. *Journal of Virology* **84**, 8231-8240.
- Prechtel, A. T., Chemnitz, J., Schirmer, S., Ehlers, C., Langbein-Detsch, I., Stülke, J., Dabauvalle, M.-C., Kehlenbach, R. H. & Hauber, J. (2006). Expression of CD83 is regulated by HuR via a novel cis-active coding region RNA element. *Journal of Biological Chemistry* **281**, 10912-10925.
- Pyle, A. M. (2011). RNA helicases and remodeling proteins. *Current Opinion in Chemical Biology* **15**, 636-642.
- Qin, D., Zeng, Y., Qian, C., Huang, Z., Lv, Z., Cheng, L., Yao, S., Tang, Q., Chen, X. & Lu, C. (2008). Induction of lytic cycle replication of Kaposi's sarcoma-associated herpesvirus by herpes simplex virus type 1: involvement of IL-10 and IL-4. *Cellular Microbiology* **10**, 713-728.
- Rappocciolo, G., Jenkins, F. J., Hensler, H. R., Piazza, P., Jais, M., Borowski, L., Watkins, S. C. & Rinaldo, C. R., Jr. (2006). DC-SIGN is a receptor for human herpesvirus 8 on dendritic cells and macrophages. *Journal of Immunology* **176**, 1741-1749.
- Read, E. K. C. & Digard, P. (2010). Individual influenza A virus mRNAs show differential dependence on cellular NXF1/TAP for their nuclear export. *Journal of General Virology* **91**, 1290-1301.
- Reed, R. & Cheng, H. (2005). TREX, SR proteins and export of mRNA. *Current Opinion in Cell Biology* **17**, 269-273.
- Reed, R. & Hurt, E. (2002). A conserved mRNA export machinery coupled to pre-mRNA splicing. *Cell* **108**, 523-531.
- Rees, D. C., Congreve, M., Murray, C. W. & Carr, R. (2004). Fragment-based lead discovery. *Nature Reviews. Drug Discovery* **3**, 660-672.
- Rehwinkel, J., Herold, A., Gari, K., Kocher, T., Rode, M., Ciccarelli, F. L., Wilm, M. & Izaurralde, E. (2004). Genome-wide analysis of mRNAs regulated by the THO complex in *Drosophila melanogaster*. *Nature Structural and Molecular Biology* **11**, 558-566.

- Renne, R., Barry, C., Dittmer, D., Compitello, N., Brown, P. O. & Ganem, D. (2001). Modulation of cellular and viral gene expression by the latency-associated nuclear antigen of Kaposi's sarcoma-associated herpesvirus. *Journal of Virology* **75**, 458-468.
- Rivas, C., Thlick, A. E., Parravicini, C., Moore, P. S. & Chang, Y. (2001). Kaposi's sarcoma-associated herpesvirus LANA2 is a B-cell-specific latent viral protein that inhibits p53. *Journal of Virology* **75**, 429-438.
- Rocak, S. & Linder, P. (2004). Dead-box proteins: The driving forces behind RNA metabolism. *Nature Reviews Molecular Cell Biology* **5**, 232-241.
- Roizman, B., Carmichael, L. E., Deinhardt, F., de-The, G., Nahmias, A. J., Plowright, W., Rapp, F., Sheldrick, P., Takahashi, M. & Wolf, K. (1981). Herpesviridae. Definition, provisional nomenclature, and taxonomy. The Herpesvirus Study Group, the International Committee on Taxonomy of Viruses. *Intervirology* **16**, 201-217.
- Roizmann, B., Desrosiers, R. C., Fleckenstein, B., Lopez, C., Minson, A. C. & Studdert, M. J. (1992). The family Herpesviridae: an update. The Herpesvirus Study Group of the International Committee on Taxonomy of Viruses. *Archives of Virology* **123**, 425-449.
- Russo, J., Bohenzky, R., Chien, M.-C., Chen, J., Yan, M., Maddalena, D., Parry, J. P., Peruzzi, D., Edelman, I., Chang, Y. & Moore, P. (1996). Nucleotide sequence of the Kaposi sarcoma-associated herpesvirus (HHV8). *Proceedings of the National Academy of Sciences of the United States of America* **93**, 14862-14867.
- Ruvolo, V., Sun, L., Howard, K., Sung, S., Delecluse, H. J., Hammerschmidt, W. & Swaminathan, S. (2004). Functional analysis of Epstein-Barr virus SM protein: identification of amino acids essential for structure, transactivation, splicing inhibition, and virion production. *Journal of Virology* **78**, 340-352.
- Sandri-Goldin, R. M. (1998). ICP27 mediates HSV RNA export by shuttling through a leucine-rich nuclear export signal and binding viral intronless RNAs through an RGG motif. *Genes and Development* **12**, 868-879.
- Sandri-Goldin, R. M. (2008). The many roles of the regulatory protein ICP27 during herpes simplex virus infection. *Frontiers in Bioscience* **13**, 5241-5256.
- Sarac, M. S., Cameron, A. & Lindberg, I. (2002). The furin inhibitor hexa-D-arginine blocks the activation of *Pseudomonas aeruginosa* exotoxin A in vivo. *Infection and Immunity* **70**, 7136-7139.
- Sarid, R., Wiezorek, J. S., Moore, P. S. & Chang, Y. (1999). Characterization and cell cycle regulation of the major Kaposi's sarcoma-associated herpesvirus (human herpesvirus 8) latent genes and their promoter. *Journal of Virology* **73**, 1438-1446.
- Schumann, S., Jackson, B., Baquero-Perez, B. & Whitehouse, A. (2013). Kaposi's sarcoma-associated herpesvirus ORF57 protein: exploiting all stages of viral mRNA processing. *Viruses* **5**, 1901-1923.
- Sei, E. & Conrad, N. K. (2011). Delineation of a core RNA element required for Kaposi's sarcoma-associated herpesvirus ORF57 binding and activity. *Virology* **419**, 107-116.
- Semmes, O. J., Chen, L., Sarisky, R. T., Gao, Z., Zhong, L. & Hayward, S. D. (1998). Mta has properties of an RNA export protein and increases cytoplasmic accumulation of Epstein-Barr virus replication gene mRNA. *Journal of Virology* **72**, 9526-9534.

- Sharp, S. Y., Boxall, K., Rowlands, M., Prodromou, C., Roe, S. M., Maloney, A., Powers, M., Clarke, P. A., Box, G., Sanderson, S., Patterson, L., Matthews, T. P., Cheung, K.-M. J., Ball, K., Hayes, A., Raynaud, F., Marais, R., Pearl, L., Eccles, S., Aherne, W., McDonald, E. & Workman, P. (2007). In vitro biological characterization of a novel, synthetic diaryl pyrazole resorcinol class of heat shock protein 90 inhibitors. *Cancer Research* **67**, 2206-2216.
- Shen, J., Zhang, L. & Zhao, R. (2007). Biochemical characterization of the ATPase and helicase activity of UAP56, an essential pre-mRNA splicing and mRNA export factor. *Journal of Biological Chemistry* **282**, 22544-22550.
- Shi, H., Cordin, O., Minder, C. M., Linder, P. & Xu, R.-M. (2004). Crystal structure of the human ATP-dependent splicing and export factor UAP56. *Proceedings of the National Academy of Sciences of the United States of America* **101**, 17628-17633.
- Shi, Y., Di Giammartino, D. C., Taylor, D., Sarkeshik, A., Rice, W. J., Yates, J. R., 3rd, Frank, J. & Manley, J. L. (2009). Molecular architecture of the human pre-mRNA 3' processing complex. *Molecular Cell* **33**, 365-376.
- Shida, H. (2012). Role of nucleocytoplasmic RNA transport during the life cycle of retroviruses. *Frontiers in Microbiology* **3**, 179.
- Shukla, D. & Spear, P. G. (2001). Herpesviruses and heparan sulfate: an intimate relationship in aid of viral entry. *The Journal of Clinical Investigation* **108**, 503-510.
- Skepper, J. N., Whiteley, A., Browne, H. & Minson, A. (2001). Herpes simplex virus nucleocapsids mature to progeny virions by an envelopment -> deenvelopment -> reenvelopment pathway. *Journal of Virology* **75**, 5697-5702.
- Song, M. J., Brown, H. J., Wu, T. T. & Sun, R. (2001). Transcription activation of polyadenylated nuclear RNA by Rta in human herpesvirus 8/Kaposi's sarcoma-associated herpesvirus. *Journal of Virology* **75**, 3129-3140.
- Soulier, J., Grollet, L., Oksenhendler, E., Cacoub, P., Cazals-Hatem, D., Babinet, P., d'Agay, M. F., Clauvel, J. P., Raphael, M., Degos, L. & Sigaux, F. (1995). Kaposi's sarcoma-associated herpesvirus-like DNA sequences in multicentric Castlemann's disease. *Blood* **86**, 1276-1280.
- Spear, P. G. & Longnecker, R. (2003). Herpesvirus entry: an update. *Journal of Virology* **77**, 10179-10185.
- Speck, S. H. & Ganem, D. (2010). Viral latency and its regulation: lessons from the gamma-herpesviruses. *Cell Host and Microbe* **8**, 100-115.
- Speese, Sean D., Ashley, J., Jokhi, V., Nunnari, J., Barria, R., Li, Y., Ataman, B., Koon, A., Chang, Y.-T., Li, Q., Moore, Melissa J. & Budnik, V. (2012). Nuclear envelope budding enables large ribonucleoprotein particle export during synaptic Wnt signaling. *Cell* **149**, 832-846.
- Staskus, K. A., Zhong, W., Gebhard, K., Herndier, B., Wang, H., Renne, R., Beneke, J., Pudney, J., Anderson, D. J., Ganem, D. & Haase, A. T. (1997). Kaposi's sarcoma-associated herpesvirus gene expression in endothelial (spindle) tumor cells. *Journal of Virology* **71**, 715-719.
- Stewart, M. (2007). Ratcheting mRNA out of the nucleus. *Molecular Cell* **25**, 327-330.

- Strasser, J. E., Arnold, R. L., Pachuk, C., Higgins, T. J. & Bernstein, D. I. (2000). Herpes simplex virus DNA vaccine efficacy: effect of glycoprotein D plasmid constructs. *Journal of Infectious Diseases* **182**, 1304-1310.
- Strässer, K., Masuda, S., Mason, P., Pfannstiel, J., Oppizzi, M., Rodriguez-Navarro, S., Rondon, A. G., Aguilera, A., Struhl, K., Reed, R. & Hurt, E. (2002). TREX is a conserved complex coupling transcription with messenger RNA export. *Nature* **417**, 304-308.
- Strauss, E. G. & Strauss, J. H. (2007). *Viruses and Human Disease*, London: Academic Press.
- Stubbs, S. H., Hunter, O. V., Hoover, A. & Conrad, N. K. (2012). Viral factors reveal a role for REF/Aly in nuclear RNA stability. *Molecular and Cellular Biology* **32**, 1260-1270.
- Stutz, F. & Izaurralde, E. (2003). The interplay of nuclear mRNP assembly, mRNA surveillance and export. *Trends in Cell Biology* **13**, 319-327.
- Sugiura, T., Sakurai, K. & Nagano, Y. (2007). Intracellular characterization of DDX39, a novel growth-associated RNA helicase. *Experimental Cell Research* **313**, 782-790.
- Sun, R., Lin, S.-F., Gradoville, L., Yuan, Y., Zhu, F. & Miller, G. (1998). A viral gene that activates lytic cycle expression of Kaposi's sarcoma-associated herpesvirus. *Proceedings of the National Academy of Sciences of the United States of America* **95**, 10866-10871.
- Sun, R., Lin, S.-F., Staskus, K., Gradoville, L., Grogan, E., Haase, A. & Miller, G. (1999). Kinetics of Kaposi's sarcoma-associated herpesvirus gene expression. *Journal of Virology* **73**, 2232-2242.
- Sun, R., Lin, S. F., Gradoville, L. & Miller, G. (1996). Polyadenylylated nuclear RNA encoded by Kaposi sarcoma-associated herpesvirus. *Proceedings of the National Academy of Sciences of the United States of America* **93**, 11883-11888.
- Taniguchi, I., Mabuchi, N. & Ohno, M. (2014). HIV-1 Rev protein specifies the viral RNA export pathway by suppressing TAP/NXF1 recruitment. *Nucleic Acids Research* **42**, 6645-6658.
- Taniguchi, I. & Ohno, M. (2008). ATP-dependent recruitment of export factor Aly/REF onto intronless mRNAs by RNA helicase UAP56. *Molecular and Cellular Biology* **28**, 601-608.
- Tanner, N. K. & Linder, P. (2001). DExD/H box RNA helicases: From generic motors to specific dissociation functions. *Molecular Cell* **8**, 251-262.
- Taylor, A., Jackson, B. R., Noerenberg, M., Hughes, D. J., Boyne, J. R., Verow, M., Harris, M. & Whitehouse, A. (2011). Mutation of a C-terminal motif affects Kaposi's sarcoma-associated herpesvirus ORF57 RNA binding, nuclear trafficking, and multimerization. *Journal of Virology* **85**, 7881-7891.
- Taylor, G. S. & Blackbourn, D. J. (2011). Infectious agents in human cancers: Lessons in immunity and immunomodulation from gammaherpesviruses EBV and KSHV. *Cancer Letters* **305**, 263-278.
- Teng, I. F. & Wilson, S. A. (2013). Mapping interactions between mRNA export factors in living cells. *PLoS ONE* **8**.
- Thomas, M., Lischka, P., Mueller, R. & Stamminger, T. (2011). The cellular DExD/H-box RNA-helicases UAP56 and URH49 exhibit a CRM1-independent nucleocytoplasmic shuttling activity. *PLoS ONE* **6**.

- Tortora, G. J., Funke, B. R. & Case, C. L. (2012). *Microbiology: An Introduction*: Benjamin Cummings Publishing Company.
- Toth, Z. & Stamminger, T. (2008). The human cytomegalovirus regulatory protein UL69 and its effect on mRNA export. *Frontiers in Bioscience* **13**, 2939-2949.
- Tugizov, S. M., Berline, J. W. & Palefsky, J. M. (2003). Epstein-Barr virus infection of polarized tongue and nasopharyngeal epithelial cells. *Nature Medicine* **9**, 307-314.
- Tunnicliffe, R. B., Hautbergue, G. M., Kalra, P., Jackson, B. R., Whitehouse, A., Wilson, S. A. & Golovanov, A. P. (2011). Structural basis for the recognition of cellular mRNA export factor REF by herpes viral proteins HSV-1 ICP27 and HVS ORF57. *PLoS Pathogens* **7**, e1001244.
- Tunnicliffe, R. B., Hautbergue, G. M., Wilson, S. A., Kalra, P. & Golovanov, A. P. (2014). Competitive and cooperative interactions mediate RNA transfer from herpesvirus saimiri ORF57 to the mammalian export adaptor ALYREF. *PLoS Pathogens* **10**, e1003907.
- Tuteja, N. & Tuteja, R. (2004). Unraveling DNA helicases - Motif, structure, mechanism and function. *European Journal of Biochemistry* **271**, 1849-1863.
- Uldrick, T. S. & Whitby, D. (2011). Update on KSHV epidemiology, Kaposi Sarcoma pathogenesis, and treatment of Kaposi Sarcoma. *Cancer Letters* **305**, 150-162.
- Uldrick, T. S., Wyvill, K. M., Kumar, P., O'Mahony, D., Bernstein, W., Aleman, K., Polizzotto, M. N., Steinberg, S. M., Pittaluga, S., Marshall, V., Whitby, D., Little, R. F. & Yarchoan, R. (2012). Phase II study of Bevacizumab in patients with HIV-associated Kaposi's sarcoma receiving antiretroviral therapy. *Journal of Clinical Oncology* **30**, 1476-1483.
- Verma, D. & Swaminathan, S. (2008). Epstein-Barr virus SM protein functions as an alternative splicing factor. *Journal of Virology* **82**, 7180-7188.
- Vieira, J., O'Hearn, P., Kimball, L., Chandran, B. & Corey, L. (2001). Activation of Kaposi's sarcoma-associated herpesvirus (human herpesvirus 8) lytic replication by human cytomegalovirus. *Journal of Virology* **75**, 1378-1386.
- Vieira, J. & O'Hearn, P. M. (2004). Use of the red fluorescent protein as a marker of Kaposi's sarcoma-associated herpesvirus lytic gene expression. *Virology* **325**, 225-240.
- Viphakone, N., Hautbergue, G. M., Walsh, M., Chang, C.-T., Holland, A., Folco, E. G., Reed, R. & Wilson, S. A. (2012). TREX exposes the RNA-binding domain of Nxf1 to enable mRNA export. *Nature Communications* **3**, 1006.
- Wang, L.-X., Kang, G., Kumar, P., Lu, W., Li, Y., Zhou, Y., Li, Q. & Wood, C. (2014). Humanized-BLT mouse model of Kaposi's sarcoma-associated herpesvirus infection. *Proceedings of the National Academy of Sciences of the United States of America* **111**, 3146-3151.
- Wang, Q. J., Jenkins, F. J., Jacobson, L. P., Kingsley, L. A., Day, R. D., Zhang, Z. W., Meng, Y. X., Pellett, P. E., Kousoulas, K. G., Baghian, A. & Rinaldo, C. R., Jr. (2001). Primary human herpesvirus 8 infection generates a broadly specific CD8(+) T-cell response to viral lytic cycle proteins. *Blood* **97**, 2366-2373.
- Wang, S. E., Wu, F. Y., Fujimuro, M., Zong, J. C., Hayward, S. D. & Hayward, G. S. (2003). Role of CCAAT/enhancer-binding protein alpha (C/EBP alpha) in activation of the

- Kaposi's sarcoma-associated herpesvirus (KSHV) lytic-cycle replication-associated protein (RAP) promoter in cooperation with the KSHV replication and transcription activator (RTA) and RAP. *Journal of Virology* **77**, 600-623.
- Wang, S. Z. E., Wu, F. Y., Chen, H. L., Shamay, M., Zheng, Q. Z. & Hayward, G. S. (2004a). Early activation of the Kaposi's sarcoma-associated herpesvirus RTA, RAP, and MTA promoters by the tetradecanoyl phorbol acetate-induced AP1 pathway. *Journal of Virology* **78**, 4248-4267.
- Wang, Y., Li, H., Chan, M. Y., Zhu, F. X., Lukac, D. M. & Yuan, Y. (2004b). Kaposi's sarcoma-associated herpesvirus ori-Lyt-dependent DNA replication: cis-acting requirements for replication and ori-Lyt-associated RNA transcription. *Journal of Virology* **78**, 8615-8629.
- Webster-Cyriaque, J., Duus, K., Cooper, C. & Duncan, M. (2006). Oral EBV and KSHV infection in HIV. *Advances in Dental Research* **19**, 91-95.
- Welch, P. J. & Wang, J. Y. J. (1992). Coordinated synthesis and degradation of cdc2 in the mammalian cell cycle. *Proceedings of the National Academy of Sciences of the United States of America* **89**, 3093-3097.
- Wen, K. W. & Damania, B. (2010). Hsp90 and Hsp40/Erdj3 are required for the expression and anti-apoptotic function of KSHV K1. *Oncogene* **29**, 3532-3544.
- Werner, F. J., Bornkamm, G. W., Fleckenstein, B. & Mulder, C. (1978). Episomal viral DNA in herpesvirus saimiri-transformed lymphoid cell lines. *IARC Scientific Publications* **24**, 125-130.
- Whitby, D., Howard, M. R., Tenant-Flowers, M., Brink, N. S., Copas, A., Boshoff, C., Hatziioannou, T., Suggett, F. E., Aldam, D. M., Denton, A. S., Miller, R. F., Weller, I. V. D., Weiss, R. A., Tedder, R. S. & Schulz, T. F. (1995). Detection of Kaposi sarcoma associated herpesvirus in peripheral blood of HIV-infected individuals and progression to Kaposi's sarcoma. *Lancet* **346**, 799-802.
- White, C. A., Stow, N. D., Patel, A. H., Hughes, M. & Preston, V. G. (2003). Herpes simplex virus type 1 portal protein UL6 interacts with the putative terminase subunits UL15 and UL28. *Journal of Virology* **77**, 6351-6358.
- Whitehouse, A., Cooper, M. & Meredith, D. M. (1998). The immediate-early gene product encoded by open reading frame 57 of herpesvirus Saimiri modulates gene expression at a posttranscriptional level. *Journal of Virology* **72**, 857-861.
- Wilson, S. J., Tsao, E. H., Webb, B. L., Ye, H., Dalton-Griffin, L., Tsantoulas, C., Gale, C. V., Du, M. Q., Whitehouse, A. & Kellam, P. (2007). X box binding protein XBP-1s transactivates the Kaposi's sarcoma-associated herpesvirus (KSHV) ORF50 promoter, linking plasma cell differentiation to KSHV reactivation from latency. *Journal of Virology* **81**, 13578-13586.
- Wu, F. Y., Ahn, J. H., Alcendor, D. J., Jang, W. J., Xiao, J. S., Hayward, S. D. & Hayward, G. S. (2001). Origin-independent assembly of Kaposi's sarcoma-associated herpesvirus DNA replication compartments in transient cotransfection assays and association with the ORF-K8 protein and cellular PML. *Journal of Virology* **75**, 1487-1506.
- Yamazaki, T., Fujiwara, N., Yukinaga, H., Ebisuya, M., Shiki, T., Kurihara, T., Kioka, N., Kambe, T., Nagao, M., Nishida, E. & Masuda, S. (2010). The closely related RNA helicases, UAP56 and URH49, preferentially form distinct mRNA export

- machineries and coordinately regulate mitotic progression. *Molecular Biology of the Cell* **21**, 2953-2965.
- Yang, Z., Yan, Z. & Wood, C. (2008). Kaposi's sarcoma-associated herpesvirus transactivator RTA promotes degradation of the repressors to regulate viral lytic replication. *Journal of Virology* **82**, 3590-3603.
- Ye, F., Lei, X. & Gao, S. J. (2011). Mechanisms of Kaposi's sarcoma-associated herpesvirus latency and reactivation. *Advances in Virology* **2011**, 193860.
- Yedavalli, V. S. R. K., Zhang, N., Cai, H., Zhang, P., Starost, M. F., Hosmane, R. S. & Jeang, K.-T. (2008). Ring expanded nucleoside analogues inhibit RNA helicase and intracellular human immunodeficiency virus type 1 replication. *Journal of Medicinal Chemistry* **51**, 5043-5051.
- Yin, J., Zhu, D., Zhang, Z., Wang, W., Fan, J., Men, D., Deng, J., Wei, H., Zhang, X.-E. & Cui, Z. (2013). Imaging of mRNA-protein interactions in live cells using novel mCherry trimolecular fluorescence complementation systems. *PLoS ONE* **8**, e80851.
- Young, L. S. & Rickinson, A. B. (2004). Epstein-Barr virus: 40 years on. *Nature Reviews. Cancer* **4**, 757-768.
- Zeng, Y., Zhang, X., Huang, Z., Cheng, L., Yao, S., Qin, D., Chen, X., Tang, Q., Lv, Z., Zhang, L. & Lu, C. (2007). Intracellular Tat of human immunodeficiency virus type 1 activates lytic cycle replication of Kaposi's sarcoma-associated herpesvirus: role of JAK/STAT signaling. *Journal of Virology* **81**, 2401-2417.
- Zenklusen, D., Vinciguerra, P., Wyss, J.-C. & Stutz, F. (2002). Stable mRNP formation and export require cotranscriptional recruitment of the mRNA export factors Yra1p and Sub2p by Hpr1p. *Molecular and Cellular Biology* **22**, 8241-8253.
- Zhang, N., Chen, H. M., Koch, V., Schmitz, H., Minczuk, M., Stepien, P., Fattom, A. I., Naso, R. B., Kalicharran, K., Borowski, P. & Hosmane, R. S. (2003). Potent inhibition of NTPase/helicase of the West Nile virus by ring-expanded ("Fat") nucleoside analogues. *Journal of Medicinal Chemistry* **46**, 4776-4789.
- Zhao, R., Shen, J., Green, M. R., MacMorris, M. & Blumenthal, T. (2004). Crystal structure of UAP56, a DExD/H-box protein involved in pre-mRNA splicing and mRNA export. *Structure* **12**, 1373-1381.
- Zhi, H., Zahoor, M. A., Shudofsky, A. M. D. & Giam, C. Z. (2014). KSHV vCyclin counters the senescence/G1 arrest response triggered by NF- $\kappa$ B hyperactivation. *Oncogene* doi:10.1038/onc.2013.567, [Epub ahead of print].
- Zhou, Z., Luo, M. J., Strässer, K., Katahira, J., Hurt, E. & Reed, R. (2000). The protein Aly links pre-messenger-RNA splicing to nuclear export in metazoans. *Nature* **407**, 401-405.